INVESTIGATION OF THE INTERCONNECTED ROLES OF CMAL AND HOPAA1-1 IN THE VIRULENCE OF *PSEUDOMONAS SYRINGAE* PV.*TOMATO* DC3000 IN *NICOTIANA BENTHAMIANA*

A Dissertation

Presented to the Faculty of the Graduate School

of Cornell University

in Partial Fulfillment of the Requirements for the Degree of

Doctor of Philosophy

by

Jay N Worley

January 2013

INVESTIGATION OF THE INTERCONNECTED ROLES OF CMAL AND HOPAA1-1 IN THE VIRULENCE OF *PSEUDOMONAS SYRINGAE* PV.*TOMATO* DC3000 IN *NICOTIANA BENTHAMIANA*

Jay N Worley, Ph.D.

Cornell University 2013

Pseudomonas syringae pv. *tomato* DC3000 (DC3000) is a model plant pathogenic bacterium that infects tomato and *Arabidopsis thaliana*. It requires the phytotoxin coronatine and the delivery of type III effector proteins (T3Es) into the host cell cytoplasm for defense suppression and virulence.

CmaL is a small protein found to be necessary for coronatine production. Coronatine is a potent molecular mimic of jasmonoyl–isoleucine, a plant hormone conjugate involved in regulating plant defenses. Coronatine is constructed of two amide bond-linked moieties, coronafacic acid and coronamic acid. CmaL was shown to be required for the production of L-*allo*-isoleucine, a precursor for coronamic acid biosynthesis.

DC3000 mutants lacking both *cmaL* and the T3E gene *hopAA1-1* are reduced in speck formation in tomato. *hopAA1-1* is member of the conserved effector locus, a group of effector genes located adjacent to the genes encoding the type three secretion apparatus that are widespread among *P. syringae* strains. HopAA1-1 is toxic to both plants and yeast upon expression within them. To gain insight into the basis for its toxicity in eukaryotic cells, the subcellular localization of HopAA1-1 was investigated.

HopAA1-1 was found to colocalize with plant peroxisomes. Truncated derivatives of HopAA1-1 that are not cytotoxic and cannot promote symptom formation do not localize with peroxisomes. Additionally, other truncated derivatives of HopAA1-1 colocalize with the endoplasmic reticulum in addition to peroxisomes, suggesting that HopAA1-1 interacts with the endomembrane system.

A DC3000 mutant with 28 T3E genes deleted (DC3000D28E) is a recently developed tool for investigating effector functions. DC3000D28E derivatives with small sets of effector genes progressively restored show increasing virulence when inoculated by infiltration with a blunt syringe into the model plant *Nicotiana benthamiana*. Because of its location in a cluster of effector genes, *cmaL* was inadvertently deleted in the construction of DC3000D28E. The importance of coronatine and its partial redundancy with HopAA1-1 in promoting an early stage of pathogenesis was revealed by restoring *cmaL* and *hopAA1-1* to selected DC3000D28E derivatives and assaying the strains by dip inoculation of *N. benthamiana* leaves, which requires bacteria to follow a natural infection route through stomata.

BIOGRAPHICAL SKETCH

Jay Noboru Worley was born on December 11th, 1983 to Paul and Faye Worley. He has one younger brother, Eric, whom he considers to be a great friend. Paul and Faye are kind and generous parents who have taught him and his brother to stand for something and to only pursue that which helps others. Most importantly, Jay and Eric were taught to be driven people – not perhaps to simply succeed, but instead to advance in ways that lift those around them. He and his brother are two very (**very**) different people, but both care deeply about how they treat those around them and the collective well-being. Jay and Eric are both Eagle Scouts.

Jay's passion for the cellular world started with a microscope in Science Research class at South Carroll High School, senior year, taught by Mr. Foor-Hogue. His project was taking pictures of zebrafish embryos and documenting the different stages of development. Eggs were collected regularly and photographed with a digital camera (that wrote to a floppy disk) hooked up to a basic microscope (using the finest plumbing technology as a mount). The eggs were allowed to develop over time, and the observations recorded in a lab notebook. Single cells developed into something with a microscopic heartbeat and then, eventually, into tiny fish. This experience introduced Jay to the tiny spirited worlds, invisible to the unaided eye, which exist everywhere. The passion that started with fish eggs has developed into a career studying the small, often with a microscope and a camera, to understand the incredible microscopic world that we live in and are made of.

Jay attended the University of Maryland beginning in 2002 and took part in the College Park Scholars program. Early on, he identified Microbiology as a field of study that interested him and sought out an internship during his Sophomore year. He worked for the FDA beginning in the Spring of 2004 as an undergraduate researcher in the lab of Dr. Keith Lampel, and later moved to the lab of Dr. Palmer Orlandi. This experience energized him to pursue a career in research, and with the blessing of his mentors, applied directly to Ph.D. programs in microbiology, and accepted enrollment at Cornell University for the term beginning in Fall 2006. He graduated magna cum laude from the University of Maryland in the Spring of 2006.

Outside of science he has an artistic drive. He has developed as a capable saxophonist and photographer outside of his studies. Perhaps his greatest legacy, outside of publications, to the Department of Plant Pathology and Plant-Microbe Interactions are the coffee break ads – each individualized to the lab hosting that week – with images of people merged into movie posters, national monuments, ads and various other images.

To my loving family for raising me well and supporting me.

To my friends for being great company.

To my mentors for developing my mind.

ACKNOWLEDGMENTS

Thanks first to Alan Collmer, who has been more patient with me than I probably deserve. Alan has a talent for inspiring hard work without being demanding. As long as I have been here, the Collmer Lab has always been the one with the lights on, and this is a testament to Alan's leadership. Once, the maintenance staff thought the motion sensor lights were broken because the log showed them turning on at 10 to 12 pm, and Sébastien and I patiently explained that the motion detectors were working just fine. I would also like to thank all of the Collmer Lab members that I have had the privilege to work with, with a few special acknowledgments: To Brian Kvitko for teaching me most of what I know about manipulating *Pseudomonas syringae* genomes, to Alistair Russell for first isolating *cmaL*, and to Kathy Munkvold for her research on HopAA1-1. Bryan Swingle has been a non-committee mentor to me in these past few years and whose insight I have enjoyed. Donna Gibson has been instrumental in producing Chapter 2 of this thesis and has been wonderful to collaborate with. To Carol Bayles, Hélène Javot and Mamta Srivastava for teaching me how to use confocal microscopes. Brittany Chao and Bong-kyo Seo were undergraduate assistants who helped with Chapter 3. Suma Chakravarthy was instrumental in developing Chapter 4 with bacterial strains and advice. The research here at Cornell was funded through a USDA/CSREES Food and Agricultural Sciences National Needs Fellowship and NSF grants MCB-0544066 and IOS-1025642.

I would like to also acknowledge three people from my academic past. To Mr. Foor-Hogue, my high school teacher for Science Research I & II; it was my experience

in those classes that drove me to pursue research opportunities in college. To Dr. Palmer Orlandi at the USFDA for giving me a stable lab environment, after the previous one fell apart, and for helping me develop professionally. To Dr. Ann Smith at the University of Maryland for teaching me how to teach and encouraging my passion for Microbiology.

I have had the great privilege of being friends with too many students and post docs here to name here. You all are dear to me.

To the many musicians around Ithaca that I have gotten to know. It may seem a silly acknowledgment for a Ph.D. thesis, but friends at Cornell come and go frequently as they graduate and move on – the friends that I have made through music have been constant throughout. Especially Asher, thank you ol' buddy.

Finally, I need to thank my family for their unwavering support throughout this degree. You are always in my heart.

TABLE OF CONTENTS

LIST OF FIGURES

LIST OF TABLES

CHAPTER 1

ROLES AND INTERPLAY BETWEEN THE TYPE THREE EFFECTORS AND PHYTOTOXINS IN *PSEUDOMONAS SYRINGAE SPP.*

Introduction to plant pathogenesis by *Pseudomonas syringae*.

Bacteria release small molecules and proteins that betray their presence to eukaryotes. Multicellular eukaryotes have developed detection arrays that monitor their intra- and extracelluar matrices for a subset of these particles, usually highly evolutionarily conserved, called pathogen associated molecular patterns (PAMPs) (Zipfel and Felix, 2005; Monaghan and Zipfel, 2012). When a PAMP is detected, a strong and appropriate defense is mounted, which pathogenic bacteria must overcome to cause disease. In response to this, bacteria have developed methods to defeat host defenses and promote their own survival and growth. The bacterial tools of invasion are adapted to each host, but involve two primary strategies that span kingdoms of hosts: secretion of small molecules that can passively travel into host cells and the direct delivery of proteins into host cytoplasm through a proteinaceous translocon. The principle of delivering biologically active proteins into a host cell cytoplasm to facilitate pathogenicity is a particularly important example of convergence as it is found in multiple kingdoms of life and viruses. Each of these two strategies is employed to deliver molecules that affect normal host function, either by lowering defenses or releasing nutrients for the pathogen.

Pseudomonas syringae follows this pattern: all pathogenic strains utilize a type-three secretion system (T3SS) to deliver effector proteins (T3Es) directly into host-cell cytoplasm, and most strains produce at least one small, diffusible molecule that interferes with host defenses (Baltrus et al., 2011). These effector repertoires are highly variable, even when two strains share a host, and contain usually between 10 to 30 individual effectors. The individual strains of these species are grouped in two ways: by pathovars, based on their primary host; and phylogenetically, based on their ancestry. Some pathovars do not align with phylogenetic relationships, nor do the individual effector repertoires.

Though several T3Es have well described targets, most do not, and additional targets have been found for already-described proteins, which means that more interactions are likely to exist even for T3Es for which at least one interactor is known. There are several examples of T3Es that are now known to contain multiple domains to facilitate various actions (Dean, 2011). There are important aspects of T3E molecular biology which have yet to be explored.

This thesis contributes new knowledge to several of these issues using the model pathogen of *Arabidopsis* and *tomato*, *P.* syringae pv. *tomato* DC3000 (*Pto* DC3000). Chapter 2 addresses the contribution to phytotoxin biosynthesis of a small ORF that we name *cmaL*. Chapter 3 is a detailed molecular dissection of *hopAA1-1* and narrows down the possible cellular pathways that it affects. Chapter 4 concerns CmaL and HopAA1-1, a T3E that is partially redundant with CmaL in speck promotion, which are reintroduced to *Pto* DC3000 deletion backgrounds to study symptom formation. Chapter 5 is a prospectus that offers an outlook on the field of pathogen

outcomes in bacterial plant pathogens. The appendix continues work with deletion backgrounds towards understanding contributions to disease at the level of bacterial colonies in leaf tissue, observing the spatial contribution to disease of various effector combinations, and aids in understanding Chapter 4.

This introduction will cover basic knowledge of T3Es and the phytotoxin coronatine in *Pseudomonas syringae*, the two major subjects of this thesis.

Coronatine biology and biosynthesis.

Almost all strains of *P. syringae* seem to encode for production of a phytotoxin (Baltrus et al., 2011). Effector proteins, then, are either insufficient to cause disease on their own and/or small molecules are much more economical to produce. The particular phytotoxin(s) produced seems to have at least some role in determining the effector repertoire of certain *P. syringae* strains, as the strains producing syringolin and syringomycin, a proteasome inhibitor and cell-membrane pore former, respectively, tend to have a smaller effector repertoire than other *P. syringae* strains (Hutchison et al., 1995; Groll et al., 2008; Baltrus et al., 2011). These phytotoxins tend to be small ribosome-independent peptides or metabolites, as reviewed (Bender et al., 1999).

Pto DC3000 produces only a single known phytotoxin, coronatine. The operons encoding coronatine production are found either plasmid-borne or in genomic regions of high genetic plasticity in several genetically diverse strains of *P. syringae*, indicating that toxin production is part of the flexible genome (Buell et al., 2003; Baltrus et al., 2011). Coronatine promotes chlorosis and necrosis, and strains of *P. syringae* that produce it have chlorosis as a symptom, typically with necrosis late in infection (Bender et al.,

1987). Coronatine is essential to the virulence of *Pto* DC3000 in dip inoculations of both *Arabidopsis thaliana* and *tomato* (Mittal and Davis, 1995). It is a molecular mimic of jasmonate-isoleucine conjugate (JA-Ile), a plant defense hormone, and through this mimicry causes the opening of stomata and the suppression of salicylic acid-mediated molecular signaling (Brooks et al., 2005; Melotto et al., 2006; Zheng et al., 2012). The major interacting protein for coronatine is CORONATINE INSENSITIVE1 (COI1), which when activated by either coronatine or JA-Ile, promotes the transcriptional response associated with jasmonic acid (Chini et al., 2007; Thines et al., 2007; Yan et al., 2009). Recently, it has been reported that another function, independent of jasmonate mimicry, is carried out by coronatine but is yet to be completely defined (Geng et al., 2012) .

A cluster of three of regulatory genes, two separate operons and one small detached gene identified in this thesis are required for producing coronatine. The *cor* genes encode an essential regulatory machinery for coronatine production, which also both relies on and contributes to the expression of the alternate sigma factor that regulates genes involved in pathogenesis more broadly, σ^L, encoded for by *hrpL* (Sreedharan et al., 2006). The *cor* genes and *hrpL* gene products are all required to express the three sets of genes believed to be sufficient for coronatine synthesis: the *cfa* operon, the *cma* operon, and *cmaL*.

Coronatine is composed of two molecules, coronafacic acid and coronamic acid, which are synthesized by the proteins encoded in the *cfa* and *cma* operons, respectively, joined by an amide bond (Ichihara et al., 1977; Brooks et al., 2004). There are two, major, unresolved issues concerning this process. The first is the identity of the ligation machinery, which links together coronafacic acid and coronamic acid. The

gene product of *cfl*, the first gene of the *cfa* operon, has been presumed to be the ligase but a direct biochemical activity has not been demonstrated (Liyanage et al., 1995; Rangaswamy et al., 1997). The second issue is addressed in this thesis. That is, the current understanding of the *cma* operon requires L-*allo*-isoleucine as a metabolic precursor, but this is a rare amino acid for which no dedicated biosynthetic machinery is known (Vaillancourt et al., 2005).

In Chapter 2 *cmaL* is identified as being required for the production of L-*allo*-isoleucine. The *cmaL* gene is located in the DC3000 genome close to the *cma* operon, but separated by several genes encoding T3Es. It is shown to be controlled by the same regulatory proteins as the *cma* operon but by separate promoter sequences.

Studying the effector pan-repertoire of *P. syringae* pathovars.

P. syringae effector repertoires are highly variable, with only a few effectors being prevalent. In DC3000, all effectors seem to be individually dispensable for disease, but are collectively essential, indicating at least some level of redundancy within repertoires (Kvitko et al., 2009). Both effectors with high or low prevalence are necessary for pathogenicity, with the highly conserved effectors hypothesized to have targets that are more evolutionarily conserved (Kvitko et al., 2009; Lindeberg et al., 2012). One hypothesis is that proteins involved in PAMP perception and subsequent signaling cascades tend to be more variable whereas proteins involved in defense deployment rely on highly conserved cellular machinery. According to this hypothesis, the most highly prevalent effectors, then, would target these highly conserved

processes while the less prevalent effectors would target the signaling cascades involved in pathogen recognition.

An overview of DC3000 effector-based evolution can be found in Fig. 1.1, which lays out a simple visualization of the different levels of plant responses and processes available for effector targeting. Surprisingly, only one receptor-like kinase (RLK), FLS2, has been described which is both broadly distributed among plants and directly responsive to a bacterially derived PAMP, the flg22 epitope of flagellin (Gomez-Gomez and Boller, 2000; Chinchilla et al., 2006). EFR is an RLK that responds to the EF-Tu peptide elf18 but is evolutionarily younger than FLS2, and has a correspondingly smaller distribution among only Brassicaceae (Zipfel et al., 2006). Other bacterial PAMPs exist, including cold-shock protein, RNP-1, and CpG DNA, but plant RLKs have not been identified for them, nor do they seem to contribute to signaling as strongly as FLS2 (Felix and Boller, 2003; Yakushiji et al., 2009). Accordingly, flg22 has been the major PTI elicitor used for studies of the signal relay downstream of RLK PAMP-perception.

PAMP-triggered immunity (PTI) is a collection of plant responses to PAMPs, which are sufficient to suppress pathogen growth (Boller and He, 2009). Although it is known that PTI can suppress pathogen growth, the exact mechanisms remain elusive. There are some hallmarks of PTI, however, that have been used to elucidate which effectors effectively suppress it: a two-stage oxidative burst, salicylic acid accumulation, formation of callose-rich papillae, and activation of specific genes, such as *pti5*, are among the hallmarks that have been used to assess PTI suppression through effector interference (Nguyen et al., 2010). These studies are performed using one effector at a

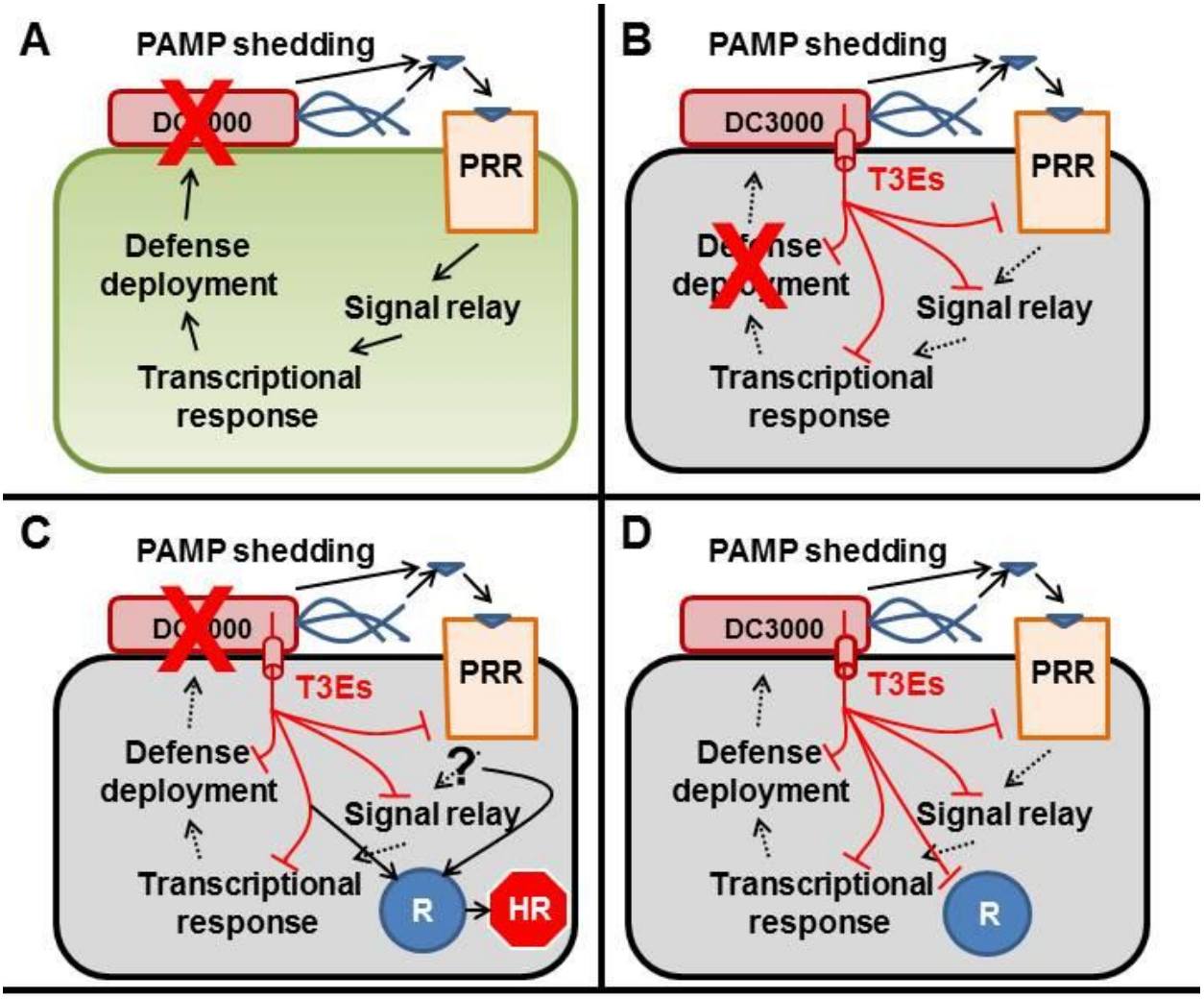

Figure 1.1. A conceptualization of disease (based on Lindeberg et al. 2012). A. Bacteria shed molecules, such as flagellin and EF-Tu, known as PAMPs, which plants can detect. These are sensed directly by pattern recognition receptors (PRR), transmembrane kinases that, upon activation, begin a signaling cascade that leads to a transcriptional response. The genes activated in this response encode a variety of defense activities which inhibit bacterial growth by PTI. B. DC3000 utilizes a T3SS (cylinder) to deliver T3Es, members of which have been found to affect each of these activities. Pathogenesis results. C. Plants have developed a stronger response for use when pathogens are detected. "R" proteins potentiate HR in response to T3E detection, either by serving as a decoy that activates upon sensing a specific T3E activity or by detecting the absence of normal defense-protein function. In HR, the host cell dies, but pathogenesis is thwarted. D. T3SS-utilizing pathogens can block HR by having additional domains or effectors that block HR initiated by R proteins. Pathogenesis is restored. In each of the cases leading to pathogenesis or HR, the host cells eventually die (gray).

time, either through delivery by *Pseudomonas fluorescens* carrying a plasmid encoding a functional T3SS or through the use of transgenic plants expressing the test effector with subsequent PAMP stimulation (Jamir et al., 2004; Oh and Collmer, 2005; Guo et al., 2009). Other studies delete one or a few effectors from pathogen genomes and look for differences in pathogen growth or persistence (Lin and Martin, 2005; Lee et al., 2012). While these studies are important for assigning impacts on disease resistance or pathogen growth, they do not directly address how these factors are functioning. Furthermore, since many of these effectors can be found in phylogenetically diverse strains of *P. syringae*, it can be inferred that there is a selective advantage to having them even in the absence of our ability to assay their function.

Some synergy has been noted between effectors that target different phases of host defense. The concept of Redundant Effector Groups (REGs) is based on groups of effectors that functionally overlap (Kvitko et al., 2009). This concept helps to explain why any of the effectors can usually be deleted without consequence, but once certain groups or combinations are deleted, the pathogen loses some of its ability to cause disease.

AvrPto and AvrPtoB belong to one REG and are T3Es found in *P. syringae* strains that have documented physical interactions with FLS2, with AvrPto additionally interacting with EFR. These two are the most heavily documented effectors of bacterial plant-pathogens. AvrPto disrupts defense signaling through this direct interaction, whereas AvrPtoB ubiquitinates FLS2, leading to its degradation (Abramovitch et al., 2006; Göhre et al., 2008; Xiang et al., 2008). Both promote disease through the disruption of PAMP recognition by directly targeting the receptor, and apparently

suppress defense through the same signal disruption as evidenced by their redundant function in promoting disease (Lin and Martin, 2005).

Downstream of this recognition, the signal is propagated by a chain of phosphorylation events. The knowledge of the kinases involved in conducting an appropriate defense response is growing and is not yet complete. Nevertheless, there are several *P. syringae* effectors known to target signal propagation. A co-receptor common to FLS2 and EFR, BAK1, is targeted by both AvrPto and AvrPtoB (Shan et al., 2008). Events downstream are targeted by effectors that inactivate kinases, and the two mechanisms discovered are, accordingly, irreversible catalyzed reactions. AvrPphB is a cysteine protease that proteolytically cleaves BIK1, whereas HopAI1 is a phosphothreonine lyase of mitogen-activated protein kinases (MAPKs) (Zhang et al., 2007; Zhang et al., 2010). AvrRpt2 and AvrRpm1 target RIN4, a component of PTI signaling, for degradation or phosphorylation, respectively, but the exact role of RIN4 in signaling is yet unknown (Kim et al., 2005). HopF2 and AvrB have been described to interfere with these signaling cascades, but with unclear mechanisms and/or targets (Cui et al., 2010; Wu et al., 2011).

The transcriptional response includes processes that directly produce or interact with plant RNAs before translation or function. In *P. syringae*, only HopU1 appears to directly modify a component of this system by ribosylating the protein GRP7, preventing it from interacting with RNAs

Finally, several effectors have been described that disrupt defense responses downstream of transcription. These responses are diverse, directing everything from vesicle trafficking to intracellular defense signaling. HopM1 suppresses PTI by

disrupting AtMIN7-assisted vesicle trafficking through directing AtMIN7 to proteasomal degradation, and has at least partial functional redundancy with AvrE (Badel et al., 2006; Nomura et al., 2006). The final example is HopI1, which disrupts plant defense-hormone biosynthesis by stimulating a chloroplast stress-response protein, Hsp70 (Jelenska et al., 2007).

Additional, but less specific knowledge about these and other T3Es comes from screens of effectors for specific plant outcomes. These screens have proven useful for figuring out how effectors affect their hosts without special mechanistic knowledge, and have revealed which effectors can, among other things, suppress cell death, stop vascular restriction, and suppress PTI, among other functions (Jamir et al., 2004; Oh and Collmer, 2005; Guo et al., 2009). These screens identify classes of effectors which, instead of interacting with specific proteins, modify specific plant functions. These screens are useful for gaining insight into what proportions of a repertoire are likely to carry out the particular functions that are thought to be essential for pathogenesis. At least for transient expression, the host makes a large difference in the ability to detect phenotype, and should be kept in mind when interpreting these experiments (Wroblewski et al., 2009). Nevertheless, screens provide useful information towards exploring repertoires. These problems are compounded by plant defenses, particularly the HR response. Detailed study of a single effector's biochemistry and cell biology in plants remains the only method for definitively observing what functions an effector might carry out.

Working with one or only a few effectors remains the primary mode of generating accurate and significant data on effector biochemistry and effector function in general.

Effectors must be carefully selected for further inquiry, as finding critical molecular mechanisms can require multiple lines of investigation and years of study. While studying an array of effectors has provided insight into repertoire themes and phenotypic similarities, these themes need to be verified and detailed through individual study. A controversial idea that has emerged from one of these inquiries is the apparent clustering of effector interactions around nodes of defense (Mukhtar et al., 2011). While, as previously noted, some plant proteins seem to be targeted by multiple effectors, the degree of this redundancy is unresolved.

In Chapter 3, the plant-cell biology of HopAA1-1 is explored. It is a single effector that was chosen for individual study because of its high prevalence among *P. syringae* strains (Baltrus et al., 2011), its identification in a screen in which its overexpression was toxic to both yeast and plant cells, and the observation that mutations to the protein that alleviate cell-death in yeast do likewise in plants (Munkvold et al., 2008). The localization patterns of several interesting mutants are explored, the apparent domains of the protein are defined, and these results are shown to be replicated almost perfectly in yeast, suggesting an interaction with deeply conserved eukaryotic machinery.

Not included in this thesis are a series of experiments carried out to try and find an interacting partner for HopAA1-1, which were unsuccessful.

Utilizing an effectorless mutant to study combinations of effectors and phytotoxins.

Recently, the Collmer lab developed a mutant strain of DC3000 with 28 effectors deleted (D28E) (Cunnac et al., 2011). Single effectors have the ability to suppress defenses and allow for pathogen growth but do not themselves enable full pathogenicity and particularly symptom development (Guo et al., 2009; Cunnac et al., 2011). This disconnect in the current understanding of pathogenesis is increased because evaluating pathogen growth and defense suppression typically rely on assays that do not allow for the formation of classic symptoms seen in a wild infection. Recent advances in our ability to use combinations of effectors allows us to probe a long-standing puzzle in the study of T3SS-utilizing hemibiotrophic plant-pathogenic bacteria: why do pathogens need complex repertoires, and what combinations of effectors are most successful?

Furthermore, some effectors have effects which seem to be context dependent and therefore would not be observed in typical assays for growth. The T3E HopAM1 suppresses basal defenses, but seems to have a pronounced effect on plants under mild drought conditions (Goel et al., 2008). HopAA1-1 is a T3E that promotes speck formation on tomato but seems to have little effect on pathogen outcome when inoculum is infiltrated via syringe (Badel et al., 2002; Munkvold et al., 2009). Finally, HopAA1-1 and HopZ3 are T3Es relevant to epiphytic populations of pathogens in *P. syringae* pv. *syringae* B728a (Lee et al., 2012). There is growing evidence that effectors that provide specific benefits with regards to specific plant-pathogen interaction contexts and effector repertoires may reveal different evolutionary pressures towards specific functions (Bogdanove et al., 2011).

In Chapter 4 a preliminary look at using specific, defined combinations of effectors and coronatine is used. The creation of an effector-depleted mutant DC3000 resulted in deletion of *cmaL*, which resides in a cluster of effectors (Buell et al., 2003). The growth profiles of D28E with up to 8 effectors has been firmly established, and Chapter 4 continues that work by investigating the ability of these strains to produce phenotypes when dip inoculated. In particular, the effect of restoring *hopAA1-1* or *cmaL* expression is examined as these are factors that redundantly promote symptom formation despite one being a small molecule and the other being a T3E (Munkvold et al., 2009).

Chapter 5 provides additional information on the growth characteristics of the backgrounds used in Chapter 4.

REFERENCES

Abramovitch, R.B., Janjusevic, R., Stebbins, C.E., and Martin, G.B. 2006. Type III effector AvrPtoB requires intrinsic E3 ubiquitin ligase activity to suppress plant cell death and immunity. Proc Natl Acad Sci USA 103:2851-2856.

Badel, J.L., Charkowski, A.O., Deng, W.L., and Collmer, A. 2002. A gene in the *Pseudomonas syringae* pv. *tomato* Hrp pathogenicity island conserved effector locus, *hopPtoA1*, contributes to efficient formation of bacterial colonies in planta and is duplicated elsewhere in the genome. Mol Plant-Microbe Interact 15:1014-1024.

Badel, J.L., Shimizu, R., Oh, H.-S., and Collmer, A. 2006. A *Pseudomonas syringae* pv. *tomato avrE1*/*hopM1* mutant is severely reduced in growth and lesion formation in tomato. Mol Plant-Microbe Interact 19:99-111.

Baltrus, D.A., Nishimura, M.T., Romanchuk, A., Chang, J.H., Mukhtar, M.S., Cherkis, K., Roach, J., Grant, S.R., Jones, C.D., and Dangl, J.L. 2011. Dynamic evolution of pathogenicity revealed by sequencing and comparative genomics of 19 *Pseudomonas syringae* isolates. PLoS Pathog 7:e1002132.

Bender, C.L., Alarcon-Chaidez, F., and Gross, D.C. 1999. *Pseudomonas syringae* phytotoxins: mode of action, regulation, and biosynthesis by peptide and polyketide synthetases. Microbiol Mol Biol Rev 63:266-292.

Bender, C.L., Stone, H.E., Sims, J.J., and Cooksey, D.A. 1987. Reduced pathogen fitness of *Pseudomonas syringae* pv. *tomato* Tn5 mutants defective in coronatine production. Physiol Mol Plant Path 30:273-283.

Bogdanove, A.J., Koebnik, R., Lu, H., Furutani, A., Angiuoli, S.V., Patil, P.B., Van Sluys, M.A., Ryan, R.P., Meyer, D.F., Han, S.W., Aparna, G., Rajaram, M., Delcher, A.L., Phillippy, A.M., Puiu, D., Schatz, M.C., Shumway, M., Sommer, D.D., Trapnell, C., Benahmed, F., Dimitrov, G., Madupu, R., Radune, D., Sullivan, S., Jha, G., Ishihara, H., Lee, S.W., Pandey, A., Sharma, V., Sriariyanun, M., Szurek, B., Vera-Cruz, C.M., Dorman, K.S., Ronald, P.C., Verdier, V., Dow, J.M., Sonti, R.V., Tsuge, S., Brendel, V.P., Rabinowicz, P.D., Leach, J.E., White, F.F., and Salzberg, S.L. 2011. Two new complete genome sequences offer insight into host and tissue specificity of plant pathogenic *Xanthomonas* spp. J Bacteriol 193:5450-5464.

Boller, T., and He, S.Y. 2009. Innate immunity in plants: an arms race between pattern recognition receptors in plants and effectors in microbial pathogens. Science 324:742-744.

Brooks, D., Hernandez-Guzman, G., Koek, A.P., Alarcon-Chaidez, F., Sreedharan, A., Rangaswarmy, V., Penaloza-Vasquez, A., Bender, C.L., and Kunkel, B.N. 2004. Identification and characterization of a well-defined series of coronatine biosynthetic mutants of *Pseudomonas syringae* pv. *tomato* DC3000. Mol Plant-Microbe Interact 17:162-174.

Brooks, D.M., Bender, C.L., and Kunkel, B.N. 2005. The *Pseudomonas syringae* phytotoxin coronatine promotes virulence by overcoming salicylic acid-dependent defences in *Arabidopsis thaliana* Mol Plant Pathol 6:629-639.

Buell, C.R., Joardar, V., Lindeberg, M., Selengut, J., Paulsen, I.T., Gwinn, M.L., Dodson, R.J., Deboy, R.T., Durkin, A.S., Kolonay, J.F., Madupu, R., Daugherty,

S., Brinkac, L., Beanan, M.J., Haft, D.H., Nelson, W.C., Davidsen, T., Liu, J., Yuan, Q., Khouri, H., Fedorova, N., Tran, B., Russell, D., Berry, K., Utterback, T., Vanaken, S.E., Feldblyum, T.V., D'Ascenzo, M., Deng, W.-L., Ramos, A.R., Alfano, J.R., Cartinhour, S., Chatterjee, A.K., Delaney, T.P., Lazarowitz, S.G., Martin, G.B., Schneider, D.J., Tang, X., Bender, C.L., White, O., Fraser, C.M., and Collmer, A. 2003. The complete sequence of the *Arabidopsis* and tomato pathogen *Pseudomonas syringae* pv. *tomato* DC3000. Proc Natl Acad Sci USA 100:10181-10186.

Chinchilla, D., Bauer, Z., Regenass, M., Boller, T., and Felix, G. 2006. The *Arabidopsis* receptor kinase FLS2 binds flg22 and determines the specificity of flagellin perception. Plant Cell 18:465-476.

Chini, A., Fonseca, S., Fernandez, G., Adie, B., Chico, J.M., Lorenzo, O., Garcia-Casado, G., Lopez-Vidriero, I., Lozano, F.M., Ponce, M.R., Micol, J.L., and Solano, R. 2007. The JAZ family of repressors is the missing link in jasmonate signalling. Nature 448:666-671.

Cui, H., Wang, Y., Xue, L., Chu, J., Yan, C., Fu, J., Chen, M., Innes, R.W., and Zhou, J.M. 2010. *Pseudomonas syringae* effector protein AvrB perturbs Arabidopsis hormone signaling by activating MAP kinase 4. Cell Host Microb 7:164-175.

Cunnac, S., Chakravarthy, S., Kvitko, B.H., Russell, A.B., Martin, G.B., and Collmer, A. 2011. Genetic disassembly and combinatorial reassembly identify a minimal functional repertoire of type III effectors in *Pseudomonas syringae*. Proc Natl Acad Sci USA 108:2975-2980.

Dean, P. 2011. Functional domains and motifs of bacterial type III effector proteins and their roles in infection. FEMS Microbiol Rev 35:1100-1125.

Felix, G., and Boller, T. 2003. Molecular sensing of bacteria in plants. The highly conserved RNA-binding motif RNP-1 of bacterial cold shock proteins is recognized as an elicitor signal in tobacco. J Biol Chem 278:6201-6208.

Geng, X., Cheng, J., Gangadharan, A., and Mackey, D. 2012. The coronatine toxin of *Pseudomonas syringae* is a multifunctional suppressor of *Arabidopsis* defense. Plant Cell 24:4763-4774.

Goel, A.K., Lundberg, D., Torres, M.A., Matthews, R., Akimoto-Tomiyama, C., Farmer, L., Dangl, J.L., and Grant, S.R. 2008. The *Pseudomonas syringae* type III effector HopAM1 enhances virulence on water-stressed plants. Mol Plant-Microbe Interact 21:361-370.

Göhre, V., Spallek, T., Häweker, H., Mersmann, S., Mentzel, T., Boller, T., de Torres, M., Mansfield, J.W., and Robatzek, S. 2008. Plant pattern-recognition receptor FLS2 is directed for degradation by the bacterial ubiquitin ligase AvrPtoB. Curr Biol 18:1824-1832.

Gomez-Gomez, L., and Boller, T. 2000. FLS2: an LRR receptor-like kinase involved in the perception of the bacterial elicitor flagellin in *Arabidopsis*. Mol Cell 5:1003-1011.

Groll, M., Schellenberg, B., Bachmann, A.S., Archer, C.R., Huber, R., Powell, T.K., Lindow, S., Kaiser, M., and Dudler, R. 2008. A plant pathogen virulence factor inhibits the eukaryotic proteasome by a novel mechanism. Nature 452:755-758.

Guo, M., Tian, F., Wamboldt, Y., and Alfano, J.R. 2009. The majority of the type III effector inventory of *Pseudomonas syringae* pv. *tomato* DC3000 can suppress plant immunity. Mol Plant-Microbe Interact 22:1069-1080.

Hutchison, M.L., Tester, M.A., and Gross, D.C. 1995. Role of biosurfactant and ion channel-forming activities of syringomycin in transmembrane ion flux: a model for the mechanism of action in the plant-pathogen interaction. Mol Plant-Microbe Interact 8:610-620.

Ichihara, A., Shiraishi, K., Sato, H., Sakamura, S., Nishiyama, K., Sakai, R., Furusaki, A., and Matsumoto, T. 1977. The structure of coronatine. J Am Chem Soc 99:636-637.

Jamir, Y., Guo, M., Oh, H.S., Petnicki-Ocwieja, T., Chen, S., Tang, X., Dickman, M.B., Collmer, A., and Alfano, J.R. 2004. Identification of *Pseudomonas syringae* type III effectors that can suppress programmed cell death in plants and yeast. Plant J 37:554-565.

Jelenska, J., Yao, N., Vinatzer, B.A., Wright, C.M., Brodsky, J.L., and Greenberg, J.T. 2007. A J domain virulence effector of *Pseudomonas syringae* remodels host chloroplasts and suppresses defenses. Curr Biol 17:499-508.

Kim, M.G., da Cunha, L., McFall, A.J., Belkhadir, Y., DebRoy, S., Dangl, J.L., and Mackey, D. 2005. Two *Pseudomonas syringae* type III effectors inhibit RIN4-regulated basal defense in *Arabidopsis*. Cell 121:749-759.

Kvitko, B.H., Park, D.H., Velásquez, A.C., Wei, C.-F., Russell, A.B., Martin, G.B., Schneider, D.J., and Collmer, A. 2009. Deletions in the repertoire of

Pseudomonas syringae pv. *tomato* DC3000 type III secretion effector genes reveal functional overlap among effectors. PLoS Pathog 5:e1000388.

Lee, J., Teitzel, G.M., Munkvold, K., del Pozo, O., Martin, G.B., Michelmore, R.W., and Greenberg, J.T. 2012. Type III secretion and effectors shape the survival and growth pattern of *Pseudomonas syringae* on leaf surfaces. Plant Physiol 158:1803-1818.

Lin, N.C., and Martin, G.B. 2005. An *avrPto*/*avrPtoB* mutant of *Pseudomonas syringae* pv. *tomato* DC3000 does not elicit Pto-specific resistance and is less virulent on tomato. Mol Plant-Microbe Interact 18:43-51.

Lindeberg, M., Cunnac, S., and Collmer, A. 2012. *Pseudomonas syringae* type III effector repertoires: last words in endless arguments. Trends Microbiol 20:199-208.

Liyanage, H., Penfold, C., Turner, J., and Bender, C.L. 1995. Sequence, expression and transcriptional analysis of the coronafacate ligase-encoding gene required for coronatine biosynthesis by *Pseudomonas syringae*. Gene 153:17-23.

Melotto, M., Underwood, W., Koczan, J., Nomura, K., and He, S.Y. 2006. Plant stomata function in innate immunity against bacterial invasion. Cell 126:969-980.

Mittal, S., and Davis, K.R. 1995. Role of the phytotoxin coronatine in the infection of *Arabidopsis thaliana* by *Pseudomonas syringae* pv. *tomato*. Mol Plant-Microbe Interact 8:165-171.

Monaghan, J., and Zipfel, C. 2012. Plant pattern recognition receptor complexes at the plasma membrane. Curr Op Plant Biol 15:349-357.

Mukhtar, M.S., Carvunis, A.-R., Dreze, M., Epple, P., Steinbrenner, J., Moore, J., Tasan, M., Galli, M., Hao, T., Nishimura, M.T., Pevzner, S.J., Donovan, S.E., Ghamsari, L., Santhanam, B., Romero, V., Poulin, M.M., Gebreab, F., Gutierrez, B.J., Tam, S., Monachello, D., Boxem, M., Harbort, C.J., McDonald, N., Gai, L., Chen, H., He, Y., Consortium, E.U.E., Vandenhaute, J., Roth, F.P., Hill, D.E., Ecker, J.R., Vidal, M., Beynon, J., Braun, P., and Dangl, J.L. 2011. Independently evolved virulence effectors converge onto hubs in a plant immune system network. Science 333:596-601.

Munkvold, K.R., Martin, M.E., Bronstein, P.A., and Collmer, A. 2008. A survey of the *Pseudomonas syringae* pv. *tomato* DC3000 type III secretion system effector repertoire reveals several effectors that are deleterious when expressed in *Saccharomyces cerevisiae*. Mol Plant-Microbe Interact 21:490-502.

Munkvold, K.R., Russell, A.B., Kvitko, B.H., and Collmer, A. 2009. *Pseudomonas syringae* pv. *tomato* DC3000 type III effector HopAA1-1 functions redundantly with chlorosis-promoting factor PSPTO4723 to produce bacterial speck lesions in host tomato. Mol Plant-Microbe Interact 22:1341-1355.

Nguyen, H.P., Chakravarthy, S., Velasquez, A.C., McLane, H.L., Zeng, L., Nakayashiki, H., Park, D.H., Collmer, A., and Martin, G.B. 2010. Methods to study PAMP-triggered immunity using tomato and *Nicotiana benthamiana*. Mol Plant-Microbe Interact 23:991-999.

Nomura, K., Debroy, S., Lee, Y.H., Pumplin, N., Jones, J., and He, S.Y. 2006. A bacterial virulence protein suppresses host innate immunity to cause plant disease. Science 313:220-223.

Oh, H.S., and Collmer, A. 2005. Basal resistance against bacteria in *Nicotiana benthamiana* leaves is accompanied by reduced vascular staining and suppressed by multiple *Pseudomonas syringae* type III secretion system effector proteins. Plant J 44:348-359.

Rangaswamy, V., Ullrich, M., Jones, W., Mitchell, R., Parry, R., Reynolds, P., and Bender, C.L. 1997. Expression and analysis of coronafacate ligase, a thermoregulated gene required for production of the phytotoxin coronatine in *Pseudomonas syringae*. FEMS Microbiol Lett 154:65-72.

Shan, L., He, P., Li, J., Heese, A., Peck, S.C., Nurnberger, T., Martin, G.B., and Sheen, J. 2008. Bacterial effectors target the common signaling partner BAK1 to disrupt multiple MAMP receptor-signaling complexes and impede plant immunity. Cell Host Microb 4:17-27.

Sreedharan, A., Penaloza-Vazquez, A., Kunkel, B.N., and Bender, C.L. 2006. CorR regulates multiple components of virulence in *Pseudomonas syringae* pv. *tomato* DC3000. Mol Plant-Microbe Interact 19:768-779.

Thines, B., Katsir, L., Melotto, M., Niu, Y., Mandaokar, A., Liu, G., Nomura, K., He, S.Y., Howe, G.A., and Browse, J. 2007. JAZ repressor proteins are targets of the SCF(COI1) complex during jasmonate signalling. Nature 448:661-665.

Vaillancourt, F.H., Yeh, E., Vosburg, D.A., O'Connor, S.E., and Walsh, C.T. 2005. Cryptic chlorination by a non-haem iron enzyme during cyclopropyl amino acid biosynthesis. Nature 436:1191-1194.

Wroblewski, T., Caldwell, K.S., Piskurewicz, U., Cavanaugh, K.A., Xu, H., Kozik, A., Ochoa, O., McHale, L.K., Lahre, K., Jelenska, J., Castillo, J.A., Blumenthal, D.,

Vinatzer, B.A., Greenberg, J.T., and Michelmore, R.W. 2009. Comparative large-scale analysis of interactions between several crop species and the effector repertoires from multiple pathovars of *Pseudomonas* and *Ralstonia*. Plant Physiol 150:1733-1749.

Wu, S., Lu, D., Kabbage, M., Wei, H.L., Swingle, B., Records, A.R., Dickman, M., He, P., and Shan, L. 2011. Bacterial effector HopF2 suppresses *Arabidopsis* innate immunity at the plasma membrane. Mol Plant-Microbe Interact 24:585-593.

Xiang, T., Zong, N., Zou, Y., Wu, Y., Zhang, J., Xing, W., Li, Y., Tang, X., Zhu, L., Chai, J., and Zhou, J.M. 2008. *Pseudomonas syringae* effector AvrPto blocks innate immunity by targeting receptor kinases. Curr Biol 18:74-80.

Yakushiji, S., Ishiga, Y., Inagaki, Y., Toyoda, K., Shiraishi, T., and Ichinose, Y. 2009. Bacterial DNA activates immunity in *Arabidopsis thaliana*. J Gen Plant Pathol 75:227-234.

Yan, J., Zhang, C., Gu, M., Bai, Z., Zhang, W., Qi, T., Cheng, Z., Peng, W., Luo, H., Nan, F., Wang, Z., and Xie, D. 2009. The *Arabidopsis* CORONATINE INSENSITIVE1 protein is a jasmonate receptor. Plant Cell 21:2220-2236.

Zhang, J., Shao, F., Li, Y., Cui, H., Chen, L., Li, H., Zou, Y., Long, C., Lan, L., Chai, J., Chen, S., Tang, X., and Zhou, J.M. 2007. A *Pseudomonas syringae* effector inactivates MAPKs to suppress PAMP-induced immunity in plants. Cell Host Microb 1:175-185.

Zhang, J., Li, W., Xiang, T., Liu, Z., Laluk, K., Ding, X., Zou, Y., Gao, M., Zhang, X., Chen, S., Mengiste, T., Zhang, Y., and Zhou, J.M. 2010. Receptor-like

cytoplasmic kinases integrate signaling from multiple plant immune receptors and are targeted by a *Pseudomonas syringae* effector. Cell Host Microb 7:290-301.

Zheng, X.Y., Spivey, N.W., Zeng, W., Liu, P.P., Fu, Z.Q., Klessig, D.F., He, S.Y., and Dong, X. 2012. Coronatine promotes *Pseudomonas syringae* virulence in plants by activating a signaling cascade that Inhibits salicylic acid accumulation. Cell Host Microb 11:587-596.

Zipfel, C., and Felix, G. 2005. Plants and animals: a different taste for microbes? Curr Op Plant Biol 8:353-360.

Zipfel, C., Kunze, G., Chinchilla, D., Caniard, A., Jones, J.D., Boller, T., and Felix, G. 2006. Perception of the bacterial PAMP EF-Tu by the receptor EFR restricts Agrobacterium-mediated transformation. Cell 125:749-760.

CHAPTER 2

PSEUDOMONAS SYRINGAE PV. *TOMATO* DC3000 CMAL (PSPTO4723), A DUF1330 FAMILY MEMBER, IS NEEDED TO PRODUCE L-*ALLO*-ISOLEUCINE, A PRECURSOR FOR THE PHYTOTOXIN CORONATINE[*]

INTRODUCTION

Pseudomonas syringae pathovar *tomato* DC3000 (*Pto* DC3000) is a model plant pathogen that causes disease in tomato and the model plants *Arabidopsis thaliana* and *Nicotiana benthamiana* (with disease in the latter plant occurring only if the *hopQ1-1* gene encoding an avirulence determinant is deleted) (Wei et al., 2007; Mansfield et al., 2012). *Pto* DC3000 subverts plant immunity primarily through the action of the phytotoxin coronatine (COR) and ca. 30 effectors injected by the type III secretion system (T3SS). COR mimics the plant stress hormone jasmonate isoleucine conjugate (JA-Ile) and has multiple activities that promote bacterial pathogenesis, including opening stomata to permit bacterial entry from the surface of plant leaves and antagonizing salicylic acid-dependent defense signaling (Brooks et al., 2005; Melotto et al., 2006; Zheng et al., 2012). COR-deficient mutants are partially reduced in bacterial growth *in planta* and strongly reduced in disease-associated chlorosis (Mittal and Davis, 1995; Brooks et al., 2004). The T3SS, in contrast, is essential for pathogenesis and is

[*]Worley, J.N., Russell, A.B., Wexler, A.G., Bronstein, P.A., Kvitko, B.H., Krasnoff, S.B., Munkvold, K.R., Swingle, B., Gibson, D.M., and Collmer, A. 2013. *Pseudomonas syringae* pv. *tomato* DC3000 CmaL (PSPTO4723), a DUF1330 family member, is needed to produce L-allo-isoleucine, a precursor for the phytotoxin coronatine. J Bacteriol 195:287-296.

encoded by a cluster of *hrp*/*hrc* genes (hypersensitive response and pathogenesis/conserved) (Tampakaki et al., 2010). Collectively, the type III effectors, designated Hops (Hrp outer proteins), are also essential for virulence (Cunnac et al., 2011). Although individual effectors are dispensable, *Pto* DC3000 polymutants lacking certain combinations of a few effectors can be substantially reduced in virulence (Alfano et al., 2000; Lin and Martin, 2005; Badel et al., 2006; Kvitko et al., 2009). A study of *Pto* DC3000 polymutants lacking effector gene cluster IX (*hopAA1,* PSPTO4719, *hopV1*, *shcV*, *hopAO1*, PSPTO4723, *hopD1'*, *IS*52, *hopG1*) revealed that PSPTO4723 is essential for the spreading chlorosis associated with bacterial speck disease in tomato (Munkvold et al., 2009).

The function of PSPTO4723 was not evident from its genomic context, sequence, or phenotype (Munkvold et al., 2009). The gene lacks upstream *hrp* promoter sequences and coding sequences for N-terminal amino acid patterns associated with type III effectors. It is linked to duplicated sequences of *corP*, a regulator of COR production, and further flanked by type III effector genes. BLAST analysis revealed PSPTO4723 to be a member of the DUF1330 family of proteins of unknown function, which are particularly prevalent in Proteobacteria, including those lacking T3SSs. Taken together, these properties suggest that PSPTO4723 is not a type III effector. However, the possibility that PSPTO4723 is an effector cannot be dismissed because an unknown *Pto* DC3000 factor, additional to COR, can promote chlorosis in infected plants (Mecey et al., 2011). Nevertheless, the most likely role for PSPTO4723 is in the production of COR (Munkvold et al., 2009).

Much is now known about COR synthesis (Gross and Loper, 2009). Several of the ca. 50 pathovars of *P. syringae* appear to be capable of producing COR, including pathovars glycinea, tomato, maculicola, atropurpurea, morsprunorum, aesculi, and oryzae (Bender et al., 1999b; Gross and Loper, 2009; Baltrus et al., 2011). The pathovars differ largely in host specificity, but COR and other phytotoxins variously produced by *P. syringae* strains have no apparent role in host specificity. Moreover, many strains of pathovar tomato do not produce COR (Hwang et al., 2005; Cai et al., 2011). The genetics, biochemistry, and regulation of COR production have been studied extensively in *P. syringae* pv. glycinea PG4180, which encodes COR biosynthesis genes compactly on a 90-kb plasmid (Bender et al., 1999a). In contrast, in *Pto* DC3000 the COR biosynthesis genes are part of a complex pathogenicity island and are more dispersed (Buell et al., 2003). COR production has been increasingly studied in *Pto* DC3000 in recent years, particularly its regulation and effects on bacterium-plant interactions.

COR is formed by amide linkage of two precursors, the polyketide coronafacic acid (CFA) and the ethylcyclopropyl amino acid coronamic acid (CMA) (Bender et al., 1999a; Gross and Loper, 2009). CFA and CMA are independently produced and can be exogenously supplied to restore COR production to corresponding *Pto* DC3000 mutants (Brooks et al., 2004; Sreedharan et al., 2006). The *cfa* and *cma* operons respectively responsible for the production of these moieties are separated by 26 kb in *Pto* DC3000, and it is noteworthy that PSPTO4723 is only 8.8 kb downstream from *cmaU*, the last gene in the *cma* operon (Buell et al., 2003; Filiatrault et al., 2011). The *cma* genes are linked with the *corR*, *corS*, and *corP* genes encoding a modified two-component

regulator system that co-regulates the *cfa* and *cma* operons (Buell et al., 2003; Sreedharan et al., 2006). Current uncertainties about COR production in *Pto* DC3000 suggest that PSPTO4723 could be involved in the regulation of COR production, the ligation of CFA and CMA, or the biosynthesis of L-*allo*-isoleucine, the first step in CMA biosynthesis.

The *Pto* DC3000 response regulator CorR regulates the production of both CFA and CMA (Sreedharan et al., 2006). The *corR* gene is preceded by *hopAQ1*, which encodes an unconfirmed candidate type III effector, and is itself preceded by a HrpL-responsive promoter (Fouts et al., 2002; Schechter et al., 2006; Sreedharan et al., 2006). HrpL is an extracytoplasmic function (ECF) class alternative sigma factor that regulates the expression of the *hrp*/*hrc* T3SS genes and the *hop* genes (Ferreira et al., 2006; Lan et al., 2006). In *Pto* DC3000, HrpL is needed to produce both CFA and CMA, and intriguingly, CorR is needed to fully express HrpL (Sreedharan et al., 2006). The dependence of CorR expression on HrpL extends to factors, such as HrpV, that act upstream of HrpL (Peñaloza-Vázquez et al., 2000), but coordination between the two virulence systems is not fully understood (Sreedharan et al., 2006). Another intriguing aspect of COR regulation is that *cmaE* and *cmaU* show significant antisense expression, which raises the possibility of further regulatory complexities in the production of CMA (Filiatrault et al., 2010).

The ligation of CFA and CMA depends on the product of *cfl* (coronofacate ligase) (Bender et al., 1993), the first gene in the *cfa* operon of both *P. syringae* pv. glycinea PG4180 and *Pto* DC3000 (Wang et al., 2002). Cfl shows similarity to enzymes that activate carboxylic acids by adenylation (Liyanage et al., 1995), which is consistent with

potential ligation of CFA-adenylate to CMA. However, the role of Cfl is unclear because it is also required for CFA production (Rangaswamy et al., 1997; Bender et al., 1999b).

Biosynthesis of L-*allo*-isoleucine, a diastereomer of L-isoleucine, is another possible role for PSPTO4723 in COR production. The biosynthesis of CMA begins with the activation of L-*allo*-isoleucine by the nonribosomal peptide synthetase adenylation domain of CmaA (Couch et al., 2004). The complete CmaA/CmaB/CmaC/CmaD/CmaE/CmaT biosynthetic pathway utilizes cryptic chlorination of thioester-tethered L-*allo*-isoleucine to produce the cyclopropyl ring in CMA. While L-*allo*-isoleucine is strongly preferred over L-isoleucine as a substrate for the CMA pathway (Parry et al., 1991; Couch et al., 2004), the source of L-*allo*-isoleucine is unknown (Gross and Loper, 2009).

Here we use *Pto* DC3000 mutants variously deficient in *hrp*/*hrc* genes, PSPTO4723, and *cfa* and *cma* genes to explore the role of PSPTO4723 using *N. benthamiana* as a test plant because it supports sufficient growth of T3SS-deficient *hrp*/*hrc* mutants for COR production in the absence of type III effectors (Kvitko et al., 2009; Cunnac et al., 2011). We demonstrate that: (i) the contribution of PSPTO4723 to chlorosis in *N. benthamiana* is independent of T3SS export functions, (ii) PSPTO4723 mutants can cross-feed CFA-deficient mutants but not CMA-deficient mutants in mixed-inoculum plant chlorosis assays, (iii) PSPTO4723 mutants are not deficient in the production of the CMA biosynthetic enzymes, (iv) such mutants accumulate CFA rather than COR in culture, and (v) COR production in culture can be restored to PSPTO4723 mutants by exogenous L-*allo*-isoleucine. These and other observations indicate that PSPTO4723

plays a role in the production of L-*allo*-isoleucine. We accordingly will refer to the PSPTO4723 gene as *cmaL* for the remainder of this report.

RESULTS

Pto DC3000 mutants unable to deliver type III effectors can produce COR-dependent chlorosis in *N. benthamiana* leaves.

We had previously noted that the *Pto* DC3000 T3SS-deficient mutant CUCPB5113 produces chlorosis and exhibits significant growth in a *N. benthamiana* leaf model of infection (Kvitko et al., 2009; Cunnac et al., 2011). We inoculated *N. benthamiana* leaves with *Pto* DC3000 derivatives with T3SS mutations differing in their regulatory impact on COR production. CUCPB5113 (Δ*hrcQ*$_B$-*hrcU*) is deficient in T3SS inner membrane export functions and is not expected to alter COR regulation (Badel et al., 2006). CUCPB5112 (Δ*hrcC::nptII*) has a nonpolar mutation resulting from insertion of an *nptII* gene lacking its promoter and terminator, and this may subtly affect COR production through altered expression of *hrpV*, which is downstream of *hrcC* and encodes a negative regulator of *hrpL* expression (Preston et al., 1998; Peñaloza-Vázquez et al., 2000). CUCPB5114 (Δ*hrpK-hrpR*::Cm^R) is lacking the *hrp*/*hrc* gene cluster, including *hrpL*, and therefore is expected to be deficient in COR production (Fouts et al., 2003). *N. benthamiana* leaves were inoculated with test strains at 3 x 10^4 CFU/ml and photographed 6 days later. Chlorosis was observed with CUCPB5113 and CUCPB5112 (Fig. 2.1). Chlorosis elicitation by CUCPB5112 was stronger, and it was COR-dependent, as indicated by its loss in derivative CUCPB5532 (Δ*hrcC* Δ*cfl-cfa9*),

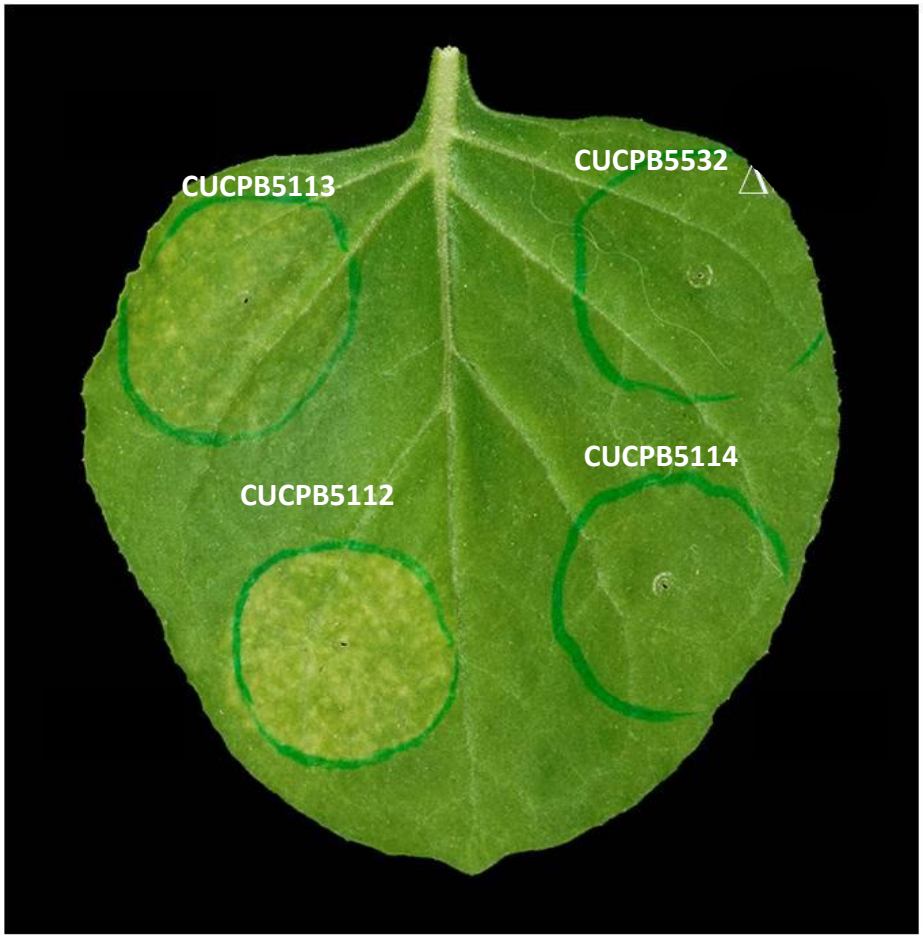

Figure 2.1. Chlorosis produced by various *Pto* DC3000 T3SS$^-$ mutants in *N. benthamiana*. *N. benthamiana* leaves were inoculated by blunt syringe with the indicated strains at 3 x 10^4 CFU/ml and then photographed 6 days later. The strains used were CUCPB5113 (Δ*hrcQ$_B$-hrcU*), CUCPB5112 (Δ*hrcC*), CUCPB5532 (Δ*hrcC* Δ*cfl-cfa9*), and CUCPB5114 (Δ*hrpK-hrpR*). For this and subsequent figures, more detailed genotypes are provided in Table 2.1.

which cannot produce CFL. These observations confirm that *Pto* DC3000 can elicit COR-dependent chlorosis in *N. benthamiana* in the absence of an active T3SS.

Chlorosis elicitation by *Pto* DC3000 in *N. benthamiana* is dependent on CmaL.

The *cmaL* gene is located in effector gene cluster IX in *Pto* DC3000 (Fig. 2.2A) and was previously shown to be important for the chlorosis produced in association with disease in tomato (Munkvold et al., 2009). Here, we introduced Δcluster IX or Δ*cmaL* mutations into a Δ*hopQ1-1* Δ*hrcQ$_B$-hrcU* background in order to determine if CmaL makes the same contribution to chlorosis in *N. benthamiana* that we previously observed in tomato. *N. benthamiana* leaves were inoculated and photographed as described above. Chlorosis was eliminated by deletion of cluster IX or *cmaL* and was fully complemented by expression of *cmaL* alone (Fig. 2.3). These observations that CmaL promotes chlorosis in *N. benthamiana* in a T3SS-independent manner suggest that CmaL is important for COR production.

Mixed inoculum experiments suggest that CmaL has a function in CMA production.

To determine if CmaL functions specifically in the production of CFA or CMA, we constructed a series of *Pto* DC3000 mutants lacking *cmaL*, *cfl-cfa9*, or *cmaD-U* in T3SS-deficient backgrounds (Δ*hrcC* or Δ*hrcQ$_B$-U*). Mutants lacking *cmaL*, *cfl-cfa9*, or *cmaD-U* failed to elicit chlorosis in *N. benthamiana* (Fig. 2.4). However, chlorosis was observed following mixed inoculation with Δ*cfl-cfa9* and Δ*cmaD-U* strains, demonstrating a capacity for cross-feeding between mutants deficient in complementary

Figure 2.2. Arrangement of the COR biosynthesis regions and *cma* operons in *Pto* DC3000 and *P. syringae* pv. glycinea B076. **A**, The relationship of the *cmaL* region to the COR biosynthesis genes of *P. syringae* pv. glycinea B076 (upper diagram), which is most closely related to PG4180 (Qi et al. 2011), and DC3000 (lower diagram). **B**, The DC3000 *cma* genes and relevant portions of the flanking regions (upper diagram), and relationship with the proposed location of *cmaL* as the first gene in an ancestral *cma* operon (lower diagram).

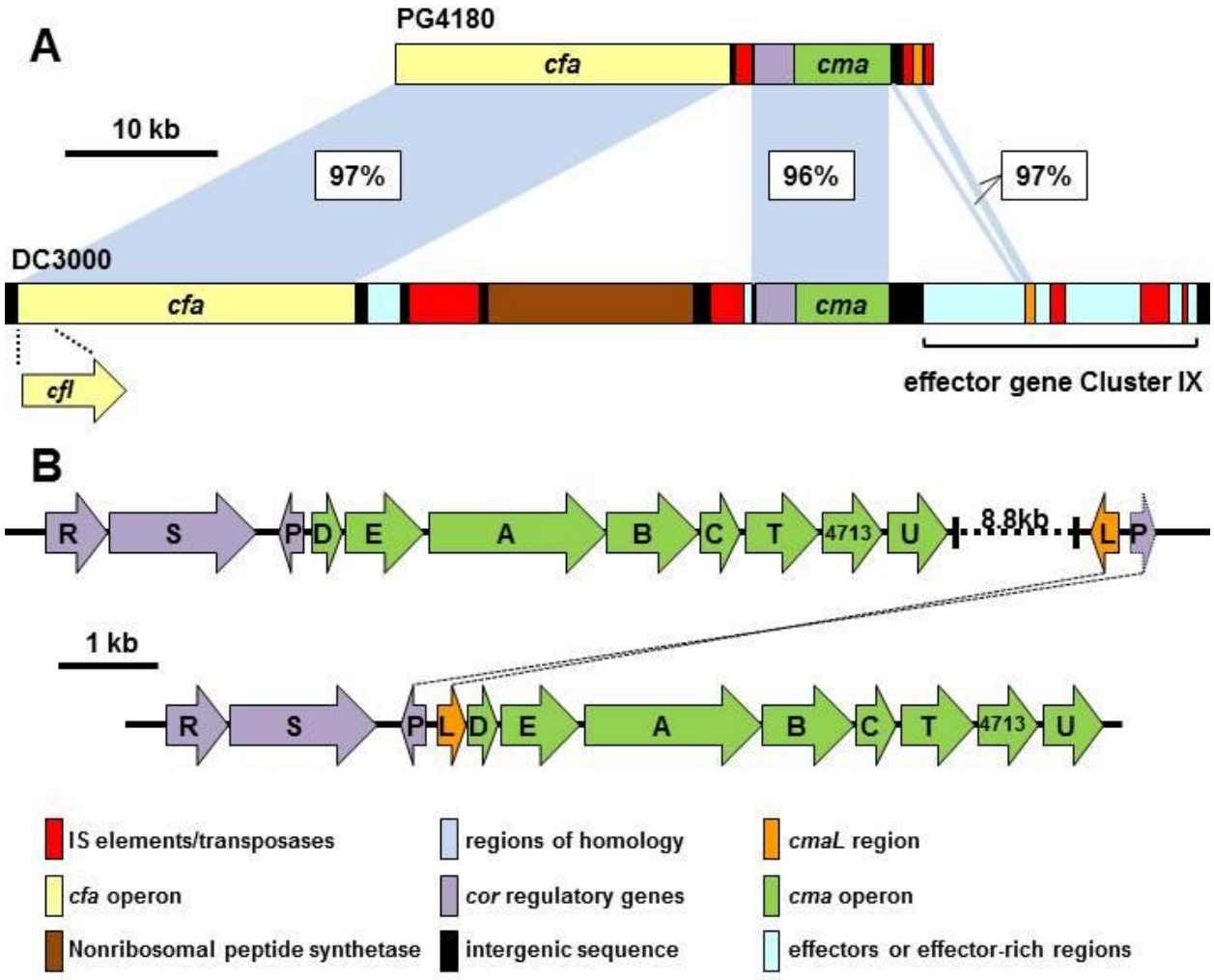
A
PG4180
cfa
cma
10 kb
97%
96%
97%
DC3000
cfa
cma
cfl
effector gene Cluster IX
B
R
S
P
D
E
A
B
C
T
4713
U
8.8kb
L
P
1 kb
R
S
P
L
D
E
A
B
C
T
4713
U
IS elements/transposases
regions of homology
cmaL region
cfa operon
cor regulatory genes
cma operon
Nonribosomal peptide synthetase
intergenic sequence
effectors or effector-rich regions

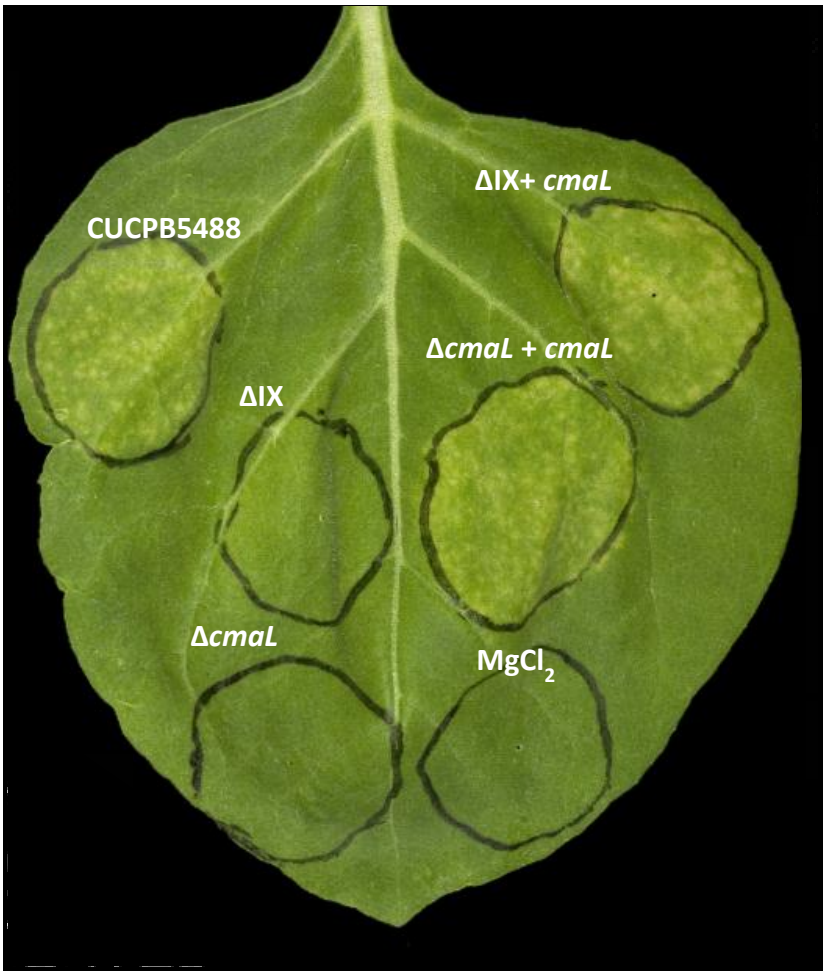

Figure 2.3. c*maL* promotes chlorosis elicitation by *Pto* DC3000 in *N. benthamiana*. Leaves were inoculated and photographed as in Figure 1. Restoration of chlorosis promotion to effector gene cluster IX deletion mutants requires *cmaL*, as shown by the indicated strains, all of which have the Δ*hrcQ*$_B$-*hrcU* Δ*hopQ1-1* background of CUCPB5488 with additional mutations indicated as such: ΔIX, CUCPB5540 (Δ*hrcQ*$_B$-*hrcU* Δ*hopQ1-1* Δ*hopAA1-2-hopG1*); Δ*cmaL*, CUCPB5570 (Δ*hrcQ*$_B$-*hrcU* Δ*hopQ1-1* Δ*cmaL*); ΔIX + *cmaL*, CUCPB5540(pCPP6001); Δ*cmaL* + *cmaL*, CUCPB5570(pCPP6001).

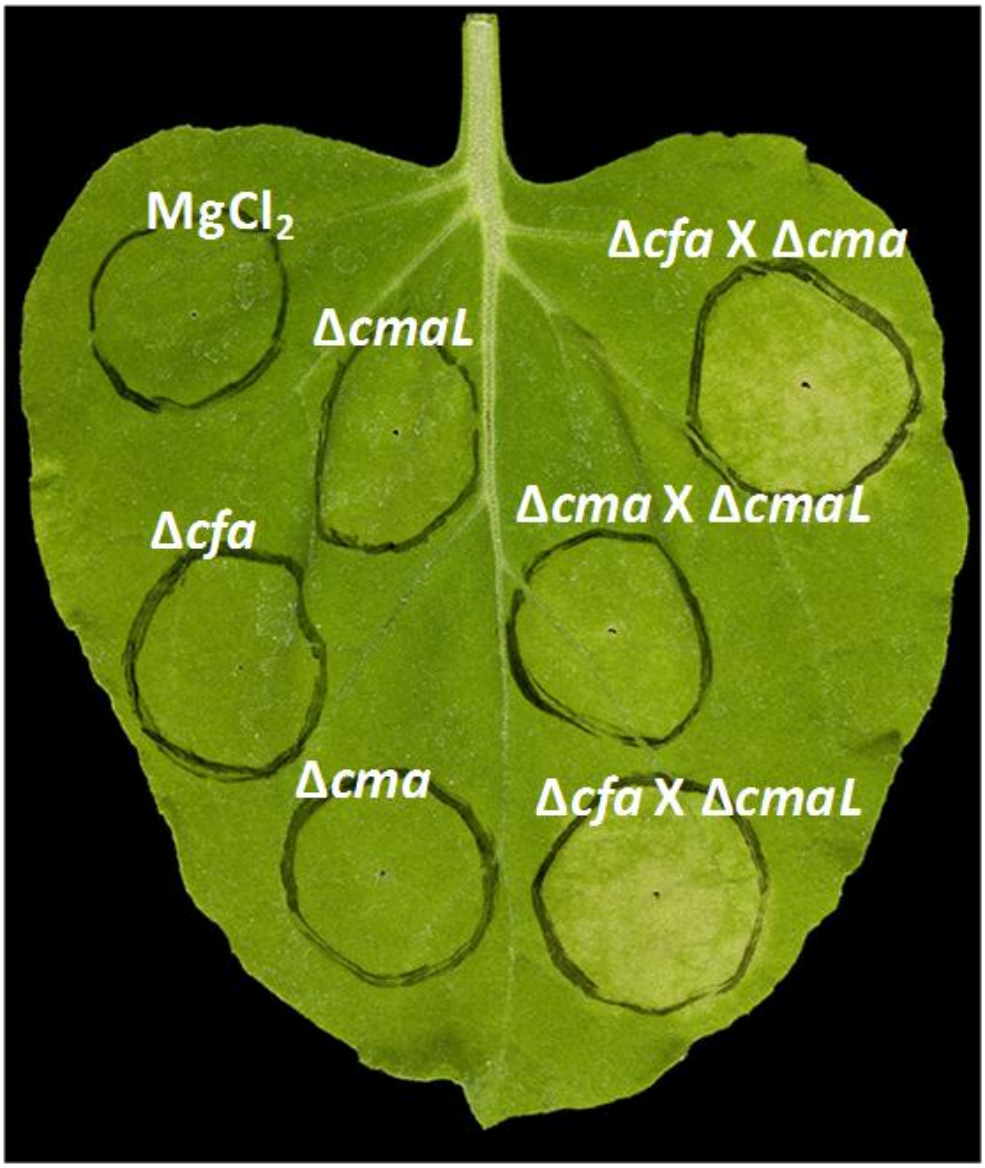

Figure 2.4. Chlorosis induction in *N. benthamiana* leaves following mixed inoculations with *Pto* DC3000 mutants deficient in CFA, CMA, and CmaL, implicate CmaL in CMA production. *N. benthamiana* leaves were inoculated with 3 x 10^6 CFU/ml of each strain and photographed as in Figure 1. The strains are all T3SS$^-$, and the "x" indicates mixed inoculum: Δ*cmaL*, CUCPB5570 (Δ*hrcQ$_B$-hrcU* Δ*hopQ1-1* Δ*cmaL*); Δ*cfa*, CUCPB5532 (Δ*hrcC* Δ*cfl-cfa9*); Δ*cma* , CUCPB5591 (Δ*hrcC* Δ*cmaD-U*); Δ*cfa* x Δ*cma*, mixed CUCPB5532 and CUCPB5591; Δ*cma* x Δ*cmaL*, mixed CUCPB5591 and CUCPB5570; Δ*cfa* x Δ*cmaL*, mixed CUCPB5532 and CUCPB5570.

pathways. Importantly, in mixed inoculations the Δ*cmaL* mutant could restore chlorosis elicitation with Δ*cfl-cfa9* but not with a Δ*cmaD-U* partner. These observations are consistent with previous reports of COR production by cross-complementation of co-cultured mutants deficient in CFA or CMA (Bender et al., 1999a), and importantly, they suggest that the Δ*cmaL* mutant is deficient in CMA production.

CmaL does not regulate *cmaE* transcript levels.

We used differentially inducing culture conditions and qRT-PCR to determine if CmaL has a regulatory role in the expression of *cmaE*, the second gene in the *cmaD-cmaU* operon (Filiatrault et al., 2011). To induce COR production in culture we used mannitol glutamate (MG) minimal medium supplemented with ferric citrate (Bronstein et al., 2008). King's medium B (KB) was used as a rich non-inducing medium (Li et al., 1998). The *Pto* DC3000 mutant CUCPB5392 (Δ*corRSP*::FRTSp^R) was used as a COR$^-$ regulatory mutant control. This mutant was compared with *Pto* DC3000 and CUCPB5563 (Δ*cmaL*::FRTSp^R) for *cmaE* transcript levels. As expected, higher levels of *cmaE* RNA accumulated in wild type *Pto* DC3000 in MG medium compared with KB medium, and this induction was strongly reduced with the Δ*corRSP* mutant (Fig. 2.5A). *cmaE* RNA levels in the inducing medium were very similar in the wild-type and Δ*cmaL* strains. Similarly, the Δ*cmaL* mutation had no effect on the expression of *cfl*, the first gene in the *cfa* operon, and *cmaU*, the last gene in the *cma* operon (Fig. 2.6). Thus, CmaL has no apparent role at the transcriptional level in regulating CMA production.

Figure 2.5. CmaL does not regulate the production of proteins enabling CMA biosynthesis, and it is produced in a *corRSP*-dependent manner. **A**, CmaL does not affect *cma* operon transcript levels. *cmaE* transcript levels were assayed by qRT-PCR after 4 h of bacterial growth in MG inducing media and KB non-inducing media. Levels were taken as abundance relative to levels of the *gap1* normalizing transcripts, and then all values were compared to wild-type under inducing conditions. Results are the mean and standard error from 4 replicates. The indicated strains are WT, *Pto* DC3000; Δ*corRSP*, CUCPB5392; Δ*cmaL*, CUCPB5563. **B**, Deletion of *cmaL* does not impact induced levels of accumulation of the six known CMA biosynthetic proteins that are encoded in the *cma* operon. A gene fusion encoding a C-terminal HA tag was introduced by recombination into *cmaD*, *cmaE*, *cmaA*, *cmaB*, *cmcC*, and *cmaT* in the genomes of strains indicated as WT (*Pto* DC3000) or Δ*cmaL* (CUCPB5563). Bacteria were grown 24 h in MG medium, and then levels of HA-tagged protein were assayed by immunoblotting. **C**, CmaL production is regulated in a *corRSP*-dependent manner. Plasmid pCPP6001 carrying *cmaL* with 200 bp of upstream DNA and encoding a C-terminal HA tag fusion was electrotransformed into various bacteria and assayed for accumulation of HA-tagged proteins under MG inducing and KB non-inducing conditions as described for the panel above. Indicated strains: WT, *Pto* DC3000; Δ*corRSP*, CUCPB5392; Δ*hrpL*, UNL134-1.

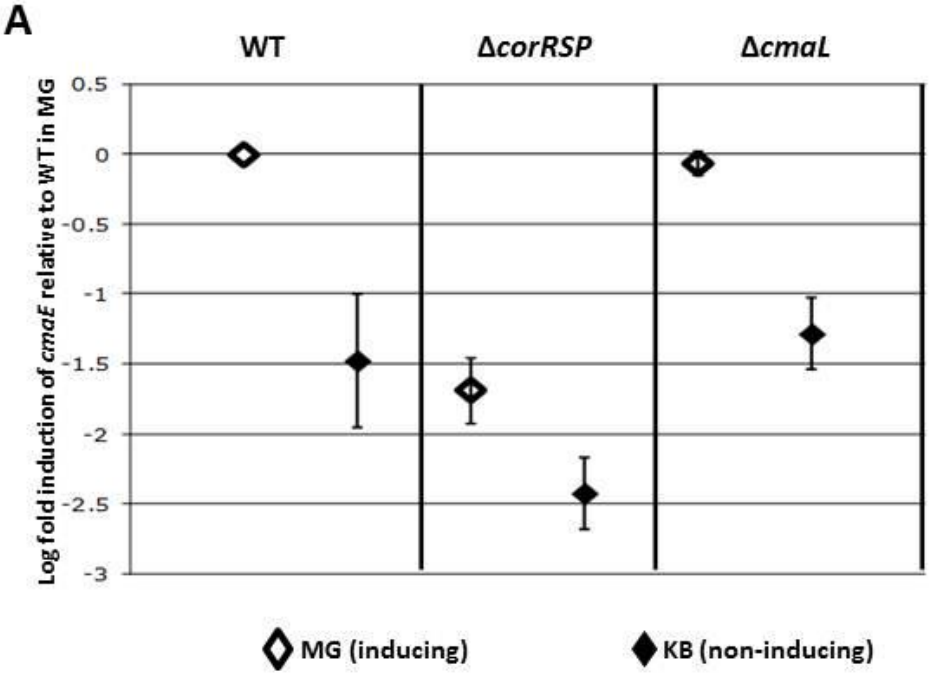
A
WT
ΔcorRSP
ΔcmaL
Log fold induction of cmaE relative to WT in MG
0.5
0
-0.5
-1
-1.5
-2
-2.5
-3
MG (inducing)
KB (non-inducing)

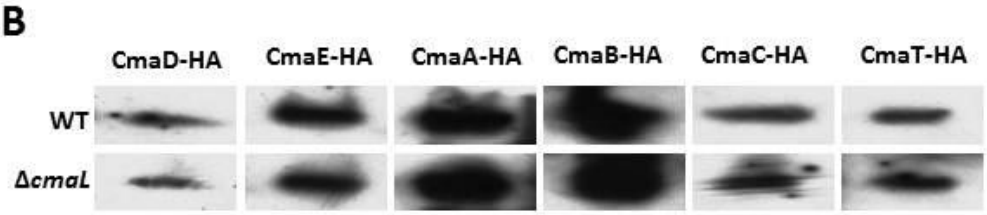
B
CmaD-HA
CmaE-HA
CmaA-HA
CmaB-HA
CmaC-HA
CmaT-HA
WT
ΔcmaL

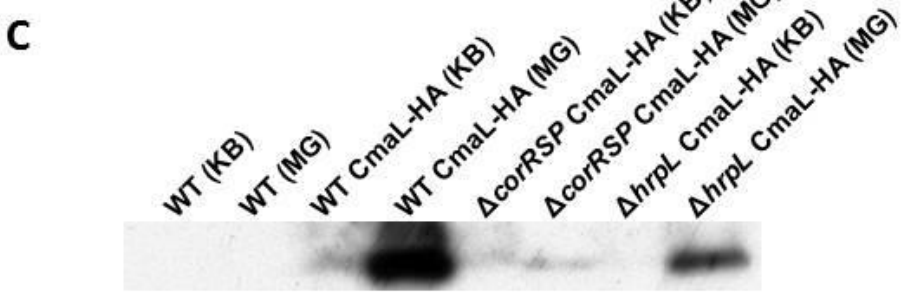
C
WT (KB)
WT (MG)
WT CmaL-HA (KB)
WT CmaL-HA (MG)
ΔcorRSP CmaL-HA (KB)
ΔcorRSP CmaL-HA (MG)
ΔhrpL CmaL-HA (KB)
ΔhrpL CmaL-HA (MG)

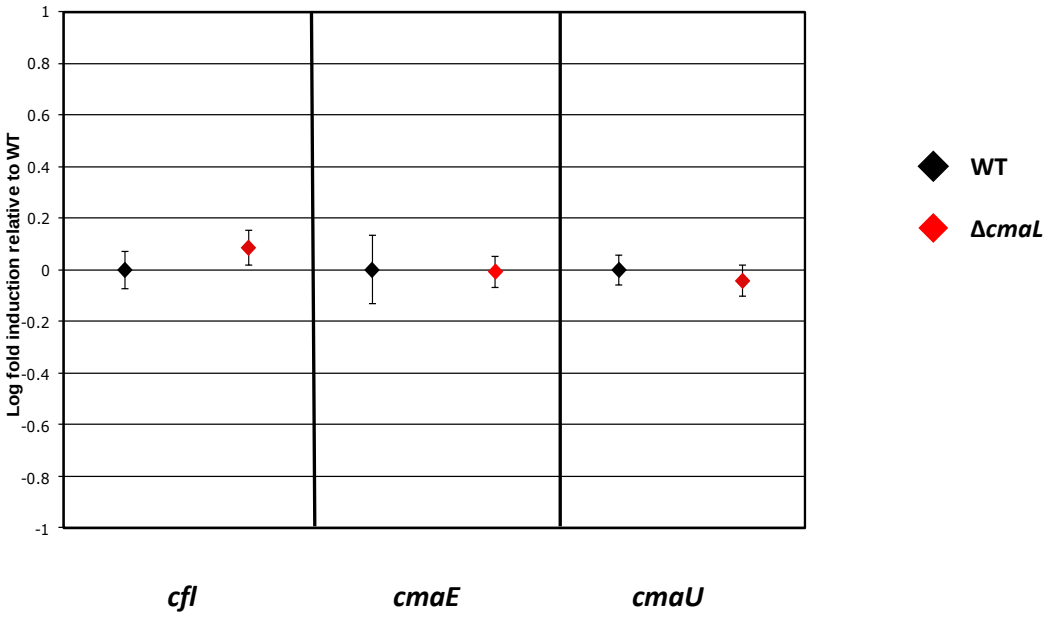

Figure 2.6. qRT-PCR reveals no significant difference in transcript abundance for *cfl* (first gene in the *cfa* operon) or *cmaU* (last gene in the *cma* operon) in wild-type and Δ*cmaL* Pto DC3000 strains under inducing conditions. Transcript levels were standardized to *gap1* before comparison, and error bars represent a standard deviation calculated from three replicates. Transcript levels were calculated for *cfl* with primers jnw123/jnw124, *cmaE* with jnw125/jnw126, and *cmaU* with jnw127/128. cDNA was prepared from MG medium-induced cultures as described in Materials and Methods.

CmaL does not regulate the accumulation of CMA biosynthesis proteins.

While CmaL does not regulate the production of the *cma* transcript, it could still regulate CMA biosynthesis proteins post-transcriptionally. To address this possibility, we constructed C-terminal HA epitope fusions to each of the genes in the *cma* operon (Fig. 2.5B). Production of proteins was then monitored by immunoblotting of cell lysates with anti-HA antibodies under inducing conditions. No product was detected for PSPTO4713, a protein with no known function in CMA biosynthesis, or for CmaU, another protein of unknown function, but predicted to be an exporter. The remaining six proteins, CmaD, CmaE, CmaA, CmaB, CmaC, and CmaT, produced detectable fusion proteins. Although the levels of the different HA-tagged Cma proteins varied, despite equal loading of bacterial protein, all six of the CMA proteins were clearly produced in Δ*cmaL* strains (Fig. 2.5B). Thus, CmaL has no apparent role at any level in regulating the expression of proteins known to be involved in the conversion of L-*allo*-isoleucine to CMA.

CmaL is produced in MG inducing medium in a CorRSP-dependent manner.

As CmaL does not appear to regulate CMA production, we considered the possibility of a role for CmaL in the biosynthesis of CMA. If CmaL is essential for production of CMA, it should be co-regulated with the known CMA biosynthesis proteins. We accordingly constructed a gene fusion producing a C-terminal HA tag from plasmid-borne, natively-expressed *cmaL* and examined CmaL-HA production under diagnostic conditions. Immunoblotting of cell lysates with anti-HA antibodies revealed that CmaL-HA was only produced in MG inducing medium (Fig. 2.5C). CmaL-HA production was

abolished in the Δ*corRSP* mutant and strongly reduced in the Δ*hrpL* mutant. Thus, the regulation of CmaL is similar to the known CMA biosynthetic enzymes.

Pto DC3000 Δ*cmaL* and Δ*cmaD-U* mutants similarly accumulate CFA rather than COR in culture.

The mixed inoculum plant chlorosis assays presented above suggested a role for CmaL in the production of CMA but not CFA. To directly test this we analyzed *Pto* DC3000 wild-type and Δ*cmaL* strains for their production of COR and CFA based on HPLC analysis of fluids from MG inducing medium cultures. COR and CFA were identified by matching retention times of standards with peaks in extracts. CMA accumulation was not measured because of technical considerations. Wild-type cultures produced COR as a major component and CFA as a minor component of the fermentation broth extract (Fig. 2.7). In contrast, the Δ*cmaL* strain produced only CFA. The analysis of CFA and COR was extended to include the Δ*cmaD-U* and Δ*cfl-cfa9* mutants and peak quantification to reveal the relative production of CFA and COR by various strains. As expected, the Δ*cfl-cfa9* mutant produced no CFA, the wild-type strain produced more COR than CFA, and the Δ*cmaL* and Δ*cmaD-U* mutants produced no COR (Fig. 2.8). In repeated testing the latter two mutants produced similar levels of CFA. Thus, the Δ*cmaL* and Δ*cmaD-U* mutants have deficiencies in COR production that are indistinguishable and consistent with a failure to produce CMA.

Exogenous L-*allo*-isoleucine restores COR production to the Δ*cmaL* mutant.

Given that the mechanism by which L-*allo*-isoleucine is produced has not been

Figure 2.7. HPLC elution profiles of sterile fluids of wild type *Pto* DC3000 and Δ*cmaL* CUCPB5563 strains grown in MG inducing medium reveal that the Δ*cmaL* mutant accumulates CFA but no COR. Culture fluids were filter-sterilized, extracted with ethyl acetate, and analyzed by HPLC.

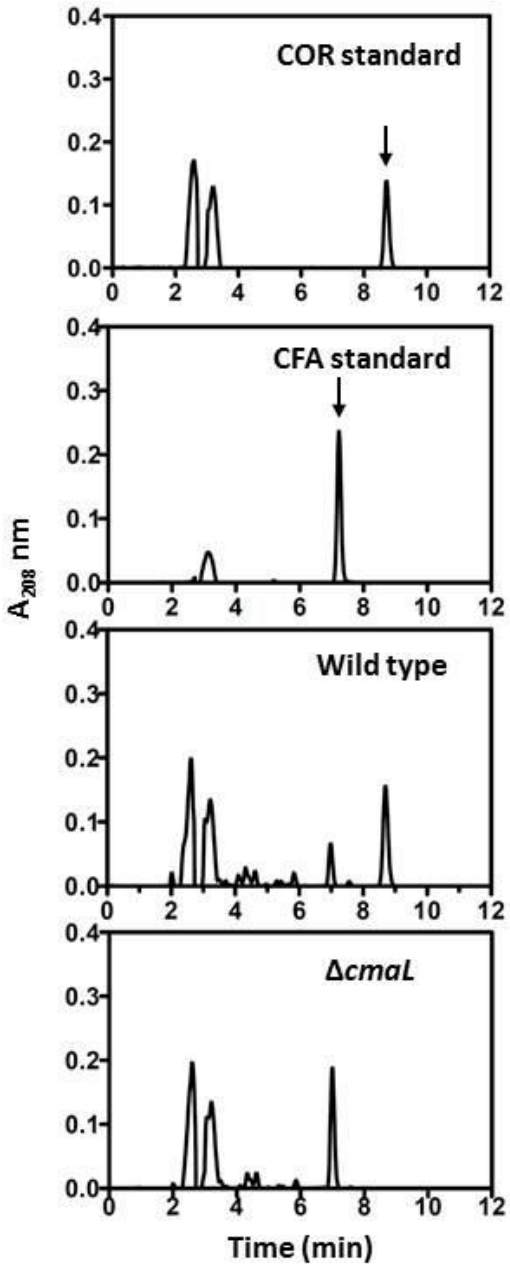
COR standard
CFA standard
Wild type
ΔcmaL
A208 nm
Time (min)

Figure 2.8. Relative levels of CFA and COR produced by *Pto* DC3000 mutants in MG inducing media reveal that Δ*cma* and Δ*cmaL* mutants similarly accumulate CFA. Concentrations of COR (RT ~ 9.5 min) were estimated using a 5-point standard curve, and CFA (RT ~ 7.5 min) was estimated as COR peak area equivalents. Indicated strains: Δ*cfa*, CUCPB5532 (Δ*hrcC* Δ*cfl-cfa9*); Δ*cma*, CUCPB5593 (Δ*cmaD-U*); Δ*cmaL*, CUCPB5563; WT, *Pto* DC3000.

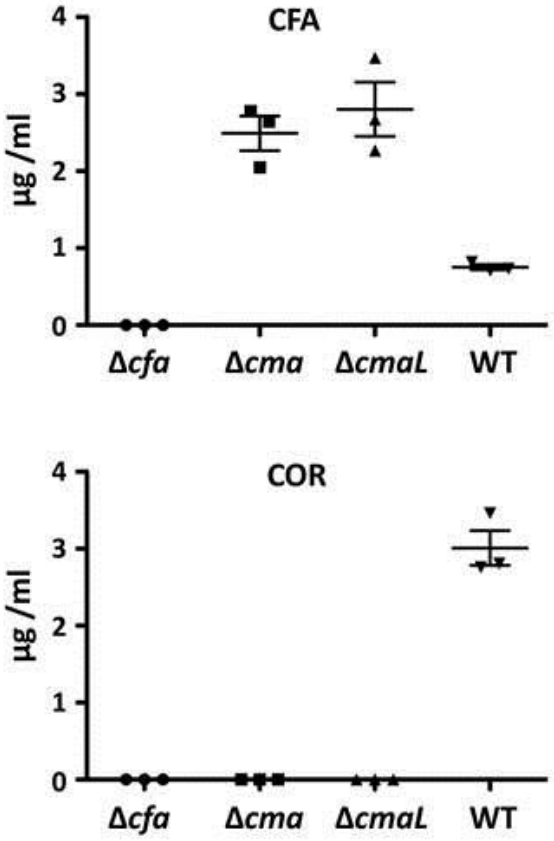
CFA
µg /ml
4
3
2
1
0
Δcfa
Δcma
ΔcmaL
WT
COR
µg /ml
4
3
2
1
0
Δcfa
Δcma
ΔcmaL
WT

described in *Pto* DC3000 and other COR-producing *P. syringae* strains, we postulated that CmaL may be required for this function and that Δ*cmaL* mutants fail to produce CMA and COR because of an L-*allo*-isoleucine deficiency. Others have previously shown that L-isoleucine is required for CMA production (Parry et al., 1991; Mitchell et al., 1994; Parry et al., 1994), through its conversion to L-*allo*-isoleucine using radiolabeled precursors (Vaillancourt et al., 2005). To test this hypothesis, we provided L-*allo*-isoleucine to the Δ*cmaL* mutant growing in MG inducing medium and analyzed culture fluids by HPLC. The supplemented Δ*cmaL* mutant produced COR, indicating that CmaL is needed for *Pto* DC3000 to produce L-*allo*-isoleucine (Fig. 2.9). We also used HPLC to determine the effects on COR production of providing the Δ*cmaL* mutant with L-isoleucine or providing the wild-type strain with either L-isoleucine or L-*allo*-isoleucine. Exogenous L-isoleucine did not enable COR production by the Δ*cmaL* mutant and did not increase COR production by the wild-type strain, whereas providing L-*allo*-isoleucine did increase COR production by the wild-type (Fig. 2.10). It should also be noted that Tn*7*-mediated integration of *cmaL* with 500 bp of upstream DNA into the genome also restored the ability to make COR to the Δ*cmaL* mutant (Fig. 2.10). Thus, COR production by a Δ*cmaL* mutant specifically requires complementation with *cmaL* or exogenous L-*allo*-isoleucine.

DISCUSSION

Study of the biosynthesis of COR has yielded several surprises over the years. These include formation of COR by ligation of two independently produced moieties

Figure 2.9. Exogenous supply of L-*allo*-isoleucine to a *Pto* DC3000 Δ*cmaL* mutant restores COR production in MG inducing media. Bacteria growing in MG inducing medium for 24 h were supplemented with 50 µg/ml L-*allo*-isoleucine and then 2 days later, culture fluids were harvested by centrifugation, filter-sterilized, extracted with ethyl acetate, and analyzed by HPLC as in Figure 6. Indicated strains: Δ*cma*, CUCPB5593 (Δ*cmaD-U*); Δ*cmaL*, CUCPB5563; WT, *Pto* DC3000.

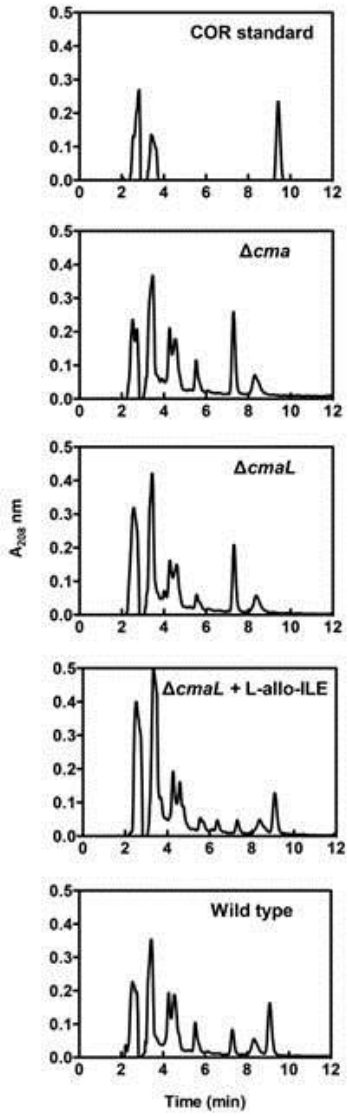
COR standard
Δcma
ΔcmaL
ΔcmaL + L-allo-ILE
Wild type
A208 nm
Time (min)

Figure 2.10. Restoration of COR production by Δ*cmaL* mutants in MG inducing medium is achieved by supplying exogenous L-*allo*-isoleucine and Tn7 based genomic integration of the genomic region containing *cmaL*, but not by L-isoleucine. **A, and B**, The blue and red lines are at the peak elution times for CFA and COR, respectively. **C**, Wild-type cultures produce CFA and COR. **D, E**, The addition of L-*allo*-isoleucine, but not L-isoleucine, causes both an increase in COR accumulation and a decrease in CFA accumulation. **F, G, and H**, The restoration of COR production by a Δ*cmaL* mutant by culture supplementation is achieved only with L-*allo*-isoleucine and not L-isoleucine. **I and J**, Integration of an ~1kb genomic fragment containing *cmaL* by Tn7 mutagenesis restores COR accumulation in MG inducing media, but an empty-vector does not.

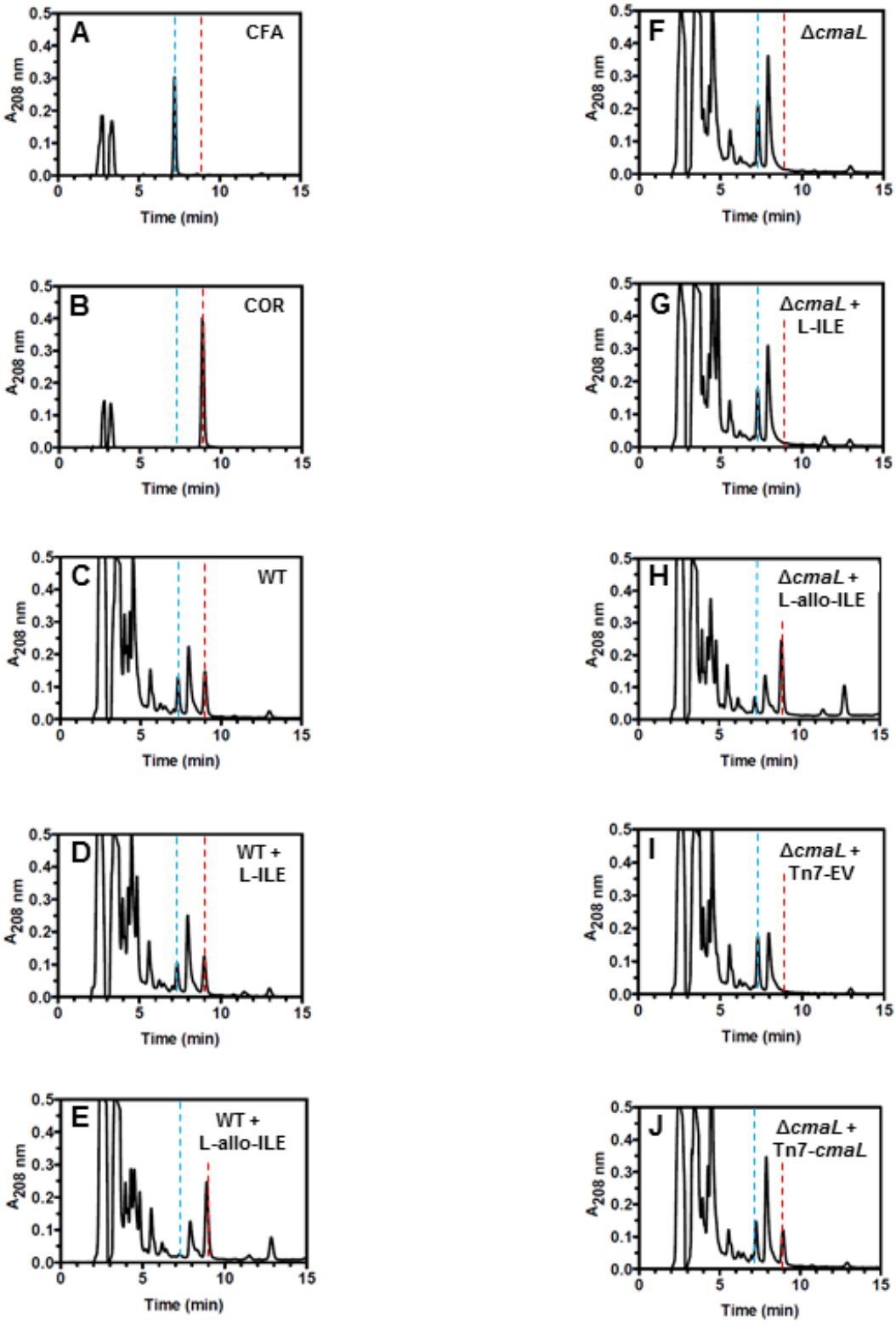
A
CFA
B
COR
C
WT
D
WT +
L-ILE
E
WT +
L-allo-ILE
F
ΔcmaL
G
ΔcmaL +
L-ILE
H
ΔcmaL +
L-allo-ILE
I
ΔcmaL +
Tn7-EV
J
ΔcmaL +
Tn7-cmaL
A208 nm
Time (min)

(CFA and CMA), the synthesis of CMA by cryptic halogenation using a new type of non-heme-Fe^{2+}-ketoglutarate-dependent halogenase, and the incorporation of an uncommon amino acid in CMA biosynthesis - L-*allo*-isoleucine, a stereoisomer of L-isoleucine at the beta carbon (Bender et al., 1999b; Couch et al., 2004; Vaillancourt et al., 2005; Gross and Loper, 2009). We have found evidence that CmaL a DUF1330 protein encoded within a cluster of type III effector genes in *Pto* DC3000, is needed for the production of L-*allo*-isoleucine, a molecule for which no enzymatic biosynthesis mechanisms are known. This appears to be the first DUF1330 protein implicated in a specific biochemical function, and it suggests that proteins in this family may facilitate isomerizations. We will discuss below the evidence that CmaL directs L-*allo*-isoleucine production, properties of the DUF1330 protein family, and the significance of *cmaL* being located among type III effector genes rather than with the known CMA biosynthesis genes. Figure 2.11 illustrates the proposed role for CmaL in Coronatine biosynthesis.

Several lines of evidence suggest that CmaL is involved in L-*allo*-isoleucine biosynthesis. (i) Although encoded among type III effector genes, CmaL promotes chlorosis independently of the T3SS. (ii) Experiments based on defined mutations in CFA and CMA pathway genes establish that CmaL is specifically needed for the production of CMA. (iii) CmaL makes no contribution to regulation of the known *cma* genes but rather is co-regulated with them by CorR, which argues against a regulatory role. (iv) A plasmid-borne region in COR-producing *P. syringae* pv. glycinea PG4180, which carries the *cma* operon and an essential downstream flank ostensibly containing *cmaL,* is sufficient to confer CMA production to a non-producing strain of *P. syringae*

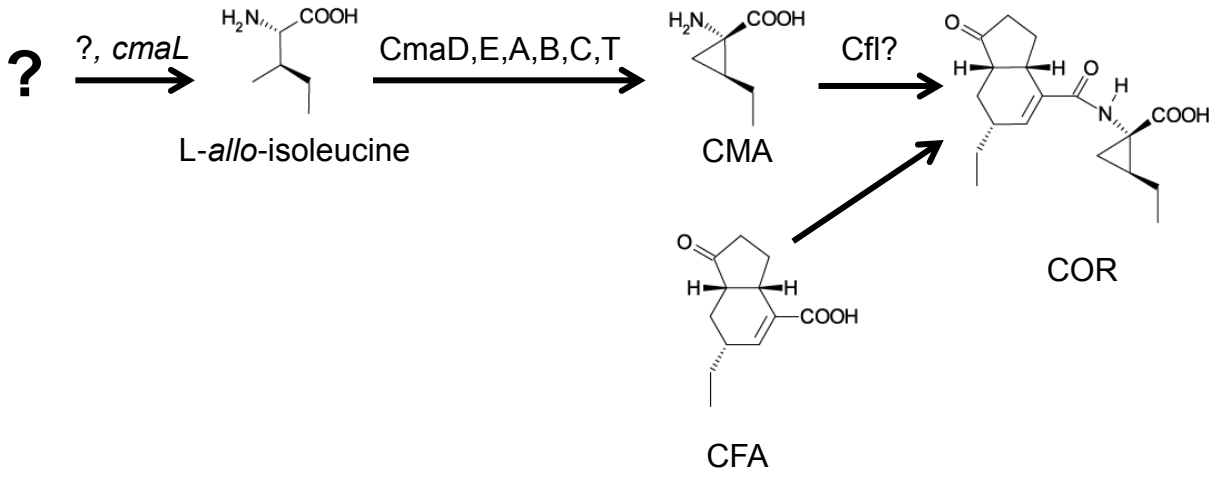

Figure 2.11. A plausible role of *cmaL* in coronatine biosynthesis. *cmaL* contributes to coronatine formation, directly or indirectly, through the biosynthesis of L-*allo*-isoleucine from an unknown precursor. *cmaL* may not be the only gene involved in the process, but is the only one known to be essential. The proteins encoded in the *cma* operon then convert L-*allo*-isoleucine to coronamic acid (CMA). An amide bond is then formed between CMA and coronafacic acid (CFA), putatively by Cfl, to produce coronatine (COR).

(Ullrich et al., 1995), suggesting that CmaL is sufficient to produce L-*allo*-isoleucine. (v) The proteins of known function in the dimeric alpha/beta-barrel superfamily of proteins (Pfam CL0032), to which DUF1330 proteins belong, are primarily enzymes with small-molecule substrates. (vi) Among 19 sequenced strains of *P. syringae* recently analyzed for their virulence genotype (Baltrus et al., 2011), *cmaL* was found only in COR-producing strains. (vii) Most tellingly, supplying L-*allo*-isoleucine to a *Pto* DC3000 Δ*cmaL* mutant restores COR production.

L-*allo*-isoleucine is an uncommon metabolite whose own accumulation has been studied largely in the context of maple syrup urine disease in humans, a metabolic disorder leading to the buildup of branched-chain amino acids (Mamer and Reimer, 1992). Two possible reactions have been proposed for the formation of the isomer L-*allo*-isoleucine (Schadewaldt et al., 2000): first, conversion of L-isoleucine to L-*allo*-isoleucine by a ketimine-enamine tautomerization and second, deamination of L-isoleucine to 2-keto-(3S) methylvaleric acid followed by keto-enol tautomerization and subsequent reamination. The former reaction was further proposed to involve activation of L-isoleucine by a pyridoxal 5'-phosphate-dependent enzyme followed by nonenzymatic tautomerization, as proposed for L-*allo*-isoleucine formation in maple syrup urine disease (Mamer and Reimer, 1992). Radiolabelled studies indicate that the second scheme is the primary course of L-*allo*-isoleucine in humans (Schadewaldt et al., 2000). A particularly relevant example of the tautomerization reaction is the macrophage migration inhibitory factor MIF, a 115 amino-acid phenyl pyruvate tautomerase whose mechanism involves a single proline as the active acid and base in tautomerization (Stamps et al., 2000). Although it is not known how this reaction is

occurring in *P. syringae*, our data indicate that CmaL is involved in production of L-alloisoleucine through an as yet unknown mechanism, as an essential step required for CMA and COR production.

The DUF1330 family is typical of DUF families in being less widely distributed than functionally annotated families (Punta et al., 2012). Distributed mostly in Proteobacteria and Actinobacteria, nearly one thousand proteins with this domain have been identified. The members of this domain family are not associated with pathogenesis, a particular environment or genetic context; without this or other corroborating information there is little basis to prefer one molecular mechanism over another, so a general function for the DUF1330 domain remains undefined.

Genes directing COR biosynthesis and production of the T3SS and effector proteins are part of the flexible genome in *P. syringae*, which is notable for its high mobile genetic element content and variability among *P. syringae* strains (Lindeberg et al., 2008). The linkage of *cmaL* with duplicated and variously fragmented sequences of *corP* in all COR-producing strains of *P. syringae* where relevant sequence data are available may provide a clue to the evolutionary origins of this arrangement. One scenario is that disruption of an ancestral *cma* operon resulted in *cmaL* being separated from the rest of the CMA biosynthesis genes (Fig. 2.2B). Evidence for this hypothesis could come from finding the proposed ancestral arrangement in a COR^+ *P. syringae* strain that has yet to be sequenced. A related question is whether there is an advantage to expressing *cmaL* and the *cmaD-U* operon independently that favors maintenance of this arrangement. Most importantly, future investigations can now focus on CmaL in exploring the mechanism of L-*allo*-isoleucine production.

MATERIALS AND METHODS

Bacterial strains and plasmids.

Bacterial strains and plasmids are listed in Table 2.1. *P. syringae* strains were cultivated on King's B (KB) at 30°C (King et al., 1954). *Escherichia coli* strains were cultivated on Luria-Burtani media (Hanahan, 1985). Antibiotics were used at the following concentrations in µg/ml: rifampicin 50; spectinomycin 50; chloramphenicol 20; gentamicin 10 for plasmids, 5 for genomic integrants; kanamycin 50.

Plasmid construction tools.

Plasmids were created as described below and transformed into *E. coli* DH5α or Top10 by standard electroporation or heat-shock procedures, respectively (Sambrook and Russel, 2001). Primers were purchased from Integrated DNA Technology. PCR reactions were performed using ExTaq DNA polymerase and PrimeSTAR HS DNA Polymerase (Takara Bio Inc.). Restriction enzymes and DNA ligation procedure enzymes were purchased from New England Biolabs. Construct sequences were verified through sequencing performed by the Cornell University Life Sciences Core Laboratories Center.

Techniques for transformations and genomic modifications.

Suicide vectors for gene deletions or single-crossover insertions were mobilized into DC3000 backgrounds through conjugation mediated either by biparental mating with the plasmid transformed into *E.coli* S17-1 or by utilizing pRK2013 in triparental mating

Table 2.1. Bacterial strains and plasmids used in this study

Designation	Genotype and relevant features	Source
Escherichia coli		
DH5α	F$^-$ *endA1 glnV44 thi-1 recA1 relA1 gyrA96 deoR nupG* Φ80*lacZ*ΔM15 Δ*(lacZYA-argF)U169, hsdR17*(r_K^- m_K^+), λ–	Invitrogen
DB3.1	F- *gyrA462 endA1 glnV44* Δ(sr1-recA) *mcrB mrr hsdS20*(r_B^-, m_B^-) *ara14 galK2 lacY1 proA2 rpsL20*(Sm^R) *xyl5* Δl*eu mtl1*	Invitrogen
DB3.1 λ*pir*	F- *gyrA462 endA1 glnV44* Δ(sr1-recA) *mcrB mrr hsdS20*(r_B^-, m_B^-) *ara14 galK2 lacY1 proA2 rpsL20*(Sm^R) *xyl5* Δl*eu mtl1* λpir-lysogen	(House et al., 2004)
S17-1	*recA pro hsdR* RP4-2-Tc::Mu-Km::Tn*7*	(Simon et al., 1983)
Top10	F- *mcrA* Δ(mrr-hsdRMS-mcrBC) φ80*lacZ*Δ*M15* Δ*lacX74 nupG recA1 araD139* Δ(*ara-leu*)7697 *galE15 galK16 rpsL*(Str^R) *endA1* λ^-	Invitrogen
Pseudomonas syringae pv. tomato		
DC3000	Rif^R	(Buell et al., 2003)
UNL134-1	Δ*hrpL*::ΩSp, Sp^R	(Ferreira et al., 2006)
CUCPB5112	Δ*hrcC*::*nptII* (*Bgl*II-*Sal*I fragment derived from Tn*5* lacking *nptII* promoter and terminator), Km^R on minimal media	(Peñaloza-Vázquez et al., 2000)
CUCPB5113	Δ$hrcQ_B$-*U*::ΩSp, Sp^R	(Badel et al., 2006)
CUCPB5114	Δ*hrpK-hrpS*::Cm^R, Gm^R	(Fouts et al., 2003)
CUCPB5392	Δ*corRSP*::FRTSp^R, Sp^R/Sm^R	This study
CUCPB5488	Δ$hrcQ_B$-*U*::ΩSp Δ*hopQ1-1*, Sp^R	This study
CUCPB5529	Δ*hopQ1-1* Δ*hopAA1-2-hopG1*::FRT	(Kvitko et al., 2009)
CUCPB5532	Δ*hrcC*::*nptII* Δ*cfl-cfa9*	This study
CUCPB5540	Δ*hopQ1-1* Δ*hopAA1-2-hopG1*::FRT Δ$hrcQ_B$-*U*::ΩSp, Sp^R	This study
CUCPB5563	Δ*cmaL*::FRTSp^R, Sp^R/Sm^R	(Munkvold et al., 2009)
CUCPB5570	Δ*hopQ1-1* Δ$hrcQ_B$-*U*::ΩSp Δ*cmaL*::FRTSp^R, Sp^R/Sm^R	This study

Table 2.1. Continued

CUCPB5591	Δ*hrcC*::*nptII* Δ*cmaD-U*::FRTSp^R, Sp^R/Sm^R	This study
CUCPB5593	DC3000 Δ*cmaD-U*::FRTSp^R, Sp^R/Sm^R	This study
CUCPB6053	*cmaD*::pCPP6338, operon interrupted	This study
CUCPB6054	*cmaE*::pCPP6339, operon interrupted	This study
CUCPB6055	*cmaA*::pCPP6340, operon interrupted	This study
CUCPB6056	*cmaB*::pCPP6341, operon interrupted	This study
CUCPB6057	*cmaC*::pCPP6342, operon interrupted	This study
CUCPB6058	*cmaT*::pCPP6343, operon interrupted	This study
CUCPB6059	PSPTO4713::pCPP6344, operon interrupted	This study
CUCPB6060	*cmaU*::pCPP6345	This study
CUCPB6061	Δ*cmaL cmaD*::pCPP6338, operon interrupted	This study
CUCPB6062	Δ*cmaL cmaE*::pCPP6339, operon interrupted	This study
CUCPB6063	Δ*cmaL cmaA*::pCPP6340, operon interrupted	This study
CUCPB6064	Δ*cmaL cmaB*::pCPP6341, operon interrupted	This study
CUCPB6065	Δ*cmaL cmaC*::pCPP6342, operon interrupted	This study
CUCPB6066	Δ*cmaL cmaT*::pCPP6343, operon interrupted	This study
CUCPB6067	Δ*cmaL* PSPTO4713::pCPP6344, operon interrupted	This study
CUCPB6068	Δ*cmaL cmaU*::pCPP6345	This study
CUCPB6076	CUCPB5563::Tn7-TcR	This study
CUCPB6084	CUCPB5563::Tn7-TcR-cmaL	This study
Plasmids		
pENTR11	Vector for basic cloning, Gateway attL1 and attL2 sites	Invitrogen
pK18mob	Small mobilizable suicide vector, Km^R	(Schafer et al., 1994)
pK18mobsacB	Small mobilizable suicide vector, Km^R, sucrose-sensitive (*sacB*)	(Schafer et al., 1994)
pKR36	pENTR/D-TOPO::Δ*corRSP* deletion construct, Km^R	This study
pRK2013	Helper plasmid for conjugation, Km^R	(Figurski and Helinski, 1979)
pCPP5209	Contains FRT flanked Gm^R cassette, Gm^R	(9)
pCPP5215	pRK415 with a Gateway cassette, Tc^R, Cm^R	(Kvitko et al., 2007)

Table 2.1 Continued.

pCPP5242	pKD4 FRT cassette plasmid with *nptII* replaced by *aadA1*, Sp^R/Sm^R	(9)
pCPP5265	pENTR/SD/D-TOPO::Δ*corRSP*::cFRTSp^R, Sp^R/Sm^R	This study
pCPP5266	pCPP5215:: Δ*corRSP*::cFRTSp^R, Sp^R/Sm^R	This study
pCPP5296	pBBR1MCS with Gateway cassette reading frame B and C-terminal HA-tag, lacks a promoter driving gateway cassette expression, Cm^R, Gm^R	(Munkvold et al., 2009)
pCPP5608	*hopQ1-1* deletion construct cloned into pK18mobsacB, Km^R	(Wei et al., 2007)
pCPP5729	pK18mobsacBGm^R::Δ*hopQ1-1*	This study
pCPP5735	pK18mobsacB::Δ*cfl-cfa9*, Km^R	This study
pCPP5762	pK18mobsacB:: Δ*cfl-cfa9*::cFRTSp^R, Sp^R/Sm^R	This study
pCPP5949	pK18mobsacB::Δ*hrcQ-U*::Ωsp, Sp^R	This study
pCPP5998	*cmaL* deletion construct cloned into pK18mobsacB, Km^R	(Munkvold et al., 2009)
pCPP5999	pK18mobsacB::Δ*cmaL*::cFRTSp^R, Sp^R/Sm^R	(Munkvold et al., 2009)
pCPP6001	pCPP5296:: *cmaL* +200 bp upstream; HA-tag; expresses *cmaL* from its native promoter, Gm^R	(Munkvold et al., 2009)
pCPP6017	pK18mobsacB::Δ*cmaD-U*, Km^R	This study
pCPP6018	pK18mobsacB:: Δ*cmaD-U*::cFRTSp^R, Sp^R/Sm^R	This study
pCPP6205	pENTR/SD/D-TOPO::*cmaL*-HA +200 bp upstream, stop codon removed, Km^R	This study
pCPP6206	pCPP5296::*cmaL*-HA +200 bp upstream; expresses *cmaL*-HA from its native promoter, Gm^R	This study
pCPP6338	pK18mob::*cmaD*-HA, Km^R	This study
pCPP6339	pK18mob::*cmaE*-HA, Km^R	This study
pCPP6340	pK18mob::*cmaA*-HA, Km^R	This study
pCPP6341	pK18mob::*cmaB*-HA, Km^R	This study
pCPP6342	pK18mob::*cmaC*-HA, Km^R	This study
pCPP6343	pK18mob::*cmaT*-HA, Km^R	This study
pCPP6344	pK18mob::PSPTO4713-HA, Km^R	This study
pCPP6345	pK18mob::*cmaU*-HA, Km^R	This study
pCPP6357	pUC18R6KT-mini-Tn7T-Tc::*cmaL*	This study

Table 2.1. Continued.

pUC18R6KT-mini-Tn7T-Tc	Mini-Tn7 vector with tetracycline resistance	(Choi and Schweizer, 2006)
pTNS2	Tn7 helper plasmid	(Choi and Schweizer, 2006)

(Figurski and Helinski, 1979; Simon et al., 1983). Deletions created using pK18mobsacB with and without FRT cassettes were performed as previously described (Wei et al., 2007; Kvitko and Collmer, 2011). Plasmid insertions using pK18mob (Schafer et al., 1994) were selected by plating on KB with kanamycin and, when appropriate, spectinomycin. Non-suicide vectors were transformed into DC3000 backgrounds by electroporation (Choi et al., 2006). Integrations were checked by PCR and/or by phenotype and antibiotic resistance.

DC3000 mutant strains created for this study.

Regions flanking the *cfa* operon were amplified by primers p2534/p2535 and p2536/p2537 (Table 2.2) from DC3000 genomic DNA, gel purified (Qiagen), digested with XmaI and ligated together, then digested with EcoRI and BamHI and cloned into pK18mobsacB to create pCPP5735. A FRT-Sp^R/Sm^R cassette, amplified with P2259/P2260 from pCPP5242, was ligated into the *XmaI* site of pCPP5735 in the reverse orientation to create pCPP5762. pCPP5762 was conjugated into CUCPB5112; integrants were selected based on spectinomycin resistance, then counter-selected based on sucrose sensitivity for vector removal to create CUCPB5532.

The Δ*hrcQ*$_B$-*hrcU*::ΩSp region of CUCPB5113 (Badel et al., 2006) was amplified using primers P1296/P2203 and blunt-end cloned into pK18mobsacB to create pCPP5949. This was integrated into CUCPB5529 (Kvitko et al., 2009), then the vector backbone removed by counter-selection to create CUCPB5540.

The FRTGm^R cassette from pCPP5209 was amplified with primer pair p2259/2260, digested with XbaI, and ligated into the *XbaI* site in pCPP5608 to create

Table 2.2. Primers used in this study.

Forward/Reverse Names	Forward sequence	Reverse sequence	Function
jnw123/jnw124	TGCTCGTCTCGTCGCCAAG	CGATACCCTTAGTTAGTCCTGTGG	For Q-PCR, *cfl*
jnw125/jnw126	GGACTTCATCCGCCAGTTCAATG	GCTGCCAAGAGTGCCAAAGG	For Q-PCR, early *cma* operon
jnw127/jnw128	GGATTGACCGCCCAGGAGAG	ACCGCAGCAGCAATGTATTCG	For Q-PCR, late *cma* operon
various/jnw147		GCGTAATCTGGAACATCGTATGGG	HA-tag reverse for checking integration
jnw166/jnw167	CAGCTCGAGATCCGTTGACCCTGGCTTCCCG	TACCTCGAGTCATGCGTAATCTGGAACATCGTATGGGTAGGCTTTATCCGCCGCAGCGGC	*cmaD*-HA construct
jnw168/jnw169	CAGCTCGAGCAATTGATTGGTCAGGTCAACGAG	TACCTCGAGTCATGCGTAATCTGGAACATCGTATGGGTATTGAATGGCCCTCTGCTTGTG	*cmaE*-HA construct
jnw170/jnw171	CAGCTCGAGTGTGCTGTTACTGACCACCTCACT	TACCTCGAGTCATGCGTAATCTGGAACATCGTATGGGTAGTCATTTCCATGTTGGCTCCT	*cmaA*-HA construct
jnw172/jnw173	CAGCTCGAGACCTTTCAAGAGTGGGTGCAGTAC	TACCTCGAGTCATGCGTAATCTGGAACATCGTATGGGTAATAAATGACTAGGGGCTTCAG	*cmaB*-HA construct
jnw174/jnw175	CAGCTCGAGTTCGGCGGCGCTATTAATGTGTGG	TACCTCGAGTCATGCGTAATCTGGAACATCGTATGGGTAACCGGTGATCTCGAACAGGCC	*cmaC*-HA construct
jnw176/jnw177	CAGCTCGAGGACAGCGTGGTCAGCCGGCTGC	TACCTCGAGTCATGCGTAATCTGGAACATCGTATGGGTAACTGCCTTGTTCATCTAGAGC	*cmaT*-HA construct
jnw178/jnw179	CAGCTCGAGTGCGATGGACGACAACCAACTGTG	TACCTCGAGTCATGCGTAATCTGGAACATCGTATGGGTAATCCACTAGGTAGATTTCGAC	PSPTO4713-HA construct
jnw180/jnw181	CAGCTCGAGTTGCACTTCGCCGCTGAAATTGTG	TACCTCGAGTCATGCGTAATCTGGAACATCGTATGGGTATGCCAATTTGGTCTTGATCAG	*cmaU*-HA construct

Table 2.2. Continued

oSWC381/oSWC382	CCGCAAGGTGATTATCTCAGC	TGGAGATGATCTGGTGCGACT	For Q-PCR, *gap*1
p1063/p1064	CACCGGTCAATTGCGGCCCGC	TGATTATGGATCCTCACTTCAGCTCGGCATAGACTACTT	Amplifies a fragment upstream of *CorRSP* for SOE PCR
p1065/p1066	TGAAGTGAGGATCCATAATCAGCTCGGCATGGACTACG	AGGGCGAACCTGCTGGTAGCG	Amplifies a fragment downstream of *CorRSP* for SOE PCR
p1296/p2203	CACCATGATGATTCGTAGCCTAAC	CACCATGACCGCACCGATCAAAA	Used for amplification of the *hrcQ-U* Ωsp region of CUCPB5113
p1683/p1753	GAAGCAGCTCCAGCCTACAC	CAAGCTGTTGAGGAACGTAAGGTAC	For checking corRSP
p1696/p1697	GTGGATCCGTGTAGGCTGGAGCTGCTTC	ACGGATCCCATATGAATATCCTCCTTA	Amplifies FRT cassettes and adds BamHI sites
p1754/p1684	GTTGATCAATTGCTACATGGTGAGG	TAAGGAGGATATTCATATG	For checking corRSP
p2259/p2260	ATTACCCGGGGTGTAGGCTGGAGCTGCTTC	ATTACCCGGGCATATGAATATCCTCCTTA	Amplifies FRT cassettes and adds XmaI sites
p2534/p2535	ATTAGAATTCGCAGCGATCAGCTCGCAT	ATTACCCGGGCAGACTCATGCTAGATCA	Amplifies a flanking region to the *cfa* operon
p2536/p2537	ATTACCCGGGTTATAAAGTCGGGCATTCTTGGA	TCACGGACACGATGCGGATCCA	Amplifies a flanking region to the *cfa* operon
p2667/p2668	GCCACGCGGCGATAGGT	AGCGTTCGGTTCTCACGGTATCG	For *cmaL* deletion confirmation

Table 2.2. Continued

p2668/p2712	AGCGTTCGGTTCTCAC GGTATCG	TAATTCTAGACCGTTAT CCACTCCCTCCAC	Amplifies *cmaL* w/o stop codon and upstream region
p2695/p2696	TAATGATATCAGCACC AGCAGGAAATCTTT	CTAGACTAGTCATGGTT TACATGCCTCGTC	Amplifies a flanking region to the *cma* operon
p2697/p2698	CTAGACTAGTTAGGTG TTAGGGAAGCTCTG	TAATGATATCTTCTCCC CAATGGTTTGGTT	Amplifies a flanking region to the *cma* operon
p2701/p2702	CTACCTTCAGATCGAG GTCG	ATAGAGCTGGCTTTGCC TTT	For *cmaD-U* deletion confirmation

pCPP5729. This was conjugated into CUPB5113 and integrants selected for with gentamicin, then the vector backbone removed by counter-selection to create CUCPB5488. *cmaL* was deleted from CUCPB5488 as described previously using pCPP5999 (Munkvold et al., 2009) to create CUCPB5570.

Flanking regions to the *cma* operon were amplified from DC3000 genomic DNA with primer pairs P2695/P2696 and P2697/P2698. These flanks were gel purified, digested with SpeI and ligated together. This ligation product was gel-purified and digested with EcoRV, then ligated into the *Eco*RV site in pk18mobsacB to create pCPP6017. A FRT-Sp/Sm^R cassette, amplified with primer pair P2259/P2260 from pCPP5242, was ligated into the *XmaI* site of pCPP6017 to create pCPP6018. pCPP6018 was conjugated into CUCPB5112 and integrants selected for with kanamycin, then the vector backbone removed by counter-selection to create CUCPB5591. pCPP6018 was then used in the same manner, but on DC3000, to create strain CUCPB5593.

Flanking regions to the genome segment encoding *corS* to *corP* were amplified by primer pairs p1063/p1064 and p1065/1066 in a SOEing PCR reaction (Horton et al., 1989) from DC3000 genomic DNA that resulted in two approximately 1-kb flanks with a *BamHI* site engineered in the middle. This was cloned into pENTR-D-TOPO using an Invitrogen TOPO cloning kit to create pKR36. A FRT-Sp^R/Sm^R cassette, amplified with primer pair P1696/1697, was ligated into the introduced *BamHI* site to create pCPP5265. pCPP5265 and pCPP5215 (Kvitko et al., 2007) were recombined using LR Clonase II (Invitrogen) to create pCPP5266. pCPP5266 was conjugated into DC3000

and integrants selected for with kanamycin, then the vector backbone removed by counter-selection to create CUCPB5392.

Single-gene-copy complementation of the Δ*cmaL* mutation for HPLC analysis of COR production, was achieved by Tn*7* mediated site-specific integration of an approximately 1.1 kb fragment containing *cmaL* with 500 bp upstream and 300 bp downstream. This fragment was amplified from DC3000 genomic DNA using primers jnw182 and jnw183 and ligated into the *Hind*III site of pUC18R6KT-mini-Tn7T-Tc to create pCPP6357. pUC18R6KT-mini-Tn7T-Tc and pCPP6357 were used in make specific insertions adjacent to *glmS* in the DC3000 Δ*cmaL* genome. Integrants were initially selected on solid MG minimal media with 5µg/ml tetracycline, and then isolated on solid KB media with rifampicin and 5µg/ml tetracycline. Confirmation of insertion in individual isolates was done using primers oSWC461 and oSWC462.

Construction of gene fusions encoding HA-tagged CMA proteins.

Genomic C-terminal HA-tag fusions were made by single crossover integrations into the target genome with a pK18mob derivative containing a ca. 1-kb region of DNA upstream of the respective *cma* gene stop codon fused to an HA tag sequence. Primers jnw166-181 (Table 2.2) were used, and the products were digested with XhoI then ligated into SalI-digested pK18mob. Single crossover recombination reactions between the resultant plasmids in the series pCPP6338-6345 were integrated into *Pto* DC3000 and CUCPB5563 to create strains CUCPB6053 to CUCPB6068. Constructs were checked by PCR with a primer upstream of the primed sequence used to create the construct and jnw147 which primes the sequence used to HA-tag all constructs.

A PCR fragment amplified by primer pair p2668/p2712 from *Pto* DC3000 genomic DNA was digested with BsaAI and XbaI and ligated into pENTR11 digested with XmnI/XbaI to create pCPP6205. pCPP6205 was LR-cloned into pCPP5296 using LR Clonase II (Invitrogen) to create pCPP6206.

Leaf chlorosis assays of *Pto* DC3000 derivatives.

DC3000 derivative strains were grown on KB media with appropriate antibiotic selection to maintain plasmids. For individual inoculations, bacteria were scraped from plates, suspended in 10mM $MgCl_2$ and diluted to 3×10^4 CFU/ml, then inoculated into leaves with a blunt syringe. For cross-feeding co-inoculation experiments, bacteria were suspended from the plate in 10mM $MgCl_2$ individually at a concentration of 3×10^6 CFU/ml each for a total bacterial concentration of 6×10^6 CFU/ml. In both experiments, plants were placed into a 16-h day, 90% relative humidity, 23°C growth chamber for 6 days to allow symptom development and then photographed.

Quantitative Reverse-Transcriptase PCR.

Bacteria were inoculated from overnight growth on KB solid media into KB broth or from mannitol-glutamate (MG) solid media (Keane et al., 1970) into MG broth supplemented with 50 µM ferric citrate at a starting OD_{600} of 0.1 and incubated for 4 h at 30°C with shaking. Bacteria in the equivalent of 1 ml of OD_{600} 0.4 of each culture were harvested by centrifugation, and the pellets were snap frozen in liquid nitrogen. RNA was extracted using the RNeasy Mini Kit from Qiagen including an on-column DNase treatment. An additional DNase treatment was performed with Ambion DNAse I

(Invitrogen) by mixing 50 µl RNA extract with 5 µl supplied buffer and 1µl of enzyme mixture and incubating at 37°C for 20m. This mixture was cleaned with the RNeasy Mini Kit RNA cleanup protocol and eluted in 50 µl nuclease free water. RNA was quantified using a NanoDrop (Thermo Scientific) and diluted to 100 ng/µl.

Reverse transcriptase PCR was performed using qScript cDNA Super Mix (Quanta BioSciences). Relative levels of gene expression were assayed in qPCR reactions using iQ SYBR Green Supermix (Bio-Rad). The primers for these reactions were designed with Beacon Designer (PREMIER Biosoft) to give similar reaction results. Primer pair oSWC381/oSWC382 was used to assay the normalizing gene, *gap1*, (PSPTO_1287 encoding glyceraldehyde 3-phosphate dehydrogenase), which has previously been used for this purpose in *Pto* DC3000 (Ferreira et al., 2006; Filiatrault et al., 2010). Primer pair jnw125/jnw126 was used to amplify a short region in the first 1.5kb of the *cma* operon that has similar amplification characteristics to that of oSWC381/oSWC382. A second primer pair, jnw127/jnw128, amplified a region in the last 1.5 kb of the *cma* operon and was used to verify that the 3' end of the operon is not regulated differently under the conditions used for this experiment (data not shown). Cycle-threshold (C_T) values were used to determine the levels of *cma* operon transcripts relative to *gap1* transcripts. The reactions were run and monitored on an iQ5 Multicolor Real-Time PCR Detection System and analyzed with its included software (Bio-Rad).

HA tag detection.

Bacteria were inoculated from overnight growth on KB solid media into KB broth or from MG solid media into MG broth supplemented with 50 µM ferric citrate at a starting

OD_{600} of 0.001 and incubated with shaking for 24 h at 30°C. Appropriate antibiotic selection was used to maintain any plasmids. Cultures in mid-log growth (OD_{600} 0.2-0.8) were harvested by centrifugation. Bacteria in an amount equal to 1 ml of OD_{600} 0.5 culture were boiled directly in 15 µl of a 5x concentrated SDS-PAGE sample loading buffer. Proteins were separated on 4-15% acrylamide gradient gels (Bio-Rad) and transferred to an Immobilon-FL membrane (Millipore). These blots were probed with rat anti-HA monoclonal (Roche) diluted 1:1000 in blocking buffer, washed, then secondarily probed with goat anti-rat IgG alkaline phosphatase conjugate (Invitrogen) diluted 1:10,000 in blocking buffer. Blots were visualized using a chemiluminescent reaction and photosensitive film. The images for production of HA-tagged Cma proteins are all derived without modification from a single blot and immunostaining procedure.

Coronatine production cultures.

Bacteria were grown overnight on solid MG media then inoculated into 100 ml MG broth cultures supplemented with 50 µM ferric citrate at a starting OD_{600} of 0.001 and incubated with shaking for 72 h at 30°C, when they were harvested for analysis. For cultures involving the addition of L-isoleucine or L-allo-isoleucine, 5 mg of powder (Sigma) was dissolved in sterile water then added to 100 ml of culture 24 h after inoculation when cultures were in late log phase. At 72 h all cultures tested were found to have an OD_{600} of 1.8 ± 0.1 regardless of genotype or amendment. Cultures were separated into cell and supernatant fractions by centrifugation at 10,000 x g for 10 min at 4^{o}C, then the supernatants were passed through a 0.2 µm filter and stored at -20°C before analysis.

Detection of coronatine pathway products.

Production of CFA and COR by *Pto* DC3000 wild-type, Δ*cmaD-U*, Δ*cfl-cfa9*, and Δ*cmaL* strains was determined by quantitative HPLC of extracted culture filtrates. Each replicate sample was extracted from 100 ml of culture filtrate as previously described (Palmer and Bender, 1993), the organic fractions were rotoevaporated to dryness, contents were transferred into a tared vial with methanol and then dried to constant weight for analysis. For HPLC, each sample was dissolved in 1 ml of methanol, and then 20 µl injections were used for the analysis. Thus, each injection represents 2 ml of culture filtrate. HPLC employed a Spherisorb Octyl column (Sigma-Aldrich, 5µm, 4.6 x 250 mm), eluted with acetonitrile:water:formic acid (35:65:0.1) at a flow rate of 1 ml/min (Waters 600 pump), with detection by UV absorbance at 208 nm (extracted from a 194-450 nm scan on a Waters 996 diode array detector), using standards for determination of retention times (COR from Sigma Chemical; CFA and CFA-isoleucine from C. Bender, Oklahoma State University). Concentrations of COR (RT ~ 9-9.5 min) were estimated using a six-point standard curve of COR (0.02, 0.05, 0.1, 0.2, 0.5, and 1 µg) to determine peak area units per µg COR and CFA (RT 7-7.5 min) amounts estimated using COR peak area equivalents. The limit of detection (LOD), established at a signal to noise ratio of 3, was estimated at 50 ng for each standard. Putative COR peaks were confirmed by comparison of spectral scans and co-injection with the standard. Presence of CFA and COR were additionally confirmed by low resolution electrospray mass spectrometry (LRESIMS) by infusion of sample solutions at 5 µL/min by a syringe pump (Harvard apparatus) into a Micromass ZMD-4000 spectrometer and comparison with

standards. Positive ion spectra were obtained with capillary cone voltages of 3.5 kV and 50 V, respectively; negative ion spectra were obtained with capillary and cone voltages of 3.5 kV and 45 V, respectively.

Chemical illustrations.

The illustrations of various chemical compounds for Figure 2.11 were produced using BKChem, available at http://bkchem.zirael.org.

REFERENCES

Alfano, J.R., Charkowski, A.O., Deng, W.-L., Badel, J.L., Petnicki-Ocwieja, T., van Dijk, K., and Collmer, A. 2000. The *Pseudomonas syringae* Hrp pathogenicity island has a tripartite mosaic structure composed of a cluster of type III secretion genes bounded by exchangeable effector and conserved effector loci that contribute to parasitic fitness and pathogenicity in plants. Proc Natl Acad Sci USA 97:4856-4861.

Badel, J.L., Shimizu, R., Oh, H.-S., and Collmer, A. 2006. A *Pseudomonas syringae* pv. *tomato avrE1*/*hopM1* mutant is severely reduced in growth and lesion formation in tomato. Mol Plant Microbe Interact 19:99-111.

Baltrus, D.A., Nishimura, M.T., Romanchuk, A., Chang, J.H., Mukhtar, M.S., Cherkis, K., Roach, J., Grant, S.R., Jones, C.D., and Dangl, J.L. 2011. Dynamic evolution of pathogenicity revealed by sequencing and comparative genomics of 19 *Pseudomonas syringae* isolates. PLoS Pathog 7:e1002132.

Bender, C.L., Alarcon-Chaidez, F., and Gross, D.C. 1999a. *Pseudomonas syringae* phytotoxins: mode of action, regulation, and biosynthesis by peptide and polyketide synthetases. Microbiol Mol Biol Rev 63:266-292.

Bender, C.L., Rangaswamy, V., and Loper, J. 1999b. Polyketide production by plant-associated pseudomonads. Annu Rev Phytopathol 37:175-196.

Bender, C.L., Liyanage, H., Palmer, D., Ullrich, M., Young, S., and Mitchell, R. 1993. Characterization of the genes controlling the biosynthesis of the polyketide

phytotoxin coronatine including conjugation between coronafacic and coronamic acid. Gene 133:31-38.

Bronstein, P.A., Filiatrault, M.J., Myers, C.R., Rutzke, M., Schneider, D.J., and Cartinhour, S.W. 2008. Global transcriptional responses of *Pseudomonas syringae* DC3000 to changes in iron bioavailability *in vitro*. BMC Microbiol 8:209.

Brooks, D., Hernandez-Guzman, G., Koek, A.P., Alarcon-Chaidez, F., Sreedharan, A., Rangaswarmy, V., Penaloza-Vasquez, A., Bender, C.L., and Kunkel, B.N. 2004. Identification and characterization of a well-defined series of coronatine biosynthetic mutants of *Pseudomonas syringae* pv. *tomato* DC3000. Mol Plant-Microbe Interact 17:162-174.

Brooks, D.M., Bender, C.L., and Kunkel, B.N. 2005. The *Pseudomonas syringae* phytotoxin coronatine promotes virulence by overcoming salicylic acid-dependent defences in *Arabidopsis thaliana* Mol Plant Pathol 6:629-639.

Buell, C.R., Joardar, V., Lindeberg, M., Selengut, J., Paulsen, I.T., Gwinn, M.L., Dodson, R.J., Deboy, R.T., Durkin, A.S., Kolonay, J.F., Madupu, R., Daugherty, S., Brinkac, L., Beanan, M.J., Haft, D.H., Nelson, W.C., Davidsen, T., Liu, J., Yuan, Q., Khouri, H., Fedorova, N., Tran, B., Russell, D., Berry, K., Utterback, T., Vanaken, S.E., Feldblyum, T.V., D'Ascenzo, M., Deng, W.-L., Ramos, A.R., Alfano, J.R., Cartinhour, S., Chatterjee, A.K., Delaney, T.P., Lazarowitz, S.G., Martin, G.B., Schneider, D.J., Tang, X., Bender, C.L., White, O., Fraser, C.M., and Collmer, A. 2003. The complete sequence of the *Arabidopsis* and tomato pathogen *Pseudomonas syringae* pv. *tomato* DC3000. Proc Natl Acad Sci USA 100:10181-10186.

Cai, R., Lewis, J., Yan, S., Liu, H., Clarke, C.R., Campanile, F., Almeida, N.F., Studholme, D.J., Lindeberg, M., Schneider, D., Zaccardelli, M., Setubal, J.C., Morales-Lizcano, N.P., Bernal, A., Coaker, G., Baker, C., Bender, C.L., Leman, S., and Vinatzer, B.A. 2011. The plant pathogen *Pseudomonas syringae* pv. *tomato* is genetically monomorphic and under strong selection to evade tomato immunity. PLoS Pathog 7:e1002130.

Choi, K.H., and Schweizer, H.P. 2006. mini-Tn*7* insertion in bacteria with single *att*Tn*7* sites: example *Pseudomonas aeruginosa*. Nat Protoc 1:153-161.

Choi, K.H., Kumar, A., and Schweizer, H.P. 2006. A 10-min method for preparation of highly electrocompetent *Pseudomonas aeruginosa* cells: application for DNA fragment transfer between chromosomes and plasmid transformation. J Microbiol Methods 64:391-397.

Couch, R., O'Connor, S.E., Seidle, H., Walsh, C.T., and Parry, R. 2004. Characterization of CmaA, an adenylation-thiolation didomain enzyme involved in the biosynthesis of coronatine. J Bacteriol 186:35-42.

Cunnac, S., Chakravarthy, S., Kvitko, B.H., Russell, A.B., Martin, G.B., and Collmer, A. 2011. Genetic disassembly and combinatorial reassembly identify a minimal functional repertoire of type III effectors in *Pseudomonas syringae*. Proc Natl Acad Sci U S A 108:2975-2980.

Ferreira, A.O., Myers, C.R., Gordon, J.S., Martin, G.B., Vencato, M., Collmer, A., Wehling, M.D., Alfano, J.R., Moreno-Hagelsieb, G., Lamboy, W.F., DeClerck, G., Schneider, D.J., and Cartinhour, S.W. 2006. Whole-genome expression profiling defines the HrpL regulon of *Pseudomonas syringae* pv. *tomato* DC3000, allows

de novo reconstruction of the Hrp *cis* element, and identifies novel co-regulated gene. Mol Plant Microbe Interact 19:1167-1179.

Figurski, D., and Helinski, D.R. 1979. Replication of an origin-containing derivative of plasmid RK2 dependent on a plasmid function provided *in trans*. Proc Natl Acad Sci USA 76:1648-1652.

Filiatrault, M.J., Stodghill, P.V., Myers, C.R., Bronstein, P.A., Butcher, B.G., Lam, H., Grills, G., Schweitzer, P., Wang, W., Schneider, D.J., and Cartinhour, S.W. 2011. Genome-wide identification of transcriptional start sites in the plant pathogen *Pseudomonas syringae* pv. *tomato* str. DC3000. PLoS One 6:e29335.

Filiatrault, M.J., Stodghill, P.V., Bronstein, P.A., Moll, S., Lindeberg, M., Grills, G., Schweitzer, P., Wang, W., Schroth, G.P., Luo, S., Khrebtukova, I., Yang, Y., Thannhauser, T., Butcher, B.G., Cartinhour, S., and Schneider, D.J. 2010. Transcriptome analysis of *Pseudomonas syringae* identifies new genes, ncRNAs, and antisense activity. J Bacteriol 192:2359-2372.

Fouts, D.E., Badel, J.L., Ramos, A.R., Rapp, R.A., and Collmer, A. 2003. A *Pseudomonas syringae* pv. *tomato* DC3000 Hrp (type III secretion) deletion mutant expressing the Hrp system of bean pathogen *P. syringae* pv. *syringae* 61 retains normal host specificity for tomato. Mol Plant-Microbe Interact 16:43-52.

Fouts, D.E., Abramovitch, R.B., Alfano, J.R., Baldo, A.M., Buell, C.R., Cartinhour, S., Chatterjee, A.K., D'Ascenzo, M., Gwinn, M.L., Lazarowitz, S.G., Lin, N.-C., Martin, G.B., Rehm, A.H., Schneider, D.J., van Dijk, K., Tang, X., and Collmer, A. 2002. Genomewide identification of *Pseudomonas syringae* pv. *tomato* DC3000

promoters controlled by the HrpL alternative sigma factor. Proc Natl Acad Sci USA 99:2275-2280.

Gross, H., and Loper, J.E. 2009. Genomics of secondary metabolite production by *Pseudomonas* spp. Nat Prod Rep 26:1408-1446.

Hanahan, D. 1985. Techniques for transformation of *E. coli*. Pages 109-135 in: DNA Cloning: A Practical Approach, D.M. Glover, ed. IRL Press, Oxford, United Kingdom.

Horton, R.M., Hunt, H.D., Ho, S.N., Pullen, J.K., and Pease, L.R. 1989. Engineering hybrid genes without the use of restriction enzymes: gene splicing by overlap extension. Gene 77:61-68.

House, B.L., Mortimer, M.W., and Kahn, M.L. 2004. New recombination methods for *Sinorhizobium meliloti* genetics. Appl Environ Microbiol 70:2806-2815.

Hwang, M.S., Morgan, R.L., Sarkar, S.F., Wang, P.W., and Guttman, D.S. 2005. Phylogenetic characterization of virulence and resistance phenotypes of *Pseudomonas syringae*. Appl Environ Microbiol 71:5182-5191.

Keane, P.J., Kerr, A., and New, P.B. 1970. Crown gall of stone fruit 2. Identification and nomenclature of *Agrobacterium* isolates. Austn J Biol Sci 23:585.

King, E.O., Ward, M.K., and Raney, D.E. 1954. Two simple media for the demonstration of pyocyanin and fluorescin. J Lab Clin Med 44:301-307.

Kvitko, B.H., and Collmer, A. 2011. Construction of *Pseudomonas syringae* pv. tomato DC3000 mutant and polymutant strains. Pages 109-128 in: Methods in Molecular Biology: Plant Immunity, J.M. McDowell, ed. Springer Science+Business Media.

Kvitko, B.H., Ramos, A.R., Morello, J.E., Oh, H.-S., and Collmer, A. 2007. Identification of harpins in *Pseudomonas syringae* pv. tomato DC3000, which are functionally similar to HrpK1 in promoting translocation of type III secretion system effectors. J Bacteriol 189:8059-8072.

Kvitko, B.H., Park, D.H., Velásquez, A.C., Wei, C.-F., Russell, A.B., Martin, G.B., Schneider, D.J., and Collmer, A. 2009. Deletions in the repertoire of *Pseudomonas syringae* pv. *tomato* DC3000 type III secretion effector genes reveal functional overlap among effectors. PLoS Pathogens 5:e1000388.

Lan, L., Deng, X., Zhou, J., and Tang, X. 2006. Genome-wide gene expression analysis of *Pseudomonas syringae* pv. *tomato* DC3000 reveals overlapping and distinct pathways regulated by *hrpL* and *hrpRS*. Mol Plant Microbe Interact 19:976-987.

Li, X.Z., Starratt, A.N., and Cuppels, D.A. 1998. Identification of tomato leaf factors that activate toxin gene expression in *Pseudomonas syringae* pv. *tomato* DC3000. Phytopathology 88:1094-1100.

Lin, N.C., and Martin, G.B. 2005. An *avrPto*/*avrPtoB* mutant of *Pseudomonas syringae* pv. *tomato* DC3000 does not elicit Pto-specific resistance and is less virulent on tomato. Mol Plant Microbe Interact 18:43-51.

Lindeberg, M., Myers, C.R., Collmer, A., and Schneider, D.J. 2008. Roadmap to new virulence determinants in *Pseudomonas syringae*: Insights from comparative genomics and genome organization. Mol Plant-Microbe Interact 21:685-700.

Liyanage, H., Penfold, D., Turner, J., and Bender, C.L. 1995. Sequence, expression and transcriptional analysis of the coronafacate lipase-encoding gene requred for coronatine biosynthesis by *Pseudomonas syringae*. Gene 153:17-23.

Mamer, O.A., and Reimer, M.L. 1992. On the mechanisms of the formation of L-alloisoleucine and the 2-hydroxy-3-methylvaleric acid stereoisomers from L-isoleucine in maple syrup urine disease patients and in normal humans. J Biol Chem 267:22141-22147.

Mansfield, J., Genin, S., Magori, S., Citovsky, V., Sriariyanum, M., Ronald, P., Dow, M., Verdier, V., Beer, S.V., Machado, M.A., Toth, I., Salmond, G., and Foster, G.D. 2012. Top 10 plant pathogenic bacteria in molecular plant pathology. Mol Plant Pathol.

Mecey, C., Hauck, P., Trapp, M., Pumplin, N., Plovanich, A., Yao, J., and He, S.Y. 2011. A critical role of *STAYGREEN*/Mendel's *I* locus in controlling disease symptom development during *Pseudomonas syringae* pv *tomato* infection of Arabidopsis. Plant Physiol 157:1965-1974.

Melotto, M., Underwood, W., Koczan, J., Nomura, K., and He, S.Y. 2006. Plant stomata function in innate immunity against bacterial invasion. Cell 126:969-980.

Mitchell, R.E., Young, S., and Bender, C.L. 1994. Coronamic acid, an intermediate in coronatine biosynthesis by *Pseudomonas syringae*. Phytochemistry 35:343-348.

Mittal, S., and Davis, K.R. 1995. Role of the phytotoxin coronatine in the infection of *Arabidopsis thaliana* by *Pseudomonas syringae* pv. *tomato*. Mol Plant-Microbe Interact 8:165-171.

Munkvold, K.R., Russell, A.B., Kvitko, B.H., and Collmer, A. 2009. *Pseudomonas syringae* pv. *tomato* DC3000 type III effector HopAA1-1 functions redundantly with chlorosis-promoting factor PSPTO4723 to produce bacterial speck lesions in host tomato. Mol Plant Microbe Interact 22:1341–1355.

Palmer, D.A., and Bender, C.L. 1993. Effects of environmental and nutritional factors on production of the polyketide phytotoxin coronatine by *Pseudomonas syringae* pv. glycinea. Appl Environ Microbiol 59:1619-1626.

Parry, R.J., Lin, M.-T., Walker, A.E., and Mhaskar, S.V. 1991. The biosynthesis of coronatine: investigations of the biosynthesis of coronamic acid. J Am Chem Soc 113:1849–1850.

Parry, R.J., Mhaskar, S.V., Lin, M.-T., Walker, A.E., and Mafoti, R. 1994. Investigations of the biosynthesis of the phytotoxin coronatine. Can J Chem 72:86-99.

Peñaloza-Vázquez, A., Preston, G.M., Collmer, A., and Bender, C.L. 2000. Regulatory interactions between the Hrp type III protein secretion system and coronatine biosynthesis in *Pseudomonas syringae* pv. *tomato* DC3000. Microbiology 146:2447-2456.

Preston, G., Deng, W.-L., Huang, H.-C., and Collmer, A. 1998. Negative regulation of *hrp* genes in *Pseudomonas syringae* by HrpV. J Bacteriol 180:4532-4537.

Punta, M., Coggill, P.C., Eberhardt, R.Y., Mistry, J., Tate, J., Boursnell, C., Pang, N., Forslund, K., Ceric, G., Clements, J., Heger, A., Holm, L., Sonnhammer, E.L., Eddy, S.R., Bateman, A., and Finn, R.D. 2012. The Pfam protein families database. Nucleic Acids Res 40:D290-301.

Rangaswamy, V., Ullrich, M., Jones, W., Mitchell, R., Parry, R., Reynolds, P., and Bender, C.L. 1997. Expression and analysis of coronafacate ligase, a thermoregulated gene required for production of the phytotoxin coronatine in *Pseudomonas syringae*. FEMS Microbiol Lett 154:65-72.

Sambrook, J., and Russel, D.W. 2001. Molecular Cloning: A Laboratory Manual. Cold Spring Harbor, NY: Cold Spring Harbor Laboratory Press.

Schadewaldt, P., Bodner-Leidecker, A., Hammen, H.W., and Wendel, U. 2000. Formation of L-alloisoleucine in vivo: an L-[^{13}C]isoleucine study in man. Pediatr Res 47:271-277.

Schafer, A., Tauch, A., Jager, W., Kalinowski, J., Thierbach, G., and Puhler, A. 1994. Small mobilizeable multi-purpose cloning vectors derived from the *Escherichia coli* plasmids pK18 and pK19: selection of defined deletions in the chromosome of *Corynebacterium glutamicum*. Gene 145:69-73.

Schechter, L.M., Vencato, M., Jordan, K.L., Schneider, S.E., Schneider, D.J., and Collmer, A. 2006. Multiple approaches to a complete inventory of *Pseudomonas syringae* pv. *tomato* DC3000 type III secretion system effector proteins. Mol Plant-Microbe Interact 19:1180-1192.

Simon, R., Priefer, U., and Puhler, A. 1983. A broad host range mobilization system for in vivo genetic engineering: Transposon mutagenesis in gram-negative bacteria. BioTechnology 1:784-791.

Sreedharan, A., Penaloza-Vazquez, A., Kunkel, B.N., and Bender, C.L. 2006. CorR regulates multiple components of virulence in *Pseudomonas syringae* pv. *tomato* DC3000. Mol Plant Microbe Interact 19:768-779.

Stamps, S.L., Taylor, A.B., Wang, S.C., Hackert, M.L., and Whitman, C.P. 2000. Mechanism of the phenylpyruvate tautomerase activity of macrophage migration inhibitory factor: properties of the P1G, P1A, Y95F, and N97A mutants. Biochemistry 39:9671-9678.

Tampakaki, A.P., Skandalis, N., Gazi, A.D., Bastaki, M.N., Sarris, P.F., Charova, S.N., Kokkinidis, M., and Panopoulos, N.J. 2010. Playing the "Harp": evolution of our understanding of *hrp*/*hrc* genes. Annu Rev Phytopathol 48:347-370.

Ullrich, M., Peñaloza-Vázquez, A., Bailey, A.-M., and Bender, C.L. 1995. A modified two-component regulatory system is involved in temperature-dependent biosynthesis of the *Pseudomonas syringae* phytotoxin coronatine. J Bacteriol 177:6160-6169.

Vaillancourt, F.H., Yeh, E., Vosburg, D.A., O'Connor, S.E., and Walsh, C.T. 2005. Cryptic chlorination by a non-haem iron enzyme during cyclopropyl amino acid biosynthesis. Nature 436:1191-1194.

Wang, X.W., Alarcón-Chaidez, F., Peñaloza-Vázquez, A., and Bender, C.L. 2002. Differential regulation of coronatine biosynthesis in *Pseudomonas syringae* pv. *tomato* DC3000 and *P. syringae* pv. *glycinea* PG4180. Physiol Mol Plant Pathol 60:111-120.

Wei, C.-F., Kvitko, B.H., Shimizu, R., Crabill, E., Alfano, J.R., Lin, N.-C., Martin, G.B., Huang, H.-C., and Collmer, A. 2007. A *Pseudomonas syringae* pv. *tomato* DC3000 mutant lacking the type III effector HopQ1-1 is able to cause disease in the model plant *Nicotiana benthamiana*. Plant J 51:32-46.

Zheng, X.Y., Spivey, N.W., Zeng, W., Liu, P.P., Fu, Z.Q., Klessig, D.F., He, S.Y., and Dong, X. 2012. Coronatine promotes *Pseudomonas syringae* virulence in plants by activating a signaling cascade that Inhibits salicylic acid accumulation. Cell Host Microbe 11:587-596.

CHAPTER 3

LOCALIZATION OF THE *PSEUDOMONAS SYRINGAE* PV. *TOMATO* DC3000 TYPE III EFFECTOR HOPAA1-1 WITH PEROXISOMES IN *NICOTIANA BENTHAMIANA* IS CORRELATED WITH THE ABILITY OF THE PROTEIN TO ELICIT EUKARYOTIC CELL DEATH AND PROMOTE BACTERIAL VIRULENCE

INTRODUCTION

The model pathogen *Pseudomonas syringae* pv. *tomato* DC3000 (*Pto* DC3000) defeats plants with ca. 28 effector proteins that it injects into host cells via the type III secretion system (T3SS). *Pto* DC3000 is a pathogen of tomato (Cuppels, 1986), Arabidopsis (Whalen et al., 1991), and *Nicotiana benthamiana* (if the gene encoding the HopQ1-1 avirulence determinant is deleted) (Wei et al., 2007). A primary function of type III effectors is to defeat the two-tiered innate immune system of plants, which is comprised of pathogen- or microbe-associated molecular pattern-triggered immunity (PTI or MTI) and effector-triggered immunity (ETI) (Jones and Dangl, 2006). PTI is triggered by conserved, surface-presented microbial features, such as flagellin. Effectors disrupt PTI, but their presence in the plant cytosol renders them vulnerable to detection by the ETI system (Boller and Felix, 2009). ETI can be defeated by the mutation of genes encoding betraying effectors or by deployment of additional effectors that suppress ETI. As a result of the coevolutionary battle over effector recognition and evasion the composition of effector repertoires among *P. syringae* strains, even those in

the same host-specific pathovar, can be remarkably different (Almeida et al., 2009; Baltrus et al., 2011; O'Brien et al., 2011).

In contrast to this diversity, the three effector genes in the conserved effector locus (CEL) of the Hrp pathogenicity island are almost universally present in the various *P. syringae* pathovars (Alfano et al., 2000). These core, ancient effectors are AvrE, HopM1, and HopAA1. The best understood of these, HopM1, targets the Arabidopsis AtMIN7 protein, a trans-Golgi network/early endosome-associated adenosine diphosphate (ADP) ribosylation factor (ARF) guanine nucleotide exchange factor (GEF) family member, for degradation by the proteasome; the disruption of AtMIN7 function likely disrupts vesicle trafficking (Nomura et al., 2006; Nomura et al., 2011). AvrE-family effectors in *P. syringae* and enterobacterial plant pathogens are also predicted to interact with small G-proteins (Ham et al., 2009), and the *Pto* DC3000 AvrE functionally overlaps with HopM1, further suggesting a potential role in vesicle trafficking (DebRoy et al., 2004; Nomura et al., 2006). HopAA1-1 carries a potential GTPase-activating (GAP) domain, but replacing the putative catalytic arginine with alanine has no apparent effect on biological activity (Munkvold et al., 2009), and HopAA1-1 does not functionally overlap with HopM1 in suppressing PTI-associated callose deposition (DebRoy et al., 2004).

A survey of 27 *Pto* DC3000 effectors for deleterious effects when inducibly expressed in yeast revealed HopAA1-1 as one of four that impaired respiration and one of two that caused cell death (Munkvold et al., 2008). Agrobacterium-mediated transient expression revealed that HopAA1-1 can also cause cell death in *N. benthamiana*, tomato, and tobacco, and that truncations to either the N- or C-terminus of HopAA1-1

that abolish cell killing in yeast have the same effect in *N. benthamiana* (Munkvold et al., 2008). *Pto* DC3000 also produces a HopAA1-1 paralog designated HopAA1-2. These two proteins are notably polymorphic at the putative GAP domain (GALRA and GAFEN, respectively), and neither HopAA1-2 nor HopAA1-$1_{LRA-FEN}$ cause cell death in yeast or *N. benthamiana* (Munkvold et al., 2009).

The *Pto* DC3000 HopAA1-1 colocalizes with the mitochondrial marker porin in yeast (Munkvold et al., 2008). The subcellular localization of the DC3000 protein in plant cells has not been investigated, but the *P. syringae* pv. syringae B728a HopAA1 protein was described as localizing to the cell periphery and probably the plasma membrane in *N. benthamiana* (Lee et al., 2012). Our knowledge of the subcellular localization of *Pto* DC3000 effectors is limited (Block and Alfano, 2011). In addition to the localization of HopM1 mentioned above, we know that HopI1 and HopN1 are targeted to chloroplasts and HopG1 to mitochondria (Jelenska et al., 2007; Block et al., 2010; Rodriguez-Herva et al., 2012); AvrPto1 and HopF2 are targeted to the plasma membrane via a myristoylation motif (Shan et al., 2000; Wu et al., 2011), and some other effectors, such as AvrPtoB, interact with plasma membrane-associated immune protein complexes (Shan et al., 2008).

Various plant interaction phenotypes have been observed for HopAA1-deficient mutants of *Pto* DC3000 and *P. syringae* pv. *syringae* B728a. Confocal microscopy of GFP-labeled wild-type and *hopAA1-1*-mutant *Pto* DC3000 in syringe-infiltrated Arabidopsis leaves revealed that the mutant displays more “failed colonies” (no larger than a T3SS-deficient control), although there is no apparent change in the ultimate size of successful colonies, total bacterial population, or disease lesions (Badel et al., 2002).

Deletion of *hopAA1-1* in *Pto* DC3000 produces a stronger phenotype of reduced lesion numbers in dip-inoculated tomato leaves if *cmaL* is also deleted; CmaL is necessary to produce L-*allo*-isoleucine, which is a precursor for coronamic acid and subsequently the phytohormone coronatine (Munkvold et al., 2009; Worley et al., 2013). A *P. syringae* pv. *syringae* B728a *hopAA1* deletion mutant is no different from the wild type when syringe-infiltrated into host *N. benthamiana* leaves, but when spray-inoculated the mutant produces increased lesion counts and bacterial populations, suggesting that HopAA1 is acting as a weak avirulence determinant (Vinatzer et al., 2006; Lee et al., 2012). Taken together, these observations suggest that HopAA1 acts very early in the bacterium-plant interaction, but its contribution to virulence may be masked by other factors, such as phytotoxins and other effectors.

Additional insights into effects of HopAA1 family members on plants have been gained by heterologous expression experiments. For example, expression of the *Pto* DC3000 HopAA1-1 in Arabidopsis protoplasts suppressed flagellin-induced transcription of the PTI-associated *NONHOST1* (*NHO1*) gene (Li et al., 2005). Similarly, expression of the *Pseudomonas fluorescens* Q8r1-96 RopAA homolog in *P. fluorescens* 55 producing a *P. syringae* T3SS and no other effector suppressed flg22 (flagellin epitope)-induced reactive oxygen species generation in *N. benthamiana*, thereby indicating an ability to suppress PTI (Mavrodi et al., 2011). Similarly expressed RopAA also showed a moderate ability to suppress ETI elicited by another effector, HopA1, in tobacco (Mavrodi et al., 2011). Finally, it is noteworthy that *P. fluorescens* expressing a T3SS and the *Pto* DC3000 HopAA1-1 (in the absence of any other effector) elicits cell death in *N. benthamiana* (Wei et al., 2007). Thus, HopAA1 is like HopM1 and several other *P.*

syringae effectors in having the ability when heterologously expressed to both suppress PTI and elicit apparent ETI, but when the effector genes are individually removed from a native genome the mutants show only subtle phenotypes (Cunnac et al., 2009).

The likely explanation for the weak phenotypes of individual effector gene mutations is redundancy. To address this problem we have constructed *Pto* DC3000D28E, which is deleted for the 28 effector genes most likely to be active and which no longer grows or causes disease symptoms in *N. benthamiana* (Cunnac et al., 2011). Reintroduction of a minimal repertoire of 8 effectors into DC3000D28E restores bacterial growth and lesion formation to near wild-type levels (Cunnac et al., 2011). HopAA1-1 is one of the effectors in the minimal repertoire, but the *hopAA1-1* gene was introduced as a block with other CEL effector genes *avrE*, *hopM1*, and *hopN1*. Thus, the contribution of HopAA1-1 to the performance of the minimal repertoire is unknown.

Here we have used Agrobacterium-mediated transient expression and confocal microscopy to determine the subcellular localization in *N. benthamiana* leaf cells of the *Pto* DC3000 HopAA1-1 and its previously described derivatives (Munkvold et al., 2009). Colocalization with fluorescent marker proteins revealed that HopAA1-1 and its derivatives localize to the surface of peroxisomes, to the endoplasmic reticulum (ER), and the cell periphery, in *N. benthamiana* leaf cells, rather than to mitochondria as was observed with yeast. Targeted reconstruction of the minimal effector repertoire in DC3000D28E produced a strain whose ability to produce chlorotic spots in dip-inoculated *N. benthamiana* leaves was qualitatively dependent on HopAA1-1. The strong phenotype enabled further resolution of the regions of HopAA1-1 required for biological activity in plants and yeast and for endomembrane localization as well as for

prevention of relocalization to the interior of peroxisomes and nuclei by heterologous targeting signals. These experiments revealed an absolute correlation between the association of HopAA1-1 with peroxisomes and endomembranes in *N. benthamiana* and all biological activities in yeast and *N. benthamiana*.

RESULTS

HopAA1-1 mutants display different localization patterns in *N. benthamiana* leaf cells.

Several HopAA1-1 variants had previously been constructed and assayed for their ability to kill yeast and *N. benthamiana* leaf cells when expressed within them (Munkvold et al., 2008; Munkvold et al., 2009). Wild-type HopAA1-1, five of the HopAA1-1 variants, and HopAA1-2 were analyzed here for their subcellular localization in *N. benthamiana*. The proteins were expressed with C-terminal YFP-HA fusions in *N. benthamiana* by *Agrobacterium*-mediated transient expression using a modified pEarleyGate101 vector, pCPP6308, containing a 35S promoter (Earley et al., 2006). HopAA1-1-YFP-HA displayed a punctate localization pattern consisting of small bodies around 1-2 µm in diameter and also a diffuse peripheral distribution (Fig. 3.1). The peripheral distribution is consistent with the reported localization of the HopAA1 protein of *P. syringae* pv. *syringae* B728a (Lee et al., 2012). The *Pto* DC3000 HopAA1-$1_{41\text{-}486}$-YFP-HA localization pattern was similar to that of wild-type HopAA1-$1_{1\text{-}486}$-YFP-HA (Fig. 3.1B), but HopAA1-$1_{41\text{-}436}$-YFP-HA showed a shift of labeling from the cell periphery to a

Figure 3.1. Truncated HopAA1-1 derivatives display distinct localization patterns in *N. benthamiana* leaf cells. All images are of C-terminal YFP fusion proteins transiently expressed 33-38 h after inoculation with *A. tumefaciens* GV3101 at OD_{600} 0.3. Variants of HopAA1-1 that were cytotoxic in *N. benthamiana* upon overexpression have their images outlined with dashes, and those that were not cytotoxic are outlined with solid lines. **A,** HopAA1-1 localizes to punctate structures (lower arrow) and also to the cell periphery (upper arrow), but there are other, smaller fluorescently labeled spots. **B,** Deleting the N-terminal 40 amino acids causes no major shift in localization pattern. **C,** Deleting the N-terminal 50 amino acids results in generalized localization to the cytoplasm. **D,** Deleting the C-terminal 50 amino acids likewise causes a major shift in localization, with a new web-like pattern, less accumulation at the cell periphery, and some large punctate structures that seem similar to wild-type. **E,** Deleting the C-terminal 100 amino acids results in bright, punctate structures of variable size. **F,** HopAA1-2 accumulates in the cytoplasm. **G,** HopAA1-$1_{LRA-FEN}$ appears to accumulate in the cytoplasm.

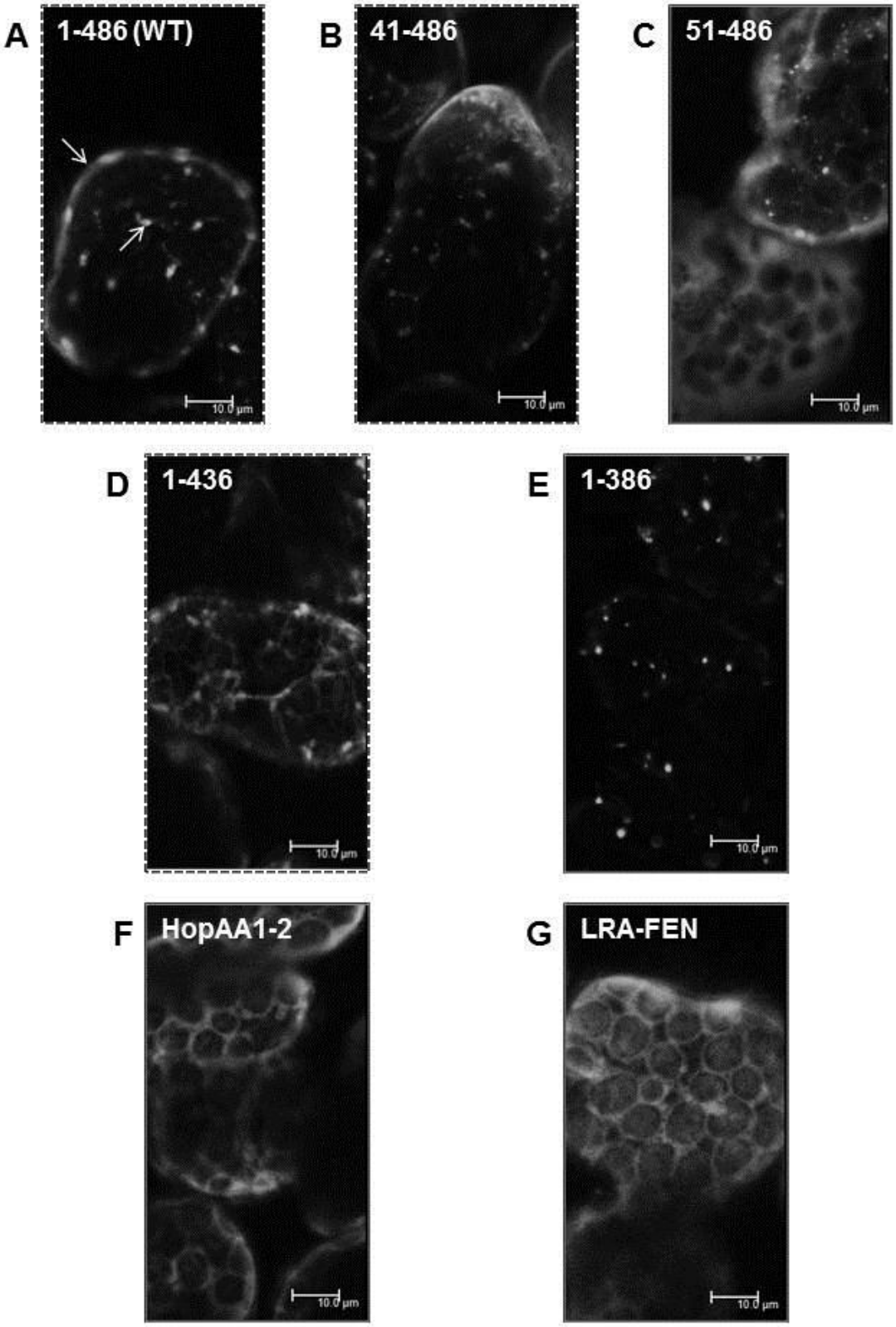
A
1-486 (WT)
B
41-486
C
51-486
D
1-436
E
1-386
F
HopAA1-2
G
LRA-FEN
10.0 µm

web-like pattern throughout the cell, while retaining labeling of the small bodies (Fig. 3.1D). HopAA1-1_{51-486}-YFP-HA, HopAA1-2-YFP-HA, and HopAA1-$1_{LRA-FEN}$-YFP-HA all showed a similar pattern that was completely different from the wild-type and suggested localization in the cytoplasm (Fig. 3.1C, F, G). In contrast, HopAA1-1_{1-386}-YFP-HA displayed scattered labeling of sharply defined, very small bodies (Fig. 3.1E). Importantly, three HopAA1-1 variants previously shown to kill yeast and *N. benthamiana* cells (HopAA1-1_{1-486}, HopAA1-1_{41-486}, and HopAA1-1_{1-436}) were also found to localize in *N. benthamiana* to small bodies around 1-2 µm in diameter, whereas HopAA1-1 variants that lacked such toxicity also failed to localize to these small bodies.

HopAA1-1 and variants that are cytotoxic colocalize with peroxisomes, and HopAA1-1_{1-436} additionally colocalizes with the endoplasmic reticulum (ER).

The size and distribution of the small bodies labeled by HopAA1-1-YFP-HA suggested possible targeting to mitochondria or peroxisomes. However, confocal microscopy experiments involving mito-tracker orange showed evidence of HopAA1-1-YFP-HA localization to mitochondria in *N. benthamiana* (data not shown). Consequently, we performed transient expression experiments using mixed inoculation with *Agrobacterium* strains harboring T-DNA constructs expressing the HopAA1-1 variants and the mCherry-px-rk peroxisomal matrix marker (Nelson et al., 2007). Colocalization with the peroxisomal marker was observed with all HopAA1-1 variants that caused cell death in *N. benthamiana* leaf cells: wild-type HopAA1-1-YFP-HA, HopAA1-1_{41-486}-YFP-HA, and HopAA1-1_{1-436}-YFP-HA (Fig. 3.2A, B, D). These images were obtained with 200x magnification, and occasionally ring-like structures were

Figure 3.2. Truncated HopAA1-1 derivatives colocalize with different fluorescently tagged markers for subcellular structures in *N. benthamiana*. HopAA1-1-YFP derivatives were transiently expressed as in Figure 3.1, but with co-inoculation with *A. tumefaciens* GV3101 delivering genes encoding mCherry-tagged proteins that localize to peroxisomes and the ER (Nelson et al., 2007). Arrows for this figure were created in the Leica LAS AF Lite software to ensure correct placement in the three panels of a sub-figure. **A,** HopAA1-1 colocalizes with peroxisomes; arrows show two examples. **B,** Deleting the N-terminal 40 amino acids from HopAA1-1 does not significantly change the wild-type localization pattern. **C,** Deleting the N-terminal 50 amino acids eliminates colocalization with the peroxisome marker. **D,** Deleting the C-terminal 50 amino acids reduces but does not eliminate colocalization with peroxisomes. **E,** Deleting the C-terminal 50 amino acids results in substantial colocalization with the ER marker. **F,** Deleting the C-terminal 100 amino acids results in cytoplasmic accumulation, exclusion from the location of peroxisomes (as exemplified by the arrow), and loss of any pattern indicative of ER localization. **G,** HopAA1-$1_{LRA\text{-}FEN}$ does not colocalize with individual peroxisomes or ER. **H, and I,** High resolution imaging with reduced exposure sensitivity reveals that HopAA1-1 and a C-terminal 50 amino acid deletion mutant localize just outside of the peroxisomal matrix, and are ostensibly located on the surface since there is only partial YFP and mCherry signal overlap around peroxisomes. H and I were imaged using 600x magnification with a water immersion objective.

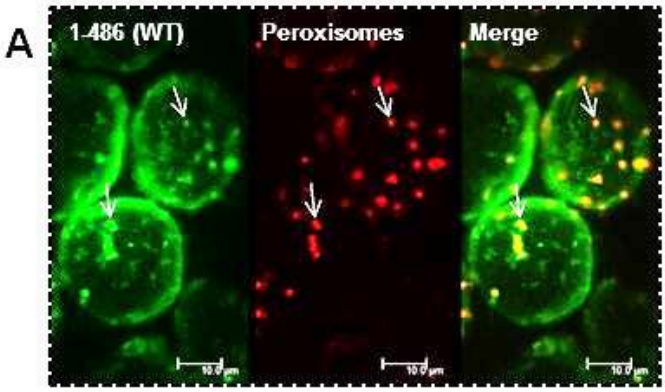
A
1-486 (WT)
Peroxisomes
Merge

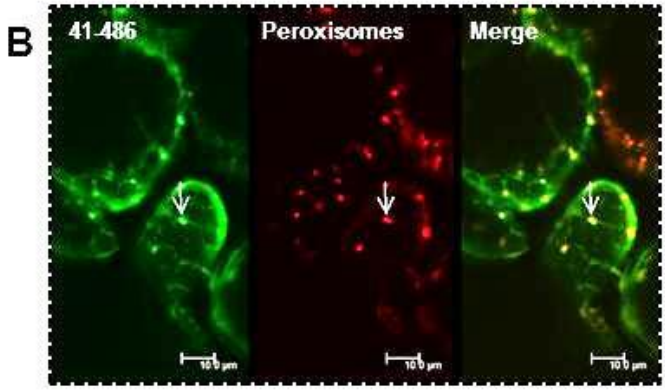
B
41-486
Peroxisomes
Merge

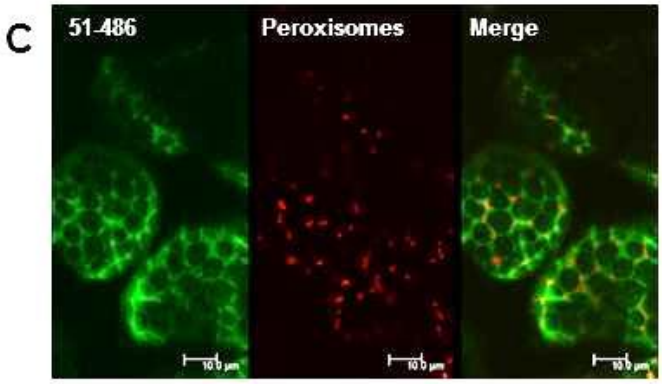
C
51-486
Peroxisomes
Merge

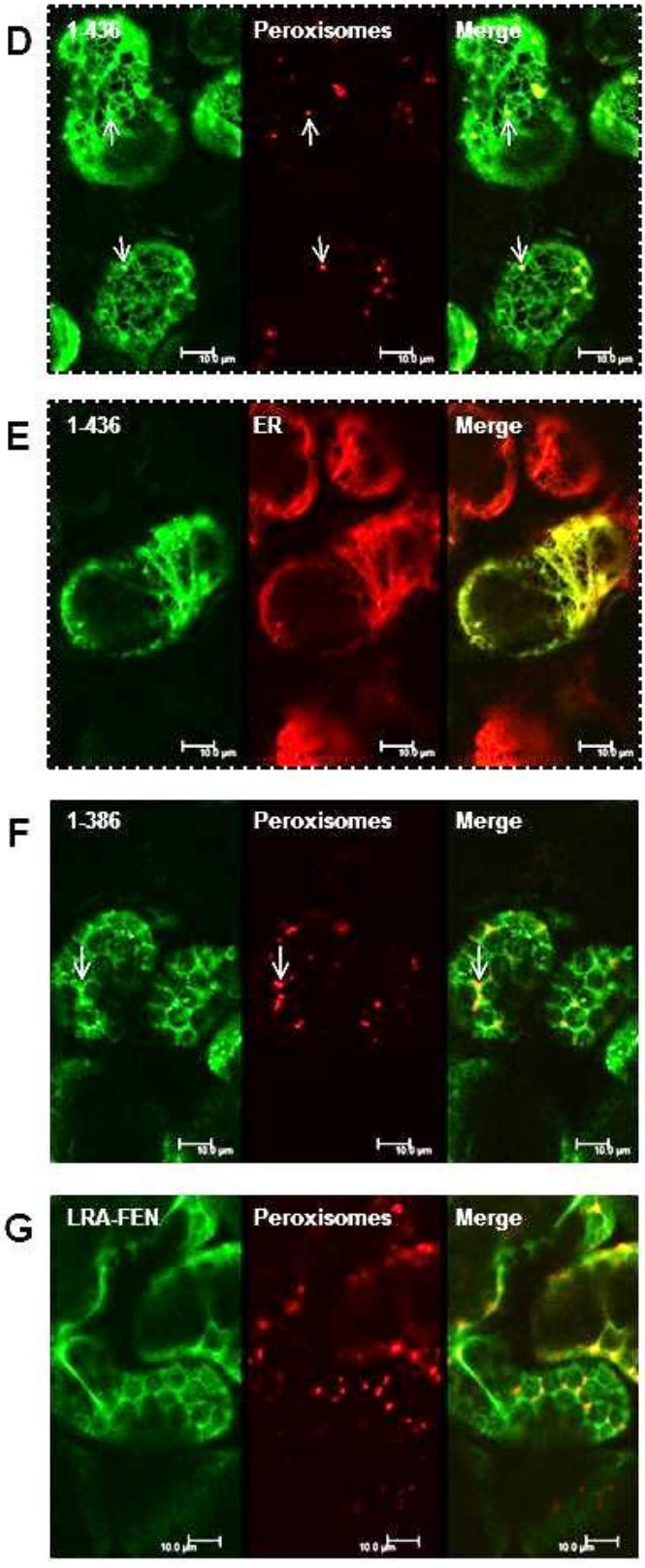
D
1-436
Peroxisomes
Merge
E
1-436
ER
Merge
F
1-386
Peroxisomes
Merge
G
LRA-FEN
Peroxisomes
Merge

H

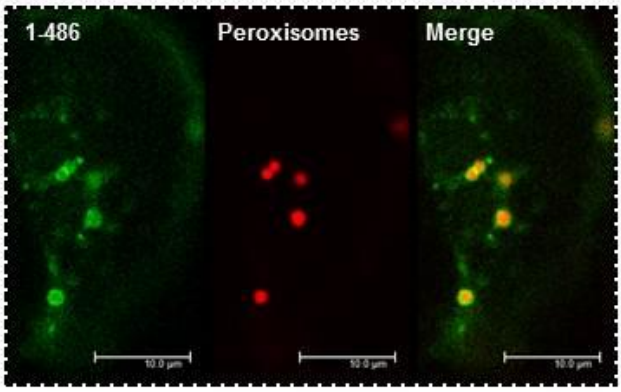

I

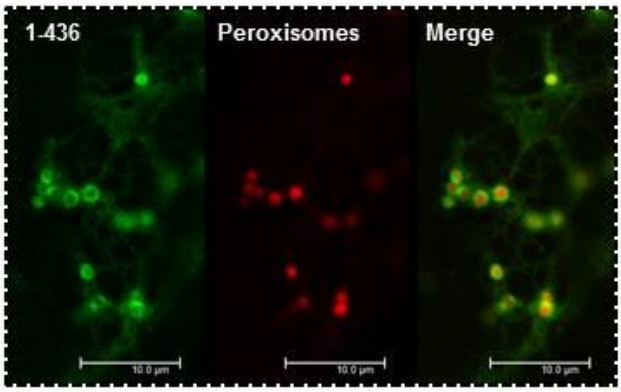

observed, as in Fig 3.2B. We used 630x magnification to explore whether HopAA1-1 localized to the surface of peroxisomes rather than to the matrix, as does the mCherry-px-rk marker. The higher magnification revealed that wild-type HopAA1-1-YFP-HA and HopAA1-1_{1-436}-YFP-HA labeled only the surface of peroxisomes (Fig. 3.2 H, I). As noted in Figure 3.1, HopAA1-1_{1-436}-YFP-HA also produced a web-like pattern suggestive of partial localization to the ER. This was confirmed by colocalization with mCherry-er-rk (Fig. 3.2E). The two HopAA1-1 variants that did not elicit cell death in *N. benthamiana* and displayed a diffuse cytoplasmic distribution (HopAA1-1_{51-486} and HopAA1-$1_{LRA-FEN}$) showed no colocalization with any distinct peroxisomal fluorescence signals (Fig. 3.2C and G). HopAA1-1_{1-386}-YFP-HA showed a punctate pattern, as seen in Figure 3.1, but there was no colocalization with peroxisomes (Fig. 3.2F). Thus, we observed a strict correlation between toxicity and localization to the surface of peroxisomes.

Additional truncations of HopAA1-1 reveal that HopAA1-1_{41-416} is close to the minimal unit for toxicity in yeast and cell death elicitation in *N. benthamiana*.

Additional deletions in *hopAA1-1* were constructed to produce proteins with C-terminal truncations in 10-amino-acid increments from residues 426 to 396. These new constructs all have a 40 amino-acid N-terminal truncation because this is the largest N-terminal truncation, within 10 amino acids, that does not disrupt toxicity in yeast (Munkvold et al., 2008). The *hopAA1-1* deletion constructs were cloned into pYES-DEST52 for galactose-inducible expression in yeast strain BY4741. *Agrobacterium* mediated transient expression was used to express the proteins with C-terminal YFP-HA fusions in *N. benthamiana*. Assays for yeast toxicity and *N. benthamiana* tissue

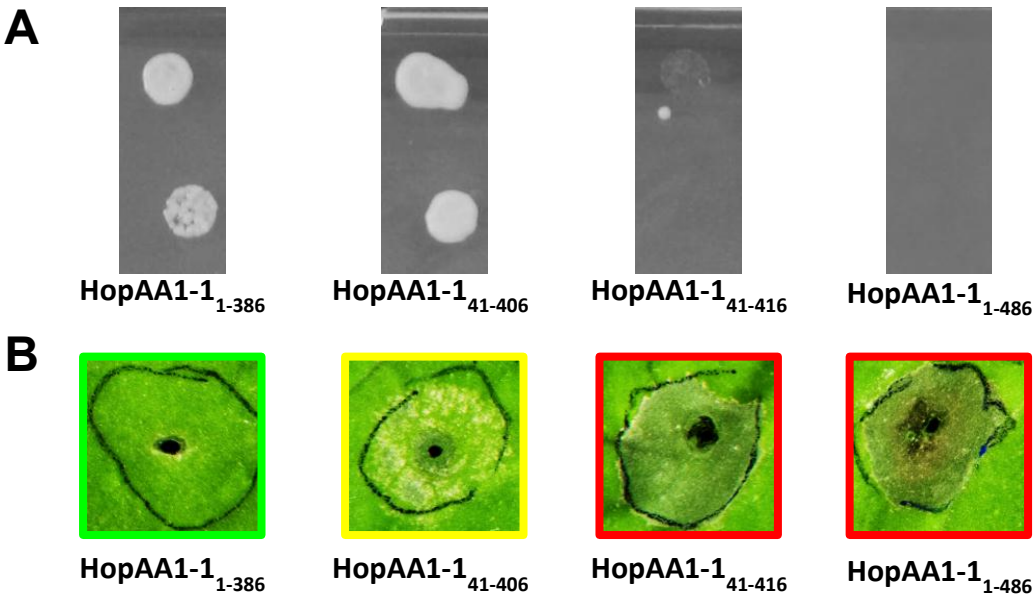

Figure 3.3. Truncations of HopAA1-1 from the N- and C-terminus reveal the minimal unit for toxicity in yeast and *N. benthamiana* with a resolution of 10 amino acids. **A**, Yeast strain BY4741a harboring the high-copy plasmid pYES-DEST52 encoding the indicated HopAA1-1 derivatives were spotted in duplicate onto medium containing galactose to induce expression of the test genes and then photographed after 2 days of incubation. Because HopAA1-1_{41-416} was unstable when expressed without a YFP tag on its C-terminus, the yeast shown here are expressing YFP fusion proteins. **B**, The indicated HopAA1-1 derivatives with C-terminal YFP fusions were produced in *N. benthamiana* leaves by *Agrobacterium*-mediated transient expression as described for Figure 3.1 and then photographed 2 days later. Representative images are shown, with a green border indicating no visible reaction, a yellow border indicating spotty chlorosis, and a red border indicating tissue death.

collapse revealed that the C-terminus of the minimal unit for toxicity is between amino acids 406 and 416 (Fig. 3.3). Although HopAA1-1_{41-406} elicited some spotty chlorosis in *N. benthamiana* (Fig. 3.3B), it showed no toxicity in yeast. HopAA1-1_{41-386} displayed no toxicity in any of these systems (Fig. 3.3). Thus, HopAA1-1_{41-416} is close to the minimal unit for toxicity in yeast and for cell death elicitation in *N. benthamiana*.

HopAA1-1_{41-416} can promote virulence of *Pto* DC3000D28E expressing a small subset of DC3000 effectors.

We had previously observed that HopAA1-1 contributed significantly to lesion formation in tomato when leaves were dip inoculated with DC3000 mutants that were also CmaL-deficient and that small subsets of the DC3000 effectors could promote virulence of the functionally effectorless polymutant DC3000D28E in *N. benthamiana* when bacteria were infiltrated into leaves with a blunt syringe (an inoculation method useful for high-throughput screening of many pathogen variants) (Munkvold et al., 2009; Cunnac et al., 2011). To facilitate further study of the contribution of HopAA1-1 to virulence, we combined these insights by dip inoculating *N. benthamiana* with CUCPB6031 expressing HopAA1-1 and key variants. CUCPB6031 is a DC3000D28E derivative that expresses AvrPtoB, HopM1, HopE1, HopG1, and HopAM1, but not CmaL (Cunnac et al., 2011). CUCPB6031 carrying an empty vector or expressing HopAA1-1_{1-406}-HA produced no symptoms when dip inoculated at 1 x 10^6 cfu/ml (Fig. 3.4). But CUCPB6031 expressing HopAA1-1_{1-416}-HA or wild-type HopAA1-1-HA produced numerous chlorotic spots by 5 days post inoculation. Although these

Figure 3.4. Wild type HopAA1-1 and HopAA1-1_{1-416} can promote virulence of *Pto* DC3000D28E expressing a minimal set of 5 DC3000 effectors. **A**, *Pto* DC3000D28E expressing HopM1, AvrPtoB, HopE1, HopG1, and HopM1 (CUCPB6031 or "D28E + 5"), along with the indicated HopAA1-1 derivatives expressed from the AvrPto promoter in plasmid pCPP5372, was inoculated into *N. benthamiana* leaves by dipping plants in inoculum at 1 x 10^6 cfu/ml. Leaves were photographed 5 days later. **B**, Chlorotic spots on *N. benthamiana* leaves inoculated and incubated as in panel C were counted. Results are mean and standard deviation for three leaves from different plants.

A

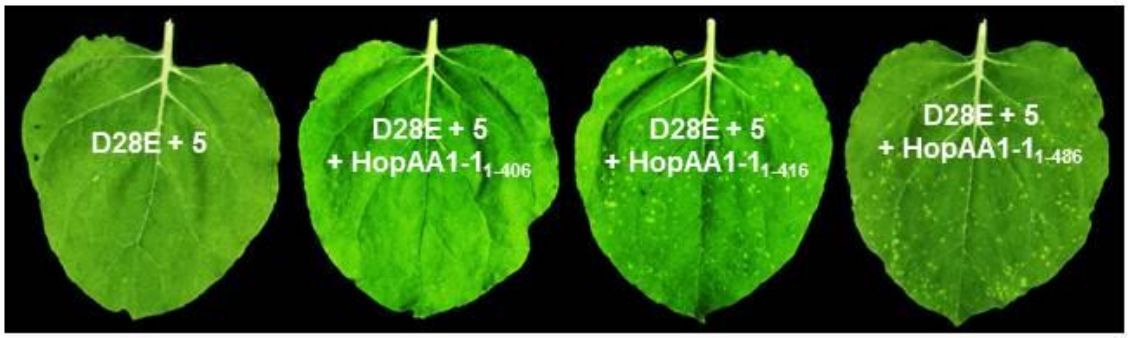
D28E + 5
D28E + 5 + HopAA1-1$_{1-406}$
D28E + 5 + HopAA1-1$_{1-416}$
D28E + 5 + HopAA1-1$_{1-486}$

B

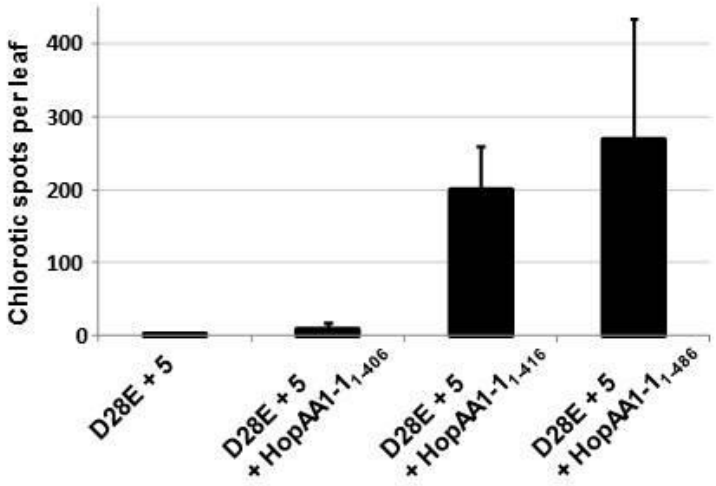
Chlorotic spots per leaf
400
300
200
100
0
D28E + 5
D28E + 5 + HopAA1-1$_{1-406}$
D28E + 5 + HopAA1-1$_{1-416}$
D28E + 5 + HopAA1-1$_{1-486}$

experiments employed HopAA1-1 derivatives with the first 40 amino acids intact because the N-terminus is needed for effector targeting to the T3SS (Schechter et al., 2004), they suggest that the minimal unit of HopAA1-1 needed for toxicity in yeast and *N. benthamiana* is the same as that needed to promote virulence.

The additional truncated variants of HopAA1-1 further define regions of the protein affecting subcellular localization in *N. benthamiana*.

We had observed above three patterns in the subcellular localization of HopAA1-1 accompanying progressive C-terminal deletions. (i) HopAA1-1_{1-486} localized to peroxisomes and the cell periphery (ii) With the deletion of 50 amino acids (HopAA1-1_{1-436}), localization shifted from the cell periphery to the ER (iii) With the deletion of 100 amino acids (HopAA1-1_{1-386}), labeling was lost for peroxisomes, ER, and the cell periphery, and a new punctate pattern appeared. Here we examined the localization of the newly constructed HopAA1-1-YFP-HA C-terminal truncations and learned that the C-terminus of the minimal unit for localization to peroxisomes and the cell periphery is between amino acids 471 and 466 (Fig. 3.5). Similarly, the C-terminus of the minimal unit for the ER localization pattern is between amino acids 416 and 406. HopAA1-14_{1-466}-YFP-HA and HopAA1-1_{41-416}-YFP-HA show a web-like pattern that is similar to the ER labeling pattern of HopAA1-1_{1-436}-YFP-HA in Figure 3.2E, but this pattern is lost with HopAA1-1_{41-406}-YFP-HA (Fig. 3.5). Thus, two defined regions of the C-terminus determine the localization pattern of HopAA1-1 in *N. benthamiana* cells. The protein constructs that were used to define the regions necessary for specific subcellular localization patterns accumulate without significant N-terminal truncations (Fig. 3.6).

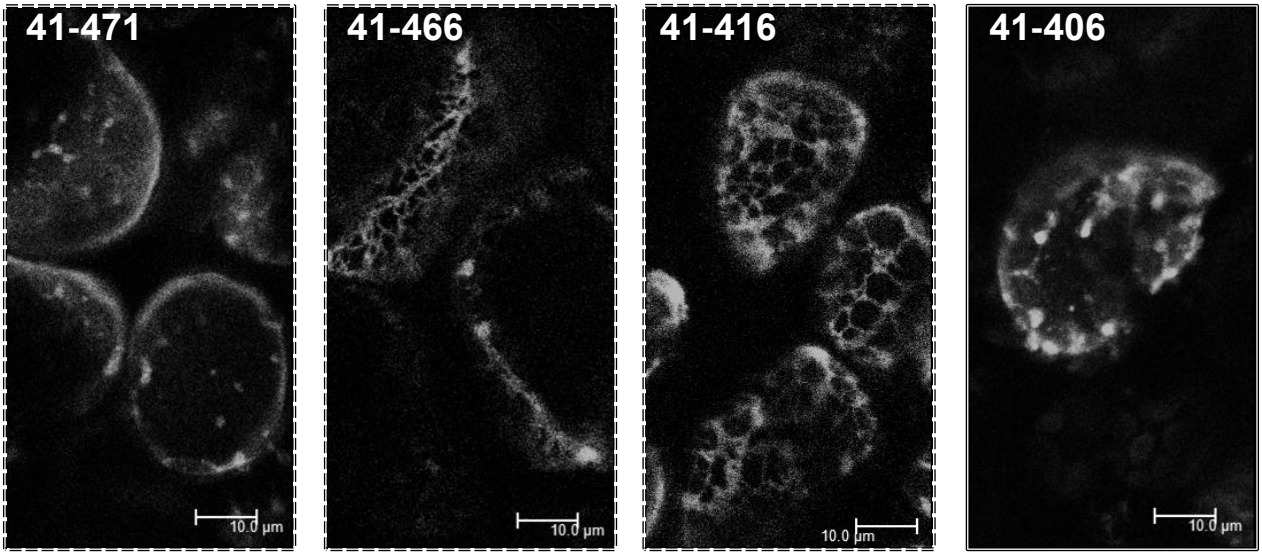

Figure 3.5. Progressive truncations of HopAA1-1 reveal changes in subcellular localization suggesting two functional C-terminal regions. *Agrobacterium*-mediated transient expression of the indicated HopAA1-1-YFP derivatives and confocal microscopy were performed as in Figure 3.1. Dashed border indicates HopAA1-1 derivatives that elicit cell death in *N. benthamiana*, whereas solid border indicates lack of cell death. HopAA1-$1_{41\text{-}471}$ localization is similar to that of HopAA1-$1_{1\text{-}486}$ and HopAA1-$1_{41\text{-}486}$ (Figs. 3.1 and 3.2), which is consistent with localization to peroxisomes and the cell periphery. HopAA1-$1_{41\text{-}466}$ and HopAA1-$1_{41\text{-}416}$ localization is similar to that of HopAA1-$1_{1\text{-}436}$ (Figs. 3.1 and 3.2), which is consistent with localization to peroxisomes and the ER.

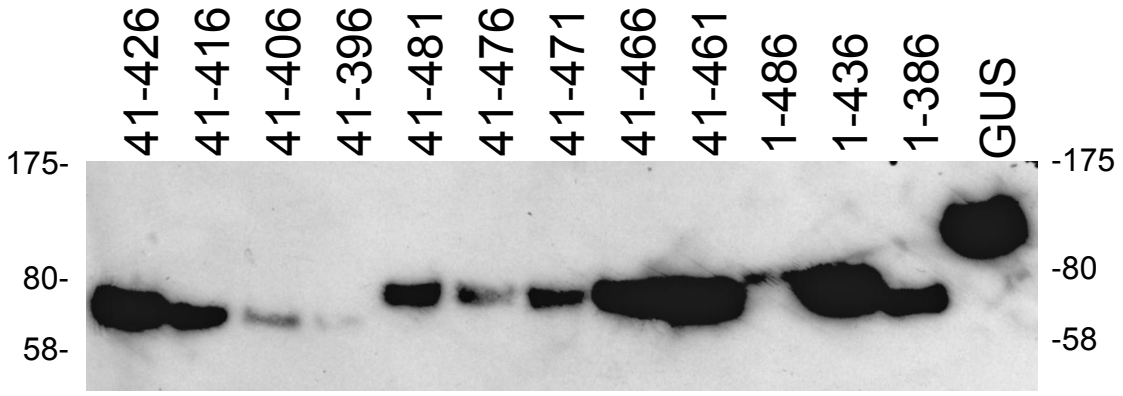

Figure 3.6. Accumulation of HopAA1-1 and derivatives with C-terminal YFP-StrepII protein fusions in *Nicotiana benthamiana* 36 hours after transformation. The StrepII protein tag was detected using Strep-Tactin alkaline phosphatase conjugate and a chemiluminescent reagent. No degredation products were observed. The predicted size for the HopAA1-1-YFP-StrepII fusion peptide is ca. 78 kDa.

The constructs which co-localize with ER tend to accumulate at elevated levels, but the significance is unknown.

HopAA1-1 variants that localize to the peroxisomal surface cannot be redirected to other subcellular targets in *N. benthamiana* by heterologous targeting signals.

To test the specificity and potential function of the subcellular targeting of HopAA1-1, we attempted to redirect the localization of three HopAA1-1 variants to the nucleus and the peroxisomal matrix. We chose three HopAA1-1 variants that represent previously defined localization patterns: wild-type HopAA1-$1_{1\text{-}486}$ (peroxisome surface and cell periphery), HopAA1-$1_{1\text{-}436}$ (peroxisome surface and ER), and HopAA1-$1_{LRA\text{-}FEN}$ (cytoplasm). The latter was also chosen because it is not deleterious when expressed in yeast or *N. benthamiana* (Munkvold et al., 2009), and it has the same size as wild-type HopAA1-1. The heterologous targeting signals were an SV40 nuclear localization sequence (Hodel et al., 2001) and the PTS1 C-terminal signal-peptide, which targets proteins to the peroxisomal matrix, (Subramani et al., 2000). C-terminal fusions of YFP-HA-NLS and YFP-HA-PTS1 were constructed with each of the fusion proteins and then produced in *N. benthamiana* by *Agrobacterium*-mediated transient expression. Neither the NLS nor PTS1 targeting signals caused a major change in the localization patterns of HopAA1-$1_{1\text{-}486}$ and HopAA1-$1_{1\text{-}436}$ (Fig. 3.7). However, HopAA1-$1_{LRA\text{-}FEN}$-YFP-HA-NLS localization was shifted entirely to the nucleus and HopAA1-$1_{LRA\text{-}FEN}$-YFP-HA-PTS1 to peroxisomes. Regarding the latter, the smaller and more sharply punctate fluorescence signals were consistent with localization to the peroxosomal matrix rather than to the peroxisomal surface.

Figure 3.7. HopAA1-1 derivatives shown to be biologically active cannot be redirected to other subcellular targets in *N. benthamiana* with heterologous targeting signals. The experimental methods and constructs used were the same as in Fig. 3.1 except for the addition of a C-terminal targeting signal: **A**, SV40 nuclear localization signal (NLS) targeting sequence (PKKKRKV) and **B**, peroxisomal matrix PTS1 targeing sequence (SKL). Only the HopAA1-1LRA-FEN derivatives show changes in pattern indicated of redirection to the nucleus (NLS) and peroxisomal martix (PTS1).

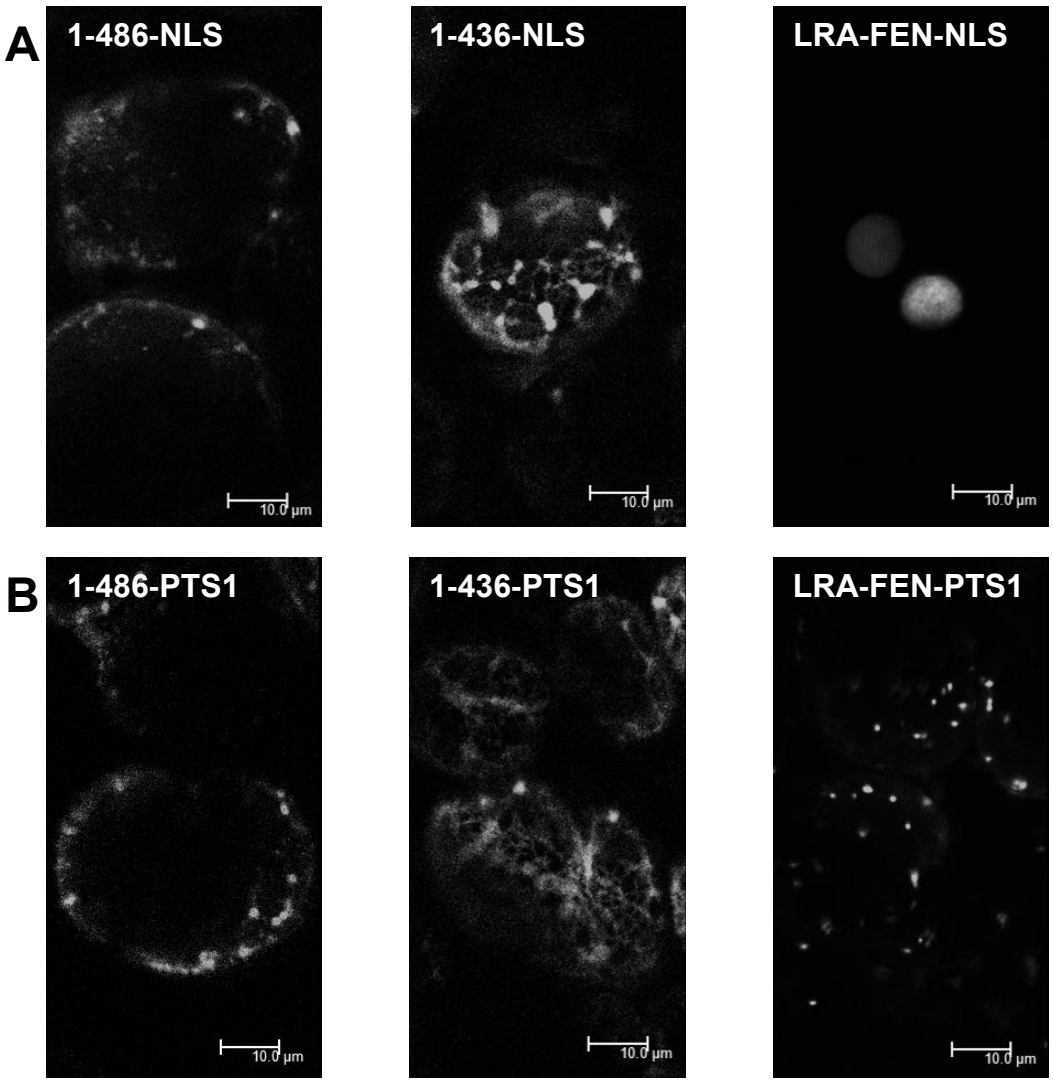
A
1-486-NLS
1-436-NLS
LRA-FEN-NLS
B
1-486-PTS1
1-436-PTS1
LRA-FEN-PTS1
10.0 µm

Subcellular distribution patterns of key HopAA1-1 variants in yeast show similarities with patterns observed in *N. benthamiana*.

The discovery of HopAA1-1 toxicity in yeast occurred through a screen of *Pto* DC3000 effectors that was motivated by the expectation that some effectors target conserved features of eukaryotes that are shared by fungi and plants (Munkvold et al., 2008). The observation that deleting more than 70 residues of the C-terminus of HopAA1-1 abolished deleterious effects in yeast and *N. benthamiana* provides further support for a common target in both organisms (Fig. 3.3). Although wild-type HopAA1-1 appears to localize to mitochondria in yeast (Munkvold et al., 2008) and peroxisomes in *N. benthamiana* (Fig. 3.2), our more detailed observations in *N. benthamiana* reveal an association with the surface of peroxisomes and endomembranes that shifts with progressive deletion of the C-terminus (Figs. 3.2 and 3.5). To determine if similar differences in localization pattern occur in yeast, we used galactose-inducible vector pYES-DEST52 to express C-terminal YFP-tagged derivatives of HopAA1-$1_{1\text{-}486}$, HopAA1-$1_{1\text{-}436}$, and HopAA1-$1_{\text{LRA-FEN}}$. The punctate, cytosolic pattern observed with HopAA1-$1_{1\text{-}486}$-YFP was consistent with localization to mitochondria and peripheral endomembranes (Fig. 3.8). The HopAA1-$1_{1\text{-}436}$-YFP pattern appeared more perinuclear, which is consistent with association with the ER. In further contrast, HopAA1-$1_{\text{LRA-FEN}}$-YFP produced a more diffuse distribution in the cytoplasm, which is similar to the pattern observed with *N. benthamiana*.

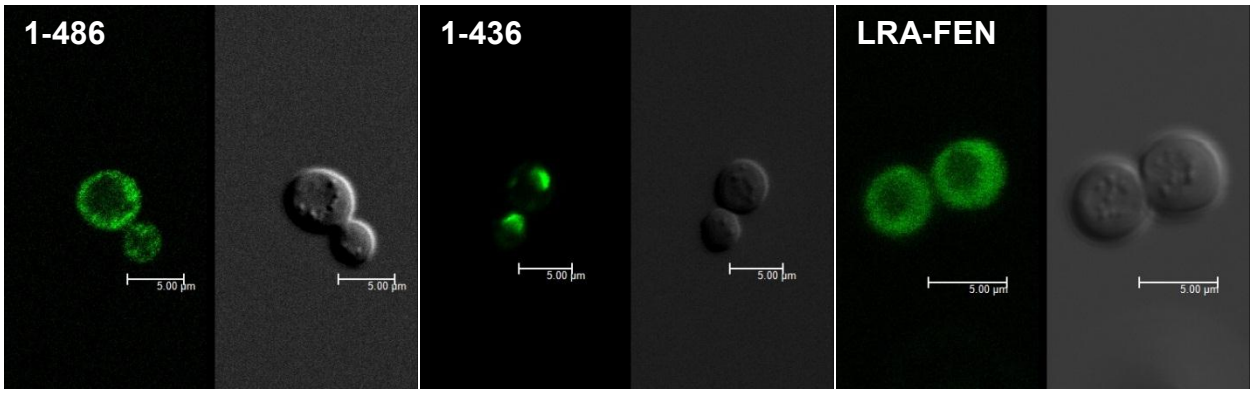

Figure 3.8. Expression of HopAA1-1-YFP variants in yeast shows three patterns of localization. C-terminal YFP fusions were expressed from a galactose-inducible promoter in yeast. Images for each construct show YFP fluorescence (left) and DIC image (right).

The minimal deleterious unit of HopAA1-1 is more conserved than the region of the C terminus not needed for biological activity.

Our observations above indicate that HopAA1-1 residues 41-416 represent the minimal unit for biological activity and that the C-terminal region (particularly 417-471) may modify localization but without a major effect on biological activity. We next asked if these functionally distinct regions are similarly conserved in the two HopAA1-1 homologs that also have been studied: *P. syringae* pv. *syringae* B728a HopAA1 and *P. fluorescens* Q8r1-96 RopAA. HopAA1-1_{41-416} shows 87% similarity with HopAA1 and 45% similarity with RopAA. However, HopAA1-$1_{417-486}$ shows only 75% similarity with HopAA1 and no detectable similarity with RopAA (Altschul et al., 1990). It is also noteworthy that alignment of HopAA1-1, HopAA1, and RopAA with CLUSTAL reveals that at the location of the LRA tripeptide essential for HopAA1-1 localization and biological properties, RopAA has the similar amino acids LRS.

DISCUSSION

We have used a defined series of HopAA1-1 variants and assays for subcellular localization and biological activity in *N. benthamiana* to gain evidence that this ancient *P. syringae* effector targets the endomembrane system and peroxisomes in plants. The series of HopAA1-1 variants showed similar changes in subcellular localization and cell death elicitation in yeast. The simplest interpretation of our observations is that HopAA1-1 targets a factor conserved in plants and yeast that is involved in interactions

between the endomembrane system and organelles, and by mechanisms awaiting elucidation, this interaction elicits cell death in eukaryotes while also promoting bacterial virulence.

The functional regions revealed by our analysis are summarized in Figure 3.9. The overriding finding is that, with the exception of T3SS-targeting signals predicted in the first 40 of the 486 amino acids in the protein, all of the major biological properties of HopAA1-1 require the region between residues 41 and 416, as well as the native LRA tripeptide in the putative GAP domain at position 120. These major biological properties are localization to organelles/endomembranes and cell death elicitation, and they are observed in both *N. benthamiana* and yeast. Further deletion of either the N- or C-terminus of the protein or substituting the FEN polymorphism found in HopAA1-2 for the LRA in HopAA1-1 completely eliminates all of these properties.

We have also observed a secondary localization behavior associated with C-terminal truncations occurring between residues 471 and 416. Such intermediate truncations produce an apparent shift of some of the HopAA1-1 from the cell periphery to the ER throughout the cell, and this shift is observed in both *N. benthamiana* and yeast. This shift and all localization patterns we observed were documented in more detail in *N. benthamiana* mesophyll cells, which are much larger than yeast cells. In *N. benthamiana*, wild-type HopAA1-1 localizes to the surface of peroxisomes and the periphery of cells. The labeling of the peroxisome surface by HopAA1-1-YFP clearly contrasts with the labeling of the peroxisome matrix by the mCherry-px-rk marker, and it also contrasts with the apparent labeling of the matrix by HopAA1-$1_{LRA\text{-}FEN}$-YFP carrying the PTS1 peroxisomal targeting signal.

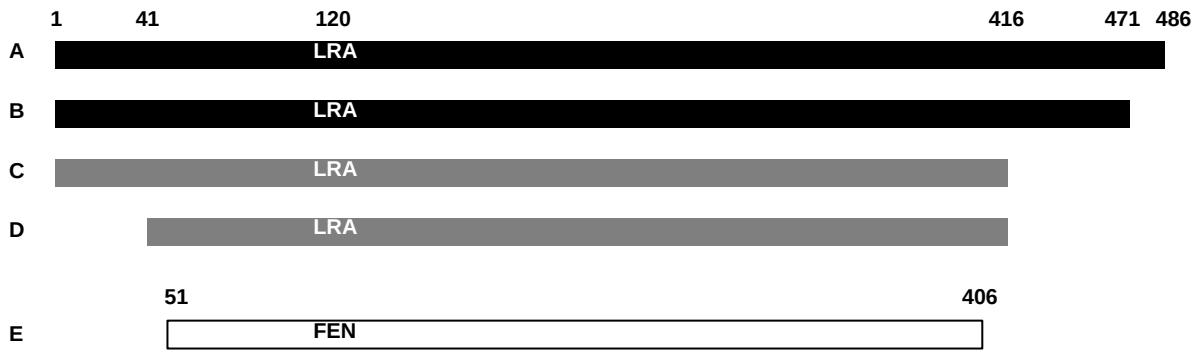

Figure 3.9. Diagram of minimal properties of HopAA1-1 needed for the biological activities reported above. The *Pto* DC3000 HopAA1-1 variants denoted with filled bars all show an ability to localize to the surface of peroxisomes and cause cell death in *N. benthamiana* leaf cells. Wild-type HopAA1-1 (A) and HopAA1-11-471 (B) also accumulate in the cell periphery (black bars). Deletion of HopAA1-1 residues between 416 and 471 produce a shift in localization from the cell periphery to the ER (C and D; gray bars); deletion of the first 41 residues (D) is expected to block targeting to the T3SS, but has no effect on localization of transiently expressed protein in *N. benthamiana*. Toxicity in yeast or *N. benthamiana*, virulence promotion, and apparent localization to peroxisomes and endomembranes is lost with either deletion of the N-terminal 51 residues, mutation of LRA to FEN, or deletion of the C-terminal 406 residues (E).

The labeling of the cell periphery by HopAA1-1-YFP appears too thick to exclusively involve the plasma membrane. In this regard, it is notable that HopAA1-1 variants with the intermediate C-terminal truncations, such as HopAA1-1_{1-436}-YFP, localize to both the ER and the surface of peroxisomes. Given that known ER associations include the plasma membrane as well peroxisomes and mitochondria (Elbaz and Schuldiner, 2011; Friedman and Voeltz, 2011), a primary interaction of HopAA1-1 with an ER-associated protein would be consistent with all of our observations, including the contradictory observations of mitochondrial localization in yeast and peroxisomal localization in *N. benthamiana*. The notion that HopAA1-1 localization is dependent upon interaction with a target protein in plants is also consistent with the lack of any apparent eukaryotic subcellular targeting signals in HopAA1-1 and with the strong impact of the LRA to FEN mutation in the putative GAP domain on localization in *N. benthamiana* cells. This impact includes allowing heterologous targeting signals to become functional.

We have no indication at this point of whether peroxisomes are the physiological target of HopAA1-1 activity in *N. benthamiana*. Models for peroxisome biogenesis in plants are evolving, but the ER clearly has a major role as the source peroxisomal lipids and some peroxisomal proteins (Hu et al., 2012). Peroxisomes are involved in the production of two phytohormones that impact *P. syringae*-plant interactions, indole acetic acid and jasmonic acid (Hu et al., 2012), and they also house the glucosinolate-activating PEN2 glycosyl hydrolase (Lipka et al., 2005; Bednarek et al., 2009; Clay et

al., 2009) and hydrogen peroxide-generating glycolate oxidases, which are both important in nonhost resistance (Rojas et al., 2012).

One concern about our observations is that the localization patterns in *N. benthamiana* cells could be an artifact of overexpression. One indicator that the observed localization is physiological is that similar shifts in localization pattern were seen with the intermediate C-terminal truncation and the LRA-FEN mutation in *N. benthamiana* and yeast. Another indicator that the observed localization is physiological is that progressive C-terminal truncations of HopAA1-1 had similar effects on cell killing in yeast and *N. benthamiana* and on promoting the virulence of *Pto* DC3000 mutant CUCPB6031 when naturally delivered by the pathogen T3SS. The latter assay, which involves more natural entry of the pathogen through dip inoculation further points to the importance of HopAA1-1 early in the infection process, and it also provides an important system for future investigation of HopAA1-1 activity in plants.

HopAA1-1 shares with the other CEL effectors, HopM1 and AvrE, a general ability to promote cell death in plants independently of any known *R* genes, as indicated by phenotypes associated with mutations and heterologous expression (Badel et al., 2006; Wei et al., 2007; Wroblewski et al., 2009). The *Pantoea stewartii* subsp. *stewartii* AvrE homolog, WtsE, also has deleterious effects when expressed in yeast and a variety of plants, and deletion derivatives that failed to elicit plant cell death also failed to promote *P. stewartii* subsp. *stewartii* virulence (Ham et al., 2008). Thus, the CEL effectors may all have targets associated with the endomembrane system in eukaryotes, which is an important participant in plant innate immunity (Kwon et al., 2008; Bednarek et al., 2010). The next challenge is identifying the molecular partner for

HopAA1-1, which is presumably present in both yeast and plants and should provide clues to the multiple biological activities of this ancient effector.

MATERIALS AND METHODS

Bacterial strains and growth conditions.

Bacterial strains and plasmids are listed in Table S1. *P. syringae* strains were cultivated on King's B (KB) at 30°C (King et al., 1954). *E. coli* strains were cultivated on Luria-Burtani media (Hanahan, 1985). Yeast were cultured using the Yeast Nitrogen Base (YNB) and Dropout Bases (DOB) from MP Biomedical. Antibiotics were used at the following concentrations in µg/ml: rifampicin 50; spectinomycin 50; chloramphenicol 20; gentamycin 10 for plasmids, 5 for genomic integrants; kanamycin 50.

Construction of HopAA1-1 truncations.

Truncation of HopAA1-1 was performed by PCR using pCPP5107 as template. Oligo jnw028* was used as the forward primer to create truncations missing the T3SS signal peptide, and jnw10 for constructs containing the signal sequence. One of oligos of BKS1-9 was used as a reverse primer. PCR products were verified by

Table 3.1. Biological strains and plasmids used in this study

Designation	Genotype/Plasmid descrpition	Source
Escherichia coli		
DH5α	F–Φ80lacZΔM15 ΔlacZYA-argF)U169 deoR recA1 endA1 hsdR17 phoA supE44 thi-1 gyrA96 relA1 λ	Invitrogen
DB3.1	F–gyrA462 endA1Δ (sr1-recA) mcrB mrr hsdS20 supE44 ara-14 galK2 lacY1 proA2 rpsL20 xyl-5 λ–leu mtl-1	Invitrogen
Top10	F- mcrA (mrr-hsdRMS-mcrBC) 80lacZM15 lacX74 recA1 ara139 (ara-leu)7697 galU galK rpsL (Sm^R) endA1 nupG	Invitrogen[
Agrobacterium tumefaciens		
GV3101	Wild type; Rif^R, Gm^R	(Weigel and Glazebrook, 2002)
Pseudomonas syringae pv. tomato		
CUCPB6030	DC3000 Δ*hopU1-hopF2* Δ*hopC1-hopH1*::FRT Δ*hopD1-hopR1*::FRT Δ*avrE-shcN*::*shcM-hopM1* EEL::(pCPP6219 *hopE1 hopAM1-1 hopG1*) Δ*hopAA1-2-hopG1*::FRT Δ*hopI1* Δ*hopAM1-1* Δ*hopAF1*::FRT Δ*avrPto* Δ*hopK1* Δ*hopB1* Δ*hopE1* Δ*hopA1*::FRT Δ*hopY1*::FRTSpR $pDC3000A^-$ $pDC3000B^-$, Rif^R	(Cunnac et al., 2011)
Saccharomyces cerevisiae		
BY4741A (KFY715)	*MAT*a; *his3*Δ*1*; *leu2*Δ*0*; *met15*Δ*0*; *ura3*Δ*0*	(Brachmann et al., 1998)
Plasmids		
pEarleyGate101	C-terminal YFP fusions driven by 35S promoter, Km^R	(Earley et al., 2006)
pCPP5107	pENTR/SD/D-TOPO::*hopAA1-1*, Km^R	(Munkvold et al., 2008)
pCPP5470	pENTR/SD/D-TOPO::$hopAA1\text{-}1_{1\text{-}436}$, Km^R	(Munkvold et al., 2008)
pCPP5471	pENTR/SD/D-TOPO::$hopAA1\text{-}1_{1\text{-}386}$, Km^R	(Munkvold et al., 2008)
pCPP5156	pENTR/SD/D-TOPO::$hopAA1\text{-}1_{41\text{-}486}$, Km^R	(Munkvold et al., 2008)
pCPP5628	pENTR/SD/D-TOPO::$hopAA1\text{-}1_{51\text{-}486}$, Km^R	(Munkvold et al., 2008)
pCPP5995	pENTR/SD/D-TOPO::$hopAA1\text{-}1_{\text{LRA-FEN}}$, Km^R	(Munkvold et al., 2008)

Table 3.1. Continued.

pCPP6358	pENTR/SD/D-TOPO::*hopAA1-1*$_{41-426}$, Km^R	This study
pCPP6359	pENTR/SD/D-TOPO::*hopAA1-1*$_{41-416}$, Km^R	This study
pCPP6360	pENTR/SD/D-TOPO::*hopAA1-1*$_{41-406}$, Km^R	This study
pCPP6361	pENTR/SD/D-TOPO::*hopAA1-1*$_{41-396}$, Km^R	This study
pCPP6362	pENTR/SD/D-TOPO::*hopAA1-1*$_{41-481}$, Km^R	This study
pCPP6363	pENTR/SD/D-TOPO::*hopAA1-1*$_{41-476}$, Km^R	This study
pCPP6364	pENTR/SD/D-TOPO::*hopAA1-1*$_{41-471}$, Km^R	This study
pCPP6365	pENTR/SD/D-TOPO::*hopAA1-1*$_{41-466}$, Km^R	This study
pCPP6366	pENTR/SD/D-TOPO::*hopAA1-1*$_{41-461}$, Km^R	This study
pCPP6401	pENTR/SD/D-TOPO::*hopAA1-1*$_{1-426}$, Km^R	This study
pCPP6402	pENTR/SD/D-TOPO::*hopAA1-1*$_{1-416}$, Km^R	This study
pCPP6403	pENTR/SD/D-TOPO::*hopAA1-1*$_{1-406}$, Km^R	This study
pCPP6404	pENTR/SD/D-TOPO::*hopAA1-1*$_{1-396}$, Km^R	This study
pCPP6405	pCPP5372:: *hopAA1-1*$_{1-426}$, Gm^R	This study
pCPP6406	pCPP5372:: *hopAA1-1*$_{1-416}$, Gm^R	This study
pCPP6407	pCPP5372:: *hopAA1-1*$_{1-406}$, Gm^R	This study
pCPP6408	pCPP5372:: *hopAA1-1*$_{1-396}$, Gm^R	This study
pCPP5372	pBBR1MCS containing *avrPto* promoter (P_{avrPto}), Gateway reading frame B cassette, and C-terminal HA tag, Gm^R, Cm^R	(Oh et al., 2007)
pCPP6349	pYES-DEST52-YFP, Ap^R, Cm^R, Ura3	This study
pCPP6409	pCPP6349::*hopAA1-1*$_{41-416}$, Ap^R, Ura3	This study
pCPP6410	pCPP6349::*hopAA1-1*$_{41-406}$, Ap^R, Ura3	This study
pCPP6411	pCPP6349::*hopAA1-14*$_{41-471}$, Ap^R, Ura3	This study
pCPP6412	pCPP6349::*hopAA1-14*$_{41-466}$, Ap^R, Ura3	This study
pCPP6293	pCPP6349::*hopAA1-1*, Ap^R, Ura3	This study
pCPP6294	pCPP6349::*hopAA1-1*$_{stop}$, Ap^R, Ura3	This study
pCPP6295	pCPP6349::*hopAA1-1*$_{N436}$, Ap^R, Ura3	This study

Table 3.1. Continued.

pCPP6296	pCPP6349::*hopAA1-1*$_{N386}$, Ap^R, Ura3	This study
pCPP6299	pCPP6349::*hopAA1-1*$_{LRA-FEN}$, Ap^R, Ura3	This study
pCPP6308	pEarleyGate101-SpR, Sp^R, Cm^R	This study
pCPP6309	pEarleyGate101-SpR-PTS1, Sp^R, Cm^R	This study
pCPP6310	pEarleyGate101-SpR-NLS, Sp^R, Cm^R	This study
pCPP6320	pEarleyGate101-SpR-StrepII, Sp^R, Cm^R	This study
pCPP6380	pCPP6320::*hopAA1-1*$_{41-426}$, Sp^R	This study
pCPP6381	pCPP6320::*hopAA1-1*$_{41-416}$, Sp^R	This study
pCPP6382	pCPP6320::*hopAA1-1*$_{41-406}$, Sp^R	This study
pCPP6383	pCPP6320::*hopAA1-1*$_{41-396}$, Sp^R	This study
pCPP6384	pCPP6320::*hopAA1-1*$_{41-481}$, Sp^R	This study
pCPP6385	pCPP6320::*hopAA1-1*$_{41-476}$, Sp^R	This study
pCPP6386	pCPP6320::*hopAA1-1*$_{41-471}$, Sp^R	This study
pCPP6387	pCPP6320::*hopAA1-1*$_{41-466}$, Sp^R	This study
pCPP6388	pCPP6320::*hopAA1-1*$_{41-461}$, Sp^R	This study
pCPP6389	pCPP6320::*hopAA1-1*, Sp^R	This study
pCPP6390	pCPP6320::*hopAA1-1*$_{1-436}$, Sp^R	This study
pCPP6391	pCPP6320::*hopAA1-1*$_{1-386}$, Sp^R	This study
pCPP6392	pCPP6320::*uidA*, Sp^R	This study
pCPP6262	pCPP6308::*hopAA1-1*, Sp^R	This study
pCPP6263	pCPP6308::*hopAA1-1*$_{stop}$, Sp^R	This study
pCPP6264	pCPP6308::*hopAA1-1*$_{41-486}$, Sp^R	This study
pCPP6265	pCPP6308::*hopAA1-1*$_{51-486}$, Sp^R	This study
pCPP6266	pCPP6308::*hopAA1-1*$_{1-436}$, Sp^R	This study
pCPP6267	pCPP6308::*hopAA1-1*$_{1-386}$, Sp^R	This study
pCPP6268	pCPP6308::*hopAA1-1*$_{LRA-FEN}$, Sp^R	This study
pCPP6269	pCPP6308::*hopAA1-2*, Sp^R	This study
px-rk	Peroxisomal marker, Km^R	(Nelson et al., 2007)
er-rk	Endoplasmic reticulum marker, Km^R	(Nelson et al., 2007)
mt-rk	Mitochondrial marker, Km^R	(Nelson et al., 2007)
g-rk	Golgi body marker, Km^R	(Nelson et al., 2007)
pCPP6324	pCPP6309::*hopAA1-1*$_{stop}$, Sp^R	This study
pCPP6311	pCPP6309::*hopAA1-1*, Sp^R	This study
pCPP6312	pCPP6309::*hopAA1-1*$_{1-436}$, Sp^R	This study
pCPP6313	pCPP6309::*hopAA1-1*$_{LRA-FEN}$, Sp^R	This study
pCPP6314	pCPP6309::*uidA*, Sp^R	This study
pCPP6315	pCPP6310::*hopAA1-1*$_{stop}$, Sp^R	This study
pCPP6316	pCPP6310::*hopAA1-1*, Sp^R	This study

Table 3.1. Continued.

pCPP6317	pCPP6310::*hopAA1-1*$_{1\text{-}436}$, Sp^R	This study
pCPP6318	pCPP6310::*hopAA1-1*$_{LRA\text{-}FEN}$, Sp^R	This study
pCPP6319	pCPP6310::*uidA*, Sp^R	This study

electrophoresis, TOPO cloned into pENTR SD/D-TOPO using Invitrogen kit K2420, then the plasmid inserts sequenced at the Cornell University Life Sciences Core Laboratories Center using HopAA1-1 specific primers (Table S2). These were introduced into Gateway destination vectors with LR Clonase II (Invitrogen).

Plasmid constructions.

pEarleyGate 101 (Earley et al., 2006) was modified with the insertion of a FRT flanked spectinomycin resistance cassette from pCPP5242 amplified with primers p2255 and p2256 and inserted into the HindIII site of pEarleyGate 101, interrupting the kanamycin resistance gene, to create pCPP6308 (pEarleyGateS 101). pCPP6308 derivatives were created by amplifying the YFP gene from pEarleyGate 101 with primers containing C-terminal additions/replacements. pCPP6320 was created by replacing the AvrII-SpeI restriction site fragment in pCPP6308 with a PCR fragment amplified by primers jnw064 and jnw051. pCPP6309 was created by replacing the AvrII-SpeI restriction site fragment in pCPP6308 with a PCR fragment amplified by primers jnw052 and jnw051. pCPP6310 was created by replacing the AvrII-SpeI restriction site fragment in pCPP6308 with a PCR fragment amplified by primers jnw053 and jnw051.

pYES-DEST52 (Invitrogen) was modified for C-terminal YFP fusion through the insertion of a PCR product, amplified off of pEarleyGate101 by primers jnw019 and jnw020, into the ApaI restriction site through a partial digest, subsequent ligation, and screening for the desired insertion by restriction digest to create pCPP6349.

Table 3.2. Primers used in this study.

Primer Name	Sequence	Function
jnw028*	caccatggagataaatgcgattgccgattac	*hopAA1-1* F from amino acid residue 41, 5’ cacc for TOPO cloning
jnw10	caccatgcacatcaaccgacgcgt	*hopAA1-1* F, 5’ cacc for TOPO cloning
p2255	attagagctcgtgtaggctggagctgcttc	FRT cassette F with sacI site
p2256	attagagctccatatgaatatcctcctta	FRT cassette R with sacI site
jnw064	agggactagtcccgggtcttaattatttttcaaattgaggatgagaccaagcgtaatctggaacatcgtatggta	for YFP-HA-StrepII in pEarleyGate background
jnw052	agggactagtcccgggtcttaattaaagcttagaagcgtaatctggaacatcgtatgggta	C-terminal PTSI in pEarleyGate101
jnw051	aagtggtgcctagggtgagcaagg	AvrII site F on pEarleyGate101
jnw053	agggactagtcccgggtcttaattaaaccttacgtttcttcttaggagcgtaatctggaacatcgtatgggta	C-terminal SV40 nuclear localization sequence in pEarleyGate101
bks1	gtcggctacgtagcctgtggt	*hopAA1-1* R, removes last 60 amino acid residues
bks2	agtcgatttcaccgtgtcc	*hopAA1-1* R, removes last 70 amino acid residues
bks3	ctcggctttttcaccgcg	*hopAA1-1* R, removes last 80 amino acid residues
bks4	cagcgcggccgtggtcc	*hopAA1-1* R, removes last 90 amino acid residues
bks5	aaacggtatttcacttggagaagccgc	*hopAA1-1* R, removes last 5 amino acid residues
bks6	tggagaagccgccgtgccccc	*hopAA1-1* R, removes last 10 amino acid residues
bks7	gccccctcttctatatcagcttc	*hopAA1-1* R, removes last 15 amino acid residues
bks8	atcagcttcacgagccgggcg	*hopAA1-1* R, removes last 20 amino acid residues
bks9	cgggcgttgacgcaggttattgac	*hopAA1-1* R, removes last 25 amino acid residues
jnw019	gagggcccagcaagggcgaggagctgttcac	apaI site YFP integration into pYES-DEST52 F
jnw020	gagggcccttagtacagctcgtccatgccgagag	apaI site YFP integration into pYES-DEST52 R
aa1-1seq1002f	gcaatgggtgcggtaagaag	Sequencing, *hopAA1-1* specific
aa1-1seq1f	atgcacatcaaccgacgcgtc	Sequencing, *hopAA1-1* specific

Table 3.2. Continued.

aa1-1seq401f	tgcagcctgcgatcaacaaggg	Sequencing, *hopAA1-1* specific
aa1-1seq1061r	cctgcaaagccacccgcca	Sequencing, *hopAA1-1* specific
aa1-1seq1461r	ttacgaccgcataggccgaaacg	Sequencing, *hopAA1-1* specific
aa1-1seq201r	ccatcagccgaatcggccg	Sequencing, *hopAA1-1* specific
aa1-1seq1241f	acggtgaaatcgactgcatccagt	Sequencing, *hopAA1-1* specific

Plant bioassays.

A. tumefaciens strains were grown overnight at 30°C in liquid LB media with selection for the plasmid marker used. Cultures were washed twice by centrifugation and resuspended in sterile 10mm MES 10 mm $MgCl_2$ pH 5.6 at a final concentration of OD_{600} 0.4 then spiked with acetosyringone to 150 µM. Spiked cultures were incubated at 30°C with shaking for 3 to 4h, then were either mixed equally with a co-inoculum strain or diluted to OD_{600} 0.2 with sterile media before inoculating into *N. benthamiana* leaves with a 1ml blunt syringe.

Bacteria were resuspended at approximately 1 x 10^8 cfu/ml, then diluted 1/100 into 1L of water with 10mM $MgCl_2$ and 0.02% Silwet L-77 (Lehle Seeds). 4 to 5 week post-transplantation *N. benthamiana* plants were inverted and the leaves submerged in the bacterial suspension for 30 s with gentle agitation. Symptoms were allowed to develop for 5 days with 16 h light and approximately 80 to 90% humidity.

Yeast growth inhibition assay.

Yeast were grown in liquid broth using yeast media from MP Biomedicals. Yeast were grown in YNB w/ ammonium sulfate supplemented either with complete supplemental media (CSM) or CSM without uracil (CSM –URA). The day before protein expression, yeast were inoculated into CSM –URA with 2% glucose then incubated overnight with shaking at 30°C. For protein expression, yeast cultures were washed twice and then resuspended in CSM –URA with 2% raffinose at an OD_{600} of 0.4 and for 2-3 h with shaking at 30°C. These cultures were then spiked to a final concentration of

2% galactose to induce protein expression. Cells were harvested or imaged 4 h post induction.

Imaging techniques.

Micrographs were taken with a Leica TCS SP5 confocal microscope at the Boyce Thompson Institute for Plant Research Plant Cell Imaging Center. YFP excitation was at 514nm with an emission spectrum captured from 524-549nm. mCherry excitation was at 561 nm with an emission spectrum captured from 600-625 nm. Chlorophyll autofluorescence was captured by excitation at 514nm with an emission spectrum captured from 653-695 nm (data not shown, used for reference in identifying cellular structures). Images have three fold line averaging. Representative images of consistent phenomena are shown. Plants were imaged between 33-40 hpi before the onset of cell death but after sufficient protein accumulation.

Immunoblot analyses.

Western blots were used to confirm correct HopAA1-1 size. For plants, two 1 cm leaf discs were ground in 100 µl 8 M urea, centrifuged, then mixed with loading buffer, run out on a gel, and transferred to an immobilon membrane (Millipore). HA-tag detection was done with Rat Anti-HA monoclonal (Roche) and Goat anti-rat AP conjugate. HopAA1-1 detection was done with rabbit polyclonal anti-hopAA1-1 and sheep anti-rabbit AP conjugate. StrepII tag detection was done with Strep-Tactin AP conjugate (IBA GmbH).

REFERENCES

Alfano, J.R., Charkowski, A.O., Deng, W.-L., Badel, J.L., Petnicki-Ocwieja, T., van Dijk, K., and Collmer, A. 2000. The *Pseudomonas syringae* Hrp pathogenicity island has a tripartite mosaic structure composed of a cluster of type III secretion genes bounded by exchangeable effector and conserved effector loci that contribute to parasitic fitness and pathogenicity in plants. Proc Natl Acad Sci USA 97:4856-4861.

Almeida, N.F., Yan, S., Lindeberg, M., Studholme, D.J., Schneider, D.J., Condon, B., Liu, H., Viana, C.J., Warren, A., Evans, C., Kemen, E., MacLean, D., Angot, A., Martin, G.B., Jones, J.D., Collmer, A., Setubal, J.C., and Vinatzer, B.A. 2009. A draft genome sequence of *Pseudomonas syringae* pv. *tomato* strain T1 reveals a repertoire of type III related genes significantly divergent from that of *Pseudomonas syringae* pv. *tomato* strain DC3000. Mol Plant-Microbe Interact 22:52-62.

Altschul, S.F., Gish, W., Miller, W., Myers, E.W., and Lipman, D.J. 1990. Basic local alignment search tool. J Mol Biol 215:403-410.

Badel, J.L., Charkowski, A.O., Deng, W.-L., and Collmer, A. 2002. A gene in the *Pseudomonas syringae* pv. *tomato* Hrp pathogenicity island conserved effector locus, *hopPtoA1*, contributes to efficient formation of bacterial colonies in planta and is duplicated elsewhere in the genome. Mol Plant-Microbe Interact 15:1014-1024.

Badel, J.L., Shimizu, R., Oh, H.-S., and Collmer, A. 2006. A *Pseudomonas syringae* pv. *tomato avrE1*/*hopM1* mutant is severely reduced in growth and lesion formation in tomato. Mol Plant Microbe Interact 19:99-111.

Baltrus, D.A., Nishimura, M.T., Romanchuk, A., Chang, J.H., Mukhtar, M.S., Cherkis, K., Roach, J., Grant, S.R., Jones, C.D., and Dangl, J.L. 2011. Dynamic evolution of pathogenicity revealed by sequencing and comparative genomics of 19 *Pseudomonas syringae* isolates. PLoS Pathog 7:e1002132.

Bednarek, P., Kwon, C., and Schulze-Lefert, P. 2010. Not a peripheral issue: secretion in plant-microbe interactions. Curr Opin Plant Biol 13:378-387.

Bednarek, P., Pislewska-Bednarek, M., Svatos, A., Schneider, B., Doubsky, J., Mansurova, M., Humphry, M., Consonni, C., Panstruga, R., Sanchez-Vallet, A., Molina, A., and Schulze-Lefert, P. 2009. A glucosinolate metabolism pathway in living plant cells mediates broad-spectrum antifungal defense. Science 323:101-106.

Block, A., and Alfano, J.R. 2011. Plant targets for *Pseudomonas syringae* type III effectors: virulence targets or guarded decoys? Curr Opin Microbiol 14:39-46.

Block, A., Guo, M., Li, G., Elowsky, C., Clemente, T.E., and Alfano, J.R. 2010. The *Pseudomonas syringae* type III effector HopG1 targets mitochondria, alters plant development, and suppresses plant innate immunity. Cell Microbiol 12:318–330.

Boller, T., and Felix, G. 2009. A renaissance of elicitors: perception of microbe-associated molecular patterns and danger signals by pattern-recognition receptors. Annu Rev Plant Biol 60:379-406.

Brachmann, C.B., Davies, A., Cost, G.J., Caputo, E., Li, J., Hieter, P., and Boeke, J.D. 1998. Designer deletion strains derived from *Saccharomyces cerevisiae* S288C: a useful set of strains and plasmids for PCR-mediated gene disruption and other applications. Yeast 14:115-132.

Clay, N.K., Adio, A.M., Denoux, C., Jander, G., and Ausubel, F.M. 2009. Glucosinolate metabolites required for an *Arabidopsis* innate immune response. Science 323:95-101.

Cunnac, S., Lindeberg, M., and Collmer, A. 2009. *Pseudomonas syringae* type III secretion system effectors: repertoires in search of functions. Curr Opin Microbiol 12:53-60.

Cunnac, S., Chakravarthy, S., Kvitko, B.H., Russell, A.B., Martin, G.B., and Collmer, A. 2011. Genetic disassembly and combinatorial reassembly identify a minimal functional repertoire of type III effectors in *Pseudomonas syringae*. Proc Natl Acad Sci USA 108:2975-2980.

Cuppels, D.A. 1986. Generation and characterization of Tn*5* insertion mutations in *Pseudomonas syringae* pv. *tomato*. Appl Environ Microbiol 51:323-327.

DebRoy, S., Thilmony, R., Kwack, Y.B., Nomura, K., and He, S.Y. 2004. A family of conserved bacterial effectors inhibits salicylic acid-mediated basal immunity and promotes disease necrosis in plants. Proc Natl Acad Sci U S A 101:9927-9932.

Earley, K.W., Haag, J.R., Pontes, O., Opper, K., Juehne, T., Song, K., and Pikaard, C.S. 2006. Gateway-compatible vectors for plant functional genomics and proteomics. Plant J 45:616-629.

Elbaz, Y., and Schuldiner, M. 2011. Staying in touch: the molecular era of organelle contact sites. Trends Biochem Sci 36:616-623.

Friedman, J.R., and Voeltz, G.K. 2011. The ER in 3D: a multifunctional dynamic membrane network. Trends Cell Biol 21:709-717.

Ham, J.H., Majerczak, D., Ewert, S., Sreerekha, M.V., Mackey, D., and Coplin, D. 2008. WtsE, an AvrE-family type III effector protein of *Pantoea stewartii* subsp. *stewartii*, causes cell death in non-host plants. Mol Plant Pathol 9:633-643.

Ham, J.H., Majerczak, D.R., Nomura, K., Mecey, C., Uribe, F., He, S.Y., Mackey, D., and Coplin, D.L. 2009. Multiple activities of the plant pathogen type III effector proteins WtsE and AvrE require WxxxE motifs. Mol Plant Microbe Interact 22:703-712.

Hanahan, D. 1985. Techniques for transformation of *E. coli*. Pages 109-135 in: DNA Cloning: A Practical Approach, D.M. Glover, ed. IRL Press, Oxford, United Kingdom.

Hodel, M.R., Corbett, A.H., and Hodel, A.E. 2001. Dissection of a nuclear localization signal. J Biol Chem 276:1317-1325.

Hu, J., Baker, A., Bartel, B., Linka, N., Mullen, R.T., Reumann, S., and Zolman, B.K. 2012. Plant peroxisomes: biogenesis and function. Plant Cell 24:2279-2303.

Jelenska, J., Yao, N., Vinatzer, B.A., Wright, C.M., Brodsky, J.L., and Greenberg, J.T. 2007. A J domain virulence effector of *Pseudomonas syringae* remodels host chloroplasts and suppresses defenses. Curr Biol 17:499-508.

Jones, J.D., and Dangl, J.L. 2006. The plant immune system. Nature 444:323-329.

King, E.O., Ward, M.K., and Raney, D.E. 1954. Two simple media for the demonstration of pyocyanin and fluorescin. J Lab Clin Med 44:301-307.

Kwon, C., Bednarek, P., and Schulze-Lefert, P. 2008. Secretory pathways in plant immune responses. Plant Physiol 147:1575-1583.

Lee, J., Teitzel, G.M., Munkvold, K., del Pozo, O., Martin, G.B., Michelmore, R.W., and Greenberg, J.T. 2012. Type III secretion and effectors shape the survival and growth pattern of *Pseudomonas syringae* on leaf surfaces. Plant Physiol 158:1803-1818.

Li, X., Lin, H., Zhang, W., Zou, Y., Zhang, J., Tang, X., and Zhou, J.M. 2005. Flagellin induces innate immunity in nonhost interactions that is suppressed by *Pseudomonas syringae* effectors. Proc Natl Acad Sci U S A 102:12990-12995.

Lipka, V., Dittgen, J., Bednarek, P., Bhat, R., Wiermer, M., Stein, M., Landtag, J., Brandt, W., Rosahl, S., Scheel, D., Llorente, F., Molina, A., Parker, J., Somerville, S., and Schulze-Lefert, P. 2005. Pre- and postinvasion defenses both contribute to nonhost resistance in *Arabidopsis*. Science 310:1180-1183.

Mavrodi, D.V., Joe, A., Mavrodi, O.V., Hassan, K.A., Weller, D.M., Paulsen, I.T., Loper, J.E., Alfano, J.R., and Thomashow, L.S. 2011. Structural and functional analysis of the type III secretion system from *Pseudomonas fluorescens* Q8r1-96. J Bacteriol 193:177-189.

Munkvold, K.R., Martin, M.E., Bronstein, P.A., and Collmer, A. 2008. A survey of the *Pseudomonas syringae* pv. *tomato* DC3000 type III secretion system effector repertoire reveals several effectors that are deleterious when expressed in *Saccharomyces cerevisiae*. Mol Plant-Microbe Interact 21:490-502.

Munkvold, K.R., Russell, A.B., Kvitko, B.H., and Collmer, A. 2009. *Pseudomonas syringae* pv. *tomato* DC3000 type III effector HopAA1-1 functions redundantly with chlorosis-promoting factor PSPTO4723 to produce bacterial speck lesions in host tomato. Mol Plant Microbe Interact 22:1341–1355.

Nelson, B.K., Cai, X., and Nebenfuhr, A. 2007. A multicolored set of *in vivo* organelle markers for co-localization studies in Arabidopsis and other plants. Plant J 51:1126-1136.

Nomura, K., Debroy, S., Lee, Y.H., Pumplin, N., Jones, J., and He, S.Y. 2006. A bacterial virulence protein suppresses host innate immunity to cause plant disease. Science 313:220-223.

Nomura, K., Mecey, C., Lee, Y.N., Imboden, L.A., Chang, J.H., and He, S.Y. 2011. Effector-triggered immunity blocks pathogen degradation of an immunity-associated vesicle traffic regulator in Arabidopsis. Proc Natl Acad Sci U S A 108:10774-10779.

O'Brien, H.E., Thakur, S., and Guttman, D.S. 2011. Evolution of plant pathogenesis in *Pseudomonas syringae*: a genomics perspective. Annu Rev Phytopathol 49:269-289.

Oh, H.-S., Kvitko, B.H., Morello, J.E., and Collmer, A. 2007. *Pseudomonas syringae* lytic transglycosylases co-regulated with the type III secretion system contribute to the translocation of effector proteins into plant cells. J Bacteriol 189:8277-8289.

Rodriguez-Herva, J.J., Gonzalez-Melendi, P., Cuartas-Lanza, R., Antunez-Lamas, M., Rio-Alvarez, I., Li, Z., Lopez-Torrejon, G., Diaz, I., Del Pozo, J.C., Chakravarthy,

S., Collmer, A., Rodriguez-Palenzuela, P., and Lopez-Solanilla, E. 2012. A bacterial cysteine protease effector protein interferes with photosynthesis to suppress plant innate immune responses. Cell Microbiol 14:669-681.

Rojas, C.M., Senthil-Kumar, M., Wang, K., Ryu, C.M., Kaundal, A., and Mysore, K.S. 2012. Glycolate oxidase modulates reactive oxygen species-mediated signal transduction during nonhost resistance in Nicotiana benthamiana and Arabidopsis. Plant Cell 24:336-352.

Schechter, L.M., Roberts, K.A., Jamir, Y., Alfano, J.R., and Collmer, A. 2004. *Pseudomonas syringae* type III secretion system targeting signals and novel effectors studied with a Cya translocation reporter. J Bacteriol 186:543-555.

Shan, L., He, P., Li, J., Heese, A., Peck, S.C., Nurnberger, T., Martin, G.B., and Sheen, J. 2008. Bacterial effectors target the common signaling partner BAK1 to disrupt multiple MAMP receptor-signaling complexes and impede plant immunity. Cell Host Microb 4:17-27.

Shan, L.B., Thara, V.K., Martin, G.B., Zhou, J.M., and Tang, X.Y. 2000. The *Pseudomonas* AvrPto protein is differentially recognized by tomato and tobacco and is localized to the plant plasma membrane. Plant Cell 12:2323-2337.

Subramani, S., Koller, A., and Snyder, W.B. 2000. Import of peroxisomal matrix and membrane proteins. Annu Rev Biochem 69:399-418.

Vinatzer, B.A., Teitzel, G.M., Lee, M.W., Jelenska, J., Hotton, S., Fairfax, K., Jenrette, J., and Greenberg, J.T. 2006. The type III effector repertoire of *Pseudomonas syringae* pv. *syringae* B728a and its role in survival and disease on host and non-host plants. Mol Microbiol 62:26-44.

Wei, C.-F., Kvitko, B.H., Shimizu, R., Crabill, E., Alfano, J.R., Lin, N.-C., Martin, G.B., Huang, H.-C., and Collmer, A. 2007. A *Pseudomonas syringae* pv. *tomato* DC3000 mutant lacking the type III effector HopQ1-1 is able to cause disease in the model plant *Nicotiana benthamiana*. Plant J 51:32-46.

Weigel, D., and Glazebrook, J. 2002. Arabidopsis: A Laboratory Manual. Cold Spring Harbor Laboratory.

Whalen, M.C., Innes, R.W., Bent, A.F., and Staskawicz, B.J. 1991. Identification of *Pseudomonas syringae* pathogens of *Arabidopsis* and a bacterial locus determining avirulence on both *Arabidopsis* and soybean. Plant Cell 3:49-59.

Worley, J.N., Russell, A.B., Wexler, A.G., Bronstein, P.A., Kvitko, B.H., Krasnoff, S.B., Munkvold, K.R., Swingle, B., Gibson, D.M., and Collmer, A. 2013. *Pseudomonas syringae* pv. *tomato* DC3000 CmaL (PSPTO4723), a DUF1330 family member, is needed to produce L-*allo*-isoleucine, a precursor for the phytotoxin coronatine. J Bacteriol 195:287-296.

Wroblewski, T., Caldwell, K.S., Piskurewicz, U., Cavanaugh, K.A., Xu, H., Kozik, A., Ochoa, O., McHale, L.K., Lahre, K., Jelenska, J., Castillo, J.A., Blumenthal, D., Vinatzer, B.A., Greenberg, J.T., and Michelmore, R.W. 2009. Comparative large-scale analysis of interactions between several crop species and the effector repertoires from multiple pathovars of *Pseudomonas* and *Ralstonia*. Plant Physiol 150:1733-1749.

Wu, S., Lu, D., Kabbage, M., Wei, H.L., Swingle, B., Records, A.R., Dickman, M., He, P., and Shan, L. 2011. Bacterial effector HopF2 suppresses *Arabidopsis* innate immunity at the plasma membrane. Mol Plant-Microbe Interact 24:585-593.

CHAPTER 4

REASSEMBLY OF THE *PSEUDOMONAS SYRINGAE* PV. *TOMATO* DC3000 TYPE III EFFECTOR REPERTOIRE AND CORONATINE BIOSYNTHESIS COMPONENTS REVEALS RELATIVE CONTRIBUTIONS OF EFFECTORS AND THE PHYTOTOXIN CORONATINE TO PATHOGENESIS

INTRODUCTION

Pseudomonas syringae pv. *tomato* DC3000 (*Pto* DC3000) defeats plant defenses with the phytotoxin coronatine (COR) and ca. 28 effector (Hop or Avr) proteins that are injected into host cells by the type III secretion system (T3SS) (Buell et al., 2003; Cunnac et al., 2011; Geng et al., 2012; Zheng et al., 2012). *Pto* DC30000 is typical of *P. syringae* strains in producing a complex effector repertoire and at least one of several toxins (O'Brien et al., 2011). Phenotypic redundancy among effectors in a repertoire and between effector repertoires and phytotoxins has been a fundamental obstacle to investigating the role of either factor in pathogenesis because it masks phenotypes associated with their activity. The existence of functional overlap between effector repertoires and toxins is suggested by two observations from widely separate perspectives. First, *P. syringae* strains that have relatively small effector repertoires, such as *P. syringae* pv. *syringae* B728a, produce particularly severe toxins (Baltrus et al., 2012). Second, the use of *Pto* DC3000 mutants deficient in the T3SS machinery or

in the production of COR reveals considerable overlap in Arabidopsis transcriptome responses attributable to each factor (Thilmony et al., 2006).

Pto DC3000 is a pathogen of tomato, Arabidopsis, and *Nicotiana benthamiana* (if effector gene *hopQ1-1* is deleted) (Wei et al., 2007), which has become a model for genetic dissection of the functions of effectors within a repertoire (Kvitko et al., 2009; Cunnac et al., 2011; Lindeberg et al., 2012) and for genetic dissection of COR production factors (Peñaloza-Vázquez et al., 2000; Brooks et al., 2004; Sreedharan et al., 2006; Worley et al., 2013). A majority of the *Pto* DC3000 effectors have a demonstrable ability to suppress one or both levels of plant innate immunity, which are pathogen- or microbe-associated molecular pattern-triggered immunity (PTI or MTI) and effector-triggered immunity (ETI), and several of these effectors also have been shown to promote bacterial growth in various hosts (Block et al., 2008; Cunnac et al., 2009; Guo et al., 2009). However, no single effector is indispensable for pathogenicity, and entire genomic clusters of multiple effector genes can be deleted without significantly affecting virulence (Wei et al., 2007; Kvitko et al., 2009; Cunnac et al., 2011). Similarly, COR has multiple immune-suppressive effects (Geng et al., 2012), but COR-deficient *Pto* DC3000 mutants retain basic pathogenicity (Brooks et al., 2004), and many field isolates of *P. syringae* pv. *tomato* lack the COR biosynthesis gene region (Almeida et al., 2009; Cai et al., 2011).

However, some effectors may be more important than others. For example, two redundant effector groups (REGs) that are particularly important for virulence have been identified in *Pto* DC3000: HopM1/AvrE/HopR1 and AvrPto/AvrPtoB (Kvitko et al., 2009). The *hopM1* and *avrE* genes are encoded in the conserved effector locus (CEL) (Alfano

et al., 2000). A strong reduction in virulence is observed with the deletion of multiple genes in a single REG, for example *avrPto* and *avrPtoB* (Lin and Martin, 2005; Kvitko et al., 2009). It is notable here that the REG concept has been useful in guiding the assembly of a minimal functional repertoire of *Pto* DC3000 effectors and in identifying novel immune suppressive activities of coronatine that are observable only in a *Pto* DC3000 ΔCEL mutant (Cunnac et al., 2011; Geng et al., 2012). Thus, genetics is becoming increasingly useful for dissecting the complex *Pto* DC3000 effector/coronatine virulence system.

Assays that involve different stages of pathogenesis or environmental conditions are also useful for observing phenotypes for virulence factors. For example, HopAM1 suppresses basal defenses but seems to have a particularly strong effect on plants under mild drought conditions (Goel et al., 2008), whereas HopAA1 and HopZ3 have a particular impact on epiphytic populations of *P. syringae* pv. *syringae* B728a (Lee et al., 2012). Similarly, the contribution of coronatine to the virulence of *Pto* DC3000 is much more evident when Arabidopsis plants are inoculated by dipping rather than by infiltration (Mittal and Davis, 1995). Finally, a study that provides the foundation for the present work reported that deletion of the *Pto* DC3000 CEL-encoded effector HopAA1-1 produced a significant phenotype (reduced numbers of lesions in tomato leaves) only when *cmaL* (PSPTO4723) was also deleted and only when bacteria were inoculated by dipping (Munkvold et al., 2009). As will be explained below, additional advances have been made in understanding the role of HopAA1-1 and CmaL.

HopAA1-1 shares several properties with the other CEL-encoded effectors, AvrE and HopM1. The genes for these ancient effectors were acquired as part of the Hrp

pathogenicity island (Alfano et al., 2000), and they are present (although sometimes disrupted) in all sequenced *P. syringae* genomes (Baltrus et al., 2011). They all have an ability to promote cell death in host and nonhost plants (Badel et al., 2006; Munkvold et al., 2008), are suggested (with varying degrees of evidence) to disrupt small G-protein signaling and to interact with the endomembrane system (Chapter 3). However, HopAA1-1 appears to promote an earlier stage in pathogenesis than AvrE and HopM1 (Badel et al., 2002; Lee et al., 2012)(Chapter 3).

Pto DC3000D28E has deletions affecting all 28 of the known, active effector genes and was constructed to facilitate the study effector functions individually or in customized, small sets (Cunnac et al., 2011). A derivative that will be referred to here as DC3000D28E+8 (AvrPtoB, HopM1, HopE1, HopG1, HopAM1, AvrE, HopAA1-1, HopN1) has a minimal functional repertoire needed to produce disease symptoms and near wild-type levels of growth following inoculation by infiltration into *N. benthamiana* leaves (Cunnac et al., 2011).

We have recently discovered that *Pto* DC3000D28E is deficient in COR production (Worley et al., 2013). COR biosynthesis in *Pto* DC3000, *P. syringae* pv. *glycinea*, and a few other *P. syringae* pathovars can be conceptualized as directed by four distinct genetic regions: the *cor* genes encoding the regulatory machinery; the *cma* operon, which is adjacent to the *cor* genes and is responsible for the conversion of L-*allo*-isoleucine to coronamic acid (CMA); the *cfa* operon, which is located at various distances from the *cor-cma* genes and is responsible for coronafacic acid (CFA) biosynthesis and, ostensibly, the linkage of CMA and CFA by an amide bond to produce COR; and *cmaL*, a single gene located at various distances downstream of the *cma*

operon and required to produce L-*allo*-isoleucine (Bender et al., 1999b; Buell et al., 2003; Worley et al., 2013).

We discovered *cmaL* and its role in the production of L-*allo*-isoleucine accidently through deletion of effector gene cluster IX, in which the *cmaL* gene is imbedded, and through finding that a Δ*hopAA1-1*Δ*cmaL* double mutant has a reduced-lesion phenotype, as noted above (Munkvold et al., 2009; Worley et al., 2013). Importantly, because DC3000D28E lacks effector gene cluster IX and therefore *cmaL*, it produces only CFA rather than the COR holotoxin. CFA is a molecular mimic of jasmonic acid that weakly displays some of the activities of COR (Ishiga et al., 2010), and CMA is structurally similar to the ethylene precursor 1-aminocyclopropane-1-carboxylic-acid (ACC) (Bender et al., 1999a). Given the multiple activities of the COR holotoxin in promoting stomatal opening, suppressing salicylic acid-mediated signaling and other defense signaling, and enhancing cell death responses and pathogen persistence after infection (Kloek et al., 2001; Brooks et al., 2004; Melotto et al., 2006; Uppalapati et al., 2007; Geng et al., 2012), we decided to restore *cmaL* to DC3000D28E and investigate the performance of key DC3000D28E derivatives in both infiltration and dip inoculation assays in *N. benthamiana*.

Here we report that restoring *cmaL* to DC3000D28E derivatives enhances chlorotic and necrotic symptoms in infiltration-inoculated *N. benthamiana*, enables DC3000D28E to produce chlorotic specks in dip-inoculated *N. benthamiana*, and further documents the functional redundancy between COR and HopAA1-1 that is observed when bacteria enter leaves through stomata from the surface.

RESULTS

Restoring *cmaL* to *Pto* DC3000D28E derivatives with small sets of effectors strongly promotes chlorosis in infiltration-inoculated *N. benthamiana* leaves.

To restore CmaL and therefore COR production to DC3000D28E and various derivatives, a 1-kb fragment containing *cmaL* and adjacent sequences was integrated into the genomes of each strain at the *glmS* locus by Tn*7* mutagenesis (Choi and Schweizer, 2006). This 1-kb fragment contains a transcriptional start site (Filiatrault et al., 2011) and flanking regions that should contain any relevant regulatory information (Fig. 4.1). The DC3000D28E derivatives were chosen to test potential interplay between COR and various effectors in the minimal functional repertoire in the production of chlorosis. We had previously observed that *Pto* DC3000 T3SS-deficient strains retain sufficient ability to grow in *N. benthamiana* to produce COR-dependent chlorosis in areas inoculated by infiltration (Worley et al., 2013). We also had previously observed that DC3000D28E growth in *N. benthamiana* is less than that of T3SS-deficient DC3000 and that some growth can be restored to DC300028E by AvrPtoB but not by HopM1. Here we observed that restoring *cmaL*-dependent COR production enabled the DC300028E+AvrPtoB strain to produce chlorosis, but it did not have this effect with the DC300028E+HopM1 strain when strains were inoculated by syringe-infiltration at 1 x 10^5 cfu/ml (Fig. 4.2). In general, chlorosis intensity correlated with previously reported ability to grow, and DC3000D28E+8 also produced spreading chlorosis that is also observed in a *cmaL*-dependent manner with wild-type DC3000 (Worley et al., 2013). It is also noteworthy, that the DC3000D28E+8 strain produced

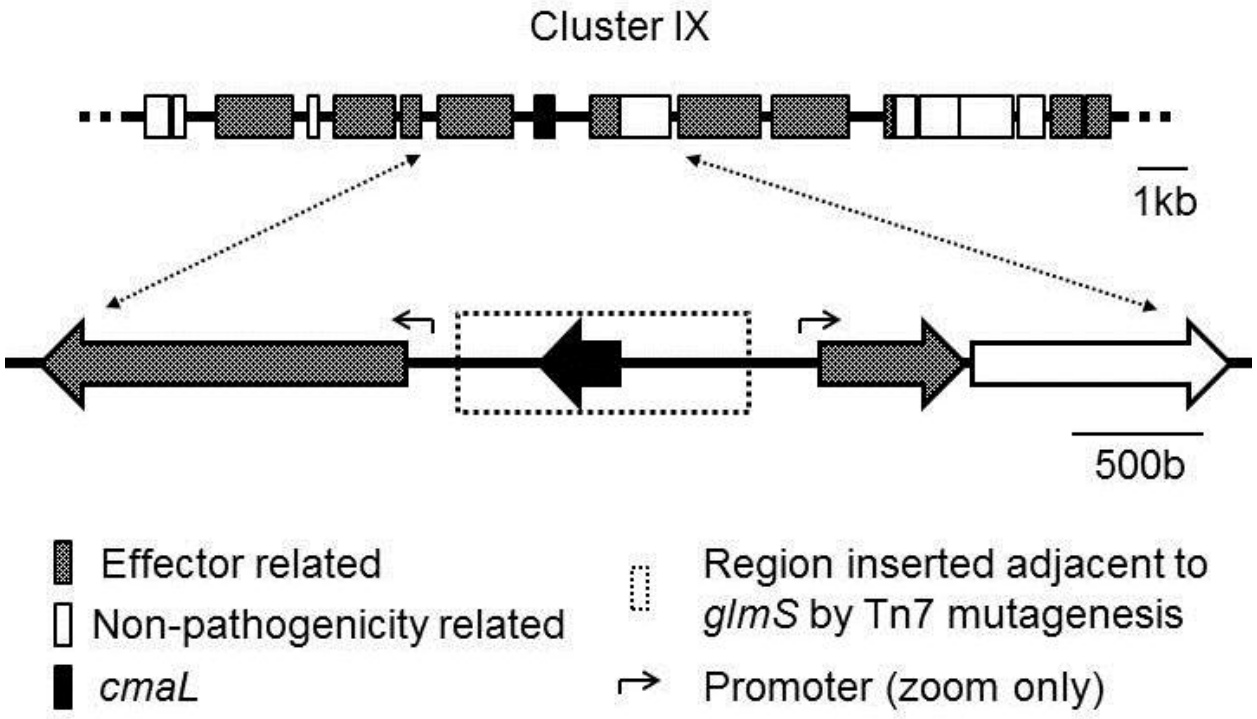

Figure 4.1. Diagram of the *cmaL* region that is inserted adjacent to *glmS* in *Pto* DC3000D28E derivatives by Tn*7* mutagenesis.

Figure 4.2. Restoring *cmaL* to *Pto* DC3000D28E derivatives that have small subsets of the DC3000 effector repertoire enhances the production of chlorosis in *N. benthamiana*. Bacterial suspensions of 1 x 10^5 cfu/ml in 10 mM $MgCl_2$ were infiltrated into leaves with a blunt syringe and incubated in a high-humidity chamber for 8 days. The arrow indicates a chlorotic flare spreading beyond the zone infiltrated with *Pto* DC3000D28E+*cmaL*.

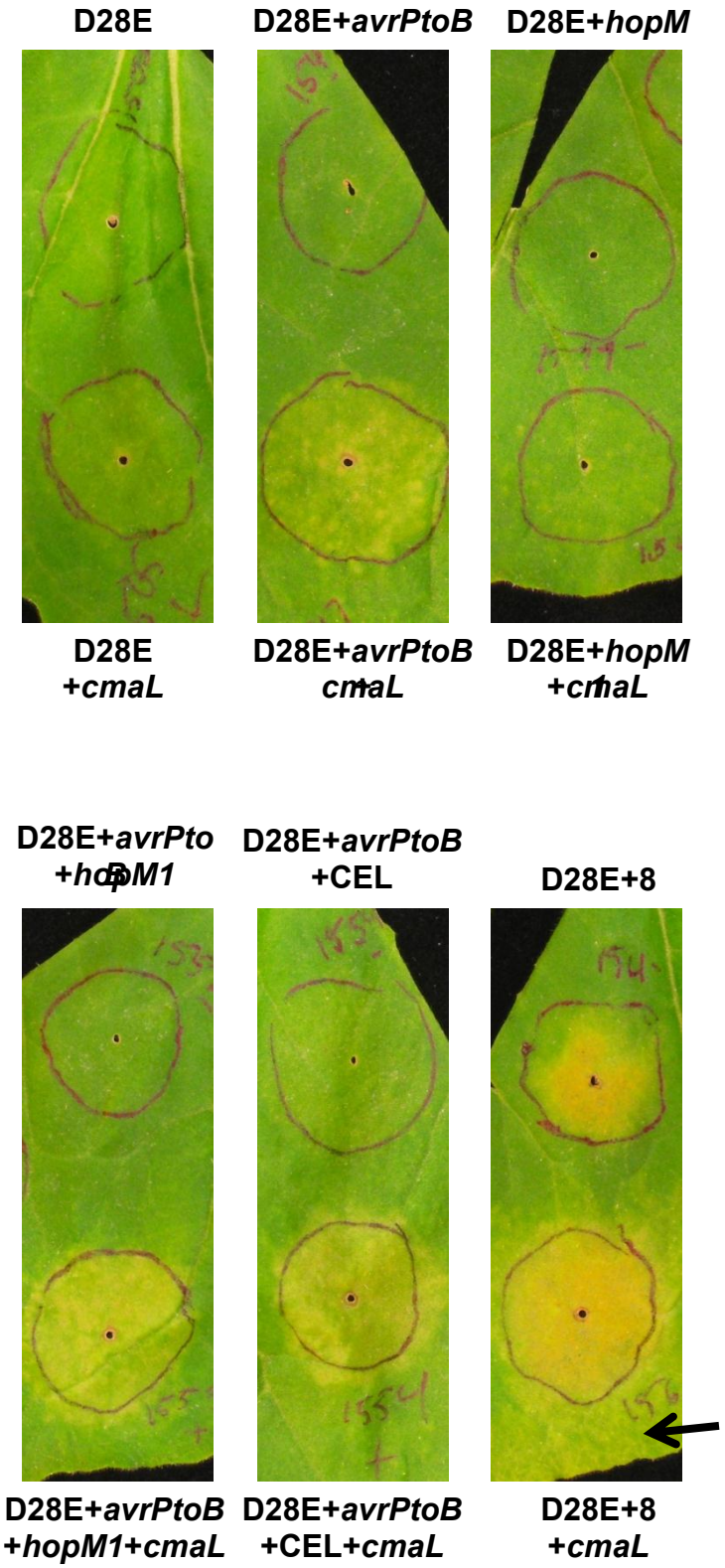
D28E
D28E+avrPtoB
D28E+hopM
D28E +cmaL
D28E+avrPtoB +cmaL
D28E+hopM +cmaL
D28E+avrPtoB +hopM1
D28E+avrPtoB +CEL
D28E+8
D28E+avrPtoB +hopM1+cmaL
D28E+avrPtoB +CEL+cmaL
D28E+8 +cmaL

local necrosis, as previously reported (Cunnac et al., 2011). Thus, CFA alone appears sufficient to promote local chlorosis, given sufficient bacterial growth, but the COR holotoxin enhances local chlorosis and enables spreading chlorosis.

Restoring *cmaL* to *Pto* DC3000D28E derivatives with small sets of effectors strongly promotes necrosis in infiltration-inoculated *N. benthamiana* leaves.

COR is linked to both chlorosis and necrosis phenotypes in *P. syringae*, so we postulated that DC3000D28E derivatives would produce stronger necrotic symptoms with the restoration of *cmaL* to the genome. We had previously observed that DC3000D28E produced some necrosis in addition to chlorosis when inoculated at a higher level (Cunnac et al., 2011), so here we syringe-infiltrated bacteria into *N. benthamiana* leaves at 1 x 10^6 cfu/ml. Because of variation in symptoms observed in preliminary tests, ten plants were inoculated to better document variation in the impact of restoring *cmaL* to the chosen DC3000D28E derivatives (Fig 4.3). DC3000D28E without effectors showed no appreciable chlorosis with or without *cmaL* (Fig. 4.3). The production of *cmaL*-dependent mild chlorosis by DC3000D28E+AvrPtoB (Fig. 4.3) was the same as observed above (Fig. 4.2). However, a striking difference was observed with the restoration of *cmaL* to DC3000D28E+AvrPtoB+CEL, which now acquired the ability to produce substantial necrosis (Fig. 4.3). Similarly, restoration of *cmaL* to DC3000D28E+8 resulted in tissue necrosis with every inoculation (Fig. 4.3). Thus, the COR holotoxin strongly promotes the induction of necrotic symptoms in *N. benthamiana* leaves by *Pto* DC3000D28E derivatives with small sets of growth-promoting effectors.

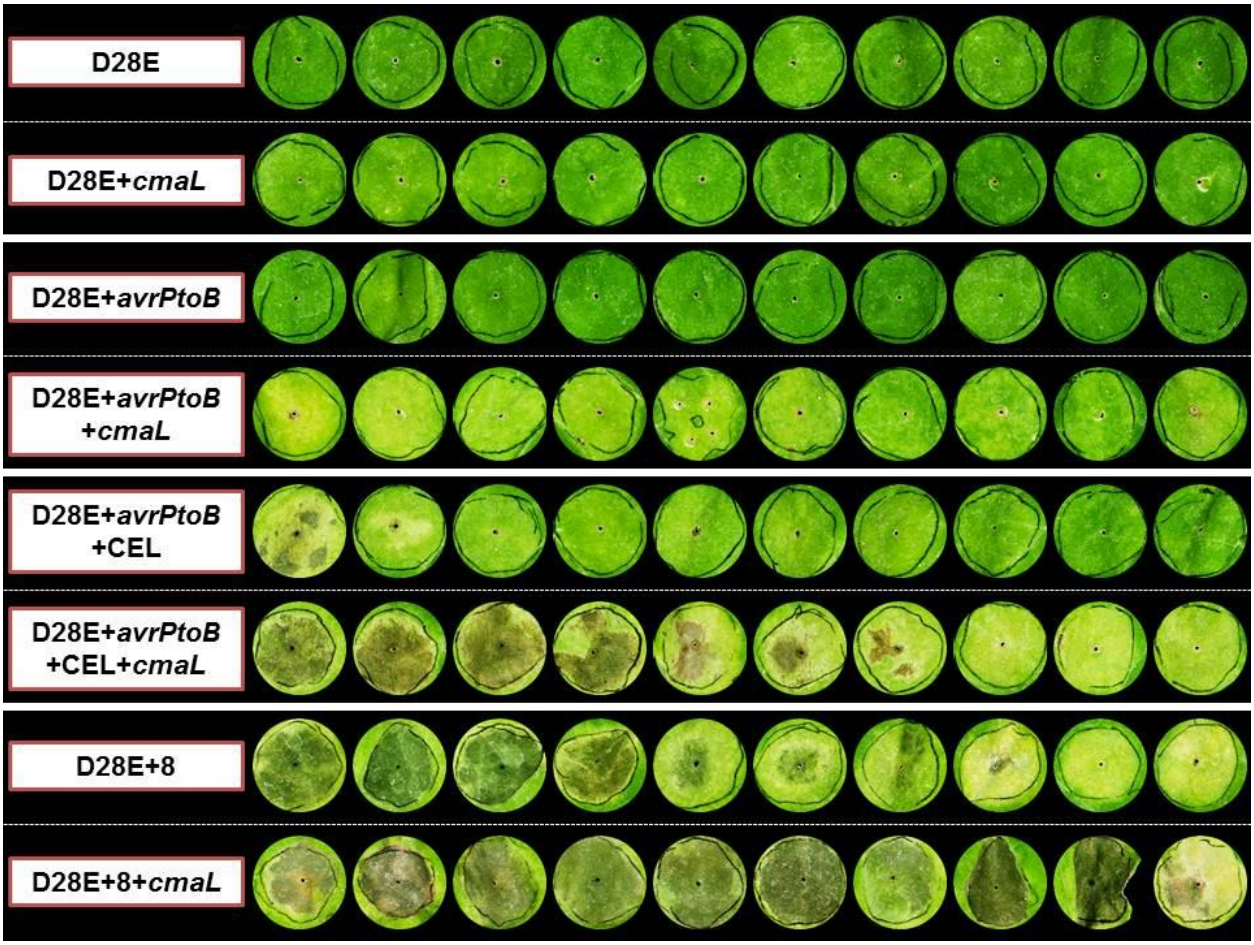

Figure 4.3. Restoring *cmaL* to *Pto* DC3000D28E derivatives that have small subsets of the DC3000 effector repertoire enhances elicitation of necrosis in *N. benthamiana* with high levels of inoculum. Concentrations of bacteria were raised from that used in Figure 4.2 to favor induction of necrosis. Bacterial suspensions of 10^6 cfu/ml in 10 mM $MgCl_2$ were infiltrated into leaves with a blunt syringe and incubated in a high-humidity chamber for 6 or 7 days. The variation in symptoms observed with some treatments in this experiment is captured by displaying infiltration zones from 10 plants for each treatment. The leaves are ranked by symptom severity and are arrayed, left to right, in decreasing order.

Restoring *cmaL* to *Pto* DC3000D28E derivatives with small sets of effectors promotes growth in infiltration-inoculated *N. benthamiana* leaves.

We had previously observed that deleting the *cfa* operon and thereby eliminating COR production had no effect on the strong growth in *N. benthamiana* of wild-type DC3000 or the residual growth of a T3SS-deficient mutant when bacteria were inoculated by syringe-infiltration into leaves (Kvitko, 2009). Here, we asked if the COR holotoxin could enhance the growth of bacteria with minimal sets of growth-promoting effectors and presumably less redundancy in the effector repertoire. We chose two DC3000D28E derivatives to test, DC3000D28E+AvrPtoB and DC3000D28E+8, because these strains bracketed the growth-promoting activities of the effector combinations employed in this study. Bacteria were inoculated at 1 x 10^4 cfu/ml, and population levels were determined 6 days later. As shown in Figure 4.4, restoring *cmaL* significantly improved the respective growth levels of both DC3000D28E+AvrPtoB and DC3000D28E+8. Thus, COR can be observed to promote bacterial growth when the inoculation method bypasses stomatal entry and the holotoxin is operating with minimal sets of growth-promoting effectors.

CFA and COR both can contribute to the ability of *Pto* DC3000 derivatives to produce spot symptoms when dip-inoculated into *N. benthamiana* leaves.

The ability of *Pto* DC3000 derivatives to produce spots when dip-inoculated into *N. benthamiana* has been shown for DC3000 Δ*hopQ1-1* (Wei et al., 2007) and DC3000D28E+5(AvrPtoB, HopM1, HopE1, HopG1, HopAM1)+HopAA1-1 (Chapter 3). We now know that these strains produce COR and CFA, respectively. Given that *Pto*

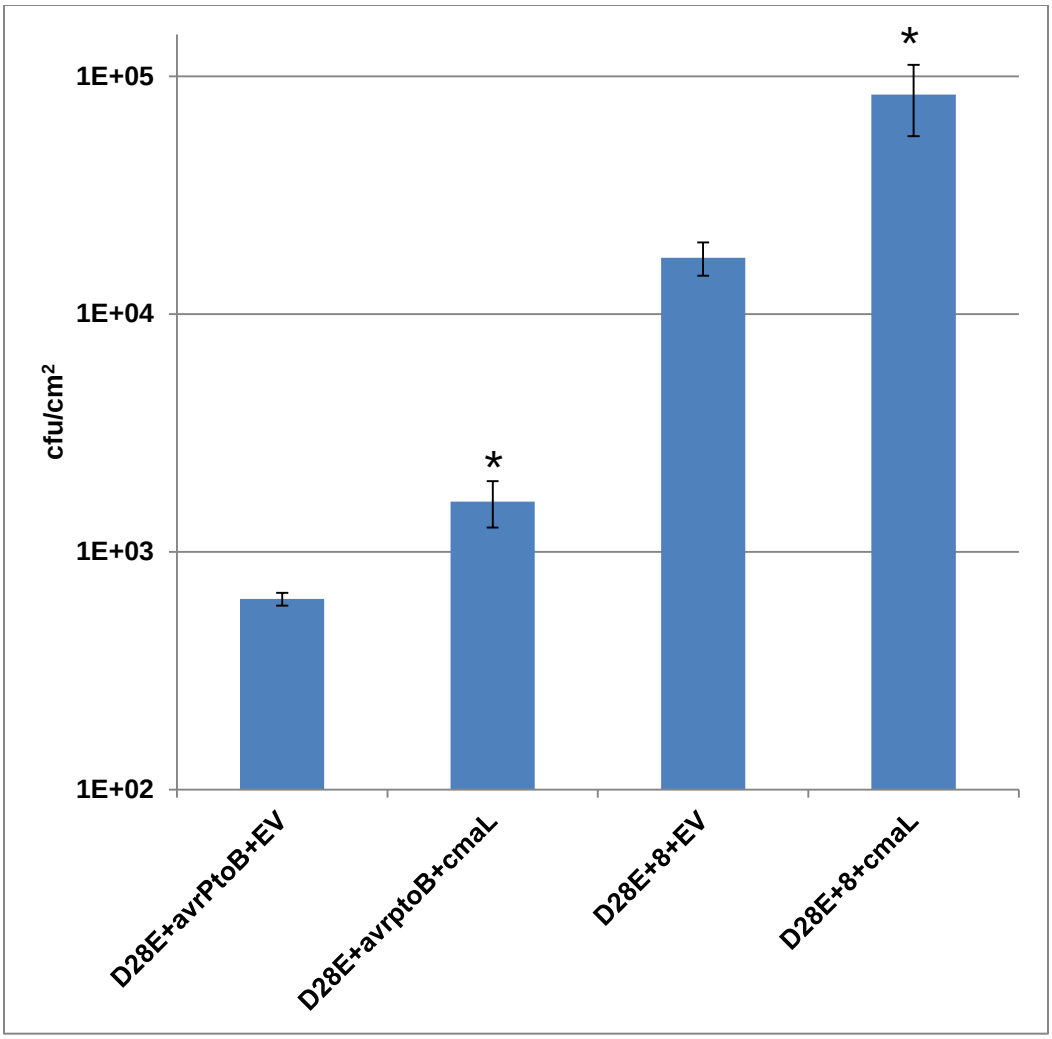

Figure 4.4. Restoring *cmaL* to two *Pto* DC3000D28E derivatives enhances their growth in *N. benthamiana*. Bacteria were suspended in 10 mM $MgCl_2$ buffer at a final concentration of 10^4 cfu/ml and infiltrated into leaves with a blunt syringe. Bacterial populations were assayed 6 dpi by plate counting. The relative growth of DC3000D28E+AvrPtoB and DC3000D28E+AvrPtoB+CmaL and of DC3000D28E+8 and DC3000D28E+8+CmaL was assayed in different experiments. Results are the mean and standard deviation from three assays, and the asterisks indicate results that are statistically different, $p < 0.05$, based on the student's T-test.

DC3000 Δ*hopQ1-1* produces a complete repertoire of effectors, we asked if that is sufficient for dip-initiated pathogenesis by deleting the *cfa* operon to eliminate both CFA and COR production. On the other hand, DC3000D28E+8 produces only CFA and a minimal set of effectors for virulence in syringe-infiltrated *N. benthamiana* leaves. We therefore asked if this strain produces lesions when dip inoculated and if such a capacity could be enhanced by restoring *cmaL* and thereby production of the COR holotoxin. Whole plants were dipped into suspensions containing 10^5 cfu/ml of the test bacteria and 0.01% Silwet and incubated in a humid chamber for 6 days before photography. Deleting the *cfa* operon strongly reduced the symptoms caused by DC3000 Δ*hopQ1-1* to just scattered, tiny, chlorotic spots (Fig. 4.5). DC3000D28E+8 was found to produce chlorotic lesions, with some lesions having necrotic centers, and restoring *cmaL* increased the number and size of these spots (Fig. 4.5). Thus, CFA is adequate to promote moderate virulence in *N. benthamiana* when bacteria are dip inoculated, but the COR holotoxin is more effective.

Symptom production by *Pto* DC3000D28E+5 in dip-inoculated *N. benthamiana* is enhanced more strongly by CmaL than by HopAA1-1

Previously, we reported that *cmaL* was partially phenotypically redundant with HopAA1-1 in speck formation following dip inoculations but not following syringe inoculations of tomato, based on single and double mutations in *Pto* DC3000 (Munkvold et al., 2009). We also observed that restoring HopAA1-1 to DC3000D28E+5 enabled the bacterium to produce chlorotic sptos in *N. benthamiana* when dip inoculated

Figure 4.5. CFA and COR contribute to the ability of *Pto* DC3000 derivatives to produce lesions when dip-inoculated into *N. benthamiana* leaves. Whole plants were dipped into bacterial suspensions containing 10^5 cfu/ml bacteria and 0.01% Silwet, and then transferred to a humid incubation chamber for 6 days before photography. Note that *Pto* DC3000Δ*hopQ1-1*Δ*cfa* is unable to produce CFA or COR, that DC3000D28E+8 produces CFA, and DC3000D28E+8+*cmaL* produces the COR holotoxin.

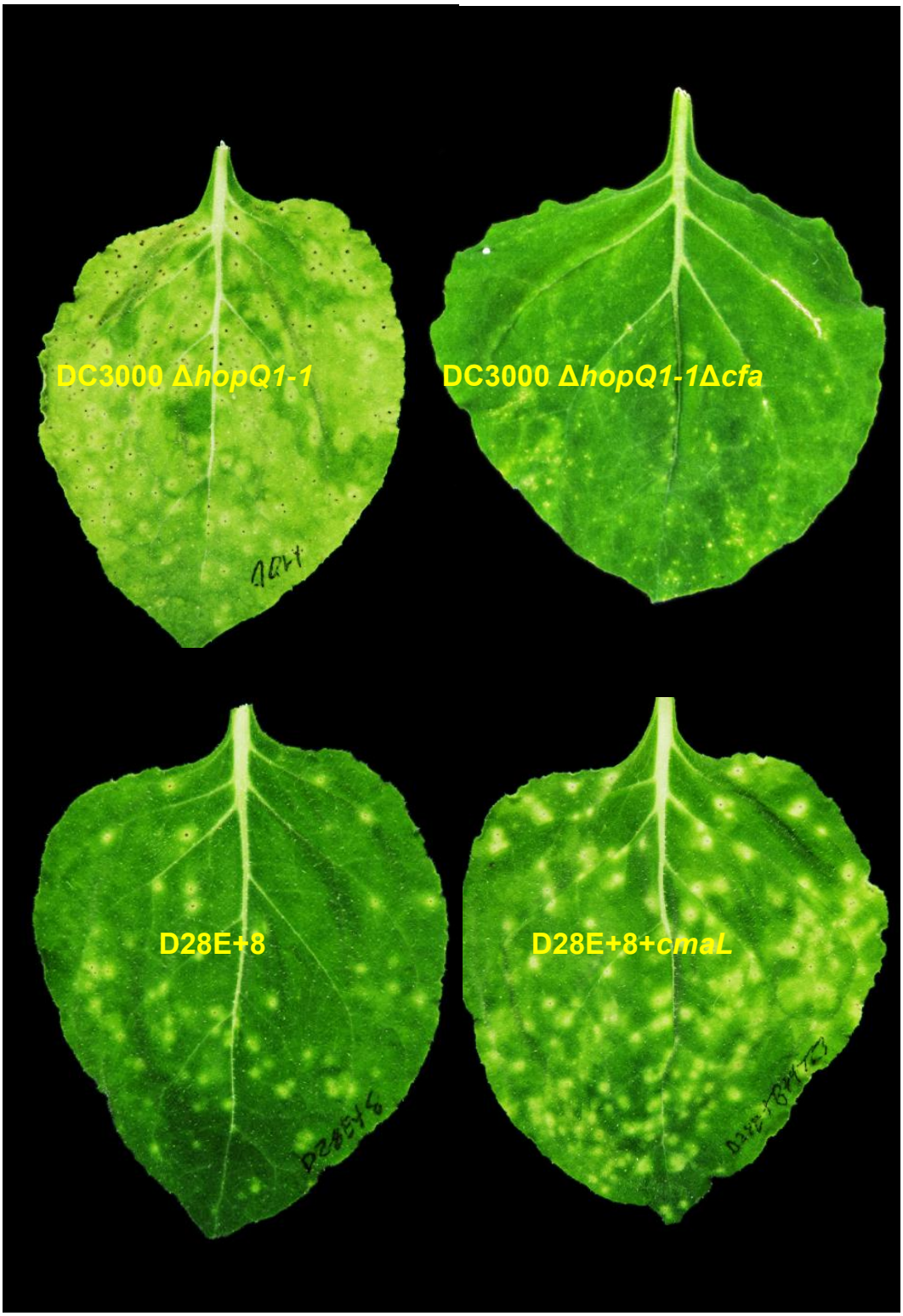
DC3000 ΔhopQ1-1
DC3000 ΔhopQ1-1Δcfa
D28E+8
D28E+8+cmaL

(Chapter 3). Here, we asked if AvrE, another CEL effector could enable DC3000D28E+5 to produce chlorotic spots when dip inoculated, and we compared the relative contribution to virulence of HopAA1-1 and CmaL. As described above, *N. benthamiana* plants were photographed 6 days after dipping in suspensions containing 1×10^5 cfu/ml of the test bacteria. DC3000D28E+5 and DC3000D28E+5+AvrE produced no chlorotic spots (Fig. 4.6). In contrast, DC3000D28E+5+HopAA1-1 produced numerous, small chlorotic spots, and DC3000D28E+5+CmaL produced more numerous and larger chlorotic spots (Fig. 4.6).

Thus, whereas CmaL and HopAA1-1 seem to contribute equally to spot formation when the rest of DC3000 effectors are present (Munkvold et al., 2009), in the context of the minimal effector repertoire CmaL outperforms HopAA1-1. The Figure 4.6 observations also suggest that HopAA1-1 functions redundantly with the COR holotoxin rather than with CFA.

CmaL and HopAA1-1 can promote the ability of additional *Pto* DC3000D28E derivatives to produce chlorotic spots in dip-inoculated *N. benthamiana* leaves.

We next asked if CmaL and HopAA1-1 can promote the production of chlorotic spots by DC3000D28E with sets of effectors smaller than five: DC3000D28E+1 (AvrPtoB), DC3000D28E+2 (AvrPtoB+HopM1), and DC3000D28E. *N. benthamiana* leaves were dip inoculated as above, and as expected, none of the aforementioned strains produced any chlorotic spots (Fig. 4.7). Remarkably, restoring CmaL was sufficient to enable all of the test strains, most notably DC3000D28E, to produce small, chlorotic spots. HopAA1-1 did not enable DC3000D28E+1 to cause any spots, but it

Figure 4.6. Production of chlorotic spots by *Pto* DC3000D28E+5 in dip-inoculated *N. benthamiana* is enhanced more strongly by CmaL than by HopAA1-1. Whole plants were dipped into bacterial suspensions containing 10^5 cfu/ml bacteria and 0.01% Silwet, and then transferred to a humid incubation chamber for 6 days before photography. DC3000D28E+5 produces AvrPtoB, HopM1, HopG1, HopE1 and HopAM1. *avrE* and the *shcE* chaperone gene were expressed from the *avrPto* promoter in broad-host-range plasmid pCPP5961. *hopAA1-1* was expressed from the *avrPto* promoter in broad-host-range plasmid pCPP5581. *cmaL* was restored to the genome via Tn*7* as described in the text. Strains labeled in white produced no chlorotic spots.

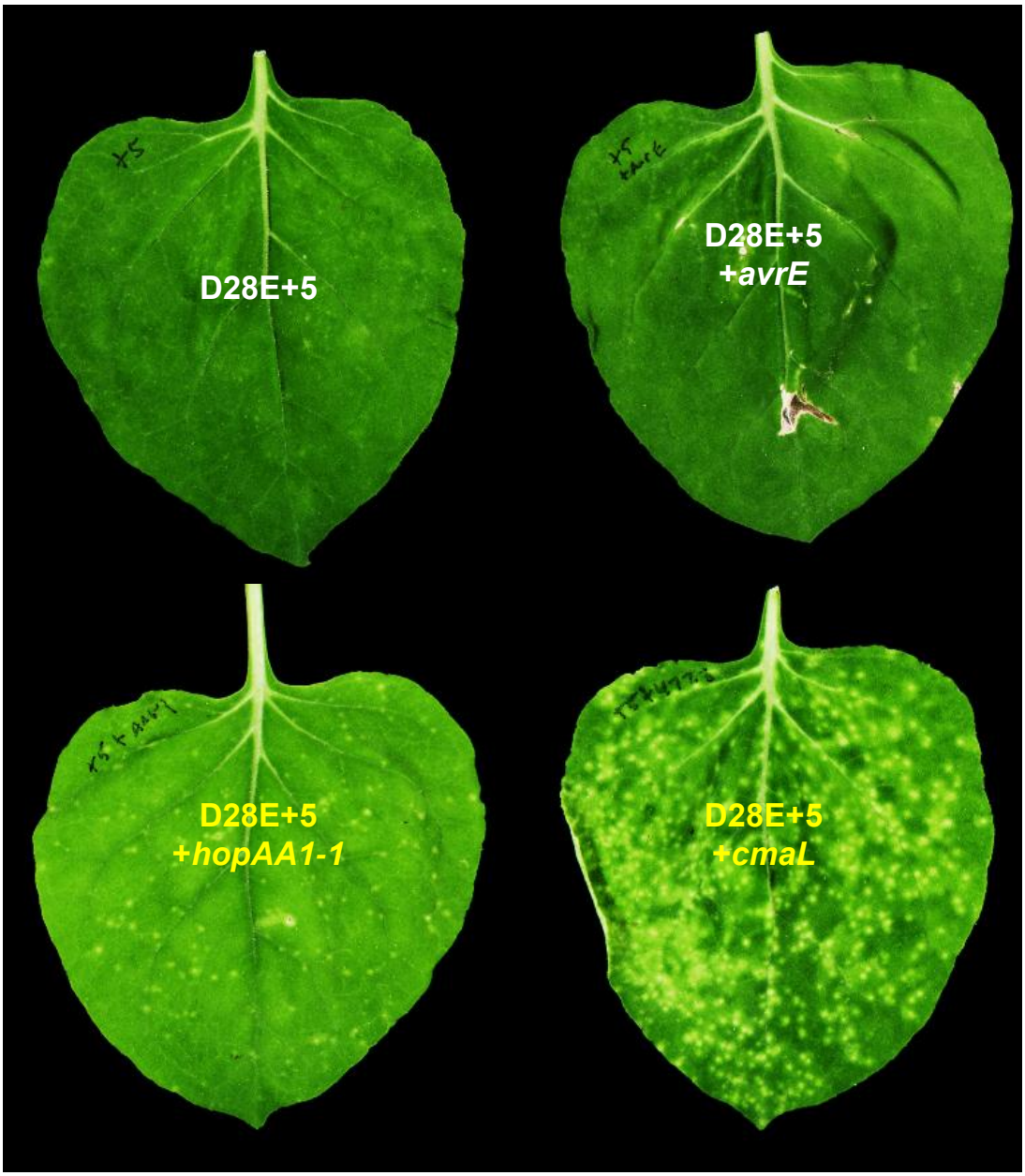
D28E+5
D28E+5
+avrE
D28E+5
+hopAA1-1
D28E+5
+cmaL

Figure 4.7. CmaL and HopAA1-1 can promote the ability of additional *Pto* DC3000D28E derivatives to produce chlorotic spots in dip-inoculated *N. benthamiana* leaves. Whole plants were dipped into bacterial suspensions containing 10^5 cfu/ml bacteria and 0.01% Silwet, and then transferred to a humid incubation chamber for 6 days before photography. DC3000D28E+1 produces AvrPtoB, and DC3000D28E+2 produces AvrPtoB and HopM1. *hopAA1-1* was expressed from the *avrPto* promoter in broad-host-range plasmid pCPP5581. *cmaL* was restored to the genome via Tn*7* as described in the text. The inset for DC3000D28E+2+HopAA1-1 shows a close-up image of chlorotic spots, which were entirely lacking in all of the strains labeled in white in the figure.

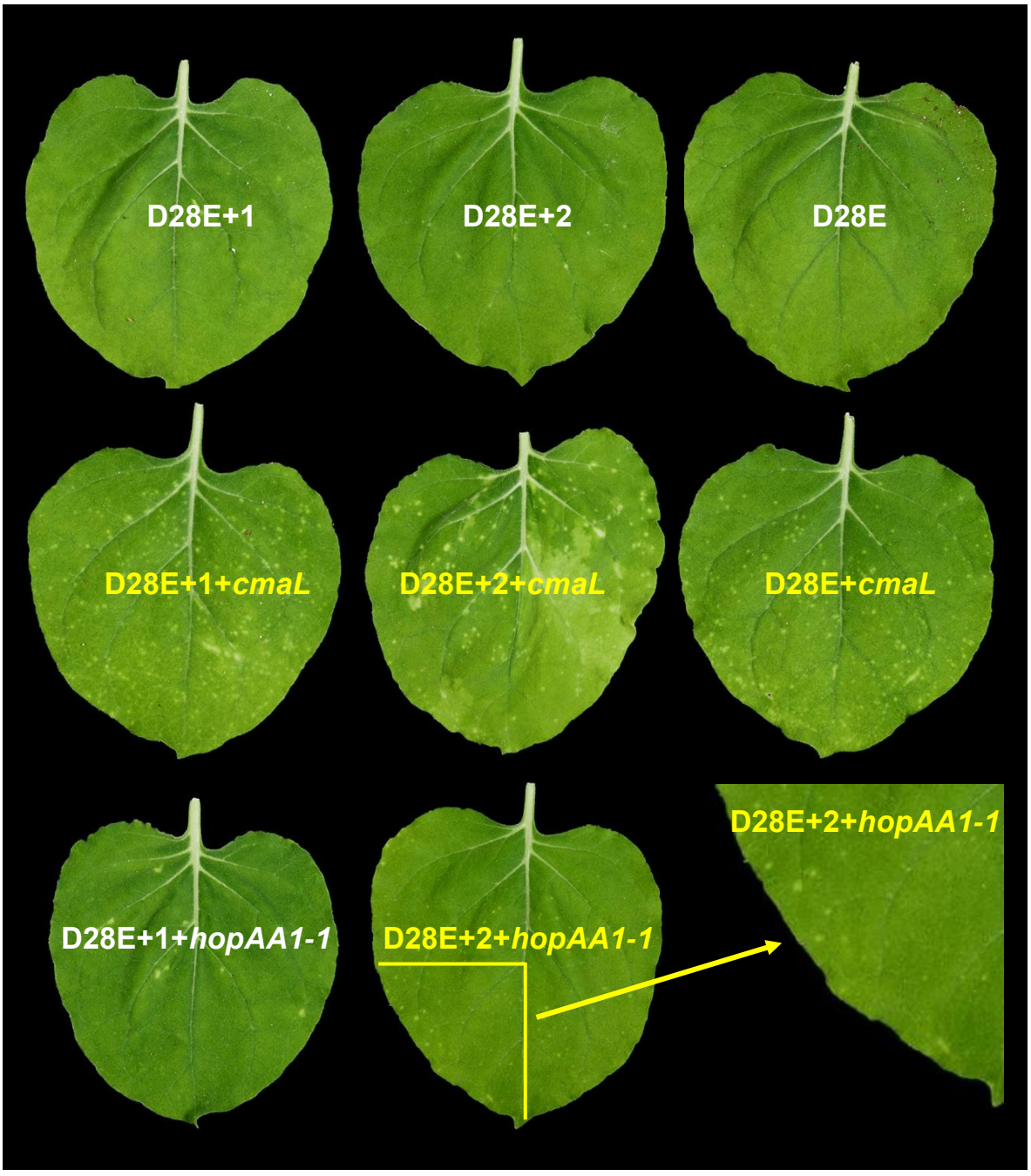
D28E+1
D28E+2
D28E
D28E+1+cmaL
D28E+2+cmaL
D28E+cmaL
D28E+1+hopAA1-1
D28E+2+hopAA1-1
D28E+2+hopAA1-1

enabled DC3000D28E+2 to produce some (Fig. 4.7). It is noteworthy that the observations in Figures 4.6 and 4.7 indicate that AvrE and HopM1 have no apparent role in enabling dip-inoculated bacteria to cause chlorotic spots, which provides further evidence that these two effectors have a fundamentally different role in pathogenesis than HopAA1-1.

DISCUSSION

P. syringae pathogenesis in plant leaves involves several stages and outcomes. The bacteria typically enter through stomata, establish successful colonies on the surface of mesophyll cells, increase their populations by several orders of magnitude, and ultimately produce necrotic spots on leaves, which in the case of *Pto* DC3000 on susceptible plants such as tomato and the model plant *N. benthamiana*, are surrounded by a bright, local chlorosis and a more diffuse, spreading chlorosis. To better understand the role of type III effectors and COR in this process, we have constructed many DC3000 mutants with combinatorial deletions (Wei et al., 2007; Kvitko et al., 2009; Cunnac et al., 2011), and we have constructed DC3000D28E, which is functionally effectorless, COR-deficient, and amenable to reassembly of minimal gene sets that can confer strong virulence phenotypes in the absence of redundant factors (Cunnac et al., 2011). By restoring CmaL (and thereby COR) and HopAA1-1 to DC3000D28E derivatives and then assaying with methods that require the entry phase of pathogenesis (dip inoculation) or bypass this phase (syringe infiltration) we have gained new insights into the actions of several key factors.

First, COR strongly promotes the entry phase, but CFA or HopAA1-1 can partially substitute in the absence of COR. The activity of COR in opening stomata is known (Melotto et al., 2006; Melotto et al., 2008). But CFA has received less attention, and here we learned that DC3000D28E derivatives with small subsets of effectors that enable growth when syringe infiltrated acquire the ability to produce chlorotic spots when dip inoculated if they also produce CmaL (and therefore COR). Similarly, DC3000 Δ*hopQ1-1*, with its repertoire of at ca. 27 effectors is strongly reduced in virulence when dip-inoculated if it is CFA-deficient (and therefore COR-deficient). On the other hand, DC3000D28E with no added effectors is able to produce small, chlorotic spots if it produces the COR holotoxin.

COR is clearly a powerful factor in the entry phase, but it is striking that in its absence, CFA or HopAA1-1 can substitute. As we had previously observed, DC3000 *cmaL* mutants retain a wild-type ability to produce lesions with small chlorotic halos in dip-inoculated tomato leaves (Munkvold et al., 2009). DC3000 *hopAA1-1* mutants similarly lack a strong virulence phenotype, however *hopAA1-1/cmaL* double mutants are strongly reduced in lesion formation when dip inoculated. Thus, HopAA1-1 and CmaL (and thereby COR) form a functional redundancy group analogous to the HopM1/AvrE/HopR1 and AvrPto/AvrPtoB REGs. More specifically, the functional overlap appears to be between HopAA1-1 and the CMA moiety in COR in a process in leaf mesophyll bacterial colony development that is early but after entry through the stomata, which is mediated by the CFA moiety of COR. It is also noteworthy that redundancy group patterns discerned in polymutants are corroborated in DC3000D28E-based reassembly experiments. As in the reassembly experiments, the partial

redundancy of HopAA1-1 and COR is not presumed to be mechanistic, yet results in overlapping contributions to symptom development.

Spreading chlorosis is a disease outcome that is dependent on production of the COR holotoxin, as similarly documented in both the disassembly and reassembly phases of our work. Thus, a DC3000Δ*hopQ1-1* Δ*cmaL* mutant loses spreading necrosis (Munkvold et al., 2009), but DC3000D28E+8 regains this ability upon restoration of *cmaL*. Less straightforward is the contribution of COR to the disease outcome of tissue necrosis. As shown in Figure 4.3, CmaL (and therefore COR) strikingly increases tissue death resulting from syringe infiltration of DC3000D28E+AvrPtoB+CEL. The CEL effectors HopM1 and AvrE are known to promote plant cell death (as discussed above), and it appears that COR, but not CFA, can potentiate this. In this regard, it is worth remembering that the CMA moiety in COR resembles the ethylene precursor ACC. Although CMA itself does not enhance ethylene production (Uppalapati et al., 2005), the CMA moiety could be responsible for such activity observed with the COR holotoxin (Ferguson and Mitchell, 1985; Kenyon and Turner, 1992), and this could have a primary role in potentiating cell death elicitation by a minimal effector repertoire.

An unexpected finding is that DC3000D28E+CmaL derivatives that produce no apparent phenotype when syringe infiltrated produce chlorotic spots when dip inoculated. It is also striking how intense the chlorosis for these individual colonies is given that they are individual colonies (see Chapter 5). A syringe infiltration can produce a mottled and somewhat diffuse chlorosis, whereas in the dip inoculations symptoms always manifested in bright, distinct spots. This suggests that there may be a different environment near the leaf surface that is more permissible to infection, and

there are several possible reasons. One is a more direct access to gaseous exchange, possibly permitting a higher aerobic metabolism. Another is that there may be fewer defense-capable cells within a certain radius, and this may have an impact on defense responses. This difference may also be mechanical – a dip inoculation may produce a low PAMP burden, whereas a syringe inoculation may cause flagellar shearing or even bacterial lysis, thereby eliciting a level of PTI that dip-inoculated bacteria do not have to overcome. New experiments involving confocal microscopy and cell biology techniques are now needed to understand the strikingly different behaviors in *N. benthamiana* of these bacteria that have simplified and defined virulence factor repertoires.

MATERIALS AND METHODS

Bacterial strains and plasmids.

Bacterial strains and plasmids are listed in Table 4.1. *P. syringae* strains were cultivated on King's B (KB) at 30°C (King et al., 1954). *Escherichia coli* strains were cultivated on Luria-Burtani media (Hanahan, 1985). Antibiotics were used at the following concentrations in µg/ml: rifampicin 50; spectinomycin 50; chloramphenicol 20; gentamicin 10 for plasmids, 5 for genomic integrants; kanamycin 50.

Plasmid constructions.

Plasmids were created as described and transformed into *E. coli* DH5α or Top10 by standard electroporation or heat-shock procedures (Sambrook and Russel, 2001). Primers were purchased from Integrated DNA Technology. PCR reactions were

Table 4.1. Bacterial strains and plasmids used in this study

Designation	Genotype/Plasmid Description	Reference
Escherichia coli		
DH5α	F–Φ80lacZΔM15 ΔlacZYA-argF)U169 deoR recA1 endA1 hsdR17 phoA supE44 thi-1 gyrA96 relA1 λ	Invitrogen
DB3.1	F–gyrA462 endA1Δ (sr1-recA) mcrB mrr hsdS20 supE44 ara-14 galK2 lacY1 proA2 rpsL20 xyl-5 λ–leu mtl-1	Invitrogen
DB3.1 λ*pir*	F−gyrA462 endA1 Δ(sr1-recA) mcrB mrr hsdS20 (r_B− m_B−) supE44 ara-14 galK2 lacY1 proA2 rpsL20 (Strr) xyl-5 Δleu mtl-1 λpir-lysogen	(House et al., 2004)
SM10 λ*pir*	sup E44 ΔlacU169 (ΦlacZΔM15) recA1 endA1 hsdR17 thi-1 gyrA96 relA1 λpir-lysogen	(Miller and Mekalanos, 1988)
HB101	F- mcrB mrr hsdS20(r_B- m_B-) recA13 leuB6 ara-14 proA2 lacY1 galK2 xyl-5 mtl-1 rpsL20(Sm^R) glnV44 λ-	(Boyer and Roulland-Dussoix, 1969)
S17-1	recA pro hsdR RP4-2-Tc::Mu-Km::Tn7	(Simon et al., 1983)
Top10	F- mcrA (mrr-hsdRMS-mcrBC) 80lacZM15 lacX74 recA1 ara139 (ara-leu)7697 galU galK rpsL (Sm^R) endA1 nupG	Invitrogen
Pseudomonas syringae pv. tomato		
DC3000	Rif^R	(Buell et al., 2003)
CUCPB5460	Δ*hopQ1-1*	(Wei et al., 2007)
CUCPB5585	DC3000D28E, Sp^R	(Cunnac et al., 2011)
CUCPB6012	DC3000D28E *avrPtoB,* Sp^R	(Cunnac et al., 2011)
CUCPB6014	DC3000D28E *hopM1,* Sp^R	(Cunnac et al., 2011)
CUCPB6016	DC3000D28E *avrPtoB hopM1,* Sp^R	(Cunnac et al., 2011)
CUCPB6019	DC3000D28E *avrPtoB* CEL, Sp^R	(Cunnac et al., 2011)
CUCPB6021	DC3000D28E *avrPtoB avrPto* CEL, Sp^R	(Cunnac et al., 2011)
CUCPB6031	DC3000D28E *avrPtoB hopM1 hopE1 hopG1 hopAM1*, Sp^R, Km^R	(Cunnac et al., 2011)

Table 4.1. Continued.

CUCPB6032	DC3000D28E *avrPtoB* CEL *hopE1 hopG1 hopAm1*, Sp^R, Km^R	(Cunnac et al., 2011)
CUCPB6046	Δ*hopQ1-1* attTn7::FRTTc, Tc^R	This study
CUCPB6069	CUCPB5585 attTn7::FRTTc, Sp^R, Tc^R	This study
CUCPB6070	CUCPB6012 attTn7::FRTTc, Sp^R, Tc^R	This study
CUCPB6071	CUCPB6014 attTn7::FRTTc, Sp^R, Tc^R	This study
CUCPB6072	CUCPB6016 attTn7::FRTTc, Sp^R, Tc^R	This study
CUCPB6073	CUCPB6019 attTn7::FRTTc, Sp^R, Tc^R	This study
CUCPB6074	CUCPB6021 attTn7::FRTTc, Sp^R, Tc^R	This study
CUCPB6075	CUCPB6032 attTn7::FRTTc, Sp^R, Tc^R, Km^R	This study
CUCPB6077	CUCPB5585 attTn7::FRTTc-*cmaL* (1kb fragment including *cmaL*, native promoter), Sp^R, Tc^R	This study
CUCPB6078	CUCPB6012 attTn7::FRTTc-*cmaL* (1kb fragment including *cmaL*, native promoter), Sp^R, Tc^R	This study
CUCPB6079	CUCPB6014 attTn7::FRTTc-*cmaL* (1kb fragment including *cmaL*, native promoter), Sp^R, Tc^R	This study
CUCPB6080	CUCPB6016 attTn7::FRTTc-*cmaL* (1kb fragment including *cmaL*, native promoter), Sp^R, Tc^R	This study
CUCPB6081	CUCPB6019 attTn7::FRTTc-*cmaL* (1kb fragment including *cmaL*, native promoter), Sp^R, Tc^R	This study
CUCPB6082	CUCPB6021 attTn7::FRTTc-*cmaL* (1kb fragment including *cmaL*, native promoter), Sp^R, Tc^R	This study
CUCPB6083	CUCPB6032 attTn7::FRTTc-*cmaL* (1kb fragment including *cmaL*, native promoter), Sp^R, Tc^R	This study
Plasmids		
pCPP5107	pENTR/SD/D-TOPO::*hopAA1-1*	(Munkvold et al., 2008)
pCPP5372	pBBR1MCS with *avrPto* promoter, Gateway reading frame B cassette, C terminal HA tag, Gm^r, Cm^r	(Oh et al., 2007)
pCPP5581	pCPP5372::*hopAA1-1*	(Munkvold et al., 2009)
pCPP5912	pENTR/D/SD-TOPO::*shcE avrE1*	(Kvitko et al., 2009)
pCPP5961	pCPP5372::*shcE avrE1*	This study
pCPP6001	Plasmid expressing *cmaL* from its native promoter.	(Munkvold et al., 2009)

Table 2.1. Continued.

pK18mob	Small mobilizable suicide vector, Km^R	(Schafer et al., 1994)
pK18mobsacB	Small mobilizable suicide vector, Km^R, sucrose-sensitive (*sacB*)	(Schafer et al., 1994)
pRK2013	Helper plasmid for conjugation, Km^R	(Figurski and Helinski, 1979)
pTNS2	Helper plasmid for Tn7 mediated insertions, pTnsABC+D, Ap^R	(Choi and Schweizer, 2006)
pUC18R6KT-mini-Tn7T-Tc	Empty vector for Tn7 mediated insertions, Tc^R	(Choi and Schweizer, 2006)
pCPP6357	pUC18R6KT-mini-Tn7T-Tc::*cmaL*	This study

performed using either ExTaq DNA polymerase or PrimeSTAR HS DNA Polymerase (Takara Bio Inc.). Restriction enzymes and DNA ligation procedure enzymes were purchased from New England Biolabs. Construct sequences were verified through sequencing performed by the Cornell University Life Sciences Core Laboratories Center.

pCPP5961 was created from an LR clonase II (Invitrogen) reaction between pCPP5912 and pCPP5372 (Table 4.2). pCPP6357 was created by the HindIII-mediated ligation of a 1-kb jnw182-183 PCR product amplified from DC3000 genomic DNA into pUC18R6KT-mini-Tn7T-Tc.

Tn7-mediated site-specific integration of synthetic constructs.

A tetraparental-mating approach was used to drive the site-specific integration of pUC18R6KT-mini-Tn7T-based donor vectors into DC3000 derivatives adjacent to *glmS*. Cultures of *E. coli* containing pTNS2, pRK2013, and the donor vector were grown in LB overnight at 30°C with shaking and antibiotic selection. Cultures of the recipient bacteria were grown in KB overnight at 30°C with shaking. Cultures were washed in 1x LM media to remove antibiotics, and 50 µl of each was added to a single tube and mixed by gentile shaking. This mixture was pelleted by centrifugation and decanted by inverting the tube, leaving approximately 50 µl of supernatant. The pellet was resuspended in this and spotted on a mating membrane on LM media. The mating was allowed to progress overnight with incubation at 30°C. The entire mating reaction was then resuspended in 1 ml LM broth by vortexing, and 100 µl of the suspension was plated on MG minimal media (Bronstein et al., 2008), amended with tetracycline at 5

Table 4.2. Primers used in this study

Forward/Reverse names	Forward sequence	Reverse sequence	Function
jnw182/jnw183	CTAAAGCTTGAG CAGCTTGCCGAA GGCCTATCA	CTGAAGCTTAGG GAGTTACCAATG CAGATCGTG	500bp upstream of PSPTO_4723 to 300bp downstream (approx 1kb)
oSWC461/oSWC462	AGTACTCCCTAG CCTACTCTTACTG	GAGTTGATCGTAT TCGCTGACGAGC	Amplifies the AttTn7 region of DC3000

µg/ml. Additional procedures involving streaking were used to achieve single colony isolation. Minimal medium was used here to select against the auxotrophic plasmid donor and maintenance strains since tetracycline resistance was not particularly robust and the combination of tetracycline and rifampicin proved to be deleterious for growth of integrants. Confirmation of siderophore production via UV-light illumination of colonies grown on MG medium was used to confirm the identity of single colony isolates. PCR reactions using primers oSWC461/oSWC462 were used to confirm insertion into the attTn*7* site.

Blunt syringe inoculation assays.

Bacteria were cultivated on KB media with tetracycline at 5 µg/ml overnight, suspended in 10 mM $MgCl_2$ to an OD_{600} of 0.1, then diluted 1000x for a final concentration of 1 x 10^5 cfu/ml. This inoculum was infiltrated directly into the youngest fully expanded leaves of 4-5 week old *N. benthamiana* plants using a blunt syringe and incubated in a 16h day, 23°C plant growth chamber. To better observe spreading chlorosis and reduce necrosis, plants were kept at a humidity of 60-80% for 8 days (Fig. 4.2). For observing maximum symptom production, including necrosis, plants were kept at 90-100% humidity for 6 days (Fig. 4.3).

Dip inoculation assays.

Bacteria were cultivated on KB media overnight with appropriate antibiotic selection for plasmid maintenance and suspended in 10 mM $MgCl_2$ to an OD_{600} of 0.1 for a final concentration of 1 x 10^8 cfu/ml. This suspension (0.5 ml) and 50 µl of Silwet

were added to 500 ml distilled water and mixed well by hand-stirring for a final concentration of 1 x 10^5 cfu/ml bacteria and 0.01% Silwet. Four to five week old *N. benthamiana* plants were covered overnight in the lab with an autoclave bag loosely tucked under the tray and removed immediately before dipping (within 5 sec). For dipping, the plants were inverted and dipped into the inoculum mixture for 30 sec with mild shaking by rocking the bucket back and forth gently. Plants were removed and let dry on the bench top, then moved to a 16h day 23°C 90-100% humidity plant growth chamber. Symptoms were imaged 5-6 days post inoculation.

Assays for bacterial growth in *N. benthamiana* leaves.

Bacteria were cultivated on KB media with appropriate antibiotic selection for Tn*7* integrants or for plasmids, then suspended in $MgCl_2$ to a final concentration of 1 x 10^4 for D28E+8 with or without *cmaL* and 3 x 10^4 cfu/ml for D28E with or without *cmaL*. Bacterial suspensions were inoculated into leaves using a blunt syringe and incubated in a 16h day 23°C 60-80% humidity plant growth chamber for 6 days. Tissue from the inoculations was ground in 10mM $MgCl_2$ and plated on KB with rifampicin as in Cunnac et al. 2009.

REFERENCES

Alfano, J.R., Charkowski, A.O., Deng, W.-L., Badel, J.L., Petnicki-Ocwieja, T., van Dijk, K., and Collmer, A. 2000. The *Pseudomonas syringae* Hrp pathogenicity island has a tripartite mosaic structure composed of a cluster of type III secretion genes bounded by exchangeable effector and conserved effector loci that contribute to parasitic fitness and pathogenicity in plants. Proc Natl Acad Sci USA 97:4856-4861.

Almeida, N.F., Yan, S., Lindeberg, M., Studholme, D.J., Schneider, D.J., Condon, B., Liu, H., Viana, C.J., Warren, A., Evans, C., Kemen, E., MacLean, D., Angot, A., Martin, G.B., Jones, J.D., Collmer, A., Setubal, J.C., and Vinatzer, B.A. 2009. A draft genome sequence of *Pseudomonas syringae* pv. *tomato* strain T1 reveals a repertoire of type III related genes significantly divergent from that of *Pseudomonas syringae* pv. *tomato* strain DC3000. Mol Plant-Microbe Interact 22:52-62.

Badel, J.L., Charkowski, A.O., Deng, W.-L., and Collmer, A. 2002. A gene in the *Pseudomonas syringae* pv. *tomato* Hrp pathogenicity island conserved effector locus, *hopPtoA1*, contributes to efficient formation of bacterial colonies in planta and is duplicated elsewhere in the genome. Mol Plant-Microbe Interact 15:1014-1024.

Badel, J.L., Shimizu, R., Oh, H.-S., and Collmer, A. 2006. A *Pseudomonas syringae* pv. *tomato avrE1*/*hopM1* mutant is severely reduced in growth and lesion formation in tomato. Mol Plant-Microbe Interact 19:99-111.

Baltrus, D.A., Nishimura, M.T., Dougherty, K.M., Biswas, S., Mukhtar, M.S., Vicente, J., Holub, E.B., and Dangl, J.L. 2012. The molecular basis of host specialization in bean pathovars of *Pseudomonas syringae*. Mol Plant-Microbe Interact 25:877-888.

Baltrus, D.A., Nishimura, M.T., Romanchuk, A., Chang, J.H., Mukhtar, M.S., Cherkis, K., Roach, J., Grant, S.R., Jones, C.D., and Dangl, J.L. 2011. Dynamic evolution of pathogenicity revealed by sequencing and comparative genomics of 19 *Pseudomonas syringae* isolates. PLoS Pathog 7:e1002132.

Bender, C.L., Alarcon-Chaidez, F., and Gross, D.C. 1999a. *Pseudomonas syringae* phytotoxins: mode of action, regulation, and biosynthesis by peptide and polyketide synthetases. Microbiol Mol Biol Rev 63:266-292.

Bender, C.L., Rangaswamy, V., and Loper, J. 1999b. Polyketide production by plant-associated pseudomonads. Annu Rev Phytopathol 37:175-196.

Block, A., Li, G., Fu, Z.Q., and Alfano, J.R. 2008. Phytopathogen type III effector weaponry and their plant targets. Curr Opin Plant Biol 11:396-403.

Boyer, H.W., and Roulland-Dussoix, D. 1969. A complementation analysis of the restriction and modification of DNA in *Escherichia coli*. J Mol Biol 41:459-472.

Bronstein, P.A., Filiatrault, M.J., Myers, C.R., Rutzke, M., Schneider, D.J., and Cartinhour, S.W. 2008. Global transcriptional responses of *Pseudomonas syringae* DC3000 to changes in iron bioavailability *in vitro*. BMC Microbiol 8:209.

Brooks, D., Hernandez-Guzman, G., Koek, A.P., Alarcon-Chaidez, F., Sreedharan, A., Rangaswarmy, V., Penaloza-Vasquez, A., Bender, C.L., and Kunkel, B.N. 2004. Identification and characterization of a well-defined series of coronatine

biosynthetic mutants of *Pseudomonas syringae* pv. *tomato* DC3000. Mol Plant-Microbe Interact 17:162-174.

Buell, C.R., Joardar, V., Lindeberg, M., Selengut, J., Paulsen, I.T., Gwinn, M.L., Dodson, R.J., Deboy, R.T., Durkin, A.S., Kolonay, J.F., Madupu, R., Daugherty, S., Brinkac, L., Beanan, M.J., Haft, D.H., Nelson, W.C., Davidsen, T., Liu, J., Yuan, Q., Khouri, H., Fedorova, N., Tran, B., Russell, D., Berry, K., Utterback, T., Vanaken, S.E., Feldblyum, T.V., D'Ascenzo, M., Deng, W.-L., Ramos, A.R., Alfano, J.R., Cartinhour, S., Chatterjee, A.K., Delaney, T.P., Lazarowitz, S.G., Martin, G.B., Schneider, D.J., Tang, X., Bender, C.L., White, O., Fraser, C.M., and Collmer, A. 2003. The complete sequence of the *Arabidopsis* and tomato pathogen *Pseudomonas syringae* pv. *tomato* DC3000. Proc Natl Acad Sci USA 100:10181-10186.

Cai, R., Lewis, J., Yan, S., Liu, H., Clarke, C.R., Campanile, F., Almeida, N.F., Studholme, D.J., Lindeberg, M., Schneider, D., Zaccardelli, M., Setubal, J.C., Morales-Lizcano, N.P., Bernal, A., Coaker, G., Baker, C., Bender, C.L., Leman, S., and Vinatzer, B.A. 2011. The plant pathogen *Pseudomonas syringae* pv. *tomato* is genetically monomorphic and under strong selection to evade tomato immunity. PLoS Pathog 7:e1002130.

Choi, K.H., and Schweizer, H.P. 2006. mini-Tn*7* insertion in bacteria with single *att*Tn*7* sites: example *Pseudomonas aeruginosa*. Nat Protoc 1:153-161.

Cunnac, S., Lindeberg, M., and Collmer, A. 2009. *Pseudomonas syringae* type III secretion system effectors: repertoires in search of functions. Curr Opin Microbiol 12:53-60.

Cunnac, S., Chakravarthy, S., Kvitko, B.H., Russell, A.B., Martin, G.B., and Collmer, A. 2011. Genetic disassembly and combinatorial reassembly identify a minimal functional repertoire of type III effectors in *Pseudomonas syringae*. Proc Natl Acad Sci U S A 108:2975-2980.

Ferguson, I.B., and Mitchell, R.E. 1985. Stimulation of ethylene production in bean leaf discs by the pseudomonad phytotoxin coronatine. Plant Physiol 77:969-973.

Figurski, D., and Helinski, D.R. 1979. Replication of an origin-containing derivative of plasmid RK2 dependent on a plasmid function provided *in trans*. Proc Natl Acad Sci USA 76:1648-1652.

Filiatrault, M.J., Stodghill, P.V., Myers, C.R., Bronstein, P.A., Butcher, B.G., Lam, H., Grills, G., Schweitzer, P., Wang, W., Schneider, D.J., and Cartinhour, S.W. 2011. Genome-wide identification of transcriptional start sites in the plant pathogen *Pseudomonas syringae* pv. *tomato* str. DC3000. PLoS One 6:e29335.

Geng, X., Cheng, J., Gangadharan, A., and Mackey, D. 2012. The coronatine toxin of *Pseudomonas syringae* is a multifunctional suppressor of *Arabidopsis* defense. Plant Cell (in press).

Goel, A.K., Lundberg, D., Torres, M.A., Matthews, R., Akimoto-Tomiyama, C., Farmer, L., Dangl, J.L., and Grant, S.R. 2008. The *Pseudomonas syringae* type III effector HopAM1 enhances virulence on water-stressed plants. Mol Plant Microbe Interact 21:361-370.

Guo, M., Tian, F., Wamboldt, Y., and Alfano, J.R. 2009. The majority of the type III effector inventory of *Pseudomonas syringae* pv. *tomato* DC3000 can suppress plant immunity. Mol Plant Microbe Interact 22:1069-1080.

Hanahan, D. 1985. Techniques for transformation of *E. coli*. Pages 109-135 in: DNA Cloning: A Practical Approach, D.M. Glover, ed. IRL Press, Oxford, United Kingdom.

House, B.L., Mortimer, M.W., and Kahn, M.L. 2004. New recombination methods for *Sinorhizobium meliloti* genetics. Appl Environ Microbiol 70:2806-2815.

Ishiga, Y., Uppalapati, S.R., Ishiga, T., and Bender, C.L. 2010. Exogenous coronatine, but not coronafacic acid or methyl jasmonate, restores the disease phenotype of a coronatine-defective mutant of Pseudomonas syringae pv. tomato on tomato seedlings. J Gen Plant Pathol 76:188-195.

Kenyon, J.S., and Turner, J.G. 1992. The stimulation of ethylene synthesis in *Nicotiana tabacum* leaves by the phytotoxin coronatine. Plant Physiol 100:219-224.

King, E.O., Ward, M.K., and Raney, D.E. 1954. Two simple media for the demonstration of pyocyanin and fluorescin. J Lab Clin Med 44:301-307.

Kloek, A.P., Verbsky, M.L., Sharma, S.B., Schoelz, J.E., Vogel, J., Klessig, D.F., and Kunkel, B.N. 2001. Resistance to *Pseudomonas syringae* conferred by an *Arabidopsis thaliana* coronatine-insensitive (*coi1*) mutation occurs through two distinct mechanisms. Plant J 26:509-522.

Kvitko, B.H. 2009. Construction of *Pseudomonas syringae* pv. *tomato* DC3000 Polymutant Strains to Uncover Functional Groups in Virulence

Kvitko, B.H., Park, D.H., Velásquez, A.C., Wei, C.-F., Russell, A.B., Martin, G.B., Schneider, D.J., and Collmer, A. 2009. Deletions in the repertoire of *Pseudomonas syringae* pv. *tomato* DC3000 type III secretion effector genes reveal functional overlap among effectors. PLoS Pathogens 5:e1000388.

Lee, J., Teitzel, G.M., Munkvold, K., del Pozo, O., Martin, G.B., Michelmore, R.W., and Greenberg, J.T. 2012. Type III secretion and effectors shape the survival and growth pattern of *Pseudomonas syringae* on leaf surfaces. Plant Physiol 158:1803-1818.

Lin, N.C., and Martin, G.B. 2005. An *avrPto*/*avrPtoB* mutant of *Pseudomonas syringae* pv. *tomato* DC3000 does not elicit Pto-specific resistance and is less virulent on tomato. Mol Plant Microbe Interact 18:43-51.

Lindeberg, M., Cunnac, S., and Collmer, A. 2012. *Pseudomonas syringae* type III effector repertoires: last words in endless arguments. Trends Microbiol 20:199-208.

Melotto, M., Underwood, W., and He, S.Y. 2008. Role of stomata in plant innate immunity and foliar bacterial diseases. Annu Rev Phytopathol 46:101-122.

Melotto, M., Underwood, W., Koczan, J., Nomura, K., and He, S.Y. 2006. Plant stomata function in innate immunity against bacterial invasion. Cell 126:969-980.

Miller, V.L., and Mekalanos, J.J. 1988. A novel suicide vector and its use in construction of insertion mutations: osmoregulation of outer membrane proteins and virulence determinants in *Vibrio cholerae* requires *toxR*. J Bacteriol 170:2575-2583.

Mittal, S., and Davis, K.R. 1995. Role of the phytotoxin coronatine in the infection of *Arabidopsis thaliana* by *Pseudomonas syringae* pv. *tomato*. Mol Plant-Microbe Interact 8:165-171.

Munkvold, K.R., Martin, M.E., Bronstein, P.A., and Collmer, A. 2008. A survey of the *Pseudomonas syringae* pv. *tomato* DC3000 type III secretion system effector

repertoire reveals several effectors that are deleterious when expressed in *Saccharomyces cerevisiae*. Mol Plant-Microbe Interact 21:490-502.

Munkvold, K.R., Russell, A.B., Kvitko, B.H., and Collmer, A. 2009. *Pseudomonas syringae* pv. *tomato* DC3000 type III effector HopAA1-1 functions redundantly with chlorosis-promoting factor PSPTO4723 to produce bacterial speck lesions in host tomato. Mol Plant Microbe Interact 22:1341–1355.

O'Brien, H.E., Thakur, S., and Guttman, D.S. 2011. Evolution of plant pathogenesis in *Pseudomonas syringae*: a genomics perspective. Annu Rev Phytopathol 49:269-289.

Oh, H.-S., Kvitko, B.H., Morello, J.E., and Collmer, A. 2007. *Pseudomonas syringae* lytic transglycosylases co-regulated with the type III secretion system contribute to the translocation of effector proteins into plant cells. J Bacteriol 189:8277-8289.

Peñaloza-Vázquez, A., Preston, G.M., Collmer, A., and Bender, C.L. 2000. Regulatory interactions between the Hrp type III protein secretion system and coronatine biosynthesis in *Pseudomonas syringae* pv. *tomato* DC3000. Microbiology 146:2447-2456.

Sambrook, J., and Russel, D.W. 2001. Molecular Cloning: A Laboratory Manual. Cold Spring Harbor, NY: Cold Spring Harbor Laboratory Press.

Schafer, A., Tauch, A., Jager, W., Kalinowski, J., Thierbach, G., and Puhler, A. 1994. Small mobilizeable multi-purpose cloning vectors derived from the *Escherichia coli* plasmids pK18 and pK19: selection of defined deletions in the chromosome of *Corynebacterium glutamicum*. Gene 145:69-73.

Simon, R., Priefer, U., and Puhler, A. 1983. A broad host range mobilization system for in vivo genetic engineering: Transposon mutagenesis in gram-negative bacteria. BioTechnology 1:784-791.

Sreedharan, A., Penaloza-Vazquez, A., Kunkel, B.N., and Bender, C.L. 2006. CorR regulates multiple components of virulence in *Pseudomonas syringae* pv. *tomato* DC3000. Mol Plant Microbe Interact 19:768-779.

Thilmony, R., Underwood, W., and He, S.Y. 2006. Genome-wide transcriptional analysis of the *Arabidopsis thaliana* interaction with the plant pathogen *Pseudomonas syringae* pv. *tomato* DC3000 and the human pathogen *Escherichia coli* O157:H7. Plant J 46:34-53.

Uppalapati, S.R., Ayoubi, P., Weng, H., Palmer, D.A., Mitchell, R.E., Jones, W., and Bender, C.L. 2005. The phytotoxin coronatine and methyl jasmonate impact multiple phytohormone pathways in tomato. Plant J 42:201-217.

Uppalapati, S.R., Ishiga, Y., Wangdi, T., Kunkel, B.N., Anand, A., Mysore, K.S., and Bender, C.L. 2007. The phytotoxin coronatine contributes to pathogen fitness and is required for suppression of salicylic acid accumulation in tomato inoculated with *Pseudomonas syringae* pv. *tomato* DC3000. Mol Plant Microbe Interact 20:955-965.

Wei, C.-F., Kvitko, B.H., Shimizu, R., Crabill, E., Alfano, J.R., Lin, N.-C., Martin, G.B., Huang, H.-C., and Collmer, A. 2007. A *Pseudomonas syringae* pv. *tomato* DC3000 mutant lacking the type III effector HopQ1-1 is able to cause disease in the model plant *Nicotiana benthamiana*. Plant J 51:32-46.

Worley, J.N., Russell, A.B., Wexler, A.G., Bronstein, P.A., Kvitko, B.H., Krasnoff, S.B., Munkvold, K.R., Swingle, B., Gibson, D.M., and Collmer, A. 2013. *Pseudomonas syringae* pv. tomato DC3000 CmaL (PSPTO4723), a DUF1330 family member, is needed to produce L-allo-isoleucine, a precursor for the phytotoxin coronatine. J Bacteriol (in press).

Zheng, X.Y., Spivey, N.W., Zeng, W., Liu, P.P., Fu, Z.Q., Klessig, D.F., He, S.Y., and Dong, X. 2012. Coronatine promotes *Pseudomonas syringae* virulence in plants by activating a signaling cascade that Inhibits salicylic acid accumulation. Cell Host Microbe 11:587-596.

CHAPTER 5

THE ABILITY OF *PSEUDOMONAS SYRINGAE* PV. *TOMATO* DC3000 TO COMPLEMENT THE GROWTH OF NON-PATHOGENIC PROTEOBACTERIA AT MODERATE DISTANCES (100 µm) IN FOLIAR INFECTIONS OF *NICOTIANA BENTHAMIANA* APPEARS TO BE DEPENDENT SOLELY ON EFFECTOR PROTEINS

INTRODUCTION

Pseudomonas syringae pv. *tomato* DC3000 (DC3000) is one of the most deeply understood bacterial plant-pathogens, and as such, a wide battery of assays has been developed to test the potency of the various aspects of its pathogenic repertoire. Among these is the ability of *P. syringae* pathovars to complement growth of crippled pathogens or non-pathogens (Macho et al., 2007). In Macho et al. 2007, the complementation of non-pathogen growth by wild-type virulence factors could be eliminated through dilution of the co-inoculated strains. The conceptual basis for this ability of complementation had not yet been explored, but has implications for how we conceptualize everyday experiments in the lab and the multiplicity of infection for individual strains. If the ability to complement can be eliminated by lowering inoculation dose, it suggests that there is an average spatial distance between individual bacteria in co-inoculations that must be achieved before these bacteria are free of each other's influence. This leaves open the possibility that at a short distance, without being a

mixed colony of bacteria growing within a leaf at a single site, non-pathogenic bacteria can benefit from the presence of pathogenic bacteria.

Individual colonies of *P. syringae* within leaf surfaces have been identified before and recently have been described as a series of monocolonies within leaf surfaces (Boureau et al., 2002; Godfrey et al., 2010). This growth dynamic of bacteria forming individual colonies from single bacterial cells when inoculated into foliar tissue demands that the complementation of non-pathogen growth must necessarily be due to complementation at a moderate distance and not due to mixed colonies of pathogen and non-pathogen.

The boundaries to non-pathogen growth within foliar tissue seem to be limited to defense responses. Apoplast fluid is capable of supporting bacterial growth without nutritional supplement, thus T3SS-deficient bacteria are able to grow in foliar environments but are ostensibly limited by PAMP-triggered immunity (PTI) (Rico and Preston, 2008). To defeat PTI, plant-pathogenic hemibiotropic bacteria primarily employ type III effectors (T3Es) delivered directly to the plant cytoplasm by a type III secretion system (T3SS) (Zhou and Chai, 2008; Cornelis Guy, 2010). These T3Es are collectively essential but individually dispensable (Lindeberg et al., 2012). Only a fraction of these are needed for near wild-type growth in *Nicotiana. benthamiana* when using the D28E derivative of DC3000, a polymutant deleted in 28 effector genes that still has a functional T3SS (Cunnac et al., 2011). Indeed, a combination of only two effectors, AvrPtoB and HopM1, is sufficient to see a synergistic boost to pathogen growth beyond the effect of either delivered alone; effector interplay must have aspects exceeding a simple additive property involving defense suppression. This idea is

supported by the diversity of functional domains present within effectors and their various apparent functions regarding signaling, PTI suppression, ETI suppression, and known plant-cell interactors in both signal perception and defense deployment in a variety of host backgrounds (Cunnac et al., 2009; Kenny and Valdivia, 2009; Deslandes and Rivas, 2012).

Beyond these observations of the role of effectors within cells, it is a relatively new concept to consider the influence of effectors between cells. One example includes HopI, and effector that disrupts signaling between cells by inhibiting plant defense-hormone biosynthesis (Jelenska et al., 2007). In DC3000, no other concrete examples exist, nor has an assay existed that is sensitive to these effects. Recent work with *Magnaporthe oryzae* has revealed that some fungal effectors are capable of cell-to-cell movement within infected leaves via plasmodesmata (Khang et al., 2010). The plasmodesmata-localized protein PDPLP5 was also recently identified as being important for resistance to bacterial pathogens, and importantly, is highly induced when exposed to bacteria, which in turn serves to decrease plasmodesmatal traffic (Lee et al., 2011). This suggests that molecular trafficking between cells via plasmodesmata is a feature of plant biology that pathogens of various types take advantage of. Not utilizing cell-to-cell communication via plasmodesmata would make bacterial plant pathogens somewhat an oddball given that viral, viroidal and fungal pathogens are able to utilize them; that they are universally abundant among plants; and that they have the ability to transmit favorable information into the surrounding tissue (Burch-Smith and Zambryski, 2012).

P. syringae strains produce small diffusible molecules, which highlights the potential for bacterial pathogens to communicate with host-cells at a distance. *P. syringae* strains tend to produce ethylene and at least one other biologically active diffusible small molecule during infections (Baltrus et al., 2011). DC3000 produces the plant-hormone mimic coronatine which is important for the opening of stomata as well as providing modest growth benefits (Brooks et al., 2004; Melotto et al., 2006; Underwood et al., 2007). Other small metabolites include syringolin, which inhibits proteasome activity; phaseolotoxin, which inhibits ornithine transcarbamoylase; and tabtoxin, which inhibits glutamine synthetase; among various other small molecules (Sinden and Durbin, 1968; Tam and Patil, 1972; Thomas et al., 1983; Templeton et al., 1984; Groll et al., 2008). These small molecules have various evolutionary histories and bacterial pathogens appear to produce far fewer different small molecules than different effectors, but almost all sequenced strains of *P. syringae* utilize at least one small diffusible molecule as part of its pathogenic repertoire (Baltrus et al., 2011).

Bacteria also release proteins that plants deploy defense response to. Pathogen associated molecular patterns (PAMPs), such as flagellin and EF-Tu, are proteins with defense-activating potential that are shed by *P. syringae*, and the resultant immunological responses may take place at cells which are not directly adjacent (Monaghan and Zipfel, 2012). The harpins present an additional layer of potentially diffusible proteins that elicit strong defense responses (Wei et al., 1992; Dong et al., 1999). HrpZ seems to forms small pores in plant plasma membranes (Lee et al., 2001), and the several harpins produced by a given strain seem to be partially redundant in their ability to form a translocon necessary for the delivery of effectors into the host cell

cytoplasm (Kvitko et al., 2007). The secretion of these factors is coordinated by HrpJ, a secreted protein that seems to time the release of harpins and effectors after pilus construction (Crabill et al., 2012), which may reduce the amount of harpins that adjacent cells are exposed to, but represents another class of potential elicitors.

Here, bacteria expressing fluorescent proteins are used to demonstrate several features of the biology of T3SS utilizing plant-pathogenic bacteria. (i) Pathogen population growth due to increased effector repertoire potency correlates with stronger colony development. (ii)The complementation of non-pathogen growth by a wild-type pathogen occurs over intermediate distances from a WT colony. (iii) Such complementation is not based on the major phytotoxin of DC3000, coronatine. (iv) Such complementation can be restored using a minimal number of effectors and seems to be dependent only on effectors.

RESULTS

Strains with increased growth *in planta* form larger colonies.

Foliar tissues do not show much autofluorescence in the mCherry signal band when infiltrated with D28E mCherry (Fig. 5.1A). D28E does not grow when syringe-inoculated into *N. benthamiana* leaves, so all signal here is presumed to be autofluorescence that is either endogenous or induced by PTI (Cunnac et al., 2011). Other corroborating images are shown later in this chapter that show low autofluorescence, and importantly, these can usually be distinguished by their strong autofluorescence in other wavelengths, such as typical YFP emission wavelengths.

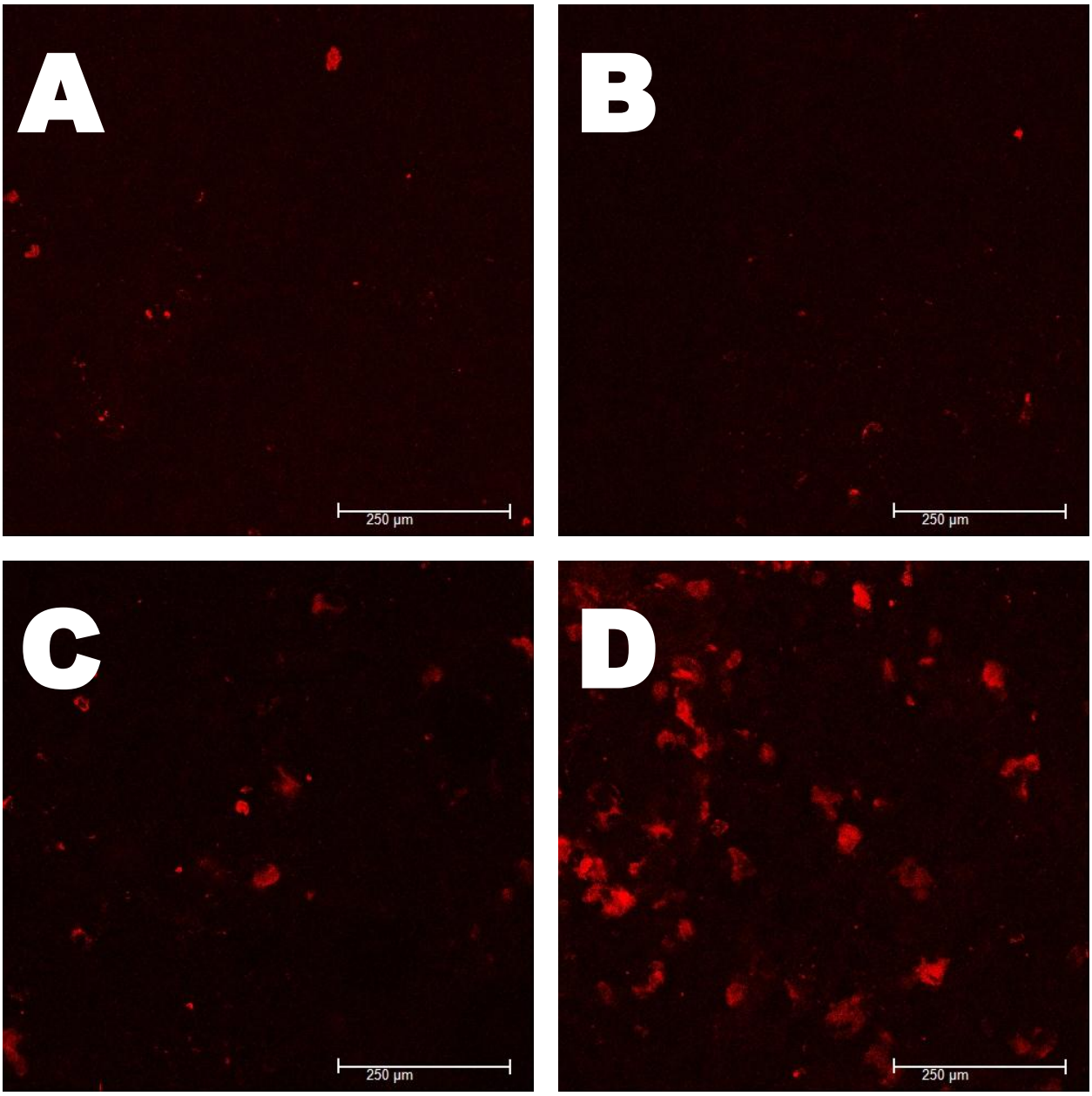

Figure 5.1. Boosts in growth from the addition of effectors can be visualized in planta. Strains are infiltrated at 10^6 cfu/ml and visualized 3 dpi. All strains are marked with a fluorescent protein expression construct integrated into the genome via Tn7 mutagenesis. Only the red channel is shown **A**, DC3000 D28E Tn7-mCherry. **B**, DC3000 D28E+*avrPtoB* Tn7-mCherry. **C**, DC3000 D28E + *avrPtoB* + *hopM1* Tn7-mCherry. **D**, DC3000 D28E+*avrPtoB* + *hopM1* + *avrE* + *hopAA1-1* Tn7-mCherry. Strains showing further additions to growth are not appear much different from the construct shown in panel D.

Restoring some growth to D28E through the restoration of AvrPtoB to the genome is not evidenced by increases in visible pathogen growth (Fig. 5.1B). Resolution at this scale is poorer than the individual bacterial scale, and further, the use of a Tn7-mediated mCherry genomic insert is limiting in its weak fluorescence signal compared to plasmid based systems. A further increase in growth with the addition of both AvrPtoB and HopM1 shows visible colonies (Fig. 5.1C). These appear as soft-bordered structures, either globular or shapes excluded from mesophyll cells, one of each highlighted by arrows. D28E+AvrPtoB+CEL, which has even more growth, appears as larger, brighter, and more frequent colonies (Fig. 5.1D). That colony size and frequency are both affected by increased effector impact implies that there are, at a minimum, at least two ways in which effectors can modulate pathogen growth.

Mixed inoculations of T3SS-deficient DC3000 with WT reveal that the helper effect is not a product of mixed colonies of bacteria.

Two basic conceptual theories exist as to why non-pathogenic bacteria are helped by co-inoculation at high but not low doses: either that the non-pathogenic bacteria are helped by mixing directly with pathogenic bacteria, or pathogenic bacteria provide some benefit to non-pathogens at a distance by modifying conditions within the host at moderate distances. To begin addressing this question, differentially labeled bacteria were co-inoculated into leaves and incubated for short durations of 2 to 3 days. T3SS- DC3000 was observed to be growing only rarely in mixed colonies with WT (Fig. 5.2A,B). This growth was not seen when T3SS$^-$ DC3000 was inoculated with itself in two separate colors (Fig. 5.2C). WT, on the other hand, had even more pronounced

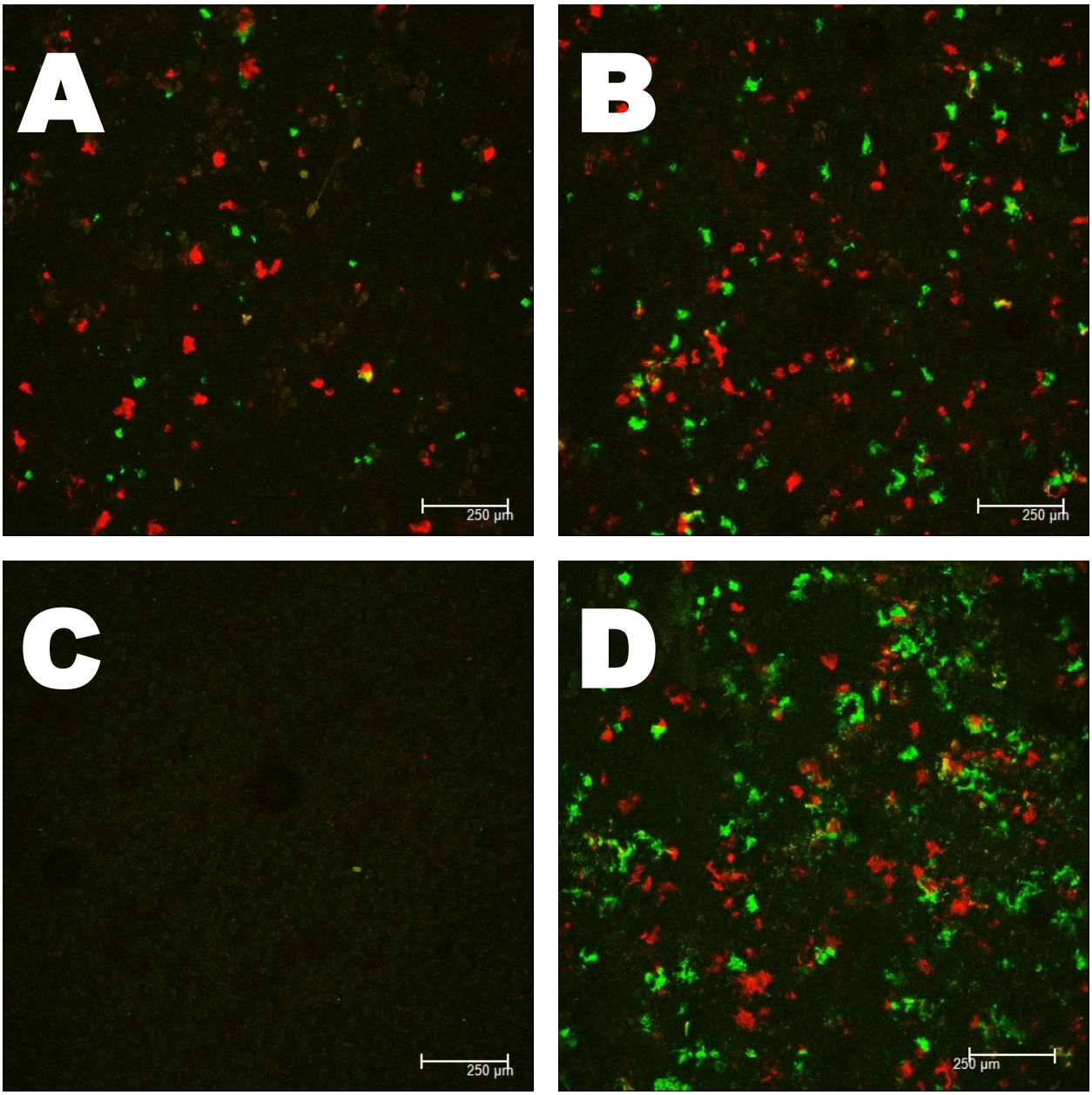

Figure 5.2. The “helper” effect of DC3000 is made by complementing colony formation over short distances in *Nicotiana benthamiana*. Individual strains were marked with a plasmid expressing either a YFP or mCherry fluorescent protein driven by an nptII promoter as noted. $1x10^6$ cfu/ml inoculum for each noted strain, introduced to the plant as a mixture by blunt syringe inoculation, incubated in standard laboratory conditions, and images taken 2 dpi. YPF is shown in green and mCherry in red. **A**, DC3000 Δ*hopQ1-1* pmCherry and DC3000 *hrcC*::*nptII* pYFP. **B**, DC3000 Δ*hopQ1-1* pYFP and DC3000 *hrcC*::*nptII* pmCherry. **C**, DC3000 *hrcC*::*nptII* pmCherry and DC3000 *hrcC*::*nptII* pYFP. **D**, DC3000 Δ*hopQ1-1* pYFP and DC3000 Δ*hopQ1-1* pmCherry

apparent growth when mixed with itself (Fig. 5.2D). This increased growth with itself points against a role for coronatine as the T3SS$^-$ mutant is COR$^+$, and instead suggests that it is the T3SS effectors which are having an effect at a moderate distance. Also, our different labeling plasmids to not show a bias at this level of analysis.

Non-plant-pathogens are helped in a similar manner to T3SS- DC3000.

The results from Fig. 5.2, however, could still be interpreted as being dependent on T3SS-related factors or growth patterns, and that perhaps other bacteria behave differently when helped. To address this, D28E (T3SS$^+$ but T3E$^-$), *Pseudomonas fluorescens* Pf0-1, and *E. coli* DH5α were co-inoculated with DC3000 in a manner similar to above. In all cases, the co-inoculated bacteria formed distinct colonies while not being competent of growth on their own (Fig. 5.3). Thus, help from WT DC3000 works in the same way independently of the identity of the helped bacteria. Another conclusion is that forming colonies within leaf tissue is not a pathogen-specific ability of DC3000 or other bacteria but instead something that is more broadly conserved among non-plant-pathogenic proteobacteria.

Individual DC3000 colonies modify host physiology enough to permit non-pathogen growth on the order of hundreds of micrometers.

If DC3000 modifies host tissue in a way that supports non-pathogen growth at distances when inoculated at a high level, then individual DC3000 colonies might create overlapping areas where non-pathogens can grow, thus accounting for the field-like distribution of non-pathogen growth in mixed infiltrations when both DC3000 and non-

Figure 5.3. Non-plant-pathogenic gram-negative bacteria are helped in identical manner to a disarmed plant-pathogen in *Nicotiana benthamiana*. All strains infiltrated at 10^6 cfu/ml and imaged 3 dpi. YFP staining is by a plasmid and mCherry staining is done by Tn7-mediated stable integration of an expression construct. YPF is shown in green and mCherry in red. **A**, *hrcC*::*nptII* pYFP. **B**, DC3000 *hrcC*::*nptII* pYFP and DC3000 Δ*hopQ1-1* Tn7-mCherry. **C**, DC3000 D28E pYFP. **D**, DC3000 D28E pYFP and DC3000 Δ*hopQ1-1* Tn7-mCherry. **E**, Pf01 pYFP. **F**, Pf01 pYFP and DC3000 Δ*hopQ1-1* Tn7-mCherry. **G**, *E. coli* DH5α pYFP. **H**, E.coli DH5α pYFP and DC3000 Δ*hopQ1-1* Tn7-mCherry.

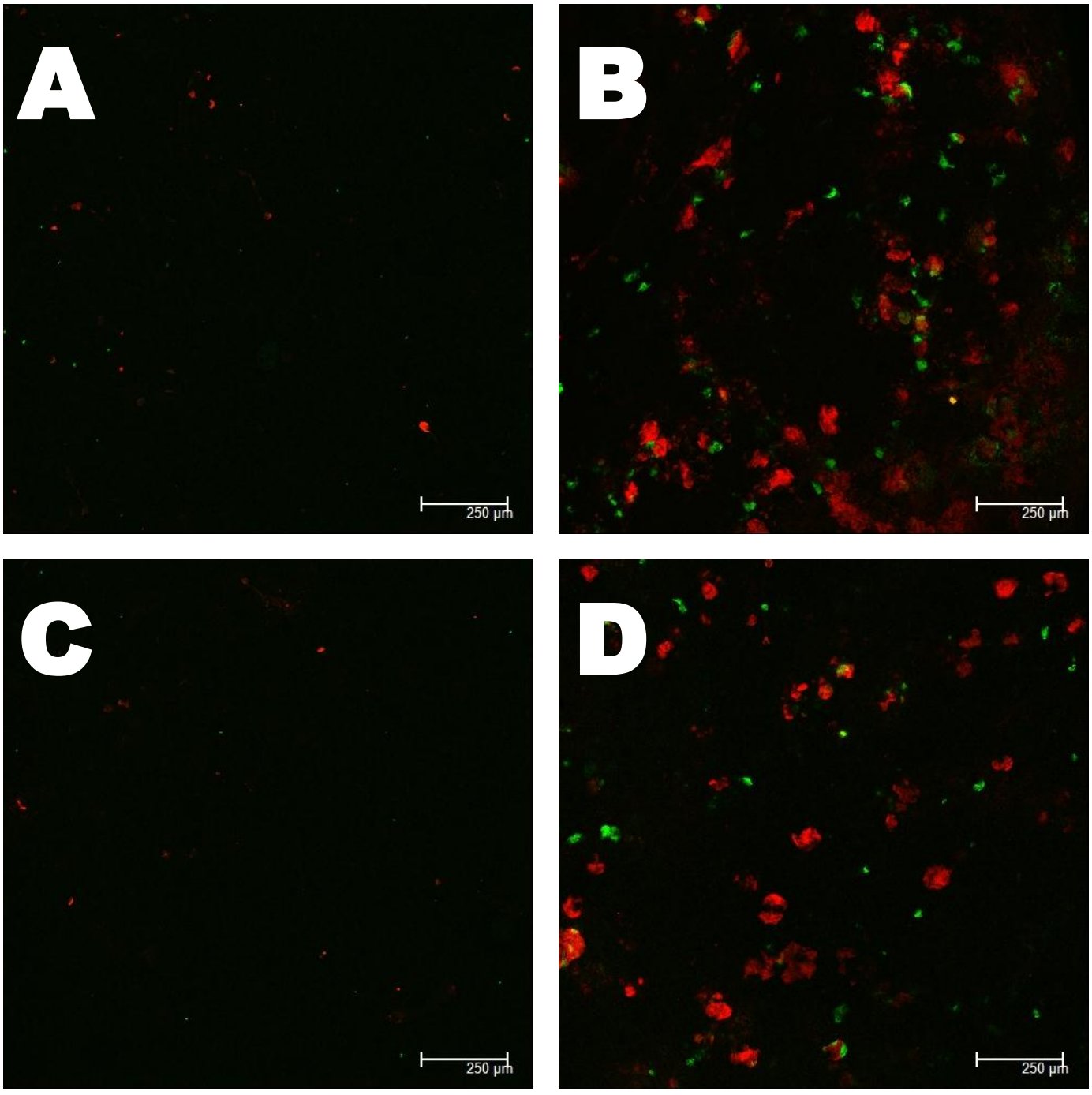
A
250 µm
B
250 µm
C
250 µm
D
250 µm

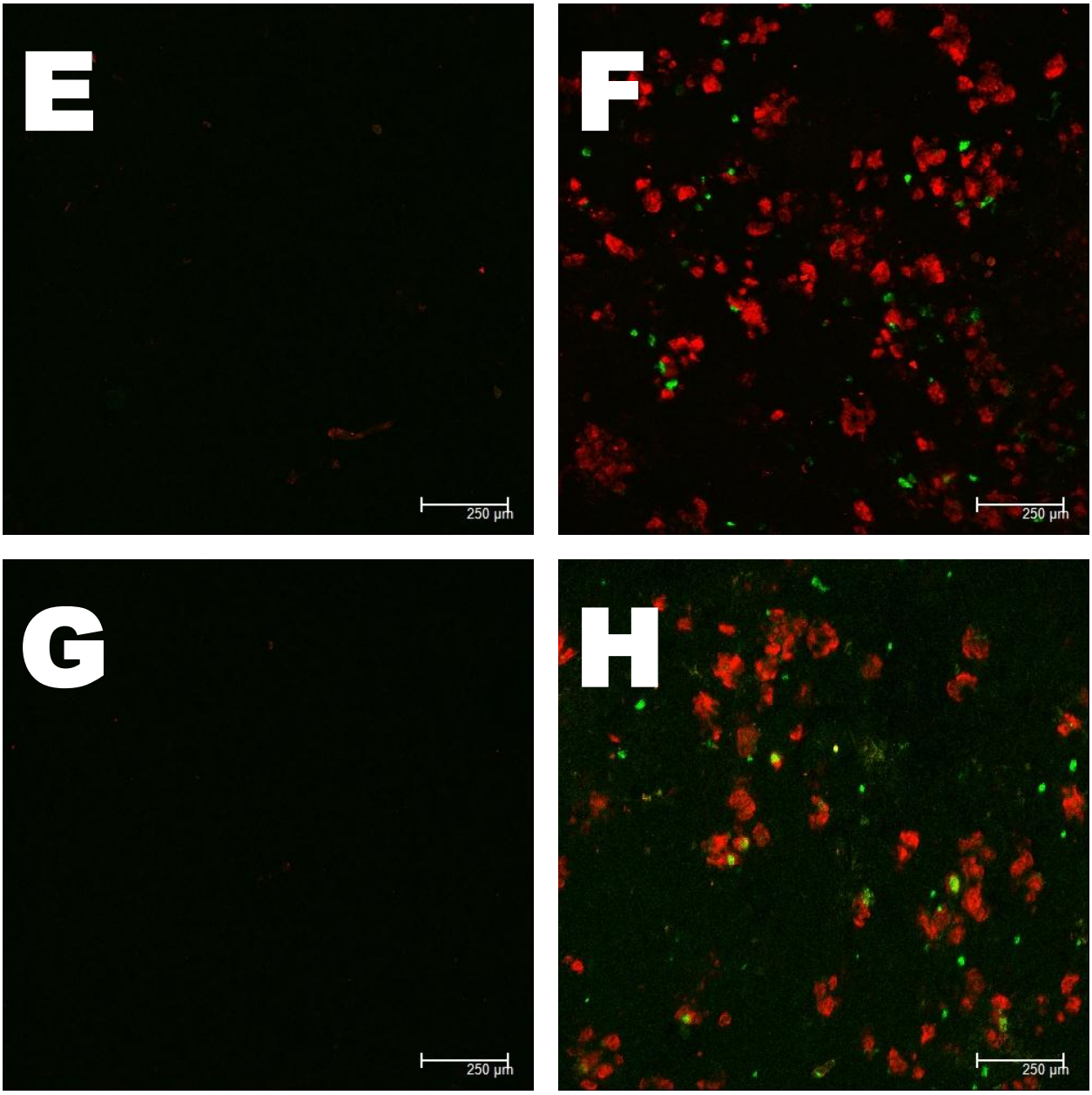
E
250 µm
F
250 µm
G
250 µm
H
250 µm

pathogen are introduced at an elevated inoculum. The previous infiltrations with both pathogen and non-pathogen at elevated inoculum levels show that, while not uniformly distributed, a reasonable coverage is achieved of the entire leaf surface that can be probed for pathogen influence since the non-pathogens will fail to grow without it. To probe fields of T3SS-deficient DC3000, the inoculum of WT DC3000 was reduced approximately 100 fold. Individual DC3000 colonies are capable of casting zones where non-pathogens are able to grow (Fig. 5.4A). When multiple colonies are present, the resulting non-pathogen growth seems to be a product of these zones overlapping (Fig. 5.4B). The magnitude of non-pathogen benefit seems to decrease with increasing distance away from the WT colony, indicating that some form(s) of diffusion are likely involved in this phenomenon.

Coronatine is not essential for non-pathogen benefit from WT growth.

The zone of non-pathogen growth facilitated by individual colonies of DC3000 seems somewhat akin to a gradient, immediately implicating a diffusible factor. Mutants deficient in COR production, however, are able to produce these zones (Fig. 5.5).

A few effectors are sufficient to support non-pathogen growth.

Effectors are essential for pathogen growth and modulate colony size and fluorescence signal intensity (Fig. 5.1). If coronatine is not essential for non-pathogen growth, then effectors are most likely the responsible party even though no mechanism has been demonstrated for effector spread between cells in bacterial pathogens. D28E

Figure 5.4. Colonies of DC3000 Δ*hopQ1-1* affect neighboring leaf tissue in *N. benthamiana* in a way which allows for non-pathogen growth. Imaging performed 3 dpi. YPF is shown in green and mCherry in red. **A**, DC3000 *hrcC*::*nptII* pYFP infiltrated at 10^6 cfu/ml and DC3000 Δ*hopQ1-1* pmCherry infiltrated at 10^4 cfu/ml. A single DC3000 Δ*hopQ1-1* colony is shown with surrounding DC3000 *hrcC*::*nptII* growth. **B**, DC3000 *hrcC*::*nptII* pYFP infiltrated at 10^6 cfu/ml and DC3000 Δ*hopQ1-1* pmCherry infiltrated at 10^4 cfu/ml. Multiple, individual colonies of DC3000 Δ*hopQ1-1* are shown with surrounding DC3000 *hrcC*::*nptII* growth and shows the convergence of influence from individual successful colonies. **C**, DC3000 Δ*hopQ1-1* pmCherry infiltrated at 10^4 cfu/ml. **D**, DC3000 *hrcC*::*nptII* pYFP infiltrated at 10^6 cfu/ml.

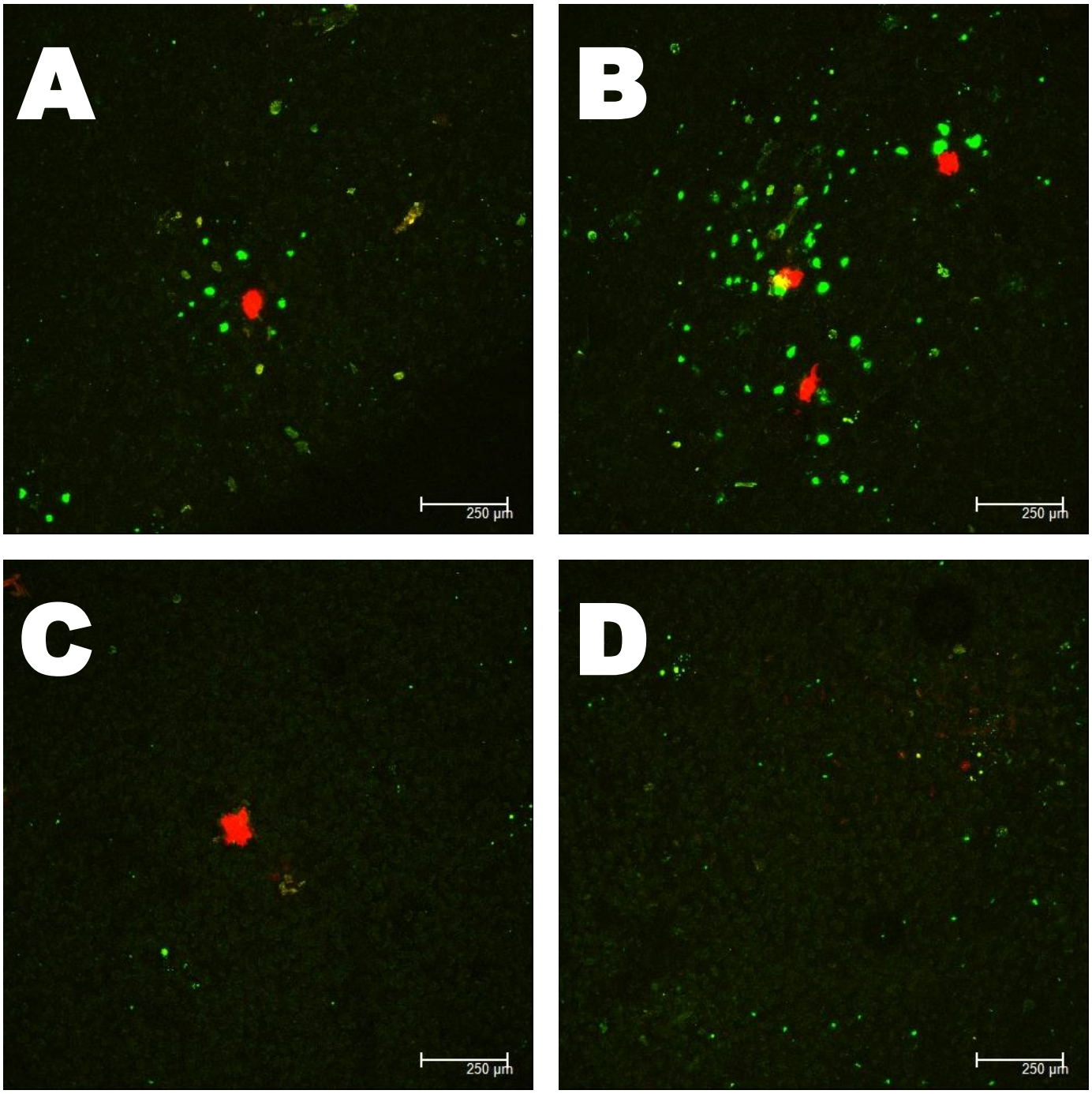
A
250 µm
B
250 µm
C
250 µm
D
250 µm

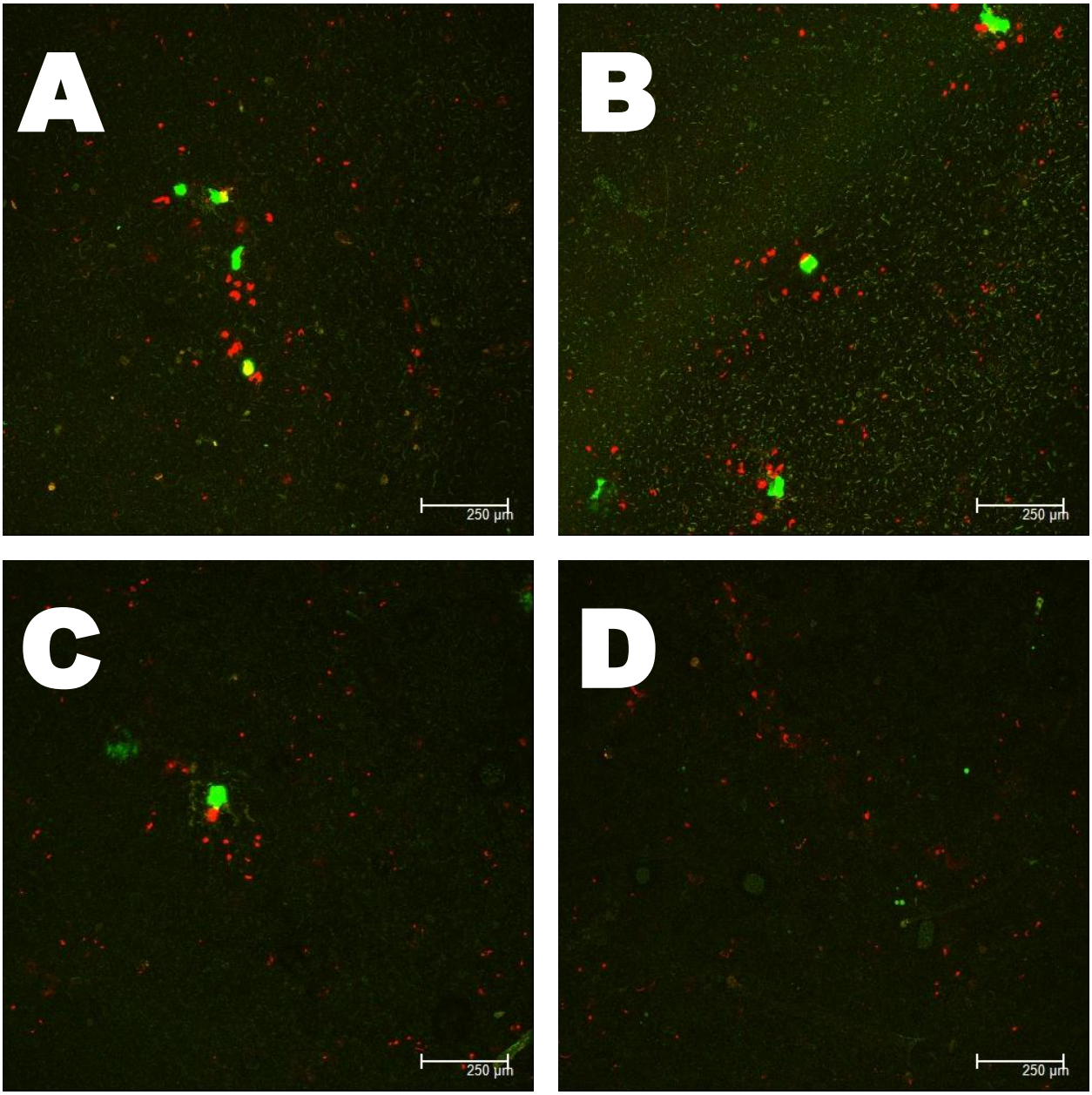

Figure 5.5. Coronatine production is not essential for ability of DC3000 to facilitate non-pathogen growth. Imaging was performed 3 dpi. YPF is shown in green and mCherry in red. DC3000 *hrcC*::*nptII* pmCherry was infiltrated at 10^6 cfu/ml, the DC3000 Δ*hopQ1-1* pYFP variant infiltrated at 10^4 cfu/ml. **A**, DC3000 *hrcC*::*nptII* pmCherry and DC3000 Δ*hopQ1-1* Δ*cfa* operon pYFP. **B**, DC3000 *hrcC*::*nptII* pmCherry and DC3000 Δ*hopQ1-1* Δ*corRS* pYFP. **C**, DC3000 *hrcC*::*nptII* pmCherry and DC3000 Δ*hopQ1-1* pYFP. **D**, DC3000 *hrcC*::*nptII* pmCherry only.

variants were labeled with mCherry by Tn7 mediated genomic integration then co-inoculated with T3SS-deficient DC3000. D28E+AvrPtoB+CEL was sufficient both for pathogen growth and non-pathogen growth in a zone around individual pathogen colonies (Fig. 5.6A). D28E + 8, which grows more strongly, shows increased pathogen growth but does not necessarily give a boost to non-pathogen growth (Fig. 5.6B). This pattern seems to hold up over many experiments where increased effector repertoires do not increase non-pathogen growth, though effectors are essential (Fig. 5.6C,D).

There are two distinct possibilities that remain after this observation – either that DC3000 is providing a nutritional benefit to surrounding non-pathogens or that DC3000 is defeating surrounding plant defenses on a local scale, ostensibly by effectors, but possibly by another mechanism.

Two effectors, delivered by a non-pathogen, is sufficient to support non-pathogen growth.

Fields of T3SS-deficient DC3000 were probed with a special derivative of *P. fluorescens* PF0-1 called “EtHAn” (Thomas et al., 2009). EtHAn contains the T3SS integrated into its genome, which makes it more useful as a tool for effector delivery absent other pathogenic factors encoded for in the DC3000 genome. EtHAn+AvrPtoB+HopM1 is enough to give a small boost to T3SS$^-$ DC3000 when co-inoculated with both at high levels of inoculum (Fig. 5.7A). The EtHAn derivative is labeled with mCherry, but visible colonies of it cannot be distinguished from background fluorescence and have not been observed (data not shown). T3SS-deficient DC3000 tends to grow better than PF01 as a helped strain, and so it is not entirely surprising that

Figure 5.6. Single colonies of DC3000D28E derivatives with several effectors can support the growth of neighboring non-pathogens in *N. benthamiana*. DC3000D28E derivatives are marked with a fluorescent protein expression construct integrated into the genome via Tn7 mutagenesis and was infiltrated at 10^4 cfu/ml. DC3000 *hrcC*::*nptII* is marked with pYFP and was infiltrated at 10^6 cfu/ml. YFP is shown in green and mCherry in red. Imaging was performed at 3 dpi. **A**, DC3000 *hrcC*::*nptII* and DC3000 D28E + *avrPtoB* + *hopM1* + *avrE* + *hopAA1-1*. **B**, DC3000 *hrcC*::*nptII* and DC3000 D28E + *avrPtoB* + *hopM1* + *avrE* + *hopAA1-1* + *avrPto* + *hopAM1-1* + *hopE1* + *hopG1*. **C**, DC3000 *hrcC*::*nptII* and DC3000 Δ*hopQ1-1*. **D**, DC3000 *hrcC*::*nptII* only.

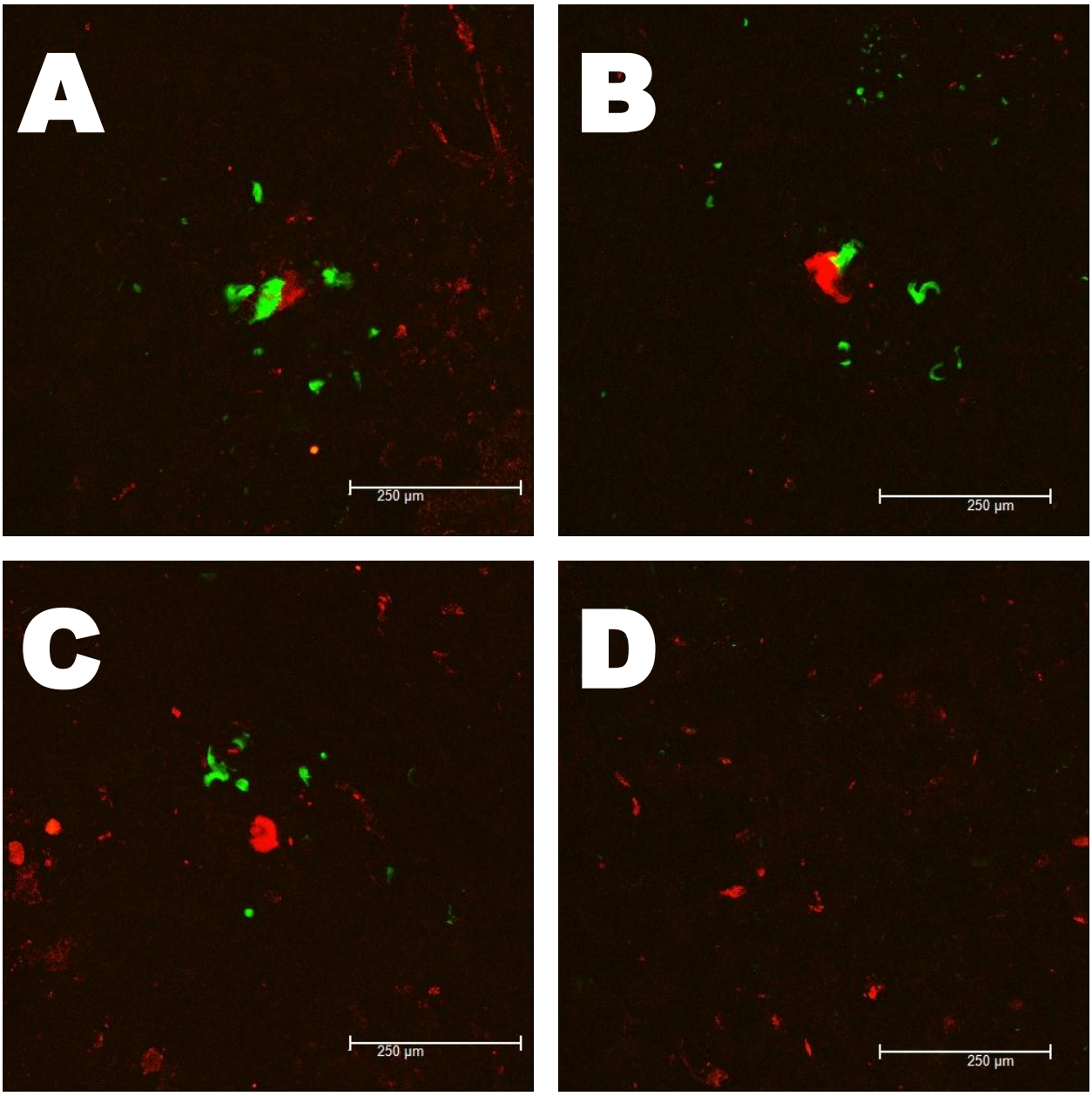
A
250 µm
B
250 µm
C
250 µm
D
250 µm

Figure 5.7. Two effectors, are sufficient to support the growth of DC3000 *hrcC*::*nptII* in a mixed inoculation. DC3000 *hrcC*::*nptII* is marked with pYFP. Pf01 “EtHAn” derivatives and DC3000D28E + *avrPtoB* + *hopM1* are marked with a mCherry fluorescent protein expression construct integrated into the genome via Tn7 mutagenesis. Strains were inoculated individually or as a mixture with each at 10^6 cfu/ml. Imaging was performed at 3 dpi. **A**, Pf01 “EtHAn” + *avrPtoB* + *hopM1* and DC3000 *hrcC*::*nptII*. **B**, DC3000 D28E + *avrPtoB* + *hopM1* and DC3000 *hrcC*::*nptII*. **C**, Pf01 “EtHAn” + *avrPtoB* and DC3000 *hrcC*::*nptII*. **D**, Pf01 “EtHAn” and DC3000 *hrcC*::*nptII*. A significant gain in the apparent growth of DC3000 *hrcC*::*nptII* is only seen with both HopM1 and AvrPtoB being delivered. HopM1 being delivered without AvrPtoB by “EtHAn” appears similar to panel C. “EtHAn” colonies were not consistently observed in any sample tested while DC3000 D28E + *avrPtoB* + *hopM1* colonies are observed with regularity, but only at 10^6 cfu/ml as in panel B.

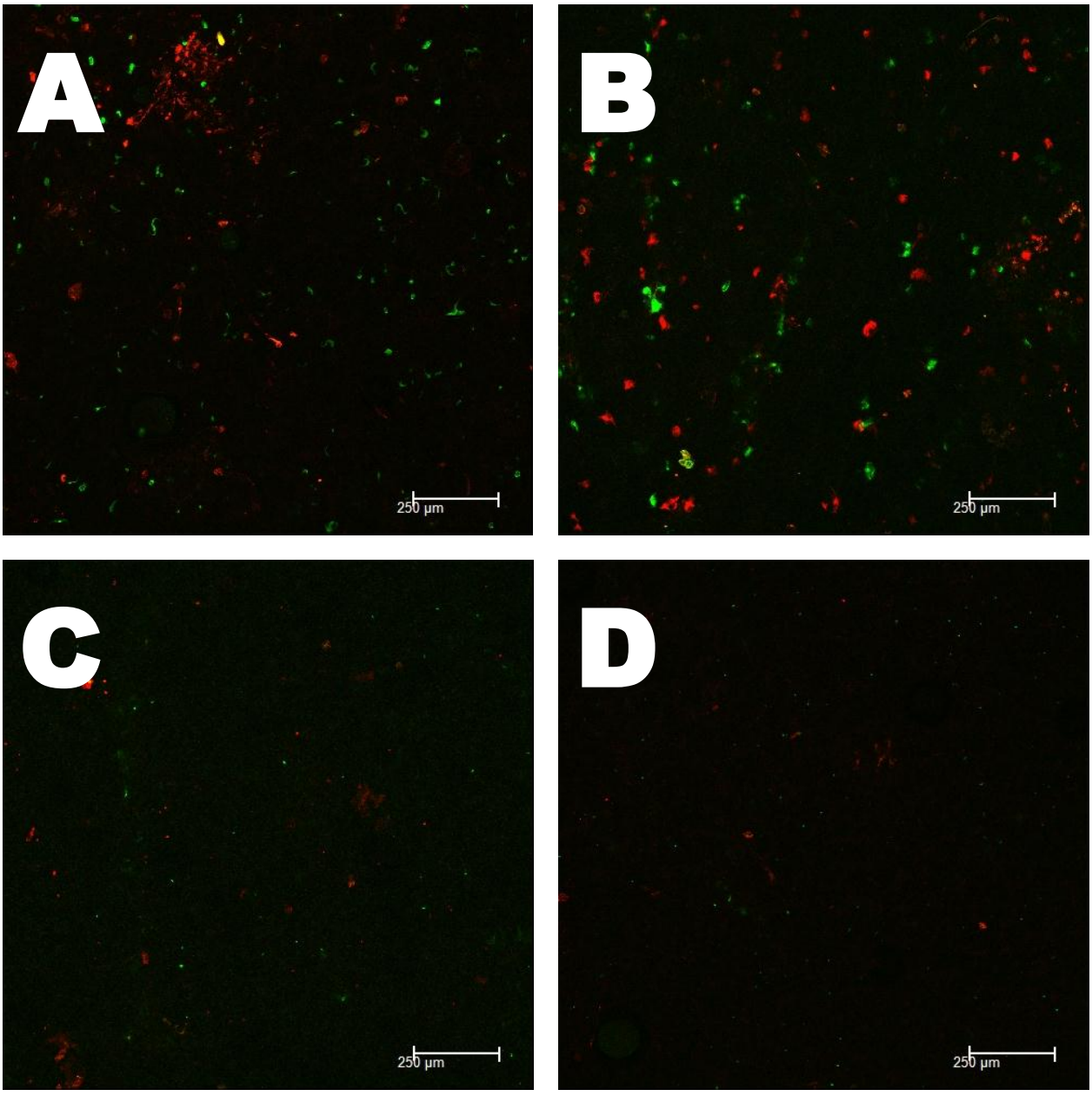
A
250 µm
B
250 µm
C
250 µm
D
250 µm

it would be helped here more than the EtHAn which is delivering it. Furthermore, given that D28E+AvrPtoB+CEL helps as much, if not better, than D28E+8, which grows better (Fig. 5.6), there may be a plant response to the T3SS which EtHAn+AvrPtoB+HopM1 cannot overcome that requires additional effectors to defeat. D28E+AvrPtoB+HopM1 can be seen growing at low levels, and similarly helps T3SS-deficient DC3000 (Fig. 5.7B). EtHAn delivering a single effector, AvrPtoB, is insufficient, as is EtHAn without effectors (Fig. 5.7C,D). Taken together, these suggest that the synergistic effect that AvrPtoB and HopM1 have on D28E growth extends to neighboring tissue. Since these effectors are both implicated in the suppression of plant defenses, the most reasonable conclusion from this work is that effectors have a physiological impact on host tissue extending several hundred micrometers out from the site of infection.

DISCUSSION

The ability of wild-type pathogens to complement non-pathogen growth at high initial inoculum levels was investigated for the nature of its spatial relationship. The surprising conclusion is that non-pathogen growth can be supported by a single colony of wild-type pathogen within a leaf and that effectors appear to be sufficient to confer this ability. Unsurprisingly, additional effectors that increase growth lead to larger colonies in plant tissue. It is remarkable, however, that true composite colonies of wild-type and non-pathogen colonies do not readily form from syringe-infiltrated mixtures. This clearly suggests that basic plant or bacterial physiology prevents bacterial congregation. Further, *P. fluorescens* and *E .coli* form colonies in plant tissue that

resemble T3SS-deficient DC3000 in these mixtures, suggesting that colony formation is not a pathogen ability per se, but is instead a result of basic plant and/or proteobacterial physiology. The formation of these adjacent colonies of non-pathogen can be partially complemented by a non-pathogen delivering two effectors by a transgenic T3SS. Thus, T3SS substrates have a radius of influence, extending out from the parent colony and strong enough to support non-pathogen growth.

The necessity for high-inoculum doses for the effect of adjacent colony growth could be interpreted in two ways – either that the entire leaf needed to be infected so strongly that the entire local physiology is changed, or that from each colony extends a radius where non-pathogens can grow as a feature of successful infection where high inoculum doses simply provide overlapping radii. Here, the second is demonstrated to be more accurate.

A mechanism for the distance effect, however, is difficult to conceive. The first and most obvious solution would be the bacterial secretion of a small metabolite either affecting plant defenses or bacterial growth. There are several lines of evidence that argue against this interpretation. Knockout mutations that affect the major phytotoxin production in DC3000 do not significantly affect the ability to complement non-pathogen growth. Secondly, because the growth complementation effect can be observed with effectors delivered by *P. fluorescens* and is not observed with high-inoculum doses of T3SS-deficient DC3000, quorum sensing factors or other bacterial-derived bacterial-growth promoters that are not effectors can be ruled out. It instead suggests that the effectors are solely responsible. Furthermore, high dosage inoculations of D28E or T3SS-deficient DC3000 fail to propagate, indicating that even with high levels of

virulence induced pathogens the production of small metabolites is not enough to achieve more than meager growth (Cunnac et al., 2011). While these small metabolites play essential functions in *P. syringae* pathogenesis, none exist without effectors and seem to play a more important role in pathogen lifestyle rather than growth.

A second explanation is the traversing of effectors between cells via plasmodesmata. Both viruses, and now fungi, extend their influence to nearby cells by spreading proteinaceous components through plasmodesmata (Khang et al., 2010; Harries and Ding, 2011). Further, callose deposits are made in response to bacterial PAMPs, a response linked to plasmodesmatal obstruction. The experiment presented in Fig. 5.7 uses only two effectors: HopM1 and AvrPtoB. The molecular weights for these two effectors are approximately 75 kDa and 59 kDa, respectively. These are either close to or exceed the size exclusion limit seen with *Magnaporthe oryzae* effector PWL2 between 45 kDa and 66 kDa (Khang et al., 2010). Components of the T3SS, notably all but one of the harpins, fall within this range, and it is possible, however unlikely, that one or more of these components modifies the size exclusion limit of plasmodesmata as in some viruses (Wolf et al., 1989; Harries and Ding, 2011). While plausible, this solution does not match with our current understanding of plant-cell biology during bacterial infection.

A third possible mechanism involves *P. syringae* T3SS substrates modifying the host-cell metabolism and/or structure to secrete small molecules favorable to pathogen growth. This would account for the irregular, graduated growth pattern of non-pathogens. Its plausibility is boosted by the known properties of the harpins. HrpZ is known to create ion-permeable membrane complexes in lipid bilayers and associate

with plasma membranes when delivered extracellularly. They are also required for the translocation of effectors, though they appear to be redundant in that all harpins must be removed before translocation is abolished (Kvitko et al., 2007). Harpins are produced in high abundance, while relatively few are conceptually necessary for effector translocation, particularly compared to T3SSs from animal pathogens, hinting at a role distinct from that of a translocon. This hypothesis fails, however, when one considers that harpins induce strong defense responses, and therefore require the presence of effectors to defeat plant defenses – indeed, neither the EtHAn nor D28E strains were able to support non-pathogen growth, including their own, in the absence of effector proteins. While harpins may play a role in non-pathogen growth, the support function of the effectors is necessary. It could be that harpins are responsible for the release of nutrients, but effector proteins are needed to suppress callose deposition at the cell wall which could block growth and nutrient release (Brown et al., 1995).

We are left with a conundrum. It is likely that the effectors seem to be responsible for non-pathogen growth at moderate distances. If this is direct, the mode of transport for this effect would almost certainly be by plasmodesmata, but the effectors are almost uniformly large in size, meaning that there would need to be an increase in the size exclusion limit of plasmodesmata. It is, perhaps, conceivable that the effectors, which are easily unfolded for transport through the T3SS, could be threaded into plasmodesmata by an analogous mechanism, dubious as the thought may be.

There are only a few functions that can possibly be driving non-pathogen growth within these mixed inoculations. (i) Suppression of defenses at moderate distances by effectors through their translocation to adjacent cells. (ii) Release of rare nutrients, such

as iron, through pores created by harpins to boost pathogen growth. (iii) Modulation of plant-cell signaling by HopM1 to relax plant defenses over moderate distances. (iv) Some unknown process that is necessary for bacterial growth in plant tissue. While intriguing, these results are ultimately unsatisfying except to suggest that there is a fundamental feature of bacterial plant-pathogens that has yet to be elucidated or understood in its proper context.

MATERIALS AND METHODS

Bacterial strains and plasmids.

Bacterial strains and plasmids are listed in Table 5.1. *Pseudomonas syringae* strains were cultivated on King's B (KB) at 30°C (King et al., 1954). *Escherichia coli* strains were cultivated on Luria-Burtani media (Hanahan, 1985). Antibiotics were used at the following concentrations in µg/ml: rifampicin 50, spectinomycin 50, chloramphenicol 20, gentamycin 10c kanamycin 50, tetracycline 5.

Plasmid construction tools.

Plasmids were created as described and transformed into *E. coli* DH5α or Top10 by standard electroporation or heat-shock procedures, respectively. Primers were purchased from Integrated DNA Technology. PCR reactions were performed using either ExTaq DNA polymerase or PrimeSTAR HS DNA Polymerase (Takara Bio Inc.). Restriction enzymes and DNA ligation procedure enzymes were purchased from New

England Biolabs. Construct sequences were verified through sequencing performed by the Cornell University Life Sciences Core Laboratories Center.

Plasmid construction.

pCPP6257 and pCPP6258 were created using a pENTR/SD/D-TOPO cloning kit from Invitrogen with PCR products amplified using primer sets Topo-mCherryF/Topo-mCherryR and TOPO-GFP for/TOPO-GFP rev. These plasmids were recombined with pBS46 using LR Clonase II from Invitrogen in order to create pCPP6261 and pCPP6260, respectively. mCherry was amplified using primer pair jnw152/jnw157 (Table 5.2) to create an enhanced expression cassette with a synthetic ribosome binding site and terminator to facilitate more efficient expression and ligated into pBS60 at the XbaI and PvuI sites to create pCPP6355. pCPP6355 was used as a template for a PCR using primer pair jnw164/jnw165, and the resultant product was ligated into pUC18R6KT-mini-Tn7T-Tc at the KpnI and EcoRI site by double digestion to create pCPP6287.

Tn7-mediated site-specific integration of synthetic constructs.

A tetraparental-mating approach was used to drive the site-specific integration of pUC18R6KT-mini-Tn7T-based donor vectors into DC3000 derivatives adjacent to *glmS*. Cultures of *E. coli* containing pTNS2, pRK2013, and the donor vector were grown in LB overnight at 30°C with shaking and antibiotic selection. Cultures of the recipient bacteria were grown in KB overnight at 30°C with shaking. Cultures were washed in 1x LM media to remove antibiotics, and 50 µl of each was added to a single tube and

Table 5.1. Bacterial strains and plasmids used in this study.

Designation	Genotype/Plasmid Description	Reference
Escherichia coli		
DH5α	F–Φ80lacZΔM15 ΔlacZYA-argF)U169 deoR recA1 endA1 hsdR17 phoA supE44 thi-1 gyrA96 relA1 λ	Invitrogen
DB3.1	F–gyrA462 endA1Δ (sr1-recA) mcrB mrr hsdS20 supE44 ara-14 galK2 lacY1 proA2 rpsL20 xyl-5 λ–leu mtl-1	Invitrogen
DB3.1 λ*pir*	F−gyrA462 endA1 Δ(sr1-recA) mcrB mrr hsdS20 (r_B− m_B−) supE44 ara-14 galK2 lacY1 proA2 rpsL20 (Strr) xyl-5 Δleu mtl-1 λpir-lysogen	House et al. 2004
SM10 λ*pir*	sup E44 ΔlacU169 (ΦlacZΔM15) recA1 endA1 hsdR17 thi-1 gyrA96 relA1 λpir-lysogen	Miller 1988
HB101	F- mcrB mrr hsdS20(r_B- m_B-) recA13 leuB6 ara-14 proA2 lacY1 galK2 xyl-5 mtl-1 rpsL20(Sm^R) glnV44 λ-	Boyer 1969
S17-1	recA pro hsdR RP4-2-Tc::Mu-Km::Tn7	Simon 1983
Top10	F- mcrA (mrr-hsdRMS-mcrBC) 80lacZM15 lacX74 recA1 ara139 (ara-leu)7697 galU galK rpsL (Sm^R) endA1 nupG	Invitrogen
Pseudomonas fluorescens		
Pf0-1	Wild type	(Silby et al., 2009)
EtHAn	Genomic integration of Psy61 *hrp* gene cluster by Tn5 mediated insertion, Cm^R	(Thomas et al., 2009)
Pseudomonas syringae pv. tomato		
DC3000	Rif^R	(Buell et al., 2003)
CUCPB5112	*hrcC*::*nptII* (no promoter), Km^R on minimal media	(Wei et al., 2000)
CUCPB5460	Δ*hopQ1-1*	(Wei et al., 2007)
CUCPB5585	DC3000 D28E, Sp^R	(Cunnac et al., 2011)
CUCPB6012	DC3000 D28E *avrPtoB,* Sp^R	(Cunnac et al., 2011)
CUCPB6014	DC3000 D28E *hopM1,* Sp^R	(Cunnac et al., 2011)
CUCPB6016	DC3000 D28E *avrPtoB hopM1,* Sp^R	(Cunnac et al., 2011)

Table 5.1. Continued

CUCPB6019	DC3000 D28E *avrPtoB* CEL, Sp^R	(Cunnac et al., 2011)
CUCPB6021	DC3000 D28E *avrPtoB avrPto* CEL, Sp^R	(Cunnac et al., 2011)
CUCPB6031	DC3000 D28E *avrPtoB hopM1 hopE1 hopG1 hopAM1*, Sp^R, Km^R	(Cunnac et al., 2011)
CUCPB6032	DC3000 D28E *avrPtoB* CEL *hopE1 hopG1 hopAm1*, Sp^R, Km^R	(Cunnac et al., 2011)
CUCPB6046	Δ*hopQ1-1* attTn7::FRTTc, Tc^R	This study
CUCPB6069	CUCPB5585 attTn7::FRTTc, Sp^R, Tc^R	This study
CUCPB6070	CUCPB6012 attTn7::FRTTc, Sp^R, Tc^R	This study
CUCPB6071	CUCPB6014 attTn7::FRTTc, Sp^R, Tc^R	This study
CUCPB6072	CUCPB6016 attTn7::FRTTc, Sp^R, Tc^R	This study
CUCPB6073	CUCPB6019 attTn7::FRTTc, Sp^R, Tc^R	This study
CUCPB6074	CUCPB6021 attTn7::FRTTc, Sp^R, Tc^R	This study
CUCPB6075	CUCPB6032 attTn7::FRTTc, Sp^R, Tc^R, Km^R	This study
CUCPB6087	CUCPB5585 attTn7::FRTTc-*mCherry* (1kb fragment including *cmaL*, native promoter), Sp^R, Tc^R	This study
CUCPB6088	CUCPB6012 attTn7::FRTTc- *mCherry* (1kb fragment including *cmaL*, native promoter), Sp^R, Tc^R	This study
CUCPB6089	CUCPB6014 attTn7::FRTTc- *mCherry* (1kb fragment including *cmaL*, native promoter), Sp^R, Tc^R	This study
CUCPB6090	CUCPB6016 attTn7::FRTTc- *mCherry* (1kb fragment including *cmaL*, native promoter), Sp^R, Tc^R	This study
CUCPB6091	CUCPB6019 attTn7::FRTTc- *mCherry* (1kb fragment including *cmaL*, native promoter), Sp^R, Tc^R	This study
CUCPB6092	CUCPB6021 attTn7::FRTTc- *mCherry* (1kb fragment including *cmaL*, native promoter), Sp^R, Tc^R	This study
CUCPB6093	CUCPB6032 attTn7::FRTTc- *mCherry* (1kb fragment including *cmaL*, native promoter), Sp^R, Tc^R	This study
Plasmids		
pBS46	pBBR1MCS5 containing Gateway reading frame B cassette for expression of HA-tagged proteins from nptII promoter, Gm^R, Tc^R	(Wei et al., 2007)

Table 5.1. Continued

pBS60	pBS46 derivative lacking the Gateway cassette, Gm^R	(Swingle et al., 2008)
pCPP5372	pBBR1MCS with *avrPto* promoter, Gateway reading frame B cassette, C terminal HA tag, Gm^r, Cm^r	(Oh et al., 2007)
pCPP5584	pCPP5372::*avrPtoB*	This study
pCPP5963	pCPP5372::*shcM-hopM1*	This study
pCPP6243	pCPP5372::*avrPtoB-shcM-hopM1*	This study
pCPP6257	pENTR/SD/D-TOPO::*mCherry*, Km^R	This study
pCPP6258	pENTR/SD/D-TOPO::*yfp*, Km^R	This study
pCPP6260	pBS46::*yfp*, Gm^R	This study
pCPP6261	pBS46::*mCherry*, Gm^R	This study
pCPP6287	pUC18R6KT-mini-Tn7T-Tc::*mCherry*, Tc^R	This study
pCPP6355	pBS60::*mCherry* with enhanced RBS and terminator	This study
pRK2013	Helper plasmid for conjugation, Km^R	Figurski et al., 1979
pTNS2	Helper plasmid for Tn7 mediated insertions, pTnsABC+D, Ap^R	Choi et al., 2005
pUC18R6KT-mini-Tn7T-Tc	Empty vector for Tn7 mediated insertions, Tc^R	Choi et al., 2005

TABLE 5.2. Primers used in this study.

Forward/Reverse names	Forward sequence	Reverse sequence	Function
jnw152/jnw157	GCTCTAGATTAACTTTAAGAAGGAGCCCTTCACCATGGTGAGCAAGGGCGAGGAGGAT	TATCGATCGAAAAAAATAAACGGCTCATTTCTGAGCCGTTTATTCGTATTGAGAGACTACTTGTACAGCTCGTCCATGCC	Amplifies *mCherry* with an enhanced ribosome binding site and terminator
jnw164/jnw165	CACGGTACCCGAGTCAGCTACTGGGCTATCTGG	GCGGAATTCTAGCACCAGGCGTTTAAGGGCACC	Amplifies from pBS60 to capture the promoter through the MCS.\
oSWC461/oSWC462	AGTACTCCCTAGCCTACTCTTACTG	GAGTTGATCGTATTCGCTGACGAGC	Amplifies the AttTn7 region of DC3000
TOPO-GFP for/TOPO-GFP rev	CACCATGAGCAAGGGCGAGGACGTGT	TTACTTGTACAGCTCGTCCATGCCGTG	Amplifies GFP and EYFP for TOPO cloning
Topo-mCherryF/Topo-mCherryR	CACCATGGTGAGCAAGGGCGAG	TTACTTGTACAGCTCGTCCATGCC	Amplifies mCherry for TOPO cloning

mixed by gentle shaking. This mixture was pelleted by centrifugation and decanted by inverting the tube, leaving approximately 50 µl of supernatant. The pellet was resuspended in this and spotted on a mating membrane on LM media. The mating was allowed to progress overnight with incubation at 30°C. The entire mating reaction was then resuspended in 1 ml LM broth by vortexing, and 100 µl of the suspension was plated on MG minimal media (Bronstein et al., 2008), amended with tetracycline at 5 µg/ml. Additional procedures involving streaking were used to achieve single colony isolation. Minimal medium was used here to select against the auxotrophic plasmid donor and maintenance strains since tetracycline resistance was not particularly robust and the combination of tetracycline and rifampicin proved to be deleterious for growth of integrants. Confirmation of siderophore production via UV-light illumination of colonies grown on MG medium was used to confirm the identity of single colony isolates. PCR reactions using primers oSWC461/oSWC462 were used to confirm insertion into the attTn*7* site.

Syringe inoculation assays.

Bacteria were cultivated on KB media with appropriate selection overnight, suspended in 10mM $MgCl_2$ to an OD_{600} of 0.1, then diluted to the desired concentration. This was infiltrated directly into the youngest fully expanded leaves of 4-5 week old *N. benthamina* plants using a blunt syringe and incubated in a 16h day 23°C plant growth chamber. Samples were prepared by punching out a leaf disk approximately 1cm across and using a wet-mount technique to image. Micrographs were taken with a Leica TCS SP5 confocal microscope at the Boyce Thompson Institute for Plant

Research Plant Cell Imaging Center. YFP excitation was at 514nm with an emission spectrum captured from 524-549nm. mCherry excitation was at 561 nm with an emission spectrum captured from 600-625 nm. Chlorophyll autofluorescence was captured by excitation at 514nm with an emission spectrum captured from 653-695 nm (data not shown, used for reference in identifying cellular structures). Images have three fold line averaging. Representative images of consistent phenomena are shown.

REFERENCES

Baltrus, D.A., Nishimura, M.T., Romanchuk, A., Chang, J.H., Mukhtar, M.S., Cherkis, K., Roach, J., Grant, S.R., Jones, C.D., and Dangl, J.L. 2011. Dynamic evolution of pathogenicity revealed by sequencing and comparative genomics of 19 *Pseudomonas syringae* isolates. PLoS Pathog 7:e1002132.

Boureau, T., Routtu, J., Roine, E., Taira, S., and Romantschuk, M. 2002. Localization of *hrpA*-induced *Pseudomonas syringae* pv. *tomato* DC3000 in infected tomato leaves. Mol Plant Pathol 3:451-460.

Bronstein, P.A., Filiatrault, M.J., Myers, C.R., Rutzke, M., Schneider, D.J., and Cartinhour, S.W. 2008. Global transcriptional responses of *Pseudomonas syringae* DC3000 to changes in iron bioavailability *in vitro*. BMC Microbiol 8:209.

Brooks, D., Hernandez-Guzman, G., Koek, A.P., Alarcon-Chaidez, F., Sreedharan, A., Rangaswarmy, V., Penaloza-Vasquez, A., Bender, C.L., and Kunkel, B.N. 2004. Identification and characterization of a well-defined series of coronatine biosynthetic mutants of *Pseudomonas syringae* pv. *tomato* DC3000. Mol Plant-Microbe Interact 17:162-174.

Brown, I., Mansfield, J., and Bonas, U. 1995. *Hrp* genes in *Xanthomonas campestris* pv. *vesicatoria* determine ability to suppress papilla deposition in pepper mesophyll cells. Mol Plant-Microbe Interact 8:825-836.

Buell, C.R., Joardar, V., Lindeberg, M., Selengut, J., Paulsen, I.T., Gwinn, M.L., Dodson, R.J., Deboy, R.T., Durkin, A.S., Kolonay, J.F., Madupu, R., Daugherty, S., Brinkac, L., Beanan, M.J., Haft, D.H., Nelson, W.C., Davidsen, T., Liu, J.,

Yuan, Q., Khouri, H., Fedorova, N., Tran, B., Russell, D., Berry, K., Utterback, T., Vanaken, S.E., Feldblyum, T.V., D'Ascenzo, M., Deng, W.-L., Ramos, A.R., Alfano, J.R., Cartinhour, S., Chatterjee, A.K., Delaney, T.P., Lazarowitz, S.G., Martin, G.B., Schneider, D.J., Tang, X., Bender, C.L., White, O., Fraser, C.M., and Collmer, A. 2003. The complete sequence of the *Arabidopsis* and tomato pathogen *Pseudomonas syringae* pv. *tomato* DC3000. Proc Natl Acad Sci USA 100:10181-10186.

Burch-Smith, T.M., and Zambryski, P.C. 2012. Plasmodesmata paradigm shift: regulation from without versus within. Annu Rev Plant Biol 63:239-260.

Cornelis Guy, R. (2010). The type III secretion injectisome, a complex nanomachine for intracellular ‘toxin’ delivery. In Biological Chemistry, pp. 745.

Crabill, E., Karpisek, A., and Alfano, J.R. 2012. The *Pseudomonas syringae* HrpJ protein controls the secretion of type III translocator proteins and has a virulence role inside plant cells. Mol Microbiol 85:225-238.

Cunnac, S., Lindeberg, M., and Collmer, A. 2009. *Pseudomonas syringae* type III secretion system effectors: repertoires in search of functions. Curr Opin Microbiol 12:53-60.

Cunnac, S., Chakravarthy, S., Kvitko, B.H., Russell, A.B., Martin, G.B., and Collmer, A. 2011. Genetic disassembly and combinatorial reassembly identify a minimal functional repertoire of type III effectors in *Pseudomonas syringae*. Proc Natl Acad Sci USA 108:2975-2980.

Deslandes, L., and Rivas, S. 2012. Catch me if you can: bacterial effectors and plant targets. Trends Plant Sci 17:644-655.

Dong, H., Delaney, T.P., Bauer, D.W., and Beer, S.V. 1999. Harpin induces disease resistance in *Arabidopsis* through the systemic acquired resistance pathway mediated by salicylic acid and the NIM1 gene. The Plant Journal 20:207-215.

Godfrey, S.A.C., Mansfield, J.W., Corry, D.S., Lovell, H.C., Jackson, R.W., and Arnold, D.L. 2010. Confocal imaging of *Pseudomonas syringae* pv. *phaseolicola* colony development in bean reveals reduced multiplication of strains containing the genomic island PPHGI-1. Mol Plant-Microbe Interact 23:1294-1302.

Groll, M., Schellenberg, B., Bachmann, A.S., Archer, C.R., Huber, R., Powell, T.K., Lindow, S., Kaiser, M., and Dudler, R. 2008. A plant pathogen virulence factor inhibits the eukaryotic proteasome by a novel mechanism. Nature 452:755-758.

Hanahan, D. 1985. Techniques for transformation of *E. coli*. Pages 109-135 in: DNA Cloning: A Practical Approach, D.M. Glover, ed. IRL Press, Oxford, United Kingdom.

Harries, P., and Ding, B. 2011. Cellular factors in plant virus movement: At the leading edge of macromolecular trafficking in plants. Virology 411:237-243.

Jelenska, J., Yao, N., Vinatzer, B.A., Wright, C.M., Brodsky, J.L., and Greenberg, J.T. 2007. A J domain virulence effector of *Pseudomonas syringae* remodels host chloroplasts and suppresses defenses. Curr Biol 17:499-508.

Kenny, B., and Valdivia, R. 2009. Host–microbe interactions: bacteria. Curr Opin Microbiol 12:1-3.

Khang, C.H., Berruyer, R., Giraldo, M.C., Kankanala, P., Park, S.-Y., Czymmek, K., Kang, S., and Valent, B. 2010. Translocation of *Magnaporthe oryzae* effectors

into rice cells and their subsequent cell-to-cell movement. Plant Cell 22:1388-1403.

King, E.O., Ward, M.K., and Raney, D.E. 1954. Two simple media for the demonstration of pyocyanin and fluorescin. J Lab Clin Med 44:301-307.

Kvitko, B.H., Ramos, A.R., Morello, J.E., Oh, H.-S., and Collmer, A. 2007. Identification of harpins in *Pseudomonas syringae* pv. *tomato* DC3000, which are functionally similar to HrpK1 in promoting translocation of type III secretion system effectors. J Bacteriol 189:8059-8072.

Lee, J.-Y., Wang, X., Cui, W., Sager, R., Modla, S., Czymmek, K., Zybaliov, B., van Wijk, K., Zhang, C., Lu, H., and Lakshmanan, V. 2011. A plasmodesmata-localized protein mediates crosstalk between cell-to-cell communication and innate immunity in *Arabidopsis*. Plant Cell 23:3353-3373.

Lee, J., Klüsener, B., Tsiamis, G., Stevens, C., Neyt, C., Tampakaki, A.P., Panopoulos, N.J., Nöller, J., Weiler, E.W., Cornelis, G.R., Mansfield, J.W., and Nürnberger, T. 2001. $HrpZ_{Psph}$ from the plant pathogen *Pseudomonas syringae* pv. *phaseolicola* binds to lipid bilayers and forms an ion-conducting pore in vitro. Proc Natl Acad Sci USA 98:289-294.

Lindeberg, M., Cunnac, S., and Collmer, A. 2012. *Pseudomonas syringae* type III effector repertoires: last words in endless arguments. Trends Microbiol 20:199-208.

Macho, A.P., Zumaquero, A., Ortiz-MartÍN, I., and BeuzÓN, C.R. 2007. Competitive index in mixed infections: a sensitive and accurate assay for the genetic analysis of *Pseudomonas syringae*–plant interactions. Mol Plant Pathol 8:437-450.

Melotto, M., Underwood, W., Koczan, J., Nomura, K., and He, S.Y. 2006. Plant stomata function in innate immunity against bacterial invasion. Cell 126:969-980.

Monaghan, J., and Zipfel, C. 2012. Plant pattern recognition receptor complexes at the plasma membrane. Curr Op Plant Biol 15:349-357.

Oh, H.-S., Kvitko, B.H., Morello, J.E., and Collmer, A. 2007. *Pseudomonas syringae* lytic transglycosylases co-regulated with the type III secretion system contribute to the translocation of effector proteins into plant cells. J Bacteriol 189:8277-8289.

Rico, A., and Preston, G.M. 2008. *Pseudomonas syringae* pv. *tomato* DC3000 uses constitutive and apoplast-induced nutrient assimilation pathways to catabolize nutrients that are abundant in the tomato apoplast. Mol Plant-Microbe Interact 21:269-282.

Silby, M.W., Cerdeno-Tarraga, A.M., Vernikos, G.S., Giddens, S.R., Jackson, R.W., Preston, G.M., Zhang, X.X., Moon, C.D., Gehrig, S.M., Godfrey, S.A., Knight, C.G., Malone, J.G., Robinson, Z., Spiers, A.J., Harris, S., Challis, G.L., Yaxley, A.M., Harris, D., Seeger, K., Murphy, L., Rutter, S., Squares, R., Quail, M.A., Saunders, E., Mavromatis, K., Brettin, T.S., Bentley, S.D., Hothersall, J., Stephens, E., Thomas, C.M., Parkhill, J., Levy, S.B., Rainey, P.B., and Thomson, N.R. 2009. Genomic and genetic analyses of diversity and plant interactions of *Pseudomonas fluorescens*. Genome Biol 10:R51.

Sinden, S.L., and Durbin, R.D. 1968. Glutamine synthetase inhibition: possible mode of action of wildfire toxin from *Pseudomonas tabaci*. Nature 219:379-380.

Swingle, B., Thete, D., Moll, M., Myers, C.R., Schneider, D.J., and Cartinhour, S. 2008. Characterization of the PvdS-regulated promoter motif in *Pseudomonas syringae* pv. *tomato* DC3000 reveals regulon members and insights regarding PvdS function in other pseudomonads. Mol Microbiol 68:871-889.

Tam, L.Q., and Patil, S.S. 1972. Mode of action of the toxin from *Pseudomonas phaseolicola*. Plant Physiol 49:808-812.

Templeton, M.D., Sullivan, P.A., and Shepherd, M.G. 1984. The inhibition of ornithine transcarbamoylase from *Escherichia coli* W by phaseolotoxin. Biochem J 224:379-370.

Thomas, M.D., Langston-Unkefer, P.J., Uchytil, T.F., and Durbin, R.D. 1983. Inhibition of glutamine synthetase from pea by tabtoxinine-beta-lactam. Plant Physiol 71:912-915.

Thomas, W.J., Thireault, C.A., Kimbrel, J.A., and Chang, J.H. 2009. Recombineering and stable integration of the *Pseudomonas syringae* pv. *syringae* 61 hrp/hrc cluster into the genome of the soil bacterium *Pseudomonas fluorescens* Pf0-1. The Plant Journal 60:919-928.

Underwood, W., Melotto, M., and He, S.Y. 2007. Role of plant stomata in bacterial invasion. Cellular Microbiol 9:1621-1629.

Wei, C.-F., Kvitko, B.H., Shimizu, R., Crabill, E., Alfano, J.R., Lin, N.-C., Martin, G.B., Huang, H.-C., and Collmer, A. 2007. A *Pseudomonas syringae* pv. *tomato* DC3000 mutant lacking the type III effector HopQ1-1 is able to cause disease in the model plant *Nicotiana benthamiana*. The Plant Journal 51:32-46.

Wei, W., Plovanich-Jones, A., Deng, W.L., Jin, Q.L., Collmer, A., Huang, H.C., and He, S.Y. 2000. The gene coding for the Hrp pilus structural protein is required for type III secretion of Hrp and Avr proteins in *Pseudomonas syringae* pv. *tomato*. Proc Natl Acad Sci USA 97:2247-2252.

Wei, Z., Laby, R., Zumoff, C., Bauer, D., He, S., Collmer, A., and Beer, S. 1992. Harpin, elicitor of the hypersensitive response produced by the plant pathogen *Erwinia amylovora*. Science 257:85-88.

Wolf, S., Deom, C.M., Beachy, R.N., and Lucas, W.J. 1989. Movement protein of *Tobacco mosaic virus* modifies plasmodesmatal size exclusion limit. Science 246:377-379.

Zhou, J.-M., and Chai, J. 2008. Plant pathogenic bacterial type III effectors subdue host responses. Curr Opin Microbiol 11:179-185.

CHAPTER 6

PROSPECTUS

This thesis has focused on the relationship between the phytotoxin coronatine and the T3Es of *Pseudomonas syringae* pv. *tomato* DC3000. These pathogenicity factors clearly have different mechanisms by which they establish interactions with plant cells, yet are connected by some functional redundancy, meaning that the small molecules and effectors are connected in their ability to promote disease. Researchers investigating *P. syringae* "omics" must be cognizant of the secreted metabolome of whatever strains they are working with. This extends to research that utilizes non *P. syringae* strains as backgrounds, such as *P. fluorescens*, where the bacterium has, ostensibly, had little selective pressure to hide itself from the constantly *en garde* leaf mesophyll cells. Tools such as *P. fluorescens* will continue to be useful, but as our ability to extract increasingly complex and accurate data sets from plant responses increases, the "omics" era requires a keen eye towards the tools used to stimulate these responses.

The bacterial side of plant-pathology is yielding an encouraging pattern in the post-genomic era. There exists a subset of effectors across *P. syringae* spp. that are highly conserved and thus make promising targets for study (Baltrus et al., 2011). These effectors are worthy of continued attention as they represent the most successful effectors known, and the most likely to reveal pathways for durable resistance. These are not without exception, though, particularly with the high variability seen in some

lineages regarding *hopM1*, suggesting that this, one of the top two most highly prevalent and ancestrally conserved effectors, may be undergoing intense selective pressure in some host-pathogen interactions (Cai et al., 2011).

The list of confirmed T3E to plant-protein targets is growing, but slowly. A few studies have attempted to address this problem, but have not yielded many confirmed and relevant interactions (Mukhtar et al., 2011). Part of this stems from a lack of compatible screens for many of the effectors. If either your effector protein or host protein is membrane associated or elicits cell death, then the yeast two-hybrid approach is not compatible. You also may lose host-machinery-dependent modifications, such as plant specific phosphorylation events, in yeast. This problem of host-modification exists also for some kinds of pull-down assays, which also can additionally struggle with low-abundance membrane bound proteins.

We may see some technologies arriving that begin to dent this problem, however. Protein arrays, once optimized, may provide good resolution for protein-protein interactions and are beginning to gain traction as a tool. This approach has the added bonus of providing a platform for radioisotopic labeling or ubiquitination experiments that can be carefully controlled. Mass spectroscopy continues to come down in price and expertise required, plus is increasing in sensitivity. If interacting protein-protein partners can be captured via covalent cross-linking and then extracted under denaturing conditions, then populations of proteins can be pulled out of plant tissue for spectroscopic analysis. It is somewhat surprising to the author that this kind of procedure has not been used in a screen utilizing Arabidopsis protoplasts and

transient expression methods with crosslinking followed by extraction and mass spectroscopy.

Although confirmed protein-protein interactions between T3Es and their hosts provides footholds for understanding plant defense and can elucidate important properties of effector repertoires, this could be considered a minor role in understanding infection. With the development of DC3000D28E, *P. syringae* research into effector biology was given a new tool in which to study effector impact. *P. fluorescens* Pf0-1 pHIR11 allowed for individual study of effector proteins but did not have a bacterial background that was programmed to fully take advantage of effector function. With an effectorless *P. syringae* mutant it seemed a propitious time to initiate combinatorial effector research, especially when armed with knowledge from an increasing number of studies of individual effectors. One advance made in this thesis is identification of a missing factor in coronatine biosynthesis, which has enabled new approaches to studying the impact of toxin-effector repertoire interactions on disease outcome.

Additionally, the DC3000D28E background may provide insights into phytotoxin roles. For instance, syringolin- and syringomycin-producing strains tend to have smaller effector repertoires (Baltrus et al., 2011). If so, a deletion of the *cfa* operon within DC3000D28E and the addition of biosynthetic pathways for syringolin and/or syringomycin would reveal if different toxin-effector repertoire dynamics are observed. Much of the focus for current research is on T3Es, and while it is a worthwhile endeavor, the interplay of all pathogenicity factors should be considered, especially since phytotoxin production is encoded on mobile elements and can move between phylogenetically distant clades.

Perhaps more promising than the bacterial side of the equation is plant defense research. Bacterial effector studies have facilitated and provided targets for plant defense research, but there is much left unresolved in signal transduction and transcription factor identification. Plant proteins are more likely to be homologous to another protein of known function than effector proteins, a property which generally makes finding specific activities easier. Additionally, if these pathways are elucidated, the effectors could be screened against a more select group of plant proteins, increasing specificity in assay design, much in the same way that effector studies have been guided by new insights from the sequencing era.

The sequencing era is bringing about a vast increase in our knowledge of allele population dynamics and, more recently, transcriptomic profiles of single lines of plants under various conditions or within specific structures. These advances can sometimes feel a bit like reading poetry in a foreign language – you can make the sounds and recognize even most of the words, but often the meaning is lost by not having the context, cultural knowledge, or knowledge of nuanced alternate meanings of words that are only accessible to those who are fluent. Like poetry, these sequencing era databanks can also reveal increasing depth and nuance with increased attention, but I would suggest, only after understanding the biochemical complexities of these interactions.

The sequencing era is bringing about a change in the ability to probe the impacts of various effectors on plant cell biochemistry, as well. Transcriptomic profiles are becoming ever cheaper to obtain, facilitating its use as a readout for the study of pathogenicity factors. These can reveal which biochemical pathways are regulated by

specific stimuli, and importantly, how these transcriptional responses are modified by pathogens. Careful attention will need to be paid to stimuli identity and other factors, such as multiplicity of infection, to determine optimal conditions for these studies. It will be particularly interesting to see how the different kinds of effectors impact the plant defense transcriptome.

Plant-pathology will continue to move towards understanding the biochemistry underlying pathogenicity factors and plant defenses. The advances in sequencing technology will continue to inform our understanding in the short term of what needs to be researched in order to reduce crop loss to pathogens. Mass spectroscopy is the technique on the horizon with the ability revolutionize how we approach not only research, but disease monitoring. As sensors increase in sensitivity and costs for basic instruments come down, using mass spectroscopy could become a common-place procedure for observing how plants are reacting to microbes on a fine scale. A particularly interesting possibility might be the application of mass spectroscopy imaging (10 μm resolution) for looking at, for example, guard cell proteomes during infection, allowing for proteome-based observation of the different cell types (Thelen and Miernyk, 2012).

REFERENCES

Baltrus, D.A., Nishimura, M.T., Romanchuk, A., Chang, J.H., Mukhtar, M.S., Cherkis, K., Roach, J., Grant, S.R., Jones, C.D., and Dangl, J.L. 2011. Dynamic evolution of pathogenicity revealed by sequencing and comparative genomics of 19 *Pseudomonas syringae* isolates. PLoS Pathog 7:e1002132.

Cai, R., Lewis, J., Yan, S., Liu, H., Clarke, C.R., Campanile, F., Almeida, N.F., Studholme, D.J., Lindeberg, M., Schneider, D., Zaccardelli, M., Setubal, J.C., Morales-Lizcano, N.P., Bernal, A., Coaker, G., Baker, C., Bender, C.L., Leman, S., and Vinatzer, B.A. 2011. The plant pathogen *Pseudomonas syringae* pv. *tomato* is genetically monomorphic and under strong selection to evade tomato immunity. PLoS Pathog 7:e1002130.

Mukhtar, M.S., Carvunis, A.-R., Dreze, M., Epple, P., Steinbrenner, J., Moore, J., Tasan, M., Galli, M., Hao, T., Nishimura, M.T., Pevzner, S.J., Donovan, S.E., Ghamsari, L., Santhanam, B., Romero, V., Poulin, M.M., Gebreab, F., Gutierrez, B.J., Tam, S., Monachello, D., Boxem, M., Harbort, C.J., McDonald, N., Gai, L., Chen, H., He, Y., Consortium, E.U.E., Vandenhaute, J., Roth, F.P., Hill, D.E., Ecker, J.R., Vidal, M., Beynon, J., Braun, P., and Dangl, J.L. 2011. Independently evolved virulence effectors converge onto hubs in a plant immune system network. Science 333:596-601.

Thelen, J.J., and Miernyk, J.A. 2012. The proteomic future: where mass spectrometry should be taking us. Biochem J 444:169-181.